IAEA-TECDOC-1287

Natural and induced radioactivity in food

INTERNATIONAL ATOMIC ENERGY AGENCY IAEA

April 2002

The originating Section of this publication in the IAEA was:

Food and Environmental Protection Section
International Atomic Energy Agency
Wagramer Strasse 5
P.O. Box 100
A-1400 Vienna, Austria

NATURAL AND INDUCED RADIOACTIVITY IN FOOD
IAEA, VIENNA, 2002
IAEA-TECDOC-1287
ISSN 1011–4289

Printed by the IAEA in Austria
April 2002

FOREWORD

One of the first questions often asked about irradiated food is whether it is radioactive. Not many people understand that food and any natural substance contains natural radioactivity which can be measurable. It is therefore important to put the issue on natural radioactivity and possible induced radioactivity in food in perspective. While there is a clear consensus among the scientific community that no radioactivity is induced when food is irradiated by gamma rays from cobalt-60 or cesium-137, electron generated by a machine with energy less than 10 million electron volt (MeV) or X rays produced generated by a machine with energy less than 5 MeV. However, data to this effect were published many years ago and are not easy to find.

As food irradiation is gaining wide acceptance in many countries, it was considered timely to compile data on natural and induced radioactivity in food into one document. We are grateful to A. Brynjolfsson, one of the few experts who have the knowledge on this subject as well as wide experience on food irradiation, who collected, compiled and evaluated all data on this subject into one report. This publication provides clear explanations not only why radioactivity cannot be induced in food irradiated by radiation sources mentioned above but to what extent the increase in dose or energy level of radiation sources would induce significantly radioactivity in food. The compilation of such data was prompted by a desire to increase the energy limit and the absorbed dose based on the need to irradiate thicker samples of food and to use sterilizing dose up to 60 kGy.

This publication concluded that the increase in radiation background dose from consumption of food irradiated to an average dose up to 60 kGy with gamma rays from cobalt-60 or cesium-137, with 10 MeV electrons or with 5 MeV X rays is insignificant. In addition, food irradiated with X ray with energy up to 7.5 MeV to a dose of 30 kGy has radioactivity well below natural radioactivity in unirradiated food. There are no adverse effect from consumption of irradiated food which contains radioactivity well below background level.

This publication should provide valuable information to anyone who has interest in food irradiation especially regulatory authorities for food safety and radiation applications as well as to consumers who might be interested in scientific matters of irradiated food. We acknowledge the excellent co-operation from M.R. Cleland, H.P. Weise, D. Ehlermann, and A. Miller in reviewing this manuscript for publication.

The IAEA officer responsible for this publication was P. Loaharanu of the Joint FAO/IAEA Division of Nuclear Techniques in Food and Agriculture.

EDITORIAL NOTE

The use of particular designations of countries or territories does not imply any judgement by the publisher, the IAEA, as to the legal status of such countries or territories, of their authorities and institutions or of the delimitation of their boundaries.

The mention of names of specific companies or products (whether or not indicated as registered) does not imply any intention to infringe proprietary rights, nor should it be construed as an endorsement or recommendation on the part of the IAEA.

CONTENTS

LIST OF TABLES

LIST OF FIGURES

SUMMARY

It is generally accepted in the scientific community that no radioactivity is induced when food is irradiated by gamma rays from cobalt-60 and cesium-137, electrons with energy less than 10 million electron-volt (MeV), and X rays produced by electrons with energy less than 5 million electron-volt (MeV), even when the doses used are as high as 10 kilogray (kGy).

The question is often raised, however, as to whether or not the energy of the electrons and the X rays, and the dose used to process the food could be increased safely beyond these limits. Since we require that no significant radioactivity be induced in the food, we must consider if increasing the dose and the energy limits would significantly increase the radiation background. We may also consider if increasing the dose requires decreasing the energy limits for electrons and X rays used in the processing. Similarly, if the dose is lowered, we might consider increasing the energy limits. For example, during inspection of food, X ray energy up to 10 MeV is permitted because the dose, less than 0.5 gray (Gy), is very low. [Anon90]

It is usually assumed that we should require that there should not be any measurable increase in the radioactivity in the food when it is irradiated. The limit for any measurable increase in food's radioactivity is usually about 1% of the natural radioactivity of unprocessed food. On this basis, the use of 10 MeV electrons and 5 MeV X rays was generally accepted.

The desire to increase the energy limit and the dose limit is driven by the need to irradiate thicker samples of food and the need, in some cases, to use sterilizing doses of up to 60 kGy. Justifying any increase in the energy and dose limits becomes increasingly difficult, because the possible health effects of "no measurable activity" limit are not well defined; and secondly, there are significant discrepancies in the onset of measurable radioactivity at higher energies as reported by the different authors.

It was found necessary, therefore, to reconsider the question closely from a theoretical point of view. First, a need exists to define in strict scientific terms the relation between health effects and any activity that is produced in the food. Secondly, there is a need to determine more accurately the magnitude of any possible induced activity, and to resolve the discrepancy in the measurements by different authors. These objectives required the present detailed evaluation, which can be used as a point of reference for further discussion.

The present report concludes that the increase in radiation background dose from consumption of food irradiated to an average dose below 60 kGy with gamma rays from cobalt-60 or Cs-137, with 10 MeV electrons, or with X rays produced by electron beams with energy below 5 MeV is insignificant. It is best characterized as zero.

1. BACKGROUND RADIATION

There are four main components of general background radiation:

(1) Natural radioactivity in food and water and inhaled air.
(2) Natural terrestrial radiation from our immediate environment, including buildings.
(3) Natural cosmic radiation from Sun, stars and from galactic and intergalactic plasma.
(4) Medical and industrial applications.

The biological effect of ionizing radiation, such as gamma rays, X rays, and fast electrons is often nearly proportional to the absorbed radiation energy; that is, it is proportional to the radiation dose. The dose is measured in units of gray (abbreviated Gy), which is equal to 1 joule of radiation energy absorbed per kilogram (1 Gy = 1 J/kg). The unit gray is very small, as it would heat water only 0.00024 ^{0}C, or 0.00043 ^{0}F. The background radiation dose exposure to humans is usually measured in the still smaller unit milligray (abbreviated mGy), which is equal to one thousandth of a gray.

When assessing radiation's health effects, the unit sievert (abbreviated Sv) is used rather than the unit gray. The number of sievert units is Q times the number of the dose units in gray. Q is called a quality factor. Q = 1 for gamma rays, X rays, and fast electrons; Q ≈10 for fast neutrons, and Q ≈ 20 for alpha particles (α-particles). Its exact value depends on the velocity of the particles and its charge. Its value indicates relative health effects of the different radiations. Corresponding to the milligray unit, the exposure dose for evaluation of radiation health effects in humans is measured in millisievert units (abbreviated mSv) and equal to 1/1000 sievert.

The average contributions to the natural background radiation from different sources are given in Table 1, which is from BEIR report; [Anon80] and in Table 2, which is from the BEIR V report. [BEIR V 90] Table 2 gives similar analysis for the USA, but includes radiations from medical uses, industrial application, and consumer products. The background radiation varies significantly from place to place and with time. The averages listed in the tables should be considered only as indicative of the average level of the background. The average dose from the background radiation is often about 3.6 millisieverts/year ($mSv \cdot y^{-1}$). For the purpose of understanding the detectable limit, let us consider the background radiation more closely.

1.1. Natural radioactivity in foods

The radioactivity is measured in units of becquerel (abbreviated Bq), where one becquerel is one nuclear change per second. In the human body, the concentration of activity of potassium (^{40}K) is about 63 Bq/kg, of carbon (^{14}C) about 66 Bq/kg, of tritium (^{3}H) about 133 Bq/kg, of polonium (^{210}Po) about 0.0002 Bq/kg, and of radium (^{226}Ra) about $2.7 \cdot 10^{-5}$ Bq/kg.

The concentration of the natural radioactivity in food is often in the range of 40 to 600 becquerel per kilogram of food. For example, the radioactivity from potassium alone may be typically 50 Bq/kg in milk, 420 Bq/kg in milk powder, 165 Bq/kg in potatoes, and 125 Bq/kg in beef. Typical of studies on the radioactivity in foods are those reported by Ramachandran and Mishra. [Ra89a] They found the concentration of ^{40}K radioactivity in different foods varies from 45.9 to 649.0 Bq/kg; that of ^{226}Ra varies from 0.01 to 1.16 Bq/kg; and that of ^{228}Th varies from 0.02 to 1.26 Bq/kg. For deriving the corresponding dose in $mSv \cdot y^{-1}$, it is necessary to take into account the energy and the fraction that is deposited in the body; and it is necessary to take into account not only the radioactive lifetime but also the biological lifetime of the isotope in the human body. For converting the activity in becquerel/kilogram ($Bq \cdot kg^{-1}$) of food intake to sievert, we must multiply the number of becquerel by

(1) The energy per disintegration.
(2) The fraction of that energy absorbed in the body.
(3) The conversion factor for the energy and mass units used.
(4) The time integrated activity, $\int A_i \cdot \exp(-t/\tau_E) \cdot dt$, where the effective lifetime τ_E is given by $1/\tau_E = 1/\tau_P + 1/\tau_R$; and τ_P and τ_R are the physiological lifetime and radioactive lifetime of the isotope in the body.
(5) The quality factor Q, which adjusts for the biological effectiveness of the different radiations relative to that of fast electrons and gamma rays.

The quality factor Q varies with the type of radiation. For example, for equal amount of activity in Bq/kg, the alpha emitters such as ^{226}Ra and ^{228}Th are biologically much more damaging than the same activity of beta and gamma emitters.

The elaborate calculations for the inclusion of these many factors (for each and every organ) have been made and the results compiled in ICRP Publication 68. [ICRP94] and [ICRP96]. We will use this compilation. For example, if an adult consumes food containing 1 becquerel (Bq) of ^{24}Na, then the dose summarized for the average adult and average lifespan will be $4.3 \cdot 10^{-10}$ sievert (Sv).

Excluding the α emitters, the natural radioactivity in foods usually contributes on the average about 0.24 to 0.6 mSv/year internal dose. The main element contributing to the dose is often potassium, which is an essential nutrient. The amount of potassium in the body is nearly constant. In the bone marrow (often considered one of the most radiation sensitive parts of the human body) the radioactivity due to the ^{40}K isotope is about 130 Bq/kg. Other beta emitters are: rubidium isotope ^{87}Rb, carbon isotope ^{14}C, tritium isotope ^{22}Na, and tritium isotope ^{3}H.

Food, water and air usually contain also trace amount of alpha emitters from the uranium, thorium, and actinium series. Some of the radon (^{222}Rn, and to lesser extent ^{220}Rn and ^{219}Rn) gas diffuses into the air and water. For example, the radon in the ground and in the water is released into the air, and its many decay products precipitate onto the field and onto the vegetation in the field. When we open the faucet in our homes, the radon and its decay products contaminate the interior of the houses. The radon also enters the houses through cracks in the floor. The radon and its decay products are suspended in the air and inhaled. Ahmed has reported values as high as 37 kBq/kg of air. [Ah91] The radiation from the alpha emitters contributes usually about 1 to 4.5 $mSv \cdot y^{-1}$, which is deposited mostly to the segmental bronchi of the lungs and to the bones.

1.2. Radiation from terrestrial sources

Terrestrial radiations from natural radioactive elements in the ground, in the stones, in the trees, and in the walls of our houses contribute on the average about 0.28 $mSv \cdot y^{-1}$. The terrestrial sources vary significantly from place to place.

The concentration of potassium is usually in the range of 1000 to 30,000 ppm. It is usually lower but more variable in basaltic rock region (1,500 to 20,000 ppm) than in acidic (high concentration of SiO_2) rock regions. For example, in granite rock, the concentration is often about 29,000 ppm. About 89 % of ^{40}K decays to ^{40}Ca by emission of β-rays with maximum energy of 1.312 MeV, while about 11 % decays by positron emission to an excited state of ^{40}Ar followed by emission of 1.46 MeV γ ray.

The concentration of rubidium (which is chemically similar to potassium) is often about 1 % of that of potassium. Accordingly, the concentration of radioactivity of rubidium is often about 60 % of that of potassium. ^{87}Rb, like ^{14}C and ^{3}H, emits only soft β-rays and contributes to internal radiation but not to the external radiation exposure.

Most of the terrestrial background radiation is due to potassium and to elements of the uranium series (^{238}U to ^{206}Pb), thorium series (^{232}Th to ^{209}Pb), and actinium series (^{235}U to ^{207}Pb). Each of these series consists of many α, β, and γ emitters. The concentration of these radioactive isotopes in the soil and water varies greatly. In certain areas, such as in the coastal areas of Kerala in India, the average dose is about 11 mSv/year. In certain areas of southwestern France, in Guarapari in Brazil, and in Ramsar in Iran the dose may be about 17 mSv/year, and in small places within these areas the dose rate may be as high as 170 to 430 mSv·y^{-1}. These levels are caused by higher than usual natural background levels of uranium and thorium isotopes in the soil. [Anon77a].

1.3. Cosmic radiation

The cosmic radiation originates in the Sun, stars, collapsed stars, such as neutron stars, quasars, and in the hot galactic and intergalactic plasma. It has many components, such as x rays, gamma rays, and particles, which may be mesons, electrons, protons, neutrons, or hyperons. The initial energy of the individual particles covers a broad spectrum from a few electronvolts (eV) to about 10^{20} eV. Cosmic radiation loses energy as it penetrates the atmosphere. The protective shield of the atmosphere and the Earth's magnetic field prevent the soft energy radiation components from penetrating the atmosphere. The hardest components, the mesons, dominate at sea level. Above about 5 km the electrons are about equal or dominate the mesons. Above about 25 km, the protons dominate. The cosmic radiation produces X rays and neutrons as it penetrates the atmosphere. Also, the primary particles often transform to new particles. Penetration of charged particles depends strongly on the magnetic field. The radiation they produce, including neutrons, depends then also on the magnetic field.

During and after slowing down in the atmosphere, the neutrons may in turn produce radioactive isotopes, such as ^{14}C, and ^{3}H. The thickness of the atmosphere corresponds to about 10 m of water, or about 4 m of concrete. Nevertheless, at the sea level the cosmic radiation contributes on the average about 0.27 millisievert/year to our body. At ground level, only a small fraction of that is due to neutrons. The cosmic radiation dose increases with altitude. At 2,500 m, it is about 0.55 mSv·y^{-1}; and at 12,000 m, the altitude for long distance air travel, it is on the order of 60 times greater or 17 mSv·y^{-1}. At a slightly higher altitude of 15,000 m and 60 degree magnetic latitude, it levels off and reaches a maximum of about 30 mSv/year.

The cosmic radiation increases with magnetic latitude, especially at higher elevations. For example, at 12,500 m altitude, the dose rate from neutrons alone increases from 8 mSv·y^{-1} at magnetic latitude of 25^0 to 19 mSv·y^{-1} at magnetic latitude of 50^0. [Na87a] A flight from Boston to San Francisco might last 6 hours at a height of 12,000 m. The extra radiation received on that flight would usually exceed 0.012 mSv.

Fig. 1 shows how the cosmic neutron dose rate at sea level and at 12,500 m altitude depends on the magnetic latitude. The neutron dose rate at sea level and magnetic latitude of 43^0 is seen to be roughly 300 times smaller than that at 12,500 m over sea level. At magnetic latitude of 50^0 the cosmic neutron dose at a height of 12,500 m over sea level is about 20 mSv/year, while at ground level and at the same magnetic latitude the cosmic ray neutron dose is about 19/300=0.063 mSv/year; see [Na87a].

2. HEALTH EFFECTS CAUSED BY LOW LEVEL RADIATION

The high levels of background radiation in some regions have not caused noticeable increase in cancer in the populations residing in these areas. [BEIR V 90] Estimates of detrimental effects of radiation exposures are based therefore on extrapolations (usually linear) from many times higher doses than those of the background radiations. In BEIR III report,[BEIR III 80] it is estimated that a single exposure to 100 mSv of radiation might cause, at most, about 6,000 excess cases of cancer deaths (other than leukemia and bone cancer) per million deaths, as opposed to a natural incidence of about 250,000 cancer deaths. The linear extrapolation indicates thus that a background radiation exposure of 3 mSv for 70 years, or a total of 210 mSv·years per person, would analogously produce about 12,600 extra cancers per million deaths of people, or about 1 radiation-induced cancer per 20 cancers. (The integration over time span of 70 years is usually considered to be excessive as it takes 5 to 30 years for cancer to develop.) Thus, the background radiation may be responsible for about 5% of all cancers or 1.26 % of all deaths. Without the background radiation, the cancer rate may vary from one human population to another, with one region to another, with many environmental factors, including smoking and drugs, as well as fungal, bacterial and viral infections. It is therefore very difficult to discern the possible 5 % increase caused by the background.

For estimating the health effects of low level radiation, the BEIR reports hypothetically assumed that any detrimental health effect increases linearly with dose D; that is,

$$H_n = a_n \cdot D ,$$

where H_n is a specific health effect and a_n is a constant. The health effect, H_n, is determined at so large a dose D that the probability for it to occur could be determined experimentally. This hypothesis is sometimes called the "linear no threshold" model, or just LNT model. Associated assumptions are usually: 1) that a health effect, such as a specific cancer, is caused by DNA damage, and 2) that the DNA damage is caused by a direct or indirect "hit" by an ionizing radiation. The indirect hit may initially result in a chemical species or compound that subsequently reacts with the DNA to produce the "hit". It is then assumed that the cell with the defect DNA multiplies and results in a chain of reactions that promotes or leads to a cancer. Some scientists believe that the effect of the background radiation is less than this linear extrapolation indicates, and very few believe that it is greater.

Fig. 2 gives examples of four different ways for extrapolating from effects observed at high doses to effects observed at low doses. Series 1 curve, the top curve, shows the relation indicated by Eq. (2), which can be considered equivalent to the LNT model given by Eq.(1). Series 2 and (3) curves show the relations indicated by Eqs. (3) and (4). In case of these two curves a linear extrapolation from high doses would indicate a threshold dose. Series 4 shows relation indicated by Eq. (5), which at very low doses shows a small beneficial effect. However, the beneficial effect is small and it would be extremely difficult to confirm it experimentally. For this illustration, the curves given by the equations have been adjusted to go through the same points at (0, 0.1) and at (5, 0.7321); and in case of equation (5), the value of A =1.5 and B = 0.5.

2.1. Basic physical effects of radiation on living matter

It is useful to view the health effects from basic physical interactions of radiation with matter. In case of gamma rays and x rays, most of the ionization and excitation are produced by the fast electrons that are knocked out of the atoms in the Compton effect and in the photoelectric effect. The chemical and the physiological effect of γ rays, X rays and electrons from an accelerator are therefore similar. The probability for interaction of the fast electrons is

proportional to number of electrons in the matter penetrated. It depends also slowly (logarithmically) on the binding energy of the electrons. However, while some interactions result in individual excitations and ionizations other interactions may result in localized large energy depositions, such as the Auger effect in phosphorus atom (P-atom is often close to the DNA). In this process a K-shell electron is ejected followed simultaneously by ejection of several electrons from the outer shells. This multi-ionization process will jolt the surrounding DNA structure; and the Auger effect is likely to result in double strand breaks. It has a G-value of approximately the same magnitude as that observed for double-strand break in the DNA. The fraction f(x) of cells subject to a specific interaction, x, with the DNA is nearly proportional to the molecular weight, M, of the DNA and proportional to radiation intensity, which in turn is proportional to the dose D. We often have then that [Br77]

$$f(x) = 1 - \exp(-10^{-10} \cdot G \cdot M \cdot D)$$

For small values of the dose D, the health effect f(x) is then given by

$$f(x) = 10^{-10} \cdot G \cdot M \cdot D = a_n \cdot D$$

Equation (2a) has the same form as equation (1). G is the number of molecular changes of the type x per 100 eV. The factor 10^{-10} (actually, $1.036 \cdot 10^{-10}$ = units of 100 eV per Gy divided by Avogadro's number) adjusts for the units used. If x is ionization, the theory and experiments show that the G-value is about 3; and for "naked" DNA in a human body the weight M of the molecule is about 10^{12} daltons. If the dose is 3 mGy, the value of f(x) for x an ionization event is $f(x) \approx 1 - \exp(-10^{-10} \cdot 3 \cdot 10^{12} \cdot 0.003) = 1 - \exp(-0.9) = 0.6$; that is, 60 % of the "naked" DNA molecules in humans have been ionized at least once when receiving a dose of 3 mGy. Some DNA molecules have been ionized more than once. The average number of ionization per year per DNA molecule is 0.9. Experiments have shown that the G-value for a single-strand break in the DNA is about 0.27. If x is a single strand break, we get then that $f(x) \approx 1 - \exp(-0.0816) = 0.078$; that is, the background dose of 3 mGy/y produces single-strand breaks in about 7.8 % of the human DNA molecules per year. The G-value for a double-strand break is about 0.026, and a 3 mGy background dose produces therefore each year a double-strand break in about 0.8 % of the DNA molecules.

There are about 10^{14} cells in our body. For a dose of 3 mGy per year, we get then that 0.8% of the 10^{14} or $8 \cdot 10^{11}$ cells per year, or about 10^8 cells per hour suffer a double-strand break. Single strand breaks are about 10 times as many, or about 10^9 cells per hour. Chemical reaction and thermal fluctuation cause many more strand breaks and other DNA errors. **Clearly, the human body must have very effective mechanisms to cope with, repair, or eliminate all those many damages or damaged cells. Any theory that does not take into account the tremendous importance of healthy repair mechanism and the variations in the repair is bound to be deficient.**

It is seen that for small doses, the single target model stipulated by equation (2) is linear in dose and without any threshold. This simple model, which dates back to 1947 analysis by Lea, [Le47] is often used for describing biological effects. The BEIR committees (see for example BEIR VI report) have been guided by similar equations. Equation (2), is usually supported by molecular experimental evidence in simple organisms, such as viruses and often also by simple bacterial models.

However, as Brynjolfsson [Br77] has shown, the experimental results for slightly more complex organisms often require a more complicated theoretical model valid for two or more targets in DNA of an organism. This multitarget model takes into account not only possible repair but also the structure and function of the DNA, which may often contain more than one copy of a gene, and which may have effective repair mechanism for the different damages. We often get a better experimental fit to the data when

$$f_j(x) = \left[1 - \exp(-10^{-10} \cdot G_j \cdot M_j \cdot D)\right]^r ,$$

where the exponent r stands for the multiplicity of significant targets of similar type in the cell. The same mathematical equation applies also if two or more cells need to be damaged to create a definite effect. Equation (3) is often named a multitarget model.

We often have also cases (see [Br77]) where several targets (genes) in the DNA must be changed to observe a significant effect. The best fit to the experimental data is then

$$f(x) = 1 - \prod_{j=1}^{s} \left(1 - \left[1 - \exp(-10^{-10} \cdot G_j \cdot M_j \cdot D)\right]^r\right),$$

where the signs $\Pi(F_j(x))$ means multiplication of function $F_j(x)$. The underlying theory and experimental evidence is similar to that used by BEIR committee for simple targets. The forms of equation (1), (2) and (3) are special cases of equation (4). Equations (3) and (4) both have a threshold when plotted against the dose D. These threshold-forms are common especially for larger and more complex cells and bacteria. The linear no threshold model of equations (1) and (2a), usually selected by the BEIR committees, are an exception rather than a rule for complex organisms such as a group of human cells. This applies not only for the death of a group of cells but also for many other specific indicators of a damaged cell, such as a loss of its ability to produce a specific enzyme.

Frequently, the organisms under investigation are not homogeneous. They usually have different sensitivity to damage. Also the threshold may be different for each type of damage, for example, for each type of cancer.

2.2. Dose-rate effects

Three different dose-rate effects affect the outcome. *First* the excitation and ionization densities around the tracks of the charged particles (such as electrons, protons, and α-particles) depend on their charge and velocity. This excitation and ionization density affects the chemical reactions in the track. We usually account for this effect by using the quality factor, Q. The *second* kind of dose rate effect occurs when the intensity of the radiation and the particles is so high that the excited states along the track of one particle have not reacted with its surrounding media before another particle track overlaps the first. The high dose-rates lead to increase of secondary order reactions, which often lead to a reduction but sometimes to an increase of a particular effect. With present radiation sources, this secondary order reaction is usually not a factor when the system is not frozen. The *third* kind of dose-rate effect occurs when the excitations and ionizations of the first track produce changes in the environment before the next excitation or ionization enters. In living systems, the first excitation event may for example activate a repair mechanism in the cell changing the response to the damage done by the second excitation. For example, the first event may activate production of a repair enzyme, or any defense mechanism similar to that when cancerous cells are destroyed or when infected cells are destroyed. This third kind of dose rate effect is usually a factor at very low dose rates of the background radiation. The first event thus may, for example, “vaccinate” the cell against further damage, provided the healthy cells are not overwhelmed. This may even lead to beneficial effects of radiation at very low doses. This third possibility may have the following mathematical form

$$f(x) = A \cdot \left(1 - \prod_{j=1}^{s} \left[1 - \left[1 - \exp(-10^{-10} \cdot G_j \cdot M_j \cdot D)\right]^r\right]\right) - B \cdot \left(\exp(-10^{-10} \cdot G_j \cdot M_j \cdot D)\right),$$

where A > B. All these possibilities expressed in equations (2) to (5) are amply supported by experimental evidence. We must therefore be very careful and never certain when we extrapolate from higher doses to lower doses. In Fig. 2, we illustrate these different possibilities.

2.3. Different consequences of primary radiation damage

Experience shows that ionization damage without a DNA strand break can usually be repaired, for example, by expelling damaged molecule(s). A single strand break in the DNA can usually also be repaired because the information about how to repair it is conserved in the compliment strand. However, a double strand break can usually not be repaired and leads to loss, changes, or deformation of a corresponding protein, enzyme etc., corresponding to the damaged part of the DNA. Bacterial cell, such as Moraxella-Acinetobacters growing on the hair of cattle where they are expose to damaging sunlight can either compensate for the damage by developing extra copies of DNA or multi-DNA structures, or by living in groups or colonies. These bacteria were observed by Maxcy and Rowley to be exceptionally resistant to radiation. [Ma78] Bacterial cells, such as some spore formers, can usually survive and form colonies on the petri dish after several (often about 10 to 20) double strand breaks. The damaged cells often require a rich medium to grow, because they have lost the ability to produce many enzymes important for survival. When returned to nature, they usually will be overgrown by the undamaged cells. Damaged human cells may also be able to survive and divide after one or more double strand breaks. They may also be recognized as foreign cells and be attacked and destroyed by the healthy cells, or by the body defense mechanism.

In addition to background radiation, many chemicals, heat fluctuations, bacteria and viruses, or the toxins they produce, may also damage the cells. At low levels of radiation, the damaged or deformed cells are usually far in between others. The inability of one or a few cells to produce a specific enzyme will not diminish the ability of the remaining cells to produce that specific enzyme; and a production of a defect enzyme may not affect significantly the ability of the rest of the cells to perform normally. Healthy cells and the defense mechanism in the human body may then be able to cope with the damaged cells and even destroy the defect cells. Thus we can understand the tremendous resilience of the human body and other multi-cellular organisms.

Determination of the constant a_n in equation (1) is usually based on a single dose far in excess of 0.3 Gy, or on exposure over extended periods to dose rates that are more than 1000 times larger than the background dose rate. In case of a single dose of 0.3 Gy, the average number of double strand breaks per cell is 0.78. The average number of single strand breaks is about 8 per cell. The density of damage just after exposure is therefore very different from that of the background radiation. Also, when we apply continuous dose rates that are more than 1000 times larger than the background dose rates, the densities of damaged cells will be much greater than that caused by background radiation. For this reason, the hypothetical linear relationship stipulated in equation (1) is questionable, especially, when applied to very low dose rates.

2.4. Threshold for harmful effects and possibility of beneficial effects

Healthy cells may sometimes destroy a defect cell, and the damaged cell may be self-destructive. The cancer would result only when the healthy cells are unable to respond or recognize the damaged cells as foreign cells, or when the healthy cells are overwhelmed. DNA-damaging reactions may also be caused by carcinogenic chemical species, viruses, and by microbial and fungal toxins. The defense and repair mechanisms against damaged cells make it reasonable to assume a threshold for many health effects. Not only may there be a threshold, but

a low level of radiation could possibly be beneficial, as some recent experimental observations indicate. The low dose rates may activate or stimulate the defense mechanisms. A vaccination, a moderate stimulation of defense mechanism, is used to defend against many diseases. Such moderate stimulation of the body is usually found to promote health.

It is possible, therefore, that a small amount of radiation is beneficial by stimulating "repair" mechanism, such as production of repair enzymes. However, as the background radiation causes only a small fraction of the DNA damage that leads to cancers, it is difficult to understand why small radiation exposure should enhance the defense mechanism. We may understand this when we realize that at low dose rates, the specific radiation damage to the DNA or any other cellular component is "spotty"; that is, the specific radiation damage is done to one cell and not to most of the surrounding cells. The damage done by the low dose rate of the background radiation is therefore likely not to overwhelm the defense mechanism, and the healthy cells have therefore relatively good opportunity to find a way to defend against the damage. On the other hand, cancer-producing chemicals, viruses, and toxins often produce damage that is not spotty, and that affects several nearby cells. The defense mechanisms may then be overwhelmed unless the cells have been "vaccinated" against that damage. It is possible that low dose rates act as "vaccinations" by creating so low a level of damage that the cells can learn how to control the damage. This hypothetical explanation is suggested only to show that we should not reject untested the hypothesis that small doses may have a beneficial effect, as some resent data suggest.

2.5. Effects on germ cells and genetic damage

The repair and defense mechanism is likely to depend on the degree of cell differentiation and development. We should therefore be careful not to extrapolate from effects on grown-up people to possible effects on the unborn.

Some mammalian cells turn over continuously (e.g., white- and red-cell series, gastrointestinal-tract cells, and basal–layer cells of the skin). Others are replaced due to hormonal stimulation, irritation, or injury. In germ cells, the DNA is usually not active before the gamete cell unites with the opposite gamete. If the DNA in one of the gametes is defect, that gamete may not function normally in its search for and reaction with the opposite gamete. A defect gamete is then less likely to produce a zygote. However, it is well established that genetic damage can be transferred from the gamete to the zygote. It is also likely that the probability to transfer a defect DNA to the zygote is proportional to the number of defect DNA gametes. In this case the zygote survival is likely to be independent of the way the damage was made. Therefore, the linear no-threshold model is likely to apply.

Still, there is a small probability that radiation immunization of the body against DNA damage can take place also in this case, and that a small increase in radiation background can promote reduction in viable DNA-damaged zygote. Again this is a hypothetical possibility and it requires experimental testing. These examples again underscore the danger of generalizing from one system to another. The experimental data are too insensitive for detecting any change in genetic defects as a consequence of low dose exposures (<100 mSv).

2.6. What should the guidelines be?

The differentiation of the cells means that we must be cautious in extrapolating or generalizing observed effects. At the present stage of inadequate understanding of the cancers, genetic effects, and many other health effects, we must be guided by direct experimental evidence to the largest extent possible. However, interference of many other factors makes it difficult or impossible to observe, or establish with certainty the effect of low-dose radiation. In

the past, we have therefore been forced to extrapolate from effects at high doses to effects at low doses. As Fig. 2 illustrates, such an extrapolation leads to uncertainties. The relatively good records over the past many years of effects of low radiation levels are starting to reveal, however, some possible beneficial effects of radiation doses below about 50 mGy/year.

Epidemiological studies of the relation between cancers and radiation background in USA by Hickey et al. [Hi81] lead to the unexpected finding that cancer rate decreased with increase radiation background. See also a letter to the editor [Ha87]. Recently, also Cohen [Co95], [Co98a] has come to similar conclusion. See also letters to the editor by Lubin [Lu98], by Smith et al. [Sm98], and response by Cohen [Co98b] and [Co98c]. Jagger [Ja98] has found that although the natural radiation background in the Rocky Mountain states is 3.2 times that in Gulf Coast states, the age-adjusted overall cancer death rate is about 1.26 times higher in the Gulf Coast states than in the Rocky Mountain states. In these studies, the higher doses are also correlated with higher altitude. It has been suggested that the lower oxygen concentration at higher altitude could produce some minor physiological changes, which could affect the observed effects. This explanation is favored in the BEIR V report [BEIR V 90]. But, there is no proof that the oxygen concentration is significantly lower in people that live at high altitude. The human body has great ability to adjust to altitude by increasing and decreasing the hemoglobin. Many other factors correlate with higher altitude, such as air quality, temperature, food habits, exercise and sedentary habits, and individual lifestyles. The studies show that it is not reasonable to invoke radiation as the important factor. Above it was shown that natural background might contribute at most about 5% of all cancers. An increase by factor 3 in the background would increase this to at most 15 %, which is difficult to detect due to the many contributing factors.

It is usually surmised that the exposure of uranium miners to radon establishes a firm basis for increase in cancer. However, the subjects of these studies are exposed to many factors correlated with the radon exposure, such as dust and air quality in the mines.

Little and Muirhead have considered the data from the Japanese atomic bomb survivors. [Li96] [Li98] They can't reject the hypothesis that there may be a threshold below about 200 mSv, but they found no proof for it. In the studies of atomic bomb survivors, the low doses are correlated with distance from the city center. This factor could possibly be correlated with life style and reduced air pollution.

Studies in India indicated a beneficial effect of low level radiation. Total mortality rate, cancer rate and cancer deaths decreased as the external background increased from about 0.1 to 0.75 mSv/year. [Na87b].

Many observations of beneficial health effects of very low levels of radiation are free from any "altitude effect" or low oxygen concentration, such as those of nuclear industry workers receiving low levels of exposure. Luckey, Sandquist, and Cuttler have presented a thorough review of the many beneficial effects of low level radiation. [Lu99] [Sa99] [Cu99]

While many studies indicate a beneficial effect of very low level radiation, or at least a threshold for harmful effect, the BEIR Committee continues to assume that "linear no threshold" model is most reasonable. We should also consider that we might have a combination of detrimental and beneficial effects. It can then be difficult to evaluate the net result.

The purpose of this paper is in no way to interject into the debate about beneficial or harmful effects, but merely to report on the limit and the best quantification of induced activity in food exposed to ionizing radiation; that is, how this activity increases as we increase the energy and the dose. For estimating the limit for induced activity, we will assume the worst case, which is represented by the linear no-threshold model in the BEIR III report. This does not indicate author's preference, but is used for the purpose of having a point of reference. We will then require that the induced activity produced in the food is so low that reasonable people would consider the effect of increased radiation insignificant. This limit has usually been based

on limits of measurements and is set at about 1% of the average natural activity in the food. The relation between radioactivity (in becquerel) in the food and the dose (in mSv) this radioactivity produces in the individual eating the food is not simple. We will therefore define it more precisely and set the integrated exposure from eating irradiated food at 0.003 $mSv \cdot y^{-1}$, because the internal background radiation due to food is about 0.3 $mSv \cdot y^{-1}$. According to the linear no-threshold model and the cancer rate estimates in the BEIR III report [BEIR III 80], this dose of 0.003 $mSv \cdot y^{-1}$ corresponds to about 0.18 cancers per year per million people consuming the irradiated food.

We will show that if each person consumes 40 kg of food irradiated with 10 MeV electrons to a dose of 60 kGy, this consumption will results in additional radiation exposure less than $3 \cdot 10^{-8}$ mSv. These $3 \cdot 10^{-8}$ mSv would according to the BEIR III report result in less than $60 \cdot 3 \cdot 10^{-8} = 1.8 \cdot 10^{-6}$ cancers in million people consuming the food. Similarly, if each person consumes 40 kg of food irradiated with 5 MeV X rays to a dose of 10 kGy, the consumption will results in additional radiation exposure less than $1.5 \cdot 10^{-5}$ mSv. These $1.5 \cdot 10^{-5}$ mSv would according to the BEIR III report result in less than $60 \cdot 1.5 \cdot 10^{-5} = 9 \cdot 10^{-4}$ cancers in million people consuming the food.

This may be compared to the extra dose of about $1.2 \cdot 10^{-2}$ mSv a person receives during the 6 hour flight at about 12,000 m when that person takes an airplane from Boston to San Francisco. Using the same assumption about the health effect, we get that the flight might result in $60 \cdot 1.2 \cdot 10^{-2} = 0.72$ cancers per million people taking such flights.

3. ELEMENTAL COMPOSITION OF FOOD

For the analysis of natural and induced radioactivity in food, it is necessary to consider the elemental composition of food. The natural radioactivity from the ^{40}K isotope, which is a constant fraction (0.0117 %) of the potassium content in the food, varies significantly with potassium concentration from food to food. Usually, the concentration of potassium is in the range of 1000 to 6000 ppm (parts per million; that is, milligram of potassium per kilogram of food). In Table 3, the concentration of potassium in a reference food is 4000 ppm. The average concentration in the human body is about 2000 ppm. Of the daily intake about 90 % is excreted in the urine and 10 % in the stool. The concentrations of many other trace elements also show great variations. As Table 4 shows, the concentration of sodium may vary from 150 to 8200 ppm, that of magnesium from 110 to 390, and that of phosphorus from 150 to 2110 ppm. The concentrations in reference food, which are shown in Table 3, are those used by professor Robert L. Becker [Be79] and many others. These concentrations are similar to those of meat, which is likely to be the food that receives the highest doses. We have to Becker's table added three elements: rubidium, iodine and gold. Table 4 gives examples of concentrations of major trace elements in actual food samples. Table 5 shows for comparison the elemental distribution in the total body of a man weighing 70 kg as assumed by the Committee Two of ICRP.

The concentrations of elements in actual food are often different from those in the human body. The main reason is that the elements of the bones contribute to the average in the human body but not to the average of food. For obtaining the activity in the actual food, the estimated activities in the reference food must be multiplied by the ratio of the actual concentration over the corresponding concentration in the reference food. Sometimes additives in the food will alter the concentration of elements significantly. For example, the actual concentration of sodium in bacon may be as high as 8,250 ppm, the estimated activities of ^{22}Na and ^{24}Na must then be multiplied by 8,250/750 =11 to obtain the actual activities. Peaches containing only 150 ppm of sodium would have 1/5 of the sodium activity in the reference food. Similarly, the iodine activity in mixed vegetable with 0.05 ppm of iodine would have 1/10 of the iodine activity in the reference food, while raw oysters with 1 ppm of iodine would have twice the iodine activity in the reference food. The concentrations used in the reference food are reasonably close to those of meats (without additives), because meats are likely to receive the highest doses.

4. ISOMERIC RADIOACTIVITY

Photons can interact with the nuclei of atoms. This process is analogous to reaction of photons with electrons in atoms. The interactions can result in excitation of nuclear states, which is analogous to excitation of atomic states. The photon's interaction can result also in an ejection of a particle, such as a neutron, a proton (H^+ ion), or an α-particle (He^{++} ion), corresponding to photon's ionization of an atom. For these reactions to be possible, the incident photon energy must transfer to the nucleus an energy quantum that is equal to or greater than the excitation energy of the nuclear state, or the binding energy of the particle emitted from the nucleus. In case of gamma rays from cobalt-60 or cesium-137, the photon energies are lower than the binding energy of the particles in any of the stable nuclei. Consequently, only one pathway is possible, namely excitation of the nuclear states.

Most of the excited nuclear states of stable nuclei decay within less than one millionth of a second to a stable state. Of the few exceptions to this rule, we will consider the 25 isotopes that have a lifetime of a nuclear isomeric state longer than about 1 minute. Any of the other short lived metastable isotopes (isomers) would have decayed to a stable isotope before exiting the facility, as it usually takes more than 10 minutes to bring the food out of the radiation facility.

In nuclear physics, long lived excited states or metastable excited states are called *isomeric states*, and the corresponding isotopes are called isomers. The formation of these isomers is called *isomeric activation*, and their decay is called *isomeric radioactivity*. All (25) isomers of natural isotopes with more than a minute half-life are listed in Table 6.

4.1. Induced isomeric radioactivity

The isotopes that can form long lived isotopes are shown in column 3 of Table 6. They are found only in trace amount or as contaminants in foods. Metastable states have a relatively long lifetime, because the corresponding transition to the lower state, usually the ground state, is forbidden. In nuclear physics, like in atomic physics, "forbidden" means that the transition is unlikely, because the angular momentum change in the transition is not equal to one as is usually the case, but greater than one. In these isotopes, the angular momentum change in the transition from the isomeric states is on the order of 5 (see column 6 of Table 6), and thus very large. When the lifetime is long, the width of the level is very narrow, and the range of frequencies that can excite the ground state to the excited metastable state is extremely narrow; that is, only photons in an extremely narrow energy interval can excite the isotope to an isomeric state, due to the uncertainty relation $\Delta t \cdot \Delta \nu \approx 1/(2 \cdot \pi)$ (or $\Delta t \cdot \Delta E \approx h/(2 \cdot \pi)$, where h is Planck constant). Therefore, the excitation of the metastable state from the ground state is very unlikely, as extremely few incident photons would be in the narrow energy interval, $\Delta E = h \cdot \Delta \nu$. Formation of the isomeric state becomes more likely if the ground state of the isotope is first excited to broad level of higher excitation state, which then in some cases decays to the lower isomeric state. The widths of the higher level states and their densities increase close to the threshold energy for emission of a particle, such as a neutron. Consequently, the activation of the metastable state (formation of the isomer) increases as the energy of the incident photon approaches or exceeds the threshold for emission of a particle.

This trend is seen in Fig. 5, which shows for strontium, cadmium, indium, and barium how the dose from consumption of irradiated food increases with photon energy. The experimental points are derived from Glass and Smith's [Gl60b] measurements. The fine structure that would show stepwise increases at the energies of the excited states cannot be discerned, because the experimental points are too far apart.

As the isomeric radioactivity induced in the food is too small to be detectable even with the best of equipment, Glass and Smith measured the activity by irradiating the pure form of the elements strontium, cadmium, indium, and barium by a dose of 50 kGy. Rough estimates of the activity in the food are then obtained by multiplying the activity induced in the pure element by concentration of the element in the food relative to that of the pure element. The values in Fig. 5 are obtained by assuming that the concentrations of the elements in food are: 0.2, 0.1, 0.01, and 0.02 parts per million (ppm) for strontium, cadmium, indium, and barium, respectively. The ordinate gives the radioactivity in the unit mSv per year from consumption of 50 kg of food irradiated to a dose of 60 kGy. The abscissa gives the energy of the gamma rays and X rays in the unit of "million electron volts" (MeV). The experimental points are for gamma rays from ^{60}Co (E_γ =1.17 and 1.33 MeV), and used fuel elements (about 2 MeV); and for X rays from 4, 8, 16, and 24 MeV electron accelerators.

Recent measurements by Lakosi et al. [La93] of the photo-excitation in ^{115}In, and ^{103}Rh show similar trend. These authors give the cross-sections rather than the activities. They also list the cross-sections obtained by several other authors. We have calculated the activities to be expected based on the cross-sections shown in Fig. 3 of the paper by Lakosi et al., and found them to be comparable to the activities measured by Glass and Smith [Gl60b]. The recent measurements (88.2, 86.4, 1361 Bq/kg of element per kGy in 61 minute irradiation of ^{87m}Sr, ^{113m}In, and ^{115m}In, respectively) by Hashizume and Nakano [Ha92], although slightly higher, are consistent with Glass and Smith's data [Gl60b]. The activity produced depends on the photon intensity in the degradation spectrum, which was not reported by any of the authors. Due to this lack of pertinent information, the data should be considered only indicative of the actual activity. However, because the activity is very low, the accuracy of the data is adequate for the present purpose.

Isomeric activity is sometimes produced when the excitation energy exceeds the threshold for photoneutron production. The approach for estimating the isomeric activity produced in this way by 7.5 and 10 MeV X rays is discussed in Section 5 about photoneutron activity induced by X rays. The corresponding activity estimates include the isomeric activity, and are shown in columns 9 and 10 of Table 8.

Similarly, isomeric activity may also be produced in electron irradiation when the electron energy exceeds the threshold for photoneutron production. The approach for estimating the isomeric activity produced by 10 MeV electrons is discussed in Section 6 about photoneutron activity induced by 10 MeV electrons. The corresponding isomeric activity estimates are included in the activity estimates shown in column 9 of Table 9.

5. PHOTONEUTRON ACTIVITY INDUCED BY X RAYS

A particle can be ejected from the nucleus if its binding energy is less than the absorbed photon energy. The remaining nucleus may be radioactive. We often use the short hand notation γ for a photon with energy $E_\gamma = h \cdot \nu$. The major reactions that can lead to photon-induced activities are:

(1) *The photoneutron reaction* or (γ, n) reaction; that is, absorption of a photon, γ, and expulsion of a neutron, n.

(2) The *photo-proton reaction* or (γ, p) reaction; that is, absorption of a photon and expulsion of a proton, $^1H^+$.

(3) The *photo-deuterium reaction* or (ν, D) reaction; that is absorption of a photon and expulsion of a nucleus of deuterium, $^2H^+$.

(4) The *photo-tritium reaction* or (γ, t) reaction; that is absorption of a photon and expulsion of a nucleus of tritium, $^3H^+$.

(5) The *photo-alpha reaction* or (γ, α) reaction; that is absorption of a photon and expulsion of an alpha particle, the nucleus of helium, $^4He^{++}$.

Each of these reactions may be considered a two-step process. The first step consists of absorption of a photon with energy $h\nu$ in the atomic nucleus and formation of an excited nucleus or excited compound nucleus. This first step is followed by the second step, which consists usually of ejection of particle such as a neutron, a proton, an electron, a tritium, or an alpha particle, and sometimes with emission of photon(s). Frequently, the two steps cannot be distinguished as separate. The remaining nucleus often retains some of the excess energy in an excited state, that is, in an isomeric state. If excited in an isomeric state, the nucleus will subsequently decay to a stable nucleus, or transform to a different unstable isotope. Usually, the lifetime of the excited nucleus is very short, and it will decay before it exits the radiation facility.

For incident photon energies of 10 MeV and below, the photoneutron reactions are most probable, while the emission of other particles become important at higher energies as shown in Section 7. There it will be shown that for equal thresholds the coulomb barrier reduces greatly the probability for emission of charged particles. As long as we limit the incident energy to about 10 MeV, the charged particles emissions can be disregarded. The emphasis in the following will be therefore on the photoneutron reactions.

5.1. Theoretical estimates of photoneutron activation

The problem of calculating the photoneutron activities produced by X rays or γ rays is solved in several steps.

(1) Calculating the number, N, of photoneutrons as a function of the incident photon energy $h\nu$ produced per joule of radiation energy absorbed, using the following Eq. (6). For these calculations, we need to know:

   (a) The photon intensity spectrum $I(h\nu, E_0)$ as a function of the incident electron energy E_0. The X ray intensity spectrum is given by Eq. (7) of Section 5.2.

   (b) The cross-section $\sigma(\gamma, n)$ for production of neutrons depends on the photon energy $E_\gamma = h \cdot \nu$ above the threshold energy E_{th}. The cross-section varies from isotope to isotope and with energy above the threshold. The important cross-sections were

obtained from measurements reported in the literature; the less important cross-sections were obtained by an interpolation method.

(c) The coefficient, $\mu_e(E_\gamma)$, for energy absorption of photons penetrating the food is about the same as that for water. This coefficient is shown for water in Fig. 24.

(2) The photoneutron activities, $A(\gamma, n)$, are calculated from the number of isotope atoms $N_A(n)$ that are initially formed per gram and per kGy. We have that $N_A(\gamma, n) \le N(h\nu, n)$ = number of neutrons that are emitted as estimated by Eq. (6) below. We may set $N_A(n) = f_A \cdot N(\gamma, n)$, where $f_A \le 1$ is the branching ratio; that is, the fraction of compound nuclei that result in the specific isotope or isomer A. The branching ratio, $f_A = f_A(\gamma)$ depends on the photon energy $E_\gamma = h \cdot \nu$. This dependence is usually not known well. Therefore, we usually list the activity as $A(\gamma, n) < A_{max}(h\nu, n)$, where $A_{max}(h\nu, n)$ is the activity that would be obtained if $f_A = 1$. The value of $A_{max}(\gamma, n)$ is obtained by dividing the number of atoms, $N(\gamma, n)$, by the radioactive lifetime $\tau = t_{1/2}/\ln 2$, where $t_{1/2}$ is the radioactive half-life of the isotope.

The results of the calculations are shown for 10 and 7.5 MeV X rays in columns 9 and 10 of Table 8, and for 10 MeV electrons in column 9 of Table 9. The threshold energies for (γ, n) and (γ, p), reactions in all stable isotopes are listed in Table 7, and shown in Fig. 6 and Fig. 7. The threshold energy for each of the major isotopes in food exceeds 10 MeV. For example, it is: 18.72 MeV for ^{12}C, 10.55 MeV for ^{14}N, and 15.67 MeV for ^{16}O. Some of the minor isotopes, such as deuterium ^{2}H, ^{13}C, ^{17}O, and ^{18}O, have lower threshold energies, but the isotopes, ^{1}H, ^{12}C, ^{16}O, and ^{17}O, formed in these reactions are stable. Many of the trace elements and contaminants in food have threshold energies slightly below 10 MeV and require therefore elaborate estimates.

The neutrons ejected in these (γ, n) reactions can be captured by some of the isotopes in food thereby producing new nuclei, which may be radioactive. The corresponding neutron capture activity is of major concern and will be discussed in Section 8.

We calculate the neutron production per unit dose for each isotope using the following equation:

$$N(\gamma,n) = \frac{10^{-27} \cdot N_{Is}}{1.602 \cdot 10^{-13}} \cdot \frac{\int \sigma \cdot \{[I(E_0, E_\gamma)]/E_\gamma\} \cdot dE_\gamma}{\int \mu_e \cdot \{[I(E_0, E_\gamma)]\} \cdot dE_\gamma}$$

$$= 6.24 \cdot 10^{-15} \cdot N_{Is} \cdot \frac{\int \sigma \cdot \{[I(E_0, E_\gamma)]/E_\gamma\} \cdot dE_\gamma}{\int \mu_e \cdot \{[I(E_0, E_\gamma)]\} \cdot dE_\gamma},$$

where $N(\gamma, n) = N(h\nu, n)$ is the number of neutrons formed per joule (J) of photon energy absorbed in the food. As one joule absorbed per gram of food is equal to a dose of one kilogray (kGy), we can say that $N(\gamma, n)$ is the number neutrons produced per gram of food for each kGy of radiation energy absorbed. N_{Is} is the number of a specific isotope atoms per gram of food; σ is the cross-section in millibarn (1 mb = 10^{-27} cm^2) for the neutron production per the specific isotope atom; 1 MeV = $1.6022 \cdot 10^{-13}$ joule; $I(E_0, E_\gamma)$ is the photon intensity spectrum in MeV per MeV for incident electrons of energy E_0 striking the X ray target; that is, the number of photons in each infinitesimal energy interval, dE_γ, times the photon energy, $E_\gamma = h\nu$, in MeV in the interval; therefore, $I(E_0, E_\gamma)/E_\gamma$ is the number of photons in each energy interval. In the denominator, we have (assuming photon-electron equilibrium) that the dose is equal to absorbed photon energy, and that μ_e is the photon's energy absorption coefficient in cm^2/g in food. (In actual operations some of the electrons knocked out may carry their energy away and deposit it

at a location different from the location of photon absorption. In photon electron equilibrium, we have that an equal number of electrons are scattered into the location of photon absorption as are scattered out.) Food irradiation usually requires relatively uniform dose. This in turn usually requires photon-electron equilibrium, which can be obtained by placing a small thickness of low Z material in front of a food sample irradiated with x rays. When the water-cooling chamber of the X ray target is made of aluminum, the photon-electron equilibrium in the food is usually adequate.

5.2. Intensity spectrum $I(E_0, E)$ of X rays

The form of the photon intensity spectrum, $I(E_0, E)$, varies only slightly with the X ray target and with the material being irradiated. E_0 is the initial energy of the incident electron, while $E = h \cdot \nu$ is the energy of the emitted X ray photon. In the present analyses, we have simplified the spectral form used by Hunt et al. [Hu63], by using one form for all elements. The actual form of the intensity varies slightly with the atomic number of the X ray target, because of the shielding of the atomic electrons. We have checked the estimates by comparing the dose in air with that found by Okulov [Ok68]. The X ray intensity at large angles is slightly softer (lower energy) than that emitted at zero angle, because the intensity at large angles is formed mainly by electrons that have been multiply scattered by the nuclei in the target and that have lost energy in collision with atomic electrons.

In the present analysis, the focus is safety, and we will then usually consider the "worst case" scenario (that which results in the highest activity). We have, therefore, assumed overall a form of the spectrum that is similar to that in the forward direction. We have also assumed a significant absorption of the low-energy photons in the X ray target. In thin food samples, or at the surface of a thick food sample, the calculated dose and activity per dose unit is about right, but slightly deeper in a thick food sample, the low energy spectrum builds up. The calculated dose in the food is then slightly lower than the actual dose, and the calculated activity per dose unit, therefore, slightly higher than the actual activity per dose unit. At these relatively large depths in the thick food sample, the calculated activity per dose unit is too high by about 6.7% at 10 MeV, and 12.8 % at 5 MeV. In thin food sample and close to the surface of a thick food sample, the dose and activity (assuming photon-electron equilibrium) is close to the actual dose and activity.

The X ray spectrum, $I(E_0, E_\gamma)$, that we use in Eq. (6) is given by

$$I\left(E_\gamma, E_0\right) = \left(1 - E_\gamma / E_0\right)^{\frac{1}{1+0.1 \cdot E_0}} \cdot \exp\left(\frac{0.067}{0.2 + E_\gamma / E_0}\right) \cdot \exp\left(0.07 \cdot \left[1 + 0.22 \cdot E_\gamma^{-3}\right]\right)$$

The X ray spectrum given by Eq. (7) is illustrated in Fig. (8) for the incident electron energy E_0 equal to: 4, 6, 8, and 10 MeV. It is similar to that used by Leboutet and Aucouturier [Le85], except that we have assumed slightly stronger absorption for the low-energy photons, as given by the last factor in Eq. (7). The slightly harder spectrum of Eq. (7) is proper when dealing with X rays from targets made from materials of high atomic numbers, tantalum, tungsten and gold, and irradiation of relatively thin food samples, because on some occasions, the facility will be used to irradiate thin food samples. For thicker samples it gives a slight overestimate of the activity produced per kGy in the food.

For correcting the dose integral for the effect of photon energy degradation with depth, it is usual for each energy interval of the photons with energy E to replace the dose integral: $\int \mu_e \cdot I(E_0, E) \cdot dE$, in the denominator of Eq. (6) by

$$\int \mu_e \cdot B_d\left(E_\gamma, x\right) \cdot I\left(E_0, E_\gamma\right) \cdot \exp\left(-\mu_t \cdot x\right) \cdot dE_\gamma \cdot$$

In an analogous manner, we may replace the cross-section integral: $\int \sigma \cdot \{[I(E_0, E_\gamma)]/E_\gamma\} \cdot dE$, in Eq. (6) by

$$\int \sigma \cdot B_c(E_\gamma, x) \cdot \{[I(E_0, E_\gamma)]/E_\gamma\} \cdot \exp(-\mu_t \cdot x) \cdot dE_\gamma.$$

For many of our applications, the threshold energy for activation is close to the incident energy E_0 of the electrons. The buildup factor, B_c, in Eq. (9) is then close to 1. On the other hand, the dose buildup factor, B_d, in Eq. (8) will increase significantly with depth. We might then be inclined to conclude, erroneously (as many have done), that therefore the dose buildup factor for the entire spectrum must increase approximately corresponding to some average of B_d (E). However, this is not the case. The reason is that the initial X ray spectrum has many low energy photons, which are removed at about the same rate, as they are built up by scattered higher energy photons. The dose buildup factor for the entire dose integral could then be about equal to 1. The exact calculations of the variation of the spectral form with depth are elaborate. In the present case, this complication of the estimate is hardly justified as the experimental conditions vary greatly, and as the variation of Eq. (6) with depth is small. The safety aspect demands that we be on the side of safety. By removing from the X ray spectrum the low energy component corresponding to the cut-off by the K-shell in the X ray target, we have reduced the dose estimate. We have therefore increased by a small amount the estimate of radioactivity per dose unit. In the first few (1 to 10) centimeters in the food, the soft component (photons between the K-shell cut-off in food and the K-shell cut-off in X ray target) will buildup and increase the dose. Our estimate could result, therefore, in an overestimate of the activity per dose unit by nearly 20 %.

In case the electrons strike a target of light materials, for example the food itself, the X ray spectrum is not cut-off by the absorption in the K-shells of the conventionally used X ray targets, which consist of materials with high atomic numbers. Instead, the spectrum is cut-off by the K-shells in food (oxygen, nitrogen and carbon). The X ray dose in food includes, therefore, the part of the spectrum that is between the K-shells of the target and the K-shells of the atoms of food. The actual radioactivity per X ray dose unit in food irradiated directly with electrons is then about 13% at 5 MeV and 6 % at 10 MeV lower than the radioactivity per X ray dose unit in food irradiated with same intensity of X rays from a tungsten target. Again, our method of calculations results usually in slight overestimate of the produced activity.

5.3. Cross-sections for the production of photoneutrons

Just above the threshold in most isotopes, the small cross-section increases first rather steeply to a low value, then it stays nearly constant corresponding to the magnetic dipole interaction; subsequently, it increases slowly and then more steeply to form the giant electrical dipole resonance curve with a maximum at about 6 to 8 MeV above the threshold. The cross-section for deuterium is different and special because of the small number of nucleons in the nuclei. The cross-section in deuterium is well known and shown in Fig. 9. It increases steeply with the photon energy from the threshold at 2.225 MeV to a maximum at the resonance at about 4.5 MeV. Above about 6 MeV, it decreases nearly exponentially with energy. We have used the analyses of Brynjolfsson [Br75] for these important cross-sections. His analysis was modified slightly to accept the absolute cross-sections between 6 and 10 MeV as determined by Birenbaum et al. [Bi85]. For other isotopes, the cross-sections are not as well known. We have used mainly the compilation of Berman [Be76] and by Dietrich and Berman [Di88] but also by Keller et al. [Ke73]. In important cases, the data were supplemented with the original observations. For the important cross-sections in ^{13}C, we used

the measurements by Jury et al. [Ju79]. For the cross-sections in ^{17}O, we used the measurements by Jury et al. [Ju80]. For the cross-sections in ^{18}O, we used the measurements by Woodworth et al. [Wo79]. Just above the threshold, the cross-section increases with atomic weight often unevenly from zero to about 0.3 to 15 millibarn per MeV. The unevenness just above the threshold, especially in the lighter atoms, is caused partially by excited states (small resonances) just above the threshold. Near the threshold, the cross-sections may often be assumed to increase proportionally with the energy difference, $(E - E_{th})$, above the threshold E_{th}. When we multiply the cross-sections with the X ray intensities below E and integrate from the E_{th} to E, we find that the neutron production is roughly proportional to the third power of the energy difference.

The activity just above the threshold is thus nearly proportional to $a \cdot (E - E_{th})^3$, where the proportionality factor, a, increases nearly proportionally with the atomic weight (or the number of nucleons in the nuclei). For the major elements of food and for important trace elements in this study, such as iodine, we have used the measured cross-sections just above the threshold. [Ra89b] These measured cross-sections just above the threshold can be assumed to have standard deviations of about 10 to 30 %. Well above the threshold, the cross-sections are usually better known. We have then assumed that the cross-sections increase linearly from zero at the threshold to the measured cross-section at the slightly higher energy. The lightest elements and isotopes with the greatest activity are treated using measured values.

Since the cross-sections just above the threshold are very small and often not well known, we have for elements producing small activities in the food used approximations by interpolating and extrapolating the better known cross-sections in silver, indium, tin, iodine and gold. For some of the lighter isotopes, these equations may overestimate the activity by as much as a factor of 2 to 10. These overestimates pertain only small activities and do not compromise the health and safety aspects.

5.4. Photoneutron activity produced by X ray irradiation

Using the X ray intensity spectrum given by Eq. (7) and the cross-sections $\sigma(E)$ for neutron production, we can calculate the neutron production for each isotope using Eq. (6). If each atom of that isotope that emits a neutron becomes a radioactive nucleus with lifetime $\tau = T_{1/2} / \ln 2$, we get that the radioactivity of that isotope is

$$A_{xrays} = 10^3 \cdot \frac{N_n}{\tau} = 10^3 \cdot \frac{N_n \cdot \ln 2}{T_{1/2}} \quad \text{Bq/(kg} \cdot \text{kGy)},$$

The unit of activity is in Bq per kg of food and per kGy of X ray dose. N_n is calculated using Eq. (6). The factor 1000 in Eq. (10) converts from activity per g of food to activity per kg of food.

Sometimes, only a fraction, f_{Is}, of atoms emitting a neutron becomes radioactive. For example, after the ^{138}Ba isotope emits a neutron, the ^{137}Ba isotope that is formed may be in an excited meta-stable state (in an isomeric state and therefore radioactive) or it may be in the ground state. We have more generally that

$$A_{xrays} = 10^3 \cdot \frac{N_n \cdot f_{Is}}{\tau} = 10^3 \cdot \frac{N_n \cdot f_{Is} \cdot \ln 2}{T_{1/2}},$$

in units of Bq/kg per kGy of X ray dose.

For the important isotopes in this study, we have used the measured cross-sections just above the threshold. These isotopes are marked with an asterisk in Tables 8 and 9. For the

small activities just above the threshold we will often use for 10 MeV X rays the approximation:

$$A_{xrays} = 10^{-13} \cdot A_{Is} \cdot \frac{N_{Is} \cdot f_{Is} \cdot \ln 2}{T_{1/2}} \cdot (10 - E_{th})^3 .$$

The X ray activity, $A_{x\ rays}$, is in Bq/kg per kGy of x ray dose; and A_{Is} the atomic weight of the isotope, N_{Is} the number of isotope atoms per gram of food; and $\tau = T_{1/2}/\ln 2$ is the lifetime of the isotope in seconds. The value of the branching ratio, f_{Is}, is usually not known; especially, for incident photons just above the threshold. Determination of f_{Is} is complicated by the fact that the branching ratio usually varies with the excitation energy. In some of these experiments, see Lakosi et al. [La93], it appears that the yield of the isomeric isotope stays constant above the threshold, or that the relative yield decreases with increasing energy above the threshold. We have used the maximum value, $f_{Is} = 1$, for estimating the activity. In these cases, we indicate the activity as being less than the indicated activity by the notation $< A_{x\ rays}$, where $A_{X\ rays}$ is the activity obtained by setting $f_{Is} = 1$.

We have also to consider the possibility that a radioactive nucleus produces a new radioactive nucleus as it decays. It is necessary, therefore, to analyze in detail all the nuclei that could be formed. Table 8 shows such analysis. In the last two columns, columns 9 and 10 of Table 8, we list the photoneutron activities produced when the food is irradiated with 10 and 7.5 MeV X rays. As can be seen, these activities are very small at 10 MeV, and usually equal to zero at 7.5 MeV.

For obtaining the corresponding activities in food irradiated with 10 MeV electrons, we can multiply the activities for 10 MeV X rays by 0.00205 as shown in Section 6.4. As we will see later, the limiting activities are determined usually by the neutron capture activities.

6. PHOTONEUTRON ACTIVITY INDUCED BY 10 MeV ELECTRONS

At energies of interest in food irradiation, the X rays generated by the incident electrons as they penetrate the food packages usually induce most of the minute activities. However, Fourier harmonics of the moving electron's electrical field can also interact directly with the nuclei and induce significant radioactivity. This fraction of the total induced activity can be taken into account as a correction to the induced activity produced by the x rays.

6.1. Relations between photon-induced and electron-induced activities

In electron irradiation, most of the photoneutron activity is produced by the X rays generated by the electrons, but at the surface where the electrons enter the food, a significant activity is produced by the virtual photon field of the electrons; that is, by the Fourier harmonics of the electrical field of the fast moving electrons. We will use a relation developed by Blair [Bl49] for the relative contribution of the X rays and the virtual photons, which is:

$$A_{ph} = \left\{Z^2 \cdot r_0^2 \cdot \left(N_0 / A\right) \cdot d \cdot \left(n - 0.5\right) \cdot F\right\} \cdot A_{el} ,$$

where A_{ph} is the measured X ray activity of the nth plate in a stack of plates being irradiated; Z is the atomic number of the isotope; $r_0 = 2.8 \cdot 10^{-13}$ cm is the classical radius of the electron; $N_0 = 6.02 \cdot 10^{23}$ is Avogadro's number; A is the atomic weight; d is the thickness in g/cm^2 of the each plate in the stack; F is a correction factor which, in principle, depends on many parameters, but which in practice is nearly constant and equal to 8.4; and A_{el} is the measured electron-produced activity of the nth plate due to virtual photons. Blair [Bl49] deduced Eq. (13) assuming that: neither the electron beam nor the bremsstrahlung lose energy in traversing the plates, and that the bremsstrahlung is predominantly in forward direction. Although these are unrealistic assumptions, they are helpful in analyzing the problem in the narrow region above the threshold and below 10 MeV.

We will assume that F is nearly constant, which is approximately correct. When the thickness $d \cdot (n–0.5)$ is small, that is close to the entrance surface, the X ray photon intensity is small. Therefore, close to the surface the photon-induced activity is small when compared with the electron-induced activity. If the thickness is relatively large, such that the electrons in fact have lost about all of their energy above the threshold, E_{th}, we can set: $d \cdot (n–0.5) \approx A \cdot (E_0 - E_{th})/(4 \cdot Z)$ g/cm^2, where E_0 is the incident electron energy in MeV. We get then from (13) that the maximum of the photon induced activity for relatively large thickness is given by

$$A_{ph} \approx \left\{Z \cdot r_0^2 \cdot N_0 \cdot F \cdot \cdot \left(E_0 - E_{th}\right)/4\right\} \cdot A_{el} \approx \left\{0.1 \cdot Z \cdot \left(E_0 - E_{th}\right)\right\} \cdot A_{el} ,$$

6.2. Photoneutron activity of trace elements in food

The X ray production is nearly proportional to the atomic number Z. Therefore, the X ray intensity per electron in food is about 7.4/Z times the intensity produced in a pure trace element with atomic number Z, and where 7.4 is the average atomic number in food. The trace element's activity in the food produced by the X ray photons is then also 7.4/Z times that produced in a pure element. The activity induced by the electrons, on the other hand, in this trace element in the food is the same as in the pure element. Therefore, the electron-

induced activity in a trace element close to the surface of the food sample relative to the maximum photon-induced activity is given by

$$A_{el} \approx \frac{A_{ph}}{0.1 \cdot Z \cdot (E_0 - E_{th})} \cdot \frac{Z}{7.4} = \frac{A_{ph}}{7.4 \cdot 0.1 \cdot (E_0 - E_{th})}.$$

One of the assumptions for Eq. (13) to (15) is that the electrons don't lose energy. A_{el} is then constant, and A_{ph} builds up proportionally with the electrons' penetration. Using these assumptions, we see also from (15) that when $(E_0 - E_{th}) \leq 1/0.74 = 1.35$ MeV, the electron-induced photoneutron activity is greater than the X ray induced activity. In fact, however, A_{el}, decreases with penetration as the electron energy decreases, and reaches zero at about $(E_0 - E_{th})/2$ cm. The relevant photon induced activity, A_{ph}, builds up with the electrons' penetration and reaches maximum at about $(E_0 - E_{th})/2$ cm. Beyond this depth, the X ray induced activity is about constant for the total thickness of the sample.

For 10 MeV $\geq E_{th} \geq$ 8.65 MeV the electron-induced activity dominates the X ray induced activity, but only in a very thin layer, less than $(E_0 - E_{th})/2$ cm. The X ray induced activity, on the other hand, will be about constant at depths $\geq (E_0 - E_{th})/2$.

For 8.65 $\geq E_{th}$ MeV, the electron induced activity at the surface will be less than the maximum X ray induced activity for a depth of about $(E_0 - E_{th})/2$ cm. Beyond this depth the activity will be approximately constant in the 3.4 cm thick sample. (The density is assumed equal to 1 g/cm^3).

These predictions are consistent with the measured activities of ^{63}Zn, ^{126}I, and ^{11}C as a function of depth in the sample irradiated with 24 MeV electrons in a report by Glass and Smith [Gl60a], see for example their Figs. 22, 23, and 24. For about 10 MeV incident electrons, the threshold energies of the trace elements are above or only slightly below 10 MeV. The total photoneutron activation per gram is then nearly independent of depth, and nearly equal to the maximum of X ray induced activity. For electron irradiation, we therefore use the X ray induced activities calculated by using the X ray spectrum just under the surface.

6.3. Effects caused by the accelerator window and the packaging

The calculations above assume that the electrons impinge on the food sample without having to penetrate the accelerator window. The window is usually made of aluminum or titanium with atomic numbers 13 and 22, respectively, while the food has an average atomic number of about 7.43. The activities produced in the food are proportional to the X ray intensities, which are nearly proportional to the atomic number. The accelerator window increases, therefore, the activity produced in the food. When penetrating 0.11 g/cm^2 thick aluminum window, the incident electron energy reduces by about 0.21 MeV. Similarly, the electron energy would be reduced 0.075 MeV by penetrating a 0.037 g/cm^2 thick titanium window. The 0.11 g/cm^2 thick aluminum foil produces about the 13/7.4 ≈ 1.8 times as much X rays per gram as the food, and the 0.037 g/cm^2 thick titanium foil about 3 times as much X rays per gram as the food. This affects the activity when the threshold is very close to 10 MeV. For example, the sulfur nuclei ^{36}S with threshold of 9.89 MeV would be activated by the X rays from the window and not directly by the electrons. The photoneutron activity of ^{35}S all through the food would increase, because it is produced by the X rays from the 0.11 g/cm^2 thick aluminum window.

However, when the threshold is very close to 10 MeV, the activity, which is proportional to $(E_0 - E_{th})^3$, is very small and therefore usually insignificant. As the threshold energy decreases, the X rays produced in the food contribute to the activity. For $E_{th} \approx$ 9.14 MeV, such as in iodine, most of the X rays are produced in the food. The effect of the window would be small, but the

activity significant. Also, for the neutron production in deuterium with threshold at 2.2 MeV and maximum cross-section at about 4.5 MeV the effect of the window would be insignificant. For simplifying the evaluation we will usually for reference disregard, therefore, the effect of the window.

The increase in activity due to food packaging is usually insignificant. For example, the aluminum plastic laminated packaging that was used to package the astronaut foods increases by insignificant amount the X ray intensity, as the thickness of the aluminum foil was only about 0.0027 g/cm^2 aluminum. On the other hand, cans containing tin and iron as those often used in heat sterilization of food would increase the activity significantly.

When the incident electron energy exceeds the thresholds for the ^{49}Ti and ^{47}Ti at 8.14, and 8.88 MeV, respectively, we must consider also the effect of neutron production in the titanium window. However, this neutron production is insignificant compared with that from the food itself.

6.4. Activities produced in electron irradiation versus X ray irradiation

In the first cm (= g/cm^2) of water about 2 MeV or 20% of the 10 MeV electron energy is absorbed. The energy emitted in the form of X rays as the electron penetrates the 1st cm is about 7.52% of 2.151 MeV total energy loss or about 0.162 MeV. The window increases the X ray dose by about 0.014 MeV. The effective X ray absorption coefficient in water for the spectrum of X rays is about 0.0232. Therefore, the corresponding dose due to the X rays in the first cm of water is about (0.162 + 0.014) · 0.0232 = 0.0041 MeV, which is very small, or 0.205 % of the 1.993 MeV energy deposited by the electrons in the first cm of water. The activity per gram and per kGy produced in the first cm by electron irradiation is then about 1/488 (=0.00205) of that produced by the X rays per gram and per kGy. Food is usually nearly water equivalent. In muscle tissue the energy emitted in form of X rays per unit dose is about 10.6 % less than that of water. The factor 1/488, valid for water, has then to be replaced by about $1/540 = 1.85 \cdot 10^{-3}$, valid for muscle tissue.

The electron induced activity, $A_{Is}^{10\ MeV\ electrons}$, produced in water equivalent food by 10 MeV electron irradiation is related to the X ray produced activity $A_{Is}^{10\ MeV\ x\ rays}$ through the relation:

$$A_{Is}^{10MeV\,electrons} = 2.05 \cdot 10^{-3} \cdot A_{Is}^{10MeV\,xrays}.$$

The unit of the activity is becquerel (Bq) per kg of food and per kGy electron dose. An electron- induced activity in a trace element according to Eq. (12) is then given by:

$$A_{Is}^{10MeV\,electrons} = 2.05 \cdot 10^{-16} \cdot (10 - E_{th})^3 \cdot \frac{A_{Is} \cdot N_{Is} \cdot F_{Is} \cdot \ln 2}{T_{1/2}}.$$

For each isotope, the photoneutron activities in becquerel (Bq) per kilogram (kg) of food and per kGy dose immediately after irradiation with 10 MeV electrons are shown in column 9 of Table 9.

These same activities are shown also in the 2nd column of Table 10. For obtaining the total activity from consumption of 50 kg/year of food irradiated with 60 kGy, the activities must be multiplied by 50·60 = 3,000. In column 5 of Table 10, we list from ICRP publication 68 the conversion factors from becquerel (Bq) to sievert (Sv) for each isotope. The total activity consumed in one year may also be multiplied by the conversion factor from Sv to mSv/year (which is obtained by multiplying by 1000 the values in column 5 of Table 10) to derive the result shown in column 6 of Table 10. We usually use the unit mSv/year because the average background radiation is about 3 mSv/year. **The main results of the photoneutron activities**

are shown in column 6 of Table 10, which gives the exposure dose in millisievert/year to humans consuming 50 kg/year of food immediately after irradiation with an average dose of 60 kGy by 10 MeV electrons.

It is extremely unlikely that humans would ever consume more than 50 kg per year of irradiation-sterilized food (radappertized food); and the maximum sterilizing dose is usually less than 60 kGy. It is also very unlikely that any individual would eat that much of radappertized food immediately after irradiation because sterilized foods are intended for long term storage. It is seen from this column that even if 50 kg/year of food is consumed immediately after irradiation with 60 kGy, the exposure dose is less than $2.4 \cdot 10^{-6}$ mSv/year, which is less than $8 \cdot 10^{-7}$ times the natural background. The assumed concentration of 0.5 ppm (see Table 2) of iodine in the reference food, which forms the basis for these calculations, is high as Tables 3 indicates, which for beef shows a value of 0.092 ppm. As it is very unlikely that the sterilized food would be consumed immediately after irradiation, we show how the exposure dose to humans consuming the food decreases with the time elapsed between irradiation and consumption in Figs. 15, 16 and 17.

7. OTHER PHOTON-INDUCED ACTIVITIES

In the introduction to Section 5, we mentioned that besides the photoneutron activities, the photons could induce other activities, such as: the *photo-proton reaction* or (γ, p), and *photo-alpha reaction* (γ, α). It can be shown, however, that these reactions are usually much less likely, and that they are insignificant in isotopes of food when the incident photons are ≤ 10 MeV.

The absorption of a photon in a nucleus results in a formation of a compound nucleus, which can decay in several ways; for example, by emission of photons, a neutron, a proton, or an α-particle. For equal binding energies, the protons are much less likely to be emitted than neutrons, because the protons must overcome or penetrate the coulomb potential barrier. The potential energy V of the coulomb barrier outside the nucleus decreases with the distance r roughly as

$$V_{Coulombbarrier} = Z_1 \cdot (Z - Z_1) \cdot e^2 / r \text{ , and } r \geq R_1 + R_2$$

where Z_1 and Z are the charges on the emitted particle and the initial nucleus, e is the elementary charge, and r the distance between the two particles. The minimum distance between the particles and maximum height of the barrier is for $r = R_1 + R_2$, where R_1 and R_2 are the radiuses of the two separated particles. It is seen that the barrier height increases with the atomic number Z. We can refine this estimate by taking into account the angular momentum and the more detailed form of the binding energy. Eq. (18) is, however, adequate for our purpose, because it makes it clear that the potential barrier will prevent or slow down the penetration of the barrier by the proton when the excitation energy of the compound nucleus exceeds only slightly the binding energy of the proton.

The photo-proton or (γ, p) reactions in isotopes of food are usually above 10 MeV, and when they are below 10 MeV the reactions result usually in stable isotopes. The first exception is the $^{33}S(\gamma, p)^{32}P$ reaction with a threshold at 9.57 MeV and with ^{32}P half-life of 14.28 days. At incident electron energy of 10 MeV, a few photons could possibly excite the compound nucleus beyond the threshold of 9.57 MeV and produce the radioactive isotope ^{32}P. However because the excitation energy exceeds by only a small amount the threshold energy, the emission of proton becomes extremely unlikely because the proton has difficulty in penetrating the coulomb barrier of about 4.51 MeV. The compound nucleus would instead emit photons, or a neutron in a (γ, n) reaction, which in this case has a threshold-energy of 8.64 MeV. The $^{33}S(\gamma, n)^{32}S$ reaction result in a stable isotope. We use Eq. (18) for the estimate of the maximum potential energy. For the proton, we have that $R_1 \approx 0.83 \cdot 10^{-13}$ cm, and for the phosphor nucleus (remaining when the proton splits from a sulfur nucleus) $R_2 \approx 3.96 \cdot 10^{-13}$ cm. From (18) we get that the maximum potential energy is given by

$$V_{Phosphor/proton} \approx 15 \cdot e^2 / (4.79 \cdot 10^{-13}) = 4.51 \text{ MeV}.$$

The $^{33}S(\gamma, p)^{32}P$ reaction with a threshold at 9.57 MeV is very unlikely, because when 10 MeV photons are absorbed, the proton (even when it absorbs all the energy) has to penetrate a coulomb barrier that is 4.51 – (10 – 9.57) = 4.08 MeV.

The $^{33}S(\gamma, p)^{32}P$ reaction as well as $^{34}S(\nu, p)^{33}P$ reaction with threshold of 10.88 MeV are mentioned by Glass and Smith [Gl60b], Meyer [Me66], and Koch and Eisenhower[Ko67]. The coulomb barrier and the thresholds in these reactions are too high for activation by 10 MeV. These reactions are therefore of no concern at 10 MeV. It should be realized that Meyer as well as Koch and Eisenhower relied on conclusions of Glass and Smith. The observations by the last mentioned authors were made using 24 MeV electrons. At these high energies these reactions are possible. The equations used by Glass and Smith, however, usually do not take the effect of

the coulomb barrier properly into account and lead to incorrect estimates for the (γ, p) reactions. In some of the experiments, they also apparently disregarded that some of the observed activity is produced by the $^{33}S(n, p)^{33}P$ reaction followed by β - decay of ^{33}P to ^{33}S. Their conclusions were misleading, therefore.

The second exception is the $^{40}K(\gamma, p)^{39}Ar$ reaction with a threshold at 7.58 MeV and a half-life of 265 years. The reaction $^{40}K(\gamma, n)^{39}K$ with threshold of 7.8 MeV is more likely, as very few protons would penetrate the coulomb barrier of about 6.24 MeV (corresponding to $R_2 = 3.32 \cdot 10^{-13}$ cm). More likely than the (γ, p) reaction would be $^{40}K(\gamma, e^+)^{40}Ar$ reaction, which results in a stable isotope, ^{40}Ar. This positron emission is very unlikely and reduces insignificantly the natural activity in ^{40}K.

The third exception is the $^{50}Cr(\gamma, p)^{49}V$ reaction with a threshold at 9.59 MeV and a half-life of 230 days. The reaction $^{50}Cr(\gamma, n)^{49}Cr$ with threshold of 13 MeV is not possible when the incident energy is ≤ 10 MeV. In the $^{50}Cr(\gamma, p)^{49}V$ reaction, practically none of the protons could penetrate the coulomb barrier of about 7.51 MeV (corresponding to $R_2 = 3.58 \cdot 10^{-13}$ cm). The fractional concentration of ^{50}Cr in the element is about 4.35 %.

The fourth exception is $^{54}Fe(\gamma, p)^{53}Mn$ reaction with a threshold at 8.85 MeV. Practically none of the protons could penetrate the coulomb barrier of about 7.96 MeV (corresponding to $R_2 = 3.69 \cdot 10^{-13}$ cm). The long half-life of $2 \cdot 10^6$ years, the small fractional concentration of 5.8% of ^{54}Fe in the element, and the high coulomb barrier means that the activity can be disregarded. Similar analyses of the remaining trace elements shows that (γ, p) reaction cannot be important.

As the mass and the charge of the emitted particle increases, the penetration of the coulomb barrier becomes increasingly difficult. Neither (γ, ^2H) nor (γ, ^3H) reaction in elements of food is possible for incident electron energies of 10 MeV. However, the large internal binding energy of the helium nucleus makes it likely that its binding energy to the rest of the nuclei is relatively low. In the heavy nuclei it may even be negative. Usually, the coulomb barrier prevents α-decay. In the ^6Li and ^7Li, the binding energy is only 1.5 and 2.5 MeV, and the coulomb barrier of about 1.05 MeV cannot prevent α-decay in a highly excited nucleus. However, the α-decay of an excited nucleus results in stable nuclei, and also, lithium is not an element in food.

The first reaction that could lead to radioactive nucleus is ^{18}O (γ, α) ^{14}C with binding energy of 6.2 MeV. We may set $r = R_1 + R_2 = 1.2 \cdot 10^{-13} + 1.3 \cdot 10^{-13} \cdot A^{1/3}$, where A is the mass of ^{14}C. The coulomb barrier is then about 4.0 MeV, and an α-particle excited by 10 MeV photons has a small possibility of penetrating the top of the coulomb barrier. However, the excitation energy of the compound nucleus would be much more likely to be emitted in the form of the faster moving neutrons with threshold at E_{th} = 8.04 MeV, which results in the $^{18}O(\gamma, n)^{17}O$ reaction. Similar analyses for other isotopes in food show that for 10 MeV electron irradiation, α-decay does not cause any radioactivity in food.

8. YIELD OF NEUTRONS IN FOOD IRRADIATED BY X RAYS

When an isotope absorbs a photon with energy exceeding the threshold energy E_{th} for the (γ, n) reaction, the compound nucleus may emit a neutron and transform into a stable isotope. For example, when food is irradiated with x rays, the photons with energy exceeding 2.2 MeV may be absorbed in deuterium (^{2}H), which then may emit a neutron, while the hydrogen isotope, ^{1}H, remaining after the emission is stable. The emitted neutron may be absorbed by the nuclei of food. This neutron capture produces a new isotope, which may be radioactive. Most of the activity produced in the food is due to this neutron capture activity. This problem requires, therefore, thorough analysis.

First, we must obtain the total number of neutrons produced in the food. The number of neutrons, N(γ, n), produced per g of food and per kGy of absorbed photon energy is given by Eq. (6) in Section 5.1:

$$N(\gamma,n) = 6.24\cdot 10^{-15}\cdot N_{Is}\cdot \frac{\int \sigma\cdot\{[I(E_0,E_\gamma)]/E_\gamma\}\cdot dE_\gamma}{\int \mu_e\cdot\{[I(E_0,E_\gamma)]\}\cdot dE_\gamma},$$

where the quantities and units used are defined as in Eq. (6). The integrations were performed numerically using intervals of 0.1 MeV.

8.1. Photoneutrons produced in food per kGy of X rays in food

When food is irradiated with X rays with energy below 10 MeV, the photoneutrons are produced mainly by deuterium, **^{2}H,** with E_{th} = 2.225 MeV; **^{13}C** with E_{th} = 4.95 MeV; **^{17}O** with E_{th} = 4.14 MeV; and **^{18}O** with E_{th} = 8.04 MeV. In all cases, the remaining isotope is stable, but the number of neutrons that is produced is significant, as we will see. When the incident electron energy is increased to 14 MeV, also the following isotopes of food contribute significantly to the photoneutron production: **^{14}N** with E_{th} = 10.55 MeV; **^{23}Na** with E_{th} = 12.42 MeV; **^{25}Mg** with E_{th} = 7.33 MeV; **^{31}P** with E_{th} = 12.31 MeV; **^{33}S** with E_{th} = 8.64 MeV; and **^{37}Cl** with E_{th} = 10.31 MeV. Table 11, and Fig. 10 and Fig. 11 show the numbers of neutrons produced per gram in the first layer of the reference food that is irradiated with 1 kGy dose of X rays.

Some times, a spectrum of high-energy photons becomes harder with penetration depth in food and in special cases could produce an increasing number of neutrons per dose unit. However, a spectrum of soft components of Compton-scattered photons between 0.03 and 0.5 MeV will buildup as the spectrum penetrates the food. These last mentioned very low-energy photons in food would buildup with depth and increase the dose slightly (up to about 13 %) and reduce therefore the number of neutrons per unit dose. The balance of more neutrons per dose due to hardening of the spectrum and the decrease in neutrons per dose unit because of increased dose from the very soft photons will depend on the initial spectrum, the packaging material, the isotope, and the incident energy. However, when using an X ray spectrum below 10 MeV, the number of neutrons per dose unit in food will be maximum close to the front of the sample (1 to 2 g/cm^2 below the surface) where the X rays enter the food, while the neutron production per dose unit at the back of the sample is close to a minimum.

To assure that the estimates are always on the side of safety, we have from the X ray spectrum removed the photon with the lowest energy (the photons absorbed in the X ray target's K shell) from the spectrum. These low energy photons are not in the initial spectrum from the X ray target, but they buildup in the food as the X rays penetrate it. They contribute to the dose but not to the activity. Removing them from the calculations reduces, therefore,

the dose in the denominator of equation (20) and increases the estimated activity per dose unit. This method assures that even when the geometry of the food changes, the estimates are close to the maximum neutron activity, and that the calculations are therefore a slight overestimate; that is, on the side of safety.

8.2. Photoneutrons from Ta, W, Au and Fe per kJ of electron beam

In addition to the number of neutrons produced in the food, a significant number of neutrons from the X ray target and the surrounding structures, such as a steel conveyor can enter the food. For calculating the neutron production in these structures, we have relied on the analysis by Swanson. [Sw79a].

Table 12 shows the number of neutrons produced in tantalum, tungsten, gold and iron per kJ of electron beam striking a semi-infinite target thickness. In Fig. 12, we illustrate these values for tantalum, tungsten, and gold; while in Fig. 13, we show the neutron production in ^{57}Fe and ^{56}Fe isotopes in a thick block of iron.

In 1.2 mm (2 g/cm^2) thickness of tantalum, and in 4 mm (3.2 g/cm^2) thickness of steel the neutron production will be about 10 % of the listed values. This may be an X ray target, a "beam catcher" that is used to stop the electron beam, a steel belt conveyor, or the food carriers.

The design of an X ray target varies. The X ray intensity varies with the energy and the angle of the forward cone. For 10 MeV, the optimal thickness of Ta, W, and Au is between 1 and 2 g/cm^2. For 10 MeV and X ray cone of 60^0, the optimal thickness is about 1.1 g/cm^2. If the thickness of tantalum, tungsten, or gold targets is 1.1 g/cm^2, the neutron production at 10 MeV will be: 5.1 %, 5.1 %, and 5.4 %, respectively, of the values listed in the Table 12 and Fig. 12, which are valid for thick targets. The neutron production in the cooling water and in the container structure of the X ray target must be added to the neutron production in Ta, W, and Au, but usually the number of these neutrons is much less than that from the primary X ray target.

At the Natick Laboratories, Natick, Massachusetts, USA, where most of the food irradiation research in the US in the 1960–1980 was conducted, the overhang carriers, the food carriers, the laminated pouches containing the food, and the beam catcher were made of 2S aluminum with E_{th} = 13.06 MeV. This material minimizes the neutron production. Other facilities often use food carriers and conveyor belts of steel. Above 8 MeV, the steel conveyor may increase slightly the neutron flux in the food.

8.3. Photoneutron production in the window

Electrons with energy ≤ 10 MeV will not produce any neutrons when they penetrate through an accelerator window made of aluminum foil, because its (γ, n) threshold is 13.06 MeV. However, if the window is made of titanium, some neutrons are produced because of the thresholds of 8.14 and 8.88 MeV for the two isotopes ^{49}Ti, and ^{47}Ti, respectively. The cross-sections for production photoneutrons (and the neutrons produced by the virtual electron field) in titanium are not known. However, the cross-sections should be similar to those for iron when adjusted for threshold energies and isotope concentrations. We may then scale the neutron production in iron shown in the last column of Table 12 by shifting the energy scale by 0.49 and 1.23 MeV, respectively for the two isotopes, and by correcting for the abundance of the isotopes. We find then that 10 MeV electrons produce about $1.1 \cdot 10^5$ neutrons per kJ in a 0.125 mm (0.0568 g·cm^{-2}) thick titanium window.

The emission of these neutrons is approximately isotropic. The spherical angle covered by the food is usually about π, corresponding to an X ray cone of 120^0; therefore, approximately 25% of the neutrons from the X ray target will enter the food; that is, at most about $0.25 \cdot 1.1 \cdot 10^5 = 2.8 \cdot 10^4$ neutrons per kJ of incident 10 MeV electron beam would enter the food from the titanium window.

Usually, about 50% of the electron beam energy is absorbed. Therefore, about 500 J per 1 kJ of 10 MeV electron beam impinging on the window would be absorbed in the food. As shown in Section 6.4, these 500 J of absorbed electron energy produce as many neutrons in the food as each joule of absorbed 10 MeV X ray energy. Table 11 shows that $1.5 \cdot 10^6$ neutrons are produced per gram per kGy (one J absorbed per g is equal to one kGy). Therefore, when 1 kJ of 10 MeV electrons impinge on the titanium window, about $(500/500) \cdot 1.5 \cdot 10^6 = 1.5 \cdot 10^6$ neutrons are produced in the food. The number of neutrons, $2.8 \cdot 10^4$, entering the food from the titanium window is therefore an insignificant fraction of the neutrons, $1.5 \cdot 10^6$, produced in the food itself.

8.4. Fraction of beam energy that enters food in the form of X rays

The X ray intensity spectrum as given by Eq. (7) is shown in Fig. 8. The intensity is directed mainly forward. When the X ray intensity, $I(E_0, h\nu, \theta)$, from a tungsten target is multiplied by the spherical angle, $2\pi \cdot \theta \cdot d\theta$, of emission and then integrated from zero to the maximum angle θ_0 in the X ray cone, we obtain the amount of X ray energy that is emitted within the angle θ_0. The results of such integrations, $\int I(\theta) \cdot 2\pi \cdot \theta \cdot d\theta$, are illustrated in Table 13 and in Fig. 14 for incident electron energies of 5, 7.5, and 10 MeV. The intensity $I(E_0, h\nu, \theta)$ used in these estimates is based on theoretical and experimental analysis of the angular distribution from an optimized tungsten target by Brynjolfsson and Martin [Br71]. There are small variations with the thickness of the X ray target. The width increases slightly as the thickness increases. However, these variations will not affect significantly the overall neutron production per kGy. For good utilization of the x rays, we should widen the angle of the forward X ray cone that is used for irradiating the food as much as is technically feasible. (One may think of vertical scanner horns and multipath overhang conveyor using food carriers that are about 4 meters high and move in a semicircle around the scanner horn.) Usually, it is difficult to utilize more of the X rays than what is within a 60^0 half-angle of the forward cone. Table 13 and Fig. 14 show that, within a half-angle of 60^0, about 5.6 %, 10 %, and 14.5 % of the incident electron beam energy would enter the food in form of X rays when the electron energies are 5, 7.5, and 10 MeV, respectively.

8.5. Fraction of neutrons from the X ray target that enters the food

The fraction of neutrons and of X rays that enter the food varies with the design in the irradiation area. The angular distribution of neutrons emitted by the (γ, n) process in the X ray target is roughly isotropic, while the angular distribution of the X rays is peaked forward. Both the neutrons and the X rays are reflected, scattered, and absorbed in the target and in the surrounding materials. The relation between the number of neutrons entering the food and the X ray dose is rather elaborate, because it depends on the materials and the geometry of objects surrounding the food samples.

From Table 13 and Fig. 14, we see that only about 10 % of 1 kJ incident 7.5 MeV electron beam energy enters in form of X rays a forward cone with half-angle $\theta_0 = 60^0$. Disregarding reflection, about 25% of the neutrons will enter the same cone, as the emission of neutrons is isotropic. The X ray energy that is absorbed in the first gram/cm^2 layer of food

is about equal to 100 J (10 % of 1 kJ) times the absorption coefficient, which is about 0.0248 cm^2/g (see Fig. 24). Thus, for an incident 1 kJ of electron beam energy on the X ray target, the amount of X ray energy absorbed in the first g/cm^2 layer of the food is therefore about $100 \cdot 0.0248 = 2.5$ J. That is, for each 1 kJ of 7.5 MeV electron beam energy striking the X ray target about 100 J of X ray energy enters the cone and about 2.5 J of this X ray energy is absorbed in the first g/cm^2 layer of the food.

According to Table 12, about $4.8 \cdot 10^8$ neutrons are produced when 1 kJ of 7.5 MeV electron beam impinges on a very thick target of tungsten. However, an X ray target is not thick. Its thickness, which is optimized for maximum X ray output, depends slightly on the size of the opening angle in the X ray cone that is utilized. At 7.5 MeV, the optimum thickness is about 1 g/cm^2 for maximum X ray intensity of the forward peak; but if the entire forward half-sphere is used, the optimum thickness increases to nearly 2 g/cm^2. About 4.7 % to 9 % of the maximum number of neutrons or about $2.3 \cdot 10^7$ to $4.3 \cdot 10^7$ neutrons/kJ is then produced in an optimized X ray target. About 25 % of these neutrons from the X ray target enter the food, because the half-angle in the forward X ray cone covering the food is about $\theta_0 = 60^0$, corresponding to a spherical angle of ¼ of 4π. The migration length of the neutrons in water is $M = \sqrt{\tau + L^2} = \sqrt{33 + 2.88^2} = 6.4$ cm, where $\sqrt{\tau} = \sqrt{33} = 5.7$ cm is the slowing-down length, and L = 2.88 cm is the diffusion length before absorption. The migration length is a measure of the neutrons' penetration depth in water. Due to slightly lower hydrogen concentration in food than in water, the migration length M is usually slightly longer in food than in water (often about 24 % longer).

An incident 1 kJ of electron beam that impinges on the X ray target of tungsten, thus, produces about $2.3 \cdot 10^7/4 = 5.8 \cdot 10^6$ to $4.3 \cdot 10^7/4 = 1.1 \cdot 10^7$ neutrons, which enter the food and penetrate about 6.4 cm. The same kJ of 7.5 MeV electron beam also results in absorption of 2.5 J of X rays in the first g/cm^2 layer of the food. The X rays produce about $8.3 \cdot 10^5$ neutrons/kGy in food. As 1 kGy is equal to 1 joule per gram, we get that about $8.3 \cdot 10^5 \cdot 2.5 = 2.1 \cdot 10^6$ neutrons are produced per gram thickness of the food that the X rays penetrate. In the first 6.4 g/cm^2 of food the X rays penetrate, they produce then about $6.4 \cdot 2.1 \cdot 10^6 = 1.3 \cdot 10^7$ neutrons. This number may be compared with about $5.7 \cdot 10^6$ to $1.1 \cdot 10^7$ neutrons that enter the food from the X ray target of tungsten. We see thus that the number of neutrons from the 7.5 MeV X ray target of tungsten (2 g/cm^2 thick) that enter the food is nearly equal to the number of neutrons produced in the first 6.4 cm of food. Therefore, irradiation of the food with 7.5 MeV X rays from a tungsten target nearly doubles the neutron activity in the outer 6.4 cm thick layers of the food. Preferably, therefore, a target of tungsten should not be used.

On the other hand, at 7.5 MeV the neutron production in a thick X ray target made of ***tantalum*** is $4.8 \cdot 10^4$ neutrons/kJ, or $1/10^4$ times that of tungsten. The number of neutrons from a tantalum target that enter the food is therefore insignificant compared with the number of neutrons produced in the food itself. The neutron production in tantalum increases steeply when the incident electron energy exceeds the 7.577 MeV threshold of the ^{181}Ta isotope. In a thick tantalum target, the neutron production is $4.0 \cdot 10^6$ neutrons per kJ for 7.75 MeV incident electrons, $5.66 \cdot 10^7$ neutrons/kJ at 8 MeV electrons, and $2.27 \cdot 10^8$ neutrons/kJ at 8.25 MeV electrons.

Similarly, X ray target of gold with $E_{th} = 8.07$ MeV, iridium with $E_{th} \geq 7.76$ MeV, iron with $E_{th} \geq 7.65$ MeV, and copper with $E_{th} \geq 9.91$ MeV could be used as X ray targets at 7.5 MeV without increasing the neutron fluence per kGy absorbed in the food.

9. THE FLUENCE OF NEUTRONS IN IRRADIATED FOOD

The fluence, Φ, is the time integral of the neutron flux, φ; that is, $\Phi = \int\varphi\cdot dt$. The neutron flux, φ, is the number of neutrons passing through a square centimeter (cm^2) of food per second (s). The neutron capture activity is proportional to the fluence, Φ_t, of thermal neutrons times the absorption coefficient for the thermal neutrons. The absorption coefficient for fast and epithermal neutrons is usually insignificant. Therefore, the focus will be on determining the fluence of thermal neutrons.

Initially, the photoneutrons have kinetic energy less than the maximum of about ($E_\gamma - E_{th}$), because some γ rays are usually emitted before or after the emission of the neutron, and because the expelled neutron transfers recoil energy to the remaining nucleus. Due to emission of γ rays and transfer of recoil energy to the remaining proton, the energy of neutrons from deuterium will be less than $(E_\gamma - E_{th})/2$. For high-energy photons, the initial neutron spectrum often peaks at about 0.7 MeV.

The fast photoneutrons that are formed initially will be scattered and slowed down and thermalized in about 18 collisions mainly with hydrogen atoms in the food. The fluence of the neutrons, as well as the activity they produce will decrease with distance from their source roughly as $\exp(-x^2/132)$. The fast neutrons, thus, are slowed down in about $(132)^{1/2} = 11.5 = 2\cdot 5.7$ cm. The energy spectrum of the fast and epithermal neutrons at the different depths will be similar. Once they have been thermalized, the neutron will diffuse with approximately constant average energy until absorbed. The microscopic *scattering* cross-section of thermalized neutrons in hydrogen depends on the binding energy of the hydrogen atoms, but is usually about 20 to 80 barn, where 1 barn is equal to 10^{-24} cm^{-2}. This corresponds to a macroscopic cross-section, Σ_s, in water of 1.9 to 7.6 cm^2. The mean free path ($\lambda_s = 1/\Sigma_s$) is therefore about 0.53 to 0.13 cm. The mean path traveled by thermal neutrons before they are *absorbed*, on the other hand, is about 45 cm in water, and 50 cm in food. Due to the scattering, the distance between the endpoint and starting point is much shorter. The thermal neutrons will diffuse from their end point of slowing down, a distance on the order of 2.45 diffusion lengths, L = 2.7 cm, for a total of 6.6 cm in water.

During the slowing down process, a significant fraction of the neutrons is scattered out of the food and absorbed in the conveyor and in the walls of the irradiation room. Also, a large fraction of the thermalized neutrons will diffuse out of the food. The number of neutrons absorbed in the food is therefore much smaller than the number produced.

Practically, only the thermal neutrons, and not the epithermal or fast neutrons, are absorbed in the food. It is important therefore to determine the thermal fluence of neutrons.

The fluence, Φ, of thermal neutrons depends on:

(1) The number of neutrons produced per dose unit, which was estimated in Section 8.

(2) The scattering coefficient for the fast neutrons in food and its containment.

(3) The diffusion coefficient for the thermal neutrons.

(4) The geometry of the food sample and containers.

(5) The absorption coefficient for thermal neutrons in the isotopes of food.

Quantification of the effect of these many parameters is complicated as it depends on the geometry and the materials in the target area that are usually not well defined.

9.1. Absorption of neutrons in elements of food

Percentage of neutrons absorbed in the major elements of food can be determined independent of many other factors. Table 15 gives in the 3rd column the percentage of

neutrons that are absorbed in the major elements of the reference food. We see from column 2, that 2004.41 neutrons are absorbed per 10^5 gram of reference food if the fluence is 1 neutron per cm^2. This corresponds to absorption of one neutron per gram if the fluence is $10^5/2004.4 \approx 50$, or to a macroscopic absorption coefficient, $_{\text{ref. food}}\Sigma_a$ = **0.0200 cm^2/g**. Therefore, if all the neutrons that are produced per kGy in the reference food are absorbed in the food, then the maximum fluence produced by one kGy dose is 1/0.020 = 50 times the number of neutrons produced per kGy of irradiation. In case of water, the macroscopic absorption coefficient is $_{\text{water}}\Sigma_a$ = **0.0222** and the corresponding maximum fluence is then 1/0.0222 = 45 times the number of produced neutrons. For example, if 5 MeV X rays produce $4.3 \cdot 10^5$ neutrons per g per kGy (see Table 11), then the maximum neutron fluence in the food is $50 \cdot 4.3 \cdot 10^5 = 2.2 \cdot 10^7$. Usually, a significant fraction of the fast neutrons that are produced will be scattered out of the food during the slowing down process, and also some of the thermalized neutrons will diffuse out of the food. The average number of neutrons absorbed in the food is, therefore, significantly smaller than the number produced. The factor 50 has then to be replaced by smaller (often much smaller) factor.

9.2. Fluence of photoneutrons in X ray facilities

How many of the produced photoneutrons, as estimated in Section 8, are slowed down, thermalized, and captured in the food depends primarily on the size of the food samples in the irradiation area. Other factors also play a role, such as neutron absorbing elements in the food, packaging, and in the carriers. In case of X ray irradiation, the food containers in the irradiation area are usually large. The density in g/cm^3 times the thickness of the food is often 20 to 40 g/cm^2. The food carriers and the conveyor may contain neutron-absorbing elements such as cadmium (in cadmium coating), and intentionally they may contain some boron (such as boron carbide in aluminum). Both of these elements would capture a significant number of thermal neutrons. However, reduction in the neutron flux caused by the packaging materials and the food containers can usually be disregarded unless they are specially designed to absorb neutrons. A relatively large fraction of the produced neutrons is then slowed down, thermalized, and captured by the nuclei of the food.

9.3. Initial distribution of thermalized neutrons

Thermalization of fast neutrons and the initial scattering width in the distribution of thermal neutrons can be estimated using the theory developed for nuclear reactors. The slowing down density, $q(r,\tau)$, or source strength of neutrons slowed down at a distance r from a fast neutron point source, line source, or a plane source is given by:

$$q(r,\tau) = \frac{\exp\left(-\frac{r^2}{4\cdot\tau}\right)}{(4\pi\tau)^{3/2}}$$ valid for a point source of fast neutrons,

$$q(r_\perp,\tau) = \frac{\exp\left(-\frac{x^2+y^2}{4\cdot\tau}\right)}{4\pi\tau}$$ valid for line source of fast neutrons,

$$q(x,\tau) = \frac{\exp\left(-\frac{x^2}{4\cdot\tau}\right)}{\sqrt{4\pi\tau}}$$ valid for plane source of fast neutrons,

where τ , the age of the neutrons, is a measure of the spatial width (slowing down width) in the neutrons distribution around the source. We may recognize that equations (21) to (23) have the same form as the normal error functions with the standard deviation $\sigma = \sqrt{2\cdot\tau}$. The value of $2\cdot\tau$ is thus also a rough measure of how far from their source the fast neutrons become thermalized. When fission spectrum neutrons are thermalized in water, their age at the point of thermalization is τ_{water} = 33 cm^2. That is, the width of the Gaussian curve for the distribution of thermal neutrons is $\sigma = \sqrt{2\cdot\tau}$ = 8.12 cm. It also means that 50 % of the neutrons will be outside $r_{1/2} = \sqrt{\tau}$ = 5.74 cm.

The age τ depends only weakly (logarithmically) on the initial neutron energy. The value 33 is strictly valid for about 2 MeV neutrons. In the reference food, the concentration of hydrogen is only about 9 % by weight, but in water it is about 11.15 %. The corresponding age of thermalized neutrons in reference food is therefore approximately $(11.15/9)^2$ times longer than that in water, or about $\tau_{ref.food}$= 50 cm, and the width σ in the distribution is about 10 cm.

The average of distance squared (the second momentum) traveled by neutrons from their emission at a point source (line source and plane source) to the point of thermalization is found from equation (21) to (23) to be respectively

$$\text{for a point source}: \overline{r^2} = 6\cdot\tau;\ \text{for line source}: \overline{x^2 + y^2} = 6\cdot\tau;\ \text{and for plane source}\ \overline{x^2} = 6\cdot\tau,$$

In water it is thus $\overline{r^2} \approx 6\cdot 33 \approx 14.1^2$, and in reference food it is $\overline{r^2} \approx 6\cdot 50 = 17.4^2$ cm^2.

In small or thin food samples as those used in electron irradiation, most of the fast neutrons would then be scattered out of the food sample surface before being thermalized; especially, the neutrons produced close to the surface of the food boxes or the food carriers.

In addition to being scattered out of the food sample during slowing down, the thermalized neutrons will diffuse a significant distance before being absorbed. The thermalized neutron may thus diffuse out of the food before being absorbed. The number of neutrons slowed down, thermalized and absorbed in the food depends strongly on the size of the food boxes being irradiated. For example, food irradiated from one side by 10 MeV electrons would usually be only about 3.4 cm thick. Therefore, very few of the neutrons produced in the food would be thermalized; and many of those that are thermalized will diffuse out of the food before being absorbed. Thus in case of electron irradiation, most of the neutrons would be scattered out of the sample, and absorbed in the walls of the irradiation room and not in the food.

Simple calculations can often be used to estimate how the sample dimensions affect slowing down distribution and the number of neutrons thermalized in the sample. Exact calculations of the number of neutrons that escape from the food samples in the target area are cumbersome, mainly because the geometry is usually not simple and because the material used in the packaging, carriers, and conveyor are usually not well defined. However, some elements of neutron leakage theory developed for homogeneous reactors (see for example, Glasstone and Edlund [GlEd]) can give useful estimates for simplified models of the samples. These estimates then serve well as guides. We find then that the fraction of fast neutrons that do not leak out during slowing down, that is, the fraction of fast neutrons thermalized in the food is given by:

$\exp\left(-B_g^2 \cdot \tau\right) \approx$ nonleakage of fast neutrons during slowing down.

where B_g is the "geometric buckling" of the food in the irradiation area, and τ is the slowing down age, which in water is equal to about 33 cm^2. In reference food $\tau_{ref.food} \approx 50$ cm^2. For a parallelepiped with dimensions a, b, and c for each of the sides, the geometric buckling is given by

$$B_g^2 = \left(\frac{\pi}{a + 4.26 \cdot \lambda_S}\right)^2 + \left(\frac{\pi}{b + 4.26 \cdot \lambda_S}\right)^2 + \left(\frac{\pi}{c + 4.26 \cdot \lambda_S}\right)^2 .$$

It is seen that $4.26 \cdot \lambda_S$, which is twice the extrapolation length, increases significantly the dimension in the denominator. The extrapolation length takes into account that the neutron density close to the surface is more than zero and approaches zero at distance that is $2.13 \cdot \lambda_S$ cm outside the surface. For water, the extrapolation length is given by $0.71 \cdot \lambda_T \approx 2.13 \cdot \lambda_S$, where $\lambda_S = 3 \cdot \lambda_T$ is the scattering length, and λ_T the transport mean free path, or transport length. The average scattering length in water during slowing down is found to be about ${}_{water}\lambda_S = 1.1$ cm corresponding to average macroscopic cross-section of ${}_{water}\Sigma_S = 0.91$ cm^2. In water, the value of $4.26 \cdot \lambda_S \approx 4.26 \cdot 1.1 = 4.7$ cm; and in reference food the corresponding value would be 5.8 cm.

In X ray irradiation, the sample may be in a form of a cube that is 30 g/cm^2 on each side, the geometric buckling for the case of water sample is about $B_g = 0.157$. Therefore, the fraction of neutrons thermalized in a water sample is exp $(-B_g^2 \cdot \tau) = 0.44$. In a reference food with the same dimensions, it is exp $(-B_g^2 \cdot \tau) = 0.32$. If a cube containing water is 20 g/cm^2 on each side, only 20 % of the fast neutrons are thermalized; and if the cube contains reference food, only 11 % of the fast neutrons are thermalized.

If in 10 MeV electron irradiation from one side only, the thickness of the sample is a = 3.4 cm and b and c practically infinite, the geometric buckling $B_g = 0.388$ in water, and the fraction of fast neutrons thermalized in the 3.4 cm thick water sample is about $\exp(-0.388^2 \cdot 33) = 0.007$. Similarly, the fraction of fast neutrons thermalized in a 3.4 thick food sample is about 0.3 %. We should realize, however, that in these two cases the "age" concept and the slowing down theory in hydrogenous materials must be applied with caution, as the theory is not strictly applicable for low atomic numbers and thin samples. The experimental determination of the age $\tau = 33$ cm^2 for the fission spectrum of neutrons in nuclear reactors reduces the uncertainty in the simple slowing down theory in hydrogen. Therefore, in spite of some shortcoming, the theory serves as a useful guide. The slowing down in thin samples is especially sensitive to the low energy part of the initial spectrum, which is more easily thermalized. Therefore, the number of thermalized neutrons in thin samples is usually slightly greater than that derived from equations (25) and (26).

Independent estimates can be made using the scattering cross-section. If the number of fast neutrons with energy E_1 in a narrow energy interval dE_1 is $N_1 \cdot dE_1$, then the number $N_2 \cdot dE_2$ of scattered neutrons in each energy interval dE_2 around $E_2 < E_1$ after the collision with a hydrogen atom is given by $N_2 \cdot dE_2 = (N_1 \cdot dE_1) \cdot (dE_2/E_1)$; that is, the spectrum of the scattered neutrons is constant. Another way to express this relation is: $d\sigma(E_2)/ dE_2 = \sigma(E_1) /E_1$, where σ is the cross-section. When the initial spectrum of fast neutrons is known, we can use this relation and iteration to derive the actual number of neutrons slowed down in the food. The scattering cross-section is needed for evaluating the fraction of neutron slowed down in thin samples. Hydrogen contributes mainly to slowing down of the neutrons, while carbon, nitrogen, and oxygen contribute to scattering of the neutrons out of the sample. The microscopic total scattering cross-section in units of barn ($=10^{-24}$ cm^2) for the fast neutrons ($E_{kin} > 1000$ eV) in hydrogen is:

$$ {}_H\sigma_T = \frac{3\cdot\pi}{1.206\cdot E + (-1.86 + 0.09415\cdot E + 0.000136\cdot E^2)^2} + \frac{\pi}{1.206\cdot E + (0.42233 + 0.13\cdot E^2)^2}. $$

The macroscopic scattering cross-section, ${}_H\Sigma_S(E)$, of hydrogen in water is obtained by multiplying the microscopic cross-section, right side of Eq. (27), by 0.0669. The following chart also illustrates the energy dependence of the scattering cross-section in units of cm^2.

Neutron energy E in MeV	0.001	0.01	0.02	0.05	0.1	0.2	0.5	1	2	5
Cross-section ${}_H\Sigma_S$ in cm^2	1.35	1.28	1.22	1.06	0.88	0.67	0.42	0.285	0.185	0.090
Scattering length ${}_H\lambda_S = 1/{}_H\Sigma_S$	0.74	0.78	0.82	0.94	1.14	1.49	2.37	3.51	5.41	11.1

At energies between 10 and about 1000 eV, the microscopic cross-section is about 20.2 barn and the macroscopic cross-section about 1.35 cm^2. When we include the microscopic scattering cross-section of neutrons on oxygen of about 4.2 barn at low energies, we get that the total macroscopic scattering cross-section in this energy range for neutrons in water is about: $1.35\cdot(20.2\cdot2+4.2)/40.4$, or ${}_{water}\Sigma_S = 1.49$ cm^2, which corresponds to a scattering length of about ${}_{water}\lambda_S = 0.67$ cm. When we include also neutrons with higher initial energy, the average scattering length in water during slowing down is found to be about ${}_{water}\lambda_{S\text{-}exp.} = 1.1$ cm corresponding to average macroscopic cross-section of ${}_{water}\Sigma_{S\text{-}exp} = 0.91$ cm^2. In the reference food the hydrogen concentration is smaller, and the corresponding average scattering cross-sections in food during slowing down, which is determined mainly by hydrogen, should be about ${}_{ref.food}\Sigma_S = (9/11.15)\cdot0.91 = 0.73$ cm^2, and average scattering length should be about ${}_{ref.food}\lambda_{S.} = 1.36$ cm.

9.4. Diffusion of thermalized neutrons

Diffusion of thermalized neutrons affects the fraction of neutrons absorbed in the food. The scattering cross-section for thermalized neutrons on hydrogen is large and the scattering length therefore short. The diffusion theory can therefore be applied to even relatively thin food samples. The scattering cross-section in hydrogen is usually significantly larger than that of the other elements of food. The macroscopic scattering cross-section in units of cm^2, ${}_H\Sigma_S$, of hydrogen in water is obtained by multiplying the microscopic cross-section by 0.0669. At energies between 10 and about 1000 eV, the microscopic cross-section is about 20.2 barn and the macroscopic cross-section therefore about 1.35 cm^2, as mentioned above. As the neutron energy decreases below about 10 eV to about 0.025 eV of the thermal energy, the cross-section for neutron scattering on hydrogen increases steeply and depends then on the binding energy and the temperature. The thermal cross-section per hydrogen atom in water is often in the range of 80 to 100 barn. The microscopic cross-section in oxygen is about 4.2 barn. The macroscopic scattering cross-section, ${}_{water}\Sigma_S$, for thermal neutrons in water is then about 5.5 to 6.8 cm^2.

The corresponding scattering length for thermal neutrons in water is ${}_t\lambda_S = 1/{}_t\Sigma_S$, or about 0.182 to 0.147 cm. In the reference food it should then be about ${}_t\lambda_S = 1/{}_t\Sigma_S \approx (11.15/9)\cdot{}_t\lambda$, or ${}_t\lambda_S \approx 0.225$ to 0.176 cm. For thermal neutrons in water and food, these scattering lengths are nearly equivalent to the diffusion coefficients for thermal neutrons in water, ${}_tD \approx 0.182$ to 0.147 cm; and in food ${}_tD \approx 0.225$ to 0.176 cm. (The diffusion coefficient ${}_tD$ is defined here as it is usually done in nuclear reactor physics. However, ${}_tD = D_0/v$, where D_0 is the conventionally defined diffusion coefficient.) The macroscopic cross-section for absorption, ${}_t\Sigma_A$, in water is about 0.0222 cm^2, but 0.020 in reference food. The scattering cross-section, ${}_t\Sigma_S$, is thus much larger than the absorption cross-section, ${}_t\Sigma_A$. The thermal neutrons can therefore diffuse a considerable distance before they are absorbed. The diffusion length L is defined by

$$L = \frac{1}{\kappa} = \sqrt{\frac{D}{\Sigma_A}} \ .$$

The diffusion length in water is then ${}_{water}L \approx 2.86$ to 2.57 cm, and in the reference food it is about ${}_{ref.food}L \approx 3.35$ to 2.97 cm.

We can apply the diffusion theory to a source of thermal neutrons emitting 1 neutron/cm^2 per second in the center plane of water like a food sample that is t = 3.4 cm thick. The neutrons would then diffuse from the center plane. The distribution of the neutron in the food sample would decrease from the center plane towards the surfaces and leak out. The diffusion theory shows that the flux φ is given by

$$\varphi_j = \frac{\sinh(k \cdot (a - x))}{2 \cdot k \cdot D \cdot \cosh(k \cdot a)}, \text{ In this equation}$$

$$\kappa = \sqrt{\Sigma_A / D} = \sqrt{0.0222 / 0.147} = 0.389 \text{ cm}^{-1}.$$

For sample thickness t = 3.4 cm, we have for "a" in equation (29) that

$$a = t/2 + 0.71 \cdot \lambda_t = t/2 + 2.13 \cdot \lambda_S = 3.4/2 + 2.13 \cdot 0.147 = 2.01 \text{ cm},$$

and for $D \approx \lambda_S$, the diffusion coefficient in water is about 0.147 cm.

We can integrate equation (29) from x = 0 to x = 1.7 cm, and get then the number of neutrons stopped to the right of the center plane in the sample per second is

$$\Phi = \frac{1}{2 \cdot \kappa^2 \cdot D}\left[1 - \frac{\cosh(\kappa \cdot (a - 1.7))}{\cosh(\kappa \cdot a)}\right] = \frac{1}{2 \cdot \Sigma_A}\left[1 - \frac{\cosh(\kappa \cdot 2.13 \cdot \lambda_S)}{\cosh(\kappa \cdot a)}\right].$$

For very thick samples, the value of κ·a >> 1, and the last term in the bracket is zero. The integrated number of neutrons per cm^2 in the right half of the sample is then $\varphi = 1/(2\Sigma_A) = 1/(2 \cdot 0.0222) = 22.5$, and in the two halves it is therefore equal to 45; that is, the fluence is 45 neutrons per cm^2 in the sample when 1 neutron per cm^2 is emitted in the center plane. We have sat $\Sigma_A = 0.0222$ equal to the macroscopic absorption cross-section in water. For $\kappa = 0.389$, a = 2.01, and $\lambda_S = 0.147$, we get that the quantity inside the bracket is 0.238, that is, about 24 % of the thermal neutrons produced in the center plane of the 3.4 cm thick water sample would be absorbed. Figure 3 shows how the fraction of absorbed thermal neutrons varies with the half-thickness of the water sample g/cm^2. For example, in a 3.4 cm thick sample (t = 1.7 cm), about 24 % of the neutrons would be absorbed in the sample.

Fig. 3 gives an example of how large a fraction of thermal neutrons emitted in the center-plane of the sample is absorbed in the food. It is seen that about 20 % of the thermal neutrons emitted in the center-plane of a 3 cm (= 3 g per cm^2) thick food sample is absorbed in the food sample. The remaining 80 % of the neutrons will diffuse out of the sample.

In the actual case the neutrons are not thermalized in the center plane but all over the sample. We can then use a different approach similar to that for slowing down of fast neutrons in homogenous reactors. We find then that the fraction of thermal neutrons not leaking out but absorbed in the sample is given by

$$\frac{1}{1 + L^2 \cdot {}_t B_g^2} \approx \text{nonleakage of thermal neutrons},$$

where $L = 1/\kappa = \sqrt{D/\Sigma_A}$ is the diffusion length of thermal neutrons. In water, the diffusion length is ${}_{water}L \approx 2.86$ to 2.57 cm, and in the reference food ${}_{ref.food}L \approx 3.35$ to 2.97 cm. ${}_tB_g$ is the geometric buckling for thermal neutrons in the food and is given by

$$ {}_tB_g^2 = \left(\frac{\pi}{a + 4.26 \cdot {}_t\lambda_S} \right)^2 + \left(\frac{\pi}{b + 4.26 \cdot {}_t\lambda_S} \right)^2 + \left(\frac{\pi}{c + 4.26 \cdot {}_t\lambda_S} \right)^2 . $$

It is analogous to buckling for scattering during slowing down, which is given by equation (26). However, the thermal diffusion length ${}_t\lambda_S \approx 0.147$ cm in water differs from the scattering length $\lambda_S \approx 1.1$ cm in water. For a water sample 3.4 cm thick and for a and b very large, the buckling for thermal neutrons is then

$$ {}_tB_g^2 = \left(\frac{\pi}{t + 2 \cdot 0.71 \cdot 3 \cdot {}_t\lambda_S} \right)^2 = \left(\frac{\pi}{3.4 + 0.626} \right)^2 = 0.609 . $$

From Eq. (31) we find that the nonleakage fraction, or the fraction of thermalized neutrons absorbed in a 3.4 cm thick water sample is 16.7 %. In the reference food about 13.6 % of the thermalized neutrons would be absorbed in a 3.4 cm thick food sample. In a cube of water 30 cm on each side, 79 % of the thermalized neutrons are absorbed; while in food with the same dimensions about 74 % of the thermalized neutrons are absorbed. Similarly, in a cube of water 20 cm on each side 64 % of the thermalized neutrons are absorbed; while in food with the same dimensions about 57 % of the thermalized neutrons are absorbed.

9.5. Scattering of fast neutrons and diffusion of thermal neutrons

The effect of scattering of fast neutrons during slowing down and diffusion of thermal neutrons can be combined. The nonleakage of fast neutrons during slowing down is given by Eq. (25), and the nonleakage of thermal neutrons during diffusion is given by Eq. (31). The total nonleakage can be obtained from Eq. (25) by increasing the age of the neutrons. The square root of the age, $\sqrt{\tau}$, is often called the *slowing down length,* and is on the order of 5.74 cm. The quantity $M = \sqrt{\tau + L^2}$ is the *migration length*, and is on the order of 6.3 cm, where the *diffusion length* is given by: $L = \sqrt{D/\Sigma_a} \approx \sqrt{0.147/0.02}22 = 2.6$ cm. Quantitatively, the nonleakage is the obtained by replacing the age in equation (25) by M^2. We get then

$$ \exp\left(-B_g^2 \cdot M^2\right) \approx \text{nonleakage of fast and thermal neutrons.} $$

A good approximation is also obtained by multiplying the right side of equations (25) and (31). We get then that the fraction of produced neutrons that is absorbed in the sample is

$$ \frac{\exp(-B_g^2 \cdot \tau)}{1 + L^2 \cdot {}_tB_g^2} = \text{fraction of neutrons absorbed in the sample} = \text{nonleakage of neutrons,} $$

where B_g^2 and ${}_tB_g^2$ are given by Eqs. (26) and (32), respectively. We use Eq. (35) for estimating the nonleakage fraction for different dimensions of the sample.

Fig. 4 shows the nonleakage fraction of neutrons, that is, how the fraction of neutrons, that are emitted uniformly throughout the sample as fast neutrons, are slowed down, thermalized, and absorbed in a water sample. This water sample is in form of a rectangular box with dimensions a, a, and t, where the thickness t is shown on the abscissa. The 5 curves from the top are for the dimension a = 50, 40, 30, 20, and 10 cm, respectively. As the dimensions increase, the fraction of the neutron absorbed increases. For example, the middle curve (a = 30 cm) shows that the fraction 0.3, or 30 %, of the produced neutrons are absorbed in a water sample with dimensions: 30 cm, 30 cm, and 24 cm, while 70 % of the produced neutrons are scattered out or diffused out of the sides of the sample. The same curve shows that about 10 % of the neutrons are absorbed if the dimensions are 30, 30, and 12 cm, respectively. It is also seen that less than 1 % of the neutrons are absorbed when the samples are less than 4 cm thick. It is

assumed that none of the neutrons that are scattered out or diffused out of the sample are reflected back into the sample.

For small dimensions of the sample, the curves indicate that the fraction of neutrons that is absorbed in the food is very low. For example for samples, 3 to 10 cm thick, the fraction absorbed for a = 50 cm is shown in the following chart.

Sample thickness in cm	3	4	5	6	7	8	9	10
Nonleakage of neutrons in %	0.05	0.22	0.69	1.6	3.0	5.0	7.3	10

As mentioned above, however, the estimates are not accurate when the samples are thin. Also, the backscattering from the surroundings becomes increasingly important. Therefore, the number of neutrons stopped in the sample becomes not only theoretically inaccurate, but also experimentally badly defined as the sample size decreases.

Materials placed around the food carriers in the irradiation area can absorb, reflect,nd produce neutrons. Ordinary concrete may reflect about 50 to 60 % of the neutrons, while iron usually reflects about 40 %. The exact values depend on the neutron energy and the incident angle. Increasing the absorption coefficient can reduce the reflection significantly. For example, 0.3 mm thick cadmium foil or coating reduces the reflection of thermal neutrons to less than 3 %. Some of the materials will also produce neutrons. For example, Table 12 shows that about $4.7 \cdot 10^7$ neutrons per kJ of 10 MeV electron beam are produced in a thick iron. If the 5 mm thick iron conveyor is placed behind the food irradiated by electrons about 8,000 neutrons are produced per cm^2 in the iron per kGy dose in the food. About 30 % or 2,400 of these neutrons would be scattered into the food. About $1.5 \cdot 10^6/500 = 3{,}000$ neutrons are produced per gram, or about 10,000 per cm^2 of food per kGy dose. It is thus seen that the iron conveyor in this case might increase the number of neutrons in the food by about 24 %. The iron conveyor would also reflect the neutrons scattered out of the food back into the food.

At Natick Laboratories where most of the astronaut food was irradiated initially, the electron beam was bent in a horizontal direction and scanned up and down in a vertical plane. As the food inside foam boxes on “see-through” overhang carriers passed horizontally through the electron beam, most of the neutrons were scattered out of the food and absorbed in the walls of the rather large irradiation room. A good design can thus prevent most back scattering. Also, a large fraction of the neutrons thermalized within the food diffuse out of it and into the walls of the irradiation room.

A good design can reduce the fluence in several ways. In the design of a 5 and 7.5 MeV X ray facility, it is reasonable to use neutron-absorbing materials, such as boron carbide in aluminum, in and around the target area. For example, the food carriers could be made of such materials, which are commercially available; and these materials could also be used as partitions in the food carriers. Commercially available materials such as 1/8" (3.2 mm) thick plate of 35 % boron carbide (grain size of boron carbide less than 0.05 mm) in aluminum would be very effective in removing the neutrons. Even half the thickness, or about 1.5 mm, would be effective.

Neutron-producing materials, such as beryllium with threshold at 1.66 MeV, should not be used. When 7.5 MeV X rays are used, the X ray target should be limited to tantalum, gold or materials that do not produce significant number of neutrons at these energies.

One way of imposing "good manufacturing design" in a X ray facility is to impose a maximum for the neutron fluence per dose unit in the food. The neutron fluence can be easily measured. While the activity induced in the food is too small to be measured, devices for measuring the small neutron fluence are available.

10. NEUTRON CAPTURE ACTIVITY IN FOOD IRRADIATED BY X RAYS

The neutron capture activity is obtained in several steps. First, assuming that the thermal fluence is one neutron per cm^2 per kGy, the number of neutrons absorbed in each isotope per gram of food is calculated from the concentration of each isotope in the food and its thermal neutron cross-section. The number of isotope atoms that have absorbed a neutron is then divided by the lifetime of the isotope formed to get the corresponding neutron capture activities. The results are shown in column 9 of Table 14.

These activity numbers are subsequently multiplied by the actual neutron fluence. The methods used for quantification of the fluence are described in Section 9.

This activity is then converted to sievert in the humans consuming the food. This conversion is done by means of standard table; see ICRP Publication 68 and 72, reference [ICRP94] and [ICRP68].

The main results of the neutron capture activities for both X ray and electron irradiations are summarized in column 6 and 7 of Table 16. These activities can be compared to the main results of the photoneutron activities, which for 10 MeV electrons are summarized in column 6 of Table 10, as discussed in Section 6.4.

10.1. Neutron-capture activities if the fluence is one neutron per cm^2

Table 14 gives the necessary data for calculation of the neutron capture activity. In columns 2 through 5, it lists the fractional abundance, the atomic mass, the concentration of the elements in ppm (that is, the concentration in mg of element per kg of food), and the number of isotope atoms per gram of the reference food. The data are from Holden [Ho99], and Heath [He80]. Column 6 lists the thermal neutron cross-section for absorption. Column 7 lists the number of neutrons absorbed in each isotope, if the neutron fluence (= the number of neutrons that cross each cm^2) is equal to one. The half-lives are listed in column 8, and the activities in $Bq \cdot g^{-1}$ for a fluence of one neutron per cm^2 in column 9. The isotopes formed and the particles emitted in the decay are shown in column 10, and the decay energy in column 11.

The elements absorbing most of the neutrons are listed in Table 15. We see from the last column that about 89.3 % of the neutrons absorbed in food are absorbed by the ^{1}H-isotope to form the stable ^{2}H-isotope; that is, deuterium from which most of the neutrons originate. About 0.16 % will be absorbed by ^{12}C to form the stable isotope ^{13}C. 8.1 % are absorbed by nitrogen, ^{14}N, to form the stable ^{15}N-isotope, and in a (n, p) reaction the radioactive ^{14}C-isotope. About 1.6 % will be absorbed in ^{35}Cl to form the relatively stable (half-life 300,000 years) isotope ^{36}Cl; about 0.016 % will in a (n, p) reaction form ^{35}S that decays to stable ^{35}Cl (half-life 87 days); and about 0.005 % of the neutrons will form ^{38}Cl that decays to stable ^{38}A (half-life 37.2 minutes).

10.2. Actual fluence and neutron-capture activities and related dose in mSv/year

In Table 16, the first 4 columns are from Table 14; the conversion factors in the 5th column are from ICRP Publication 68. [ICRP94] In column 6, we list the dose in millisievert/year from consumption of 40 kg of food immediately after exposure to a fluence of 10^5 neutrons per cm^2. This fluence is considered as representing the maximum fluence in food irradiated with a sterilizing dose of 60 kGy by 10 MeV electrons. The fluence of 10^5 neutrons per cm^2 in food irradiated with a dose of 60 kGy by 10 MeV electrons is obtained as follows:

(a) According to Table 11, the number of neutrons produced per gram by 1 kGy of 10 MeV X rays is $1.5 \cdot 10^6$. From Section 6.4, we have that the number of neutrons produced per

gram by 1 kGy of 10 MeV electron irradiation of in muscel tissue is then: $1.5 \cdot 10^{6} \cdot 1.85 \cdot 10^{-3} = 2.8 \cdot 10^{3}$.

(b) Then the number of neutrons produced per gram of food by 60 kGy of 10 MeV X rays is $9 \cdot 10^{7}$; and the number produced per gram of food by 60 kGy of 10 MeV electron irradiation is $1.67 \cdot 10^{5}$.

(c) According to Section 9.1, the maximum fluence is in reference food irradiated by 10 MeV electrons is $50 \cdot 1.665 \cdot 10^{5} = 8.3 \cdot 10^{6}$.

(d) According to Fig. 4, the fraction of neutrons absorbed in 3.4 cm thick sample is less than about 1 % and in 8 cm thick sample less than about 6 %. Therefore, the fluence in a 3.4 cm thick sample irradiated with 10 MeV electrons to a dose of 60 kGy is less than about $8.3 \cdot 10^{4}$, or less than about 1,400 neutrons per cm^2 and per kGy. Similarly, the fluence in a sample that is 8 cm thick and irradiated to a dose of 60 kGy with 10 MeV electrons is less than $5 \cdot 10^{5}$ neutrons/cm^2, or 8,300 neutrons per cm^2 and per kGy.

Usually, the 10 MeV electrons will be used to irradiate about 3.4 cm thick food-sample from one side. Therefore, a fluence of 10^{5} neutrons per cm^2 in food irradiated to a dose of 60 kGy by 10 MeV electrons is used as a conservative estimate of the representative fluence in column 6 of Table 16. If the water content in the food increases, the number of neutrons from ^{2}H is likely to increase. However, the number of neutrons from ^{13}C is likely to decrease. The variation in the neutron production is thus likely to vary less than the variation in the water concentration.

The background radiation is about 3 mSv/year. It is seen that immediately after irradiation, the dose is about 1/10,000,000 of the background. The dose is caused mainly by $2.29 \cdot 10^{-7}$ from ^{24}Na and $1.62 \cdot 10^{-7}$ from ^{42}K. The half-lives are 15 and 12.36 hours, respectively. At the time of actual consumption, the activities would be much smaller.

In column 7 of Table 16, we list the corresponding dose in $mSv \cdot y^{-1}$ from consumption of 40 kg/year of food irradiated with 30 to 60 kGy. The fluence is assumed to be about $3 \cdot 10^{8}$ neutrons per cm^2. This fluence represents the maximum fluence in food irradiated with a sterilizing dose of 60 kGy by 5 MeV x rays, or with a dose of 30 kGy by 7.5 MeV X rays (using an X ray target of tantalum or gold). The fluence of $3 \cdot 10^{8}$ neutrons per cm^2 in food irradiated with a dose of 60 kGy by 5 MeV X rays is obtained as follows:

(a) According to Table 11, the number of neutrons produced per gram by 1 kGy of 5 MeV X rays is $4.3 \cdot 10^{5}$ in reference food.

(b) Then the maximum fluence in reference food irradiated with 60 kGy by 5 MeV X rays is: $60 \cdot 50 \cdot 4.3 \cdot 10^{5} = 1.29 \cdot 10^{9}$ neutrons per cm^2.

(c) From Fig. 4, we get that about 13 % of the neutrons are absorbed in the food if the sample dimensions are 20 cm × 20 cm × 20 cm; and about 35 % are absorbed if the dimensions are 30 cm × 30 cm × 30 cm. These dimensions are considered typical. The average of 24 % of $1.29 \cdot 10^{9}$, or $3 \cdot 10^{8}$ is therefore considered as representative fluence of neutrons per cm^2 in food irradiated with a dose of 60 kGy by 5 MeV x rays.

It is seen from column 7 in Table 16, that immediately after irradiation the dose in mSv/year is about $1.3 \cdot 10^{-3}$ or about $4.3 \cdot 10^{-4}$ of the background of about 3 mSv/year. Due to the decay, the activities of the sterilized food, which is usually consumed weeks or months after irradiation, would be smaller at the actual time of consumption. The main activities would then be from ^{32}P and ^{35}S, as can be seen from Figs. 22 and 23. Usually, the doses applied would be much smaller. These activities are best characterized as negligible or zero activities, as the natural background radiation is more than 10,000 times larger than the induced activity at the time of consumption.

11. COMPARING WITH OTHER AUTHORS' THEORETICAL ESTIMATES

The theoretical estimates and the experimental determinations of the activities by different authors often appear to be in disagreement. In the following, we will seek to explain these discrepancies by analyzing both the theoretical estimates and the experimental results of other authors.

11.1. Comparing with other theoretical estimates of photoneutron activities

The estimates by Becker are usually lower than the present estimates. The estimates of the photoneutron activities in Table 9 are usually higher than the corresponding estimates by Becker [Be77], [Be79], and [Be83] for induced activity in 10 MeV electron irradiation facilities. The highest activities, that of ^{137m}Ba, ^{114}In, and ^{108m}Ag isotopes, were not mentioned by Becker because they will have disappeared before the food is consumed as the half-lives are short. In Table 10 we consider only activities with half-lives greater than 10 minutes.

Becker estimated that the ^{199m}Hg activity produced in the ^{200}Hg(γ, n)^{199m}Hg reaction is about $2.2\cdot10^{-5}$ Bq/kg per kGy ($\approx 7\cdot10^{-4}$ Bq/kg per 32 kGy). This should be compared with the present estimate listed in Table 9 as something less than $2.8\cdot10^{-3}$ Bq/kg per kGy (or $< 2.8\cdot10^{-3}$ Bq/kg per kGy) for the same reaction. The upper limit in the present estimate is therefore about 127 times larger than Becker's value, but it is not inconsistent with Becker's value estimate. When the neutron is emitted, it may carry with it the entire excitation energy, or it may leave the compound nucleus in an excited state. We have not tried to estimate the branching ratio, but from the neutron cross-section in ^{198}Hg, it appears that the branching ratio is about 120. If this is the case, then Becker's estimates are in complete agreement with present estimates. In addition to this reaction, it is also possible to form the ^{199m}Hg isomer by exciting ^{199}Hg isotope directly, especially because the E_{th} = 6.6 MeV for the (γ, n) reaction is relatively low. The half-life is only 42.6 minutes. The activity will usually have disappeared long before the food is consumed.

Becker estimated the ^{203}Hg activity to be $2.2\cdot10^{-8}$ Bq/kg per kGy (= $7\cdot10^{-7}$ Bq/kg per 32 kGy), which is 1/55 of the present estimate of $1.2\cdot10^{-6}$.

Becker estimated the ^{69m}Zn activity to be $4.7\cdot10^{-6}$ Bq/kg per kGy (=$1.5\cdot10^{-4}$ Bq/kg per 32 kGy), which is 1/49 of the present estimate of $2.31\cdot10^{-4}$. Judging from neutron cross-section in ^{68}Zn, the branching ratio is about 1/10, which brings the present estimate to about $2.31\cdot10^{-5}$.

Becker estimated the ^{203}Pb activity to be $9.4\cdot10^{-7}$ Bq/kg per kGy (= $3\cdot10^{-5}$ Bq/kg per 32 kGy), which is 1/29 of the present estimate, $2.7\cdot10^{-5}$.

Becker estimated the ^{129m}Te activity to be $9.4\cdot10^{-9}$ Bq/kg per kGy (= $3\cdot10^{-7}$ Bq/kg per 32 kGy), which is 1/43 of the present estimate of $4.0\cdot10^{-7}$. From neutron cross-section in ^{128}Te, the branching ratio is about 1/11, which brings the present estimate to $4.4\cdot10^{-8}$ Bq/kg per kGy.

Thus Becker's estimates, when disregarding the actual branching ratio, appear only 1/30 to 1/130 of the present estimates. However, when we take the branching ratio into account the agreement is much better.

For estimating the cross-sections, Becker relied heavily on parameters that characterize the cross-sections around the giant resonance. He extrapolated these to the cross-sections close to the threshold. While this approach is reasonable for energies far above the threshold, they are not good approximations when the incident energy exceeds the threshold by small amount. The present estimates, on the other hand, focus directly on the measured cross-sections just above the threshold for the isotopes, indicated by star in columns 6 and 7 of

Table 9. For other isotopes the present values are obtained by interpolation, using the general characteristics of measured cross-sections just above the thresholds.

The estimates by Lone are similar to the present estimates. Lone [Lo90] has calculated the photonuclear activity for two isotopes in food irradiated with 10 MeV electrons. For ^{199m}Hg with a half-life of 42.6 minutes, he finds $2.1 \cdot 10^{-3}$ Bq/(kg·kGy), which is about 3/4 of the present estimate of $2.8 \cdot 10^{-3}$ Bq/(kg·kGy) in Table 9. Like Becker, he disregards the possibility for direct excitation of the isomer from ^{199}Hg. Considering that both Lone's estimate and the present estimates disregarded the branching ratio, the actual estimate should be close to $2.3 \cdot 10^{-5}$ Bq/kg per kGy

For ^{69m}Zn, Lone finds $1.4 \cdot 10^{-3}$ Bq/(kg·kGy) which is about 6.1 times greater than that of the present estimate of $2.3 \cdot 10^{-4}$ Bq/(kg·kGy). Taking the branching ratio into account would bring the present estimates to $2.3 \cdot 10^{-5}$ Bq/(kg·kGy), and Lone's estimate is the 61 times greater. However, Lone erroneously assumed that the activity was determined by the half-life of 58 minutes of the ^{69}Zn rather than by the half-life of 13.76 hours of the ^{69m}Zn metastable isotope. This results in a factor of 14.7 (=13.76·60/58). The estimate by Lone would then be 4.1 (= 61/14.7) times greater than the actual activity. The initial ratio of these two states of the isotope may vary with the exact excitation energy. In the present estimates it is assumed that all the initial activity is due to ^{69m}Zn, because this assumption results in greatest exposure (in mSv) to those consuming the food, and because any estimate must be on the side of safety. Lone's estimates are reasonably consistent with present estimates.

The estimates by Leboutet et Aucoutier are similar to the present estimates. Leboutet and Aucouturier [Le85] have estimated the activity of ^{126}I in food irradiated with 10 MeV X rays to be given by: $15000 \cdot (10\text{-}9.3)^{2.5}/(t_{1/2} / \ln 2) = 3.8 \cdot 10^{-3}$ Bq/kg per kGy. This value is 28 % of the value of $1.35 \cdot 10^{-2}$ Bq/kGy per kg in Table 8. The difference is due to the following:

(a) We use cross-sections that increase nearly linearly from zero at 9.14 to a value of 26.6 mb at 9.9 MeV, instead of their value of $15 \cdot (E\text{-}9.3)^{1/2}$ mb.

(b) We use one half of the concentration, or 0.5 ppm instead of 1 ppm, which reduces the present estimates by one half.

(c) We use slightly higher X ray intensity per kGy in the important region; for example, for 10 MeV X rays the present estimates use 48 % higher photon numbers at 8 MeV and 85 % higher at 9 MeV photon energy than those used by Leboutet and Aucouturie.

For 10 MeV x rays, Leboutet and Aucouturier [Le85] used for (γ, n) cross-sections in ^{124}Sn the values of {2.5· (E - 8.5)} mb, and a concentration of $1.2 \cdot 10^{14}$ atoms of ^{124}Sn per gram of food. For the photon number they used $\{3 \cdot 10^{12} \cdot (10 - E)/4\}$ per kGy between 6 and 10 MeV. The integration results in an activity of $3.75 \cdot 10^{-2} \cdot (10 - 8.5)^3/(t_{1/2}/\ln 2) = 7.9 \cdot 10^{-6}$ Bq/kg per kGy. This is about 1/2 of our value of $1.7 \cdot 10^{-5}$ Bq/kg per kGy of Table 8. Leboutet and Aucouturier used concentration that was about four times greater, and a cross-section that was about one fourth of that used in the present calculations. The difference is, therefore, partly due to a small difference in X ray intensity per kGy, and partly due to simplifications Leboutet and Aucouturier made; for example, the linear approximation that they used for the photon number.

The present theoretical estimates of photoneutron activities at 10 MeV are thus about equal to or larger than the above estimates by the above mentioned authors. The present estimates have sought to be on the side of safety and therefore assumed conservative estimates, and can therefore be expected to be slightly larger than the other estimates. As seen from column 6 of Table 10, the photoneutron activities are nevertheless insignificant. The

dose in mSv/year is due mainly to ^{126}I. For consumption of 50 kg/year of reference food irradiated with 10 MeV electrons to a dose of 60 kGy, the exposure dose is less than $2.35 \cdot 10^{-6}$ mSv/year, or less than 1/1,000,000 of the natural background of about 3 mSv/year. The assumption made that about 50 kg of sterilized food would be consumed immediately after irradiation is close to maximum.

11.2. Comparing with other theoretical estimates of neutron-capture activities

The different neutron capture activities are often best evaluated by comparing the neutron fluences used to obtain the activities; because if we know the fluence used, the capture activities can be determined from the cross-sections and decay times, which are usually well known. In Section 10.2, we estimated the fluence in samples 3.4 cm thick irradiated with 10 MeV electrons to be less than about 1400 neutrons per cm^2 per kGy. In Table 16, we assume a fluence value of 10^5 neutrons per cm^2 for 60 kGy irradiation, which corresponds to 1666 neutrons per cm^2 per kGy. This higher value is merely to be on the side of safety.

Becker [Be77], [Be79], [Be83] lists the activity of ^{24}Na in food irradiated by 12 MeV electrons to a dose of 32 kGy as $3 \cdot 10^{-3}$ Bq/kg, or about $9.4 \cdot 10^{-5}$ Bq/kg per kGy. At 10 MeV, Becker estimates the activity to be about $7.2 \cdot 10^{-5}$ Bq/kg per kGy, or a factor of 1.3 times smaller (mainly due to smaller X ray intensity) than at 12 MeV. He assumed (as is done in this paper) that the sodium concentration in food is 750 ppm. From Table 14 and 15, we see that the activity of sodium for the same concentration is $1.33 \cdot 10^{-7}$ Bq/kg when the fluence is one neutron per cm^2. Therefore, the fluence that Becker used must have been about 541 $=7.2 \cdot 10^{-5}/(1.33 \cdot 10^{-7})$ neutrons per cm^2 and per kGy of 10 MeV electron irradiation. Becker's value for the fluence at 10 MeV is therefore about 40% of about 1,400 neutrons per cm^2 and per kGy estimated in Section 10.2. This difference is insignificant, because of the uncertainty in determination of the fluence in thin samples. It may also be that Becker underestimated the neutron production in ^{13}C, ^{18}O, ^{14}N, and ^{17}O. At 10 MeV, the neutron production from deuterium is 44 % of the total neutron production in food, which would explain the difference between Becker's and present results.

Lone [Lo90] lists similarly the activity of ^{24}Na in food irradiated by 10 MeV electrons as being $3.9 \cdot 10^{-3}$ Bq/(kg·kGy), when the sodium concentration in food is 750 ppm. Therefore, the fluence that Lone used must have been about $2.9 \cdot 10^4$ $=3.9 \cdot 10^{-3}/(1.33 \cdot 10^{-7})$ neutrons per cm^2 and per kGy of 10 MeV electron irradiation. The large fluence, about 21 $(=2.9 \cdot 10^4/1400)$ times larger than the present estimates, is caused by different estimates in the number of neutrons scattered out of the sample (90 % versus 99 % in the present estimate). Like Becker, Lone used Monte Carlo methods for calculating the slowing down and absorption of the neutrons. Caution must however be exercised when using such general programs, as they may not yield high accuracy for relatively thin, 3.4 g/cm^2, sample. Many of the neutrons that are nearly thermalized may be scattered out of the sample, and many of the thermalized neutrons will diffuse out of the sample. However, if the value estimated by Lone is assumed right, it would result in a fluence at 60 kGy with 10 MeV electrons, that is $1.7 \cdot 10^6$ neutrons per cm^2. Even this 21-times larger number than that used in Table 16 would result in insignificant neutron capture activities when the food is irradiated with 10 MeV electrons.

Leboutet and Aucouturier [Le85] estimated in their Table 6 that the neutron production is $3.2 \cdot 10^3$ neutrons per gram per kGy for irradiation. This number is about the same as our number of $1.5 \cdot 10^6/485$ $=3.1 \cdot 10^3$. They estimated the macroscopic absorption cross-section in food to be between 0.024 and 0.020 cm^2/g. This is consistent with our value for the reference food of 0.020 cm^2/g in food and 0.022 in water. **Leboutet and Aucouturier** estimated the number of neutrons captured per gram in 10 MeV electron irradiation of a sample that is 8 cm

thick to be about 3645 per 2 kGy (see Table 6 of their paper), or 1822 per gram and per kGy. Thus, they find that about 57 % of the produced neutrons are absorbed in the 8 cm thick sample, while the present calculations, according to Fig. 4 estimates that only 6 % are absorbed in the 8 cm thick sample. Their fluence number is therefore about 9 times larger than the present estimates. The corresponding activities would still be insignificant.

.

12. COMPARING THE THEORY WITH EXPERIMENTAL RESULTS

The extensive experimental work by Glass and Smith [Gl60a], Smith [Sm62], Kruger and Wilson [Kr60], and Meneely [Me64] failed to detect any induced activity in food irradiated with 50 kGy and electron energies at or below 11.2 MeV. This is consistent with the present estimates, with experiments at Natick Laboratories, and with experiments by Miller and Jensen [Mi87] at Risoe. Still, some of the experiments at higher energies may appear to be inconsistent with the theoretical predictions and will therefore be discussed.

12.1. Comparing with experimental results of Glass and Smith

The present estimates of photoneutron activities are consistent with direct experimental results by Glass and Smith [Gl60a] who indicated that no measurable photoneutron activity could be detected. For increasing their sensitivity, they measured the activity produced in pure elements. In the case of iodine, Glass and Smith measured, for 12 MeV x rays, an ^{126}I activity of $5.25 \cdot 10^5$ Bq/(kg·kGy) per gram of pure element (= 0.71 microcuries per gram and per 5 Megarad). This corresponds to 0.26 Bq/(kg·kGy) for a concentration of 0.5 ppm of ^{127}I in the food irradiated with 12 MeV x rays. Using the measured cross-sections for ^{127}I(ν, n)^{126}I reaction, and the present theoretical estimates for the X ray spectra, we obtain a theoretical estimate of 0.16 Bq/(kg·kGy) for a concentration of 0.5 ppm of ^{127}I in the food irradiated with 12 MeV x rays. We believe that the difference between 0.26 and 0.16 Bq/(kg·kGy) is within the experimental accuracy of both the cross-section and the dose measurements.

12.2. Comparing with experimental results of Smith

At 12 MeV, Smith measured the neutron capture activity of ^{24}Na in ham in a No. 10 can to be about 0.5 Bq/kg per kGy. He reports finding 0.68 ± 0.24 pCi per gram of ham per 5 Mrad. (See, for example, Table IV of the final report by Smith [Sm62]).

We will adjust for energy difference. According to present Table 11, the neutron production at 12 MeV is about 2.07 (= $3.1 \cdot 10^6/(1.5 \cdot 10^6)$) times that at 10 MeV. In the 3.4 cm thick sample, the neutron fluence at 12 MeV is then less than about 1,400·2.07 = 2,800, and the ^{24}Na activity at 12 MeV should be less than about $2800 \cdot 1.33 \cdot 10^{-7} = 3.7 \cdot 10^{-4}$ Bq/kg per kGy. The activity measured by Smith is then 1350 times the present estimate for the 3.4 cm thick sample. For resolving this apparent discrepancy between Smith's and our results, we will in the following consider the experimental designs and assumptions made.

We will correct for the concentration effect. The concentration of sodium in the ham sample that Smith used is not known. (The sodium may be in the form of sodium chloride, sodium nitrate and nitrite, and possibly also in the form of sodium phosphates and sodium ascorbate). It is likely to have been about 7,500 to 9,800 ppm (corresponding to 2 to 2.5 % salt), and thus containing about 11.5 (= 8650/750) times the amount of sodium assumed in our reference sample. After this correction there still remains a significant difference, a factor on the order of 1350/11.5 = 117 when compared with present estimates at 12 MeV.

We will correct for increased X ray intensity. Smith irradiated the food in a tinplated No. 10 can, which is about 15.2 cm (6") in diameter, 17.8 cm (7") high, and contains about 3 kg of ham. The can is usually made of iron (90%) and tin (10%). The beam was made to strike the lid (the end) of the can, which therefore was an X ray target of iron, about 0.134 g/cm^2 and tin 0.013 g/cm^2. This "X ray target" increases the total X ray intensity penetrating the food, and therefore also the neutron production in the food by approximately 36 %. In addition, to obtain an average dose of 1 kGy, the authors increased the dose by about

a factor of 3 (17.8/6), because the length of the can is about 3 times the maximum penetration. The actual neutron production per gram of food is then 3·1.36 = 4.1 times larger. To this we must add the neutron production in the can, which increases the neutron production by about 12% as the X rays enter and exit the can. The total neutron production is then about factor 4.6 times larger than in food irradiated in thin, flexible packages. The discrepancy factor is then reduced from 117 to 117/4.6 = 25.5.

We will correct for the irradiation geometry. The present estimates assumed the irradiation procedures and the irradiation geometry that were used at U. S. Army Natick Laboratories. At these Laboratories, the electron energy was well defined and calibrated within a narrow half-width at half maximum of ± 0.25 MeV. The accelerator window was made of 0.4 mm thick aluminum foil. The food, packaged in thin plastic aluminum laminates, was irradiated in thermally insulating plastic-foam boxes (for thermal insulation) in open, or see through, aluminum carriers on an overhanging conveyor. The thickness of the food in flexible packages at 10 MeV was less than 3.4 cm. Therefore, a very small fraction (about 1%) of the neutrons produced are thermalized and absorbed in the food. Behind the overhanging carriers, the "beam catcher" (which absorbs that part of the beam that penetrates the sample, or passes between the samples) was made of a water cooled aluminum (2S-aluminum, which is very pure aluminum). The threshold for the (γ, n) reaction in aluminum is 13.06 MeV. Because of this high threshold energy, no neutrons are emitted from the aluminum. Thus, at Natick the selection of materials in the target area was intentionally made so as to minimize the X ray and neutron production. We will consider this design and procedures as being in accordance with good manufacturing practices.

On the other hand, Smith used the linear accelerator facility at General Atomics, La Jolla, San Diego, California. This accelerator was made for higher energy about 24 to 32 MeV [SM62]. Usually, when the energy is lowered to 12 MeV from optimum at 24 MeV, the energy spectrum becomes rather broad. For selecting the energy, the beam was magnetically bent and made to go through slits. In that process, X rays and neutrons are created. Also the apparatus holding and moving the can of food will create X rays and produce neutrons. The description is not adequate to predict accurately the effect. However, the effect on neutron fluence in the can could be significant and result in neutron fluence increase by a factor of 1.2 to 2. This brings the factor 25.5 down to 21 to 13.

We will correct for the escape of neutrons from the large food sample. The large food sample, No. 10 can, in Smith's experiments means that a large fraction of the neutrons that are produced will be slowed down, thermalized, and absorbed in the food. The can and the surrounding structure used to rotate the can act as neutron reflectors and moderators.

In the 3.4 cm thick food sample assumed in the present estimates, the fraction of produced neutrons that are slowed down and absorbed is about 1 %. In No. 10 can, the fraction of neutrons slowed down (according to Eq. (13)) is about 24% of those produced; and the fraction of thermal neutrons that are absorbed is about 55%. Thus, of the neutron produced about 24·0.55 = 13.2% is absorbed. Of the neutrons produced about, 13.2 times greater number is absorbed in number 10 can than in 3.4 cm sample. The structures that hold the can will reflect the fast and thermal neutrons produced in the food back into the food and thereby increase the neutron fluence in the food by 40 %. The factor 13.2 is then increased to about 18. This brings the factor 21 to 1.2 and the factor 13 to 0.7.

Although these are only rough estimates, they indicate that the many differences in experimental design adequately explain the difference between the theoretical estimates and Smith's measurements, which therefore can be considered to be in agreement with present estimates. We draw attention to the fact that the experiments by Smith do not represent actual applications, as the sample thickness (17.8 cm) is much too large for uniform dose distribution at the lower energies (12 MeV). This was fully realized by Smith; but the main

focus of his experiment was activity at about 24 MeV, for which his design is more appropriate.

12.3. Comparing with experimental results of Miller and Jensen

Some of the topics discussed above can help explain the relatively large activity of ^{24}Na observed by Miller and Jensen [Mi87] at the relatively high energy of 13.5 MeV. These researchers measured about 80 times higher ^{24}Na activity than that predicted by Becker. They used the linear accelerator at Risø in Denmark, where the beam is directed vertically down on the beef sample in an aluminum tray on a horizontal steel belt conveyor. The sample thickness was 2.5 cm and the area 20×20 cm^2 for a weight of about 1 kg. The energy spread, shown in their Fig. 1, was very large. The sodium concentration was 692 ppm in the beef versus 750 ppm assumed in Becker's and the present estimates.

First, we will correct for neutron production in the food. Becker [Be79]) and Becker and Martin [Be80] assumed that the neutron production in deuterium dominated that of other isotopes. As Table 11 shows, the total neutron production at 13.5 MeV in reference food is about $5.3 \cdot 10^6$ per g and per kGy X ray dose in food versus $6.4 \cdot 10^5$ from deuterium alone, or 8.3 times greater than that from deuterium alone. Therefore, Becker underestimated the neutron production at 13.5 MeV by factor of about 8.3 per kGy X ray dose. This correction to Becker's estimates reduces the discrepancy from a factor of 80 to 9.6 (= 80/8.3).

Second, we will correct for energy spread. As Figure 1 of Miller and Jensen's paper shows, some of the maximum beam energy reaches beyond 14.5 MeV when the average energy was listed as 13.5 MeV. Considering that the induced activity is roughly proportional to $(E - E_{th})^3$, where E is the beam energy and E_{th} the threshold for (γ, n) reaction, means that the activity increases sharply with energy. For the same beam energy distribution, the average of $(E - E_{th})^3$ is slightly higher than $(E_{av} - E_{th})^3$, where E_{av} is the average energy. In the present case, where many of the neutron emitters have relatively low thresholds, this causes only a small correction to the number of neutrons produced in the food, but not for those produced in the aluminum tray and iron conveyor.

Third, we will correct for the neutron production in the conveyor. The number of neutrons produced per gram of food at 13.5 MeV is about 3.53 times greater than at 10 MeV (see Table 11). The total number of neutrons produced by 13.5 MeV electrons in 2.5 cm thick food sample is then about: $(5.3 \cdot 10^6/500) \cdot 2.5 = 2.7 \cdot 10^4$ per cm^2 per kGy. This number should be compared with the number of neutrons entering the food from surroundings.

At 13.5 MeV, neutrons from iron conveyor and the aluminum tray may enter the food. At Risø, the horizontal conveyor belt is made of rather heavy steel wire netting rolling on steel rollers. As shown in Table 12 and Fig. 11, a thick "beam catcher" of steel irradiated with 13.5 MeV electrons will emit about $2.8 \cdot 10^9$ neutrons per kJ of incident beam power. The X rays that produce the neutrons in the conveyor are in the present case generated mostly when the electrons are stopped in the food (and not in the steel conveyor). The intensity in the X rays produced in the food is 3.27 times smaller than that produced in the iron. We have therefore that at 13.5 MeV, 1 kJ per cm^2 of incident beam power, which corresponds to $74 \cdot 10^{-6}$ coulomb per cm^2, will result in about 150 kGy electron dose in the food. Therefore, if the beam is stopped in the food and the X rays produced in the food impinge on a thick plate of steel behind the food, then the number of neutrons produced in the steel is about $2.8 \cdot 10^9/(150 \cdot 3.27) = 5.7 \cdot 10^6$ per kGy electron dose in the food. The steel plate (actually, steel belt, steel rollers, and a conveyor structure of steel) behind the food is not thick, but only about 5 mm. This will reduce the number of neutrons produced in the steel conveyor by about a factor of 8.5 to about $5.7 \cdot 10^6/8.5 = 6.7 \cdot 10^5$ neutrons per kGy electron dose in the food. The initial emission of the neutrons from the steel is isotropic. It appears reasonable that about 30

% of $6.7 \cdot 10^5$, or about $2 \cdot 10^5$ of the neutrons from the iron conveyor will reach the food per kGy.

We also have that a significant fraction of the electron beam exceeds the 13.06 MeV threshold in aluminum. With the energy spread shown by Miller and Jensen, about $5 \cdot 10^6$ neutrons are produced per g of aluminum per kGy in the food. About 0.3 % of $5 \cdot 10^6$ is produced in the window and about 2.0 % in the aluminum tray, for a total of $1.1 \cdot 10^5$. Of these, about 30 % of $1.1 \cdot 10^5$, or $3.3 \cdot 10^4$ neutrons per kGy will enter the food. The numbers of neutrons: $2 \cdot 10^5$ from the steel conveyor, $3.3 \cdot 10^4$ from the aluminum tray and window, and $2.7 \cdot 10^4$ from the food add for a total of $2.85 \cdot 10^5$ neutrons produced per cm^2. This is about 10 times the total number $2.7 \cdot 10^4$ per cm^2 of neutrons produced in the food. This would change the discrepancy factor from 9.6 to 0.96.

These are only rough estimates (and the agreement is better than is to be expected), but they indicate that the difference in experimental design adequately explains the difference between the theoretical estimates and Miller and Jensen's observations. These experiments can therefore be considered to confirm the present theoretical estimates.

Miller and Jensen could not detect any neutron activity at 10 MeV, because of 60 times lower neutron production in the steel conveyor and none in the aluminum trays, and because of lower neutron production in ^{13}C, ^{14}N, ^{18}O, and ^{17}O in the food; see Table 11. The observation by Miller and Jensen are thus consistent with the present estimates. Their observations underscore the importance of adhering to "good manufacturing practices" and present guidelines of the international Codex Alimentarius Commission.

12.4. Comparing with experimental results of McKeown et al.

The recent experiments by McKeown et al. [Mc98] are consistent with present estimates. They found that a 2.5 g/cm^2 (=1.5 mm) thick tantalum target produced at 10 MeV $1.8 \cdot 10^9$ and at 11 MeV $4.2 \cdot 10^9$ neutrons per kJ of incident electron beam. This result may be compared with the values in Table 12, which for very thick targets show $1.1 \cdot 10^{10}$ and $3.0 \cdot 10^{10}$ neutrons per kJ at 10 and 11 MeV. We adjust these production numbers by taking into account the attenuation in the target; that is, we multiply the production number by $(1 - \exp(-\mu_t \cdot x))$. We get then for a target that is $x = 2.5$ g/cm^2 thick, that the number produced is $0.112 \cdot 1.1 \cdot 10^{10} = 1.2 \cdot 10^9$ and $0.114 \cdot 3.0 \cdot 10^{10} = 3.4 \cdot 10^9$ neutrons per kJ. These theoretical estimates, within the error margin, are in agreement with the experiments by McKeown et al. The authors' results show that at 10 MeV, the neutron production in the tantalum X ray target is very significant. However, as Table 12 shows, the neutron production at 7.5 MeV is insignificant.

13. GOOD MANUFACTURING PRACTICES

For food in trade, "good manufacturing practices" (GMP) in all aspects of food production, food handling, and processing are usually mandatory. This includes proper design and operational controls of food irradiation facilities, which usually would have to be licensed for processing the food; see for example, the Codex Alimentarius General Standards for Irradiated Foods [Anon84].

Besides the usual good hygienic aspects in food processing facilities, it is of course necessary to assure adherence to all regulations about workers' safety, and all health physics aspects, including design of facilities, radiation monitoring, and control; see for example, Brynjolfsson and Martin III [Br71], Swanson [Sw79b] and [IAEA96]. National and international standards are already in place.

For processing of food, good manufacturing practices require that the proper dose be calibrated, monitored and recorded. In case of accelerators, it is usually reasonable to require that the electron energy be calibrated, monitored and recorded. The Codex Alimentarius General Standards for Irradiated Foods also requires the staff to receive training that assures proper operation of the facilities.

In research facilities and in medical applications of electron accelerators, the rather low beam power is used for relatively short duration each day. The buildup of induced activity in the shielding and the equipment within the irradiation room is then not a problem.

However, when powerful accelerators are used for X ray production by industry in nearly continuous operation, the possible buildup of small activity within the conveyor and the irradiation room must be considered. This is usually of concern only in facilities operating at energies higher than those used for food irradiation; see for example, a monograph on the subject by Swanson [Sw79b]. When we draw attention to this in the case of food irradiation facilities, it is because we should be unusually strict about preventing any contamination.

13.1. Good manufacturing practices in gamma ray facilities

Good manufacturing practices for the processing, encapsulation, and shipping, of γ ray sources, and for design and maintenance of the irradiation facilities are well established. Since no activity is induced in food or in the irradiation cell or its shielding, no additional "good manufacturing practices" are required. "Good manufacturing practices" for operation and for dose control are described elsewhere. See for example, references [Anon77b] and [Anon84].

13.2. Good manufacturing practices in electron accelerator facilities

Good manufacturing practices in all aspects of food production, food handling and processing in electron accelerator facilities are also well established. The dose control differs from that in isotope facilities; but also in this case, the "good manufacturing practices" for the dose control are well established, and are described elsewhere. See, for example, references [Anon77b] and [Anon84]; International Organization for Standard, ISO 11137, (1994); and American Standards for Testing and Materials, Annual Book of ASTM Standards, ASTM Standard E 1204-88, (1993). The two last mentioned standards are frequently updated and the latest versions should be used.

Certain aspects of the energy control and design of electron accelerator facilities are relevant to induced activity production and will therefore be considered here. Good energy control in an electron facility is important. Many aspects such as dose control, dose monitoring, and recording are easier if the energy is well controlled because the energy affects

the depth dose distribution and scanner width. Also, the accelerator operation is likely to be more reliable when energy is fairly homogeneous. The electron beam is then more easily focused and is less likely to hit internal structures of the accelerator, which causes out-gassing, that in turn may lead to instabilities. Methods for automatic control and recording of energy, scanner-width and dose have been developed; see for example, references [Br73] and [Anon77b].

Even for powerful (above 30 kW electron beam power) electron accelerators below 10 MeV, buildup of activity is not a problem except within 1 meter of the target area where some activities can buildup in some materials. Within these areas, small activities of ^{64}Cu, with half-life of 12.9 hours will buildup due to neutron capture, ^{63}Cu (n,γ)^{64}Cu, and photoneutrons, ^{65}Cu (γ, n)^{64}Cu, reactions. Manganese in steel and iron (often 1 to 2 % and exceptionally 10%) has a relatively high absorption coefficient for thermal neutrons. Some activity of ^{56}Mn, with half-life of 2.58 hours, will then buildup in steel structures in the target area. Steel often contains also a significant amount of chromium (1 to 20 %). Some ^{51}Cr with half-life of 27.7 days may then buildup. If pure aluminum, aluminum magnesium alloy, or aluminum containing boron carbide is the material used in the conveyor and the carriers that are used for bringing food into the irradiation area, this should not be a problem. For reducing the neutron exposure, materials containing boron or cadmium can be used. The walls, ceiling, and floor can be painted by relatively radiation resistant epoxy paints for the purpose of reducing dust in the air.

For an electron accelerator facility, we suggest that good manufacturing practices stipulate that:

(1) The maximum of the energy shall be less or equal to 10 MeV.
(2) Less than 2% of the beam electrons shall have energy above 10.5 MeV.
(3) The irradiation area should not contain materials that produce neutrons, such as uranium, lead, or tungsten.
(4) The design should aim at reducing the thermal neutron fluence for the dose applied to the food to a value less than 10^5 per cm^2 in one-sided irradiation (3.4 cm thick sample) and to a value of less than 10^6 per cm^2 in a two sided irradiation (about 8 cm thick sample).

The low fluence values are not dictated by need, but rather by the fact that a higher value indicates less than good practice in the design and operation of the facility.

13.3. Good manufacturing practices in X ray facilities

Although several orders of magnitude smaller than the natural activity in food, the induced activity produced in a 5 to 7.5 MeV X ray facility will usually be several orders of magnitude greater than that produced in a 10 MeV electron accelerator facility. The activities produced by 5 MeV X rays are due to captures of neutrons produced from ^{2}H in the food. At 7.5 MeV, some neutrons are also produced from ^{13}C, and ^{17}O. Neutron absorbers in the target area and in the food carriers can reduce the neutron-capture activities. When the facility is designed and operated properly, the activities are insignificant.

In a 5 MeV X ray facility, the only activity of concern is that induced by neutrons produced from deuterium in the food. Proper design and good manufacturing practices require that the energy is well calibrated and monitored, and that care is taken in the design such as to eliminate neutron production in beryllium or heavy water.

In a 7.5 MeV X ray facility, the neutron production in the food would be about factor 2 greater than that in a 5 MeV facility. About $8.3 \cdot 10^5$ neutrons per kGy are produced at 7.5 MeV and about $4.3 \cdot 10^5$ neutrons per kGy at 5 MeV, as can be seen from the last column in Table 11.

At 7.5 MeV, the neutron production in the X ray target can be significant. However, it can be reduced or eliminated by proper design; that is, by selecting in the target area only materials with threshold energies above 7.5 MeV. For minimizing the neutron production in the X ray target, it is recommended that the X ray target be made of tantalum or gold, and not of the frequently used tungsten, which at 7.5 MeV produces a significant number of neutrons. Production of neutrons from water, including cooling water, in the X ray area can be minimized and made insignificant. Neutron absorbers can reduce the neutron flux where their use is feasible.

Cost considerations will usually favor the use of electrons directly for high dose applications; and the cost considerations will often limit the use of X rays to low dose applications, such as insect disinfestation, elimination of trichina in pork (1 kGy), etc. As the activity is proportional to dose, the neutron activation is insignificant in well-designed facilities for these applications. The X rays would compete with gamma ray sources, principally, cobalt-60.

For a large industrial X ray facility, we suggest that good manufacturing practices stipulate that: 1) with exception of natural levels of ^{2}H, ^{13}C, and ^{17}O in food and water, no neutron producing materials should be used in the target area (including the X ray converter); 2) no part of the energy distribution in the electron beam should exceed the threshold energy for neutron production except for the mentioned natural isotopes in food and water; 3) the walls, ceiling, and the floors in the irradiation room should preferably be made of boron-containing concrete; 4) the walls, ceiling and floors should be painted with epoxy paints or similar radiation resistant paints; 5) the materials used in the conveyor and the carriers should not result in buildup of any significant activities; and 6) for the dose applied to the food, the design should reduce the average thermal neutron fluence in every carrier load of food to a value less than $3 \cdot 10^{8}$ per cm^{2}.

13.4. Monitoring the neutron fluence in X ray facilities for food irradiation

As the neutron flux depends on many design parameters that may not have been anticipated in these estimates, the above calculations, estimates and recommendations should only serve as rough guide. In X ray facilities, it is important therefore to measure the neutron fluence in the food to assure compliance with the requirement that the food should not have any significant amount of any induced radioactivity as discussed in Section 2.5. There are many different methods of neutron detection. One method consists of activation of indium foil (sometimes, 100 cm^{2} and 0.5 mm thick). Indium has a very large cross-section for thermal neutrons. In food it is a contaminant usually with concentration less than 10^{-8}. The element has a density of 7.31 $g \cdot cm^{-3}$. A one square centimeter of 0.5 mm thick plate of indium would have a macroscopic cross-section of about 0.134 cm^{2} for the reaction of interest to us (that is, transformation of ^{115}In to ^{116m}In, followed by a decay with a half-life of 54.1 minute to ^{116}Sn). Another method is based on activation of gold foils. If the food has the elemental composition of the reference food, and if it is to be consumed 48 hours after exiting the radiation cell, the fluence should be less than $3 \cdot 10^{8}$. Neutron absorbers could be used wherever possible for reducing the neutron exposure dose. For example, in the carriers bringing the food into the irradiation area, materials containing boron could be used. Epoxy paints that are fairly resistant to irradiation are often used on the wall, ceiling, and floors to reduce dust.

14. CONCLUSIONS

The increase in radiation background dose from consumption of food irradiated with gamma rays from cobalt-60 or Cs-137 to an average dose below 60 kGy, is insignificant. It is best characterized as zero, as the increase from consumption of 50 kg/year immediately after irradiation is less than 10^{-8} mSv/year, or less than 1/300,000,000 of the natural background exposure, which is about 3 mSv/year.

The increase in dose from consumption of food irradiated with 10 MeV electrons to an average dose below 60 kGy, is insignificant. It is best characterized as zero, as the increase from consumption of 50 kg/year immediately after irradiation is less than $5 \cdot 10^{-6}$ mSv/year, or less than 5/3,000,000 of the natural background exposure.

Radioactivity produced in food when irradiated to a dose of 60 kGy with 5 MeV X rays, or to a dose of 30 kGy with 7.5 MeV X rays is larger than that produced by 10 MeV electrons; but it is an insignificant fraction of the natural radioactivity in the food. An individual consuming annually 40 kg of food more than two days after irradiation with a dose of 30 kGy in case of 7.5 MeV X rays and 60 kGy in case of 5 MeV X rays would receive less than 10^{-4} mSv/year. This exposure dose level is 1/30,000 of the natural background exposure.

For comparison it is useful to realize that the increase in background due to one flight from Boston to San Francisco is about 0.012 mSv, or about 10,000 times greater than the annual increase in background from consuming food sterilized by 10 MeV electrons immediately after irradiation, and about 100 times greater than the increase due to consumption of food sterilized by X rays.

The normal variation in the background radiation caused by natural radioactivity in food is many times greater than that received by airplane passengers on their flight from Boston to San Francisco.

REFERENCES

[Ah91] **Ahmed, J. U.** (1991). High levels of natural radiation: Report of an international conference in Ramsar. IAEA Bulletin **33**(2), 36–38.

[Anon77a]. (1977). "Sources and effects of ionizing radiation." United Nations Scientific Committee on Effects of Atomic Radiation 1977 Report to the General Assembly, with annexes. United Nations Publications. Sales No. E.77.IX.I. United Nations, New York.

[Anon77b]. (1977). "Manual of food irradiation dosimetry." Technical Report Series No. 178. International Atomic Energy Agency. Published by IAEA, Vienna. STI/DOC/10/178; ISBN 92-0-115277-9.

[Anon80] (1980). **BEIR** report. "The effects on populations of exposure to low levels of radiation." Report of the Committee on the Biological Effects of Ionizing Radiations, Division of Medical Sciences, National Research Council. National Academy Press, Washington, D. C.

[Anon84] (1984). "Codex alimentarius standards for irradiated foods" and "Recommended international code of practice for the operation of radiation facilities used for the treatment of foods." In Joint FAO/WHO Food Standards Programme, Codex Alimentarius Commission Vol. XV. Published by Food and Agricultural Organization of the United Nations and World Health Organization, Rome, 1984.

[Anon90] (1990). Food safety aspects relating to the application of X ray surveillance equipment: memorandum from a WHO meeting. Bull. WHO 68, 297–301.

[Be77] **Becker, R. L.** (1977). "Radioactivity induced in foods by 10-MeV electron irradiation." Contract No. DAAG17-76-0060. U. S. Army Natick Research and Development Command, Natick, Massachusetts 01760.

[Be79] **Becker, R. L.** (1979). "A determination of the radioactivity induced in foods as a result of irradiation by electrons of energy between 10 and 16 MeV." Contract No. DAAK60-78-R-0007. U. S. Army Natick Research and Development Command, Natick, Massachusetts 01760.

[Be83] **Becker, R. L.** (1983). Absence of induced radioactivity in irradiated foods. In: Recent advances in food irradiation. Eds. Elias, P. S. and Cohen, A. J. Published by Elsevier Biomedical. ISBN 0-444-80499-4. Pp. 285–313.

[Be80] **Becker, R. L. and Martin, T. G. III.** (1980). "Radioactivity induced in food by electron irradiation." An unpublished report. (See also Becker 1979 above.)

[BEIR III 80] (1980). **BEIR III** report. "The effect on populations of exposure to low levels of ionizing radiation" A report by the Committee on Biological Effects of Ionizing Radiations, Board on Radiation Effects Research Commission on Life Sciences, National Research Council, USA. National Academy Press, Washington, D.C. 524 pp.

[BEIR V 90] (1990). **BEIR V** Report. "Health effects of exposure to low levels of ionizing radiation." A report by the Committee on the Biological Effects of Ionizing Radiations, Board on Radiation Effects Research Commission on Life Sciences, National Research Council, USA. National Academy Press, Washington, D. C.

[Be76] **Berman, B. L.** (1976). "Atlas of photoneutron cross-sections obtained with monoenergetic photons." Report sponsored by U. S. Energy Research and Development Administration under W-7405-Eng-48.

[Bi85] **Birenbaum, S., Kahane, S., and Moreh, R.** (1985). Absolute cross-section for the photodisintegration of deuterium. *Phys. Rev. C.* **32**(6), 1825–1829.

[Bl49] **Blair, J. S.** (1949). Electro-disintegration of nuclei. *Phys. Rev.* **75**, 907–908.

[Br73] **Brynjolfsson, A.** (1973). Definition and control of processing parameters for radappertization of beef for wholesomeness studies in the United States of America. In "Radiation Preservation of Food." (Proceedings of an International Symposium Bombay, 13 – 17 November 1972, Jointly organized by the IAEA and FAO of the United Nations.) Published by IAEA, Vienna, 1973, STI/PUB/317. Pp. 549–560.

[Br75] **Brynjolfsson, A.** (1975). Photonuclear Reactions in Water. Chapter 9.1.10.5 in "Engineering compendium on radiation shielding, Vol. II, Shielding materials." Ed. R. Jaeger et al. Sponsored by International Atomic Energy Agency. Springer-Verlag, Berlin, Heidelberg, New York. Chapter 9.1.10, pp. 46–55.

[Br77] **Brynjolfsson, A.** (1978). Mathematical models for microbial kill by radiation. In "Food Preservation by Irradiation." (Proceedings of an International Symposium on Food Preservation by Irradiation, Jointly organized by the IAEA, FAO, of the United Nations, and WHO, and held in Wageningen, 21 – 25 November 1977.) Published by IAEA, Vienna, 1978, STI/PUB/470, ISBN 92-0-010278-6. Vol. I; pp. 227–239.

[Br71] **Brynjolfsson, A., and Martin, T. G.** (1971). Bremsstrahlung production and shielding of static and linear electron accelerators below 50 MeV. Toxic gas production, required exhaust rates, and radiation protection instrumentation. *Int. J. Appl. Radiat. Isot.* **22**, 29–40.

[Co95] **Cohen, B. L.** (1995). Test of the linear-no threshold theory of radiation carcinogenesis for inhaled radon decay products. *Health Phys.* **68**(2), pp. 157–174.

[Co98a] **Cohen, B. L.** (1998). Lung cancer rate vs. mean radon level in U.S. counties of various characteristics. *Health Phys.* **72**(1), pp. 114–119.

[Co98b**] Cohen, B. L.** (1998). Response to Lubin's proposed explanations of our discrepancy. *Health Phys.* **75**(1).

[Co98c] **Cohen, B. L.** (1998). Response to criticisms of Smith et al. *Health Phys.* **75**(1).

[Ca89] **Clarke, R. H., and Southwood, T. R. E.** (1989). Risks from ionizing radiation. *Nature* **338**, 197–198.

[Cu99] **Cuttler J. M.** (1999). "Resolving the controversy over beneficial effects of ionizing radiation." In Proceedings of WONUC Conference on the Effects of Low and Very Low Doses of Ionizing Radiation on Health Organized by the World Council of Nuclear Workers, held in Versailles, France, 1999 June 16–18.

[Di88] **Dietrich, S. S., and Berman, B. L.** (1988). Atlas of photoneutron cross-sections obtained with monoenergetic photons. *Atomic Data and Nuclear Tables* **38**(2), 199–338.

[Do96] **Doe, John B.** (1996). "Conceptual planning: A guide to a better planet," 3d ed. Reading, MA: SmithJones.

[Gl60a] **Glass, A., and Smith H. D.** (1960). "Radioactivities produced in foods by high-energy electrons." Report No. 10. Summary Technical Report, dated January 14, 1960, under contract: DA 19-129-QM -1100. Stanford Research Institute Project No. SU-2424. Prepared for Quartermaster Food and Container Institute for the Armed Forces, Chicago, IL, and Research and Engineering Center, Natick, MA. See in particular pp. 45 to 52.

[Gl60b] **Glass, A., and Smith H. D.** (1960). "Radioactive isomer production in foods by gamma rays and x rays." Final report, dated October 3, 1960, under contract: DA 19-129-QM-1511. Stanford Research Institute Project No. SU-3081. Quartermaster Food and Container Institute for the Armed Forces, Research and Engineering Command, Quartermaster Corps, U. S. Army, Chicago, IL. See in particular Table IV.

[GlEd] **Glasstone, S., and Edlund, M. C.** No publication date. "The elements of nuclear reactor theory." MacMillan and Co. Limited, St. Martin's Street, London. See in particular chapter VII.

[Ha87] **Harley, J. H.** (1987). Including reply by Hickey et al. In *Health Physics*, Vol. **52**(1); pp. 103–104.

[Ha92] **Hashizume, A., and Nakano, K.** (1992). "Induced radioactivity by gamma rays. Photonuclear reactions by gamma rays below 10 MeV." The final report of the Food Irradiation Research Committee for 1986–1991. Published by Japan Radioisotope Association, Tokyo, Japan. Pp. 29–45. (The values of 88.2, 86.4, 1361 Bq/kg of element per kGy in 61 minute irradiation of Sr-87m, In-113m, and In-115m, respectively, are obtained through private communication, a fax dated Sep. 19, 1997 to Dr. F. Käferstein, Food Safety Unit, WHO)

[He80] **Heath, R. L.** (1968) and (1980). Table of isotopes. In "CRC Hand Book of Chemistry and Physics," 49th edition; editor: R. C. Weast; pp. B-4 to B-92. A different version was published ibid., 61st edition (1980), pp. B-258 to B-342.

[Hi81] **Hickey, R. J.; Bowers, E. J.; Spence, D. E. Zemel, B. S.; Clelland, A. B., and Clelland, R. C.** (1981). Low level ionizing radiation and human mortality: Multi-regional epidemiological studies. *Health Physics* **40**; pp. 625–641. See also a letter to the editor by John H. Harley and Hickey et al.'s resply in *Health Physics*, Vol. **52**(1); pp. 103–104, 1987.

[Ha87] **Harley, J. H.** (1987); and Hickey et al.'s reply in *Health Physics*, Vol. **52**(1); pp. 103–104, 1987.

[Ho99] **Holden, N. E.** (1991) and (1999). Table of the isotopes. Report (revised 1991) from the High Flux Beam Reactor, Reactor Division, Brookhaven National Laboratory, Upton, New York, 11973. A similar version is also found in "CRC Handbook of Chemistry and Physics," 79th edition, 1998–1999; editor: D. R. Lide; CRC Press, Bocca Raton, Boston, London, New York, Washington DC; pp. 11–41 to 11–149.

[Hu63] **Hunt, D. O., Brynjolfsson, A., and Cooper, R. D.** (1963). "Handbook of photonuclear reactions." Tech. Rep. FD-1; Proj. Ref. 1-K-0-25601-A-033; U. S. Army Natick Laboratories, Natick, MA 01760.

[IAEA96] (1996). "International basic safety standards for protection against ionizing radiation and for the safety of radiation sources." Jointly sponsored by: Food and Agricultural Organization of the United Nations, International Atomic Energy Agency, International Labor Organization, Nuclear Energy Agency of the Organization for Economic Co-operation and Development, Pan American Health Organization, World Health Organization."Safety series No. 115 Published by International Atomic Energy Agency, Vienna, 1996.

[ICRP94] **ICRP** Publication 68. (1994). "Dose coefficients for intakes of radionuclides by workers" (Replacement of ICRP Publication 61. Published for the International Commission on Radiological Protection. *Annals of the ICRP* Vol. **24**(4), 1994. See also IAEA. 1996. International basic safety standards for protection against ionizing radiation and for the safety of radiation sources. Jointly sponsored by: Food and Agricultural

Organization of the United Nations, International Atomic Energy Agency, International Labor Organization, Nuclear Energy Agency of the Organization for Economic Co-operation and Development, Pan American Health Organization, World Health Organization." Safety series No. 115 Published by International Atomic Energy Agency, Vienna, 1996.

[ICRP96] **ICRP** Publication 72. (1996). "Age-dependent doses to members of the public from intake of radionuclides: Part 5 Compilation of ingestion and inhalation dose coefficients." (Adopted by ICRP in 1995; and copyrighted by ICRP 1996.) *Annals of the ICRP* (Printed by Elsevier Science Inc. 660 White Plains Road, Tarrytown, New York 10591-5153, USA. ISBN 008042737 5; ISSN 0146-6453); March 1996.

[Ja98] **Jagger, J.** (1998). Natural background radiation and cancer death in Rocky Mountain states and Gulf states. *Health Phys.* **75**(4), pp. 428–430.

[Ju79] **Jury, J. W., Berman, B. L., Faul, D. D., Meyer, P., McNeill, K. G., and Woodworth, J. G.** (1979). Photoneutron cross-sections for ^{13}C. *Phys. Rev. C.* **19**(5), 1684–1692.

[Ju80] **Jury, J. W., Berman, B. L., Faul, D. D., Meyer, P., and Woodworth, J. G.** (1980). Photoneutron cross-sections for ^{17}O. *Phys. Rev. C.* **21**(2), 503–511.

[Ke73] **Keller, K. A., Lange, J., Münzel, H.** (1973). "Q-values and excitation functions of nuclear reactions." Editor: H. Schopper. Landolt-Börnstein, Numerical Data and Functional Relationships in Science and Technology, New Series, editor in chief: K.-H. Hellwege; Group I: Nuclear and Particle Physics, Vol. 5, Part a. Springer-Verlag, Berlin, Heidelberg, New York, 1973.

[Ko67] **Koch, H. W., Eisenhower, E. H.** (1967). Radioactivity criteria for radiation processing of foods. In "Radiation preservation of foods." Advances in Chemistry Series 65. American Chemical Society, Washington D.C. 1967. Proceedings of a Symposium in Atlantic City Sept.16–17, 1965. pp.87–108.

[Kr60] **Kruger, P., and Wilson. C. R.** (1960). "Determination of neutron dosages by food irradiation devices." Final report, May 1960, under contract DA-19-129-QM-741. Nuclear Science & Engineering Corp. Pittsburgh, PA. Quartermaster Food and Container Institute for the Armed Forces, Research and Engineering Command, Quartermaster Corps, U. S. Army, Chicago, IL.

[La93] **Lakosi. L., S f r, J., Veres, A., Sekine, T., Kaji, H., and Yoshihara, K.** (1993). Photoexcitation by gamma ray scattering near threshold and giant dipole resonance. *J. Phys. G: Nucl. Part. Phys.*, **19**, 1037–1043.

[Le47] **Lea, D. E.** (1947). "Actions of radiation on living cells." Cambridge University Press, New York, 1946. *Brit. J. Radiol. Suppl*. **1**, 59– .

[Le85] **Leboutet H., and Aucouturier, J.** (1985) Theoretical evaluation of induced radioactivity in food products by electron - or X ray beam sterilization. In: Proceedings of the 5th Int. Meeting on Radiation Processing, in San Diego, U. S. A., 22–26 Oct. 1984. Published in *Radiat. Phys. Chem.* **25**, 233–242.

[Li96] **Little, M. P., Muirhead, C. R.** (1996). Evidence for curvilinearity in cancer incidence dose – response in the Japanese atomic bomb survivors. *Int. J. Radiat. Biol.* **70**(1), pp. 83–94.

[Li98] **Little, M. P., Muirhead, C. R.** (1998). Curvature in the cancer mortality dose response in Japanese atomic bomb survivors: Absence of evidence of threshold. *Int. J. Radiat. Biol.* **74**(4), pp. 471–480.

[Lo90] **Lone M. A.** (1990). Induced radioactivity from industrial radiation processing. *Nucl. Instrum. and Meth. in Phys. Res.* **A299**, pp. 656–660.

[Lu98] **Lubin J. H.** (1998). On the discrepancy between epidemiologic studies in individuals of lung cancer and residential radon and Cohen's ecologic regression. *Health Phys.* **75**(1) 1998.

[Lu99] **Luckey, T. D.** (1999). A novel application for radioactive waste – as a nutritional supplement! In: Proceedings of the International Conference on Future Nuclear Systems Aug. 29 to Sept. 3, 1999, Jackson Hole, Wyoming.

[Ma78] **Maxcy, R. B., Rowley, D. B.** (1978). Radiation-resistant vegetative bacteria in proposed system of radappertization of meats. In: Food preservation by irradiation. (Proceedings of a Symposium, Wageningen, 21–25 November 1977. Jointly organized by IAEA,FAO, and WHO. Published by IAEA, Vienna, 1978STI/PUB/470; ISBN 92-0-010278-6. Vol. I, pp. 347–357, 1978.

[Mc98] **McKeown, J., Armstrong. L., Cleland, M. R., Drewell, N. H., Dubeau, J., Lawrence, C. B., Smyth, D.** (1998). Photon energy limits for food irradiation: a feasibility study. *Radiation Physics and Chemistry,* **53**, 55–61.

[Me64] **Meneely, G. R.** (1964). "Radioisotopes in radiation processed food." Final report for period August, 1962–January 1964, under contract DA-49-MD-2315. Department of Medicine, School of Medicine, Northwestern University and University of Texas, M. D. Anderson Hospital and Tumor Institute, Houston, TX. U. S. Army Medical Research and development Command, Office of the Surgeon General, Washington 25, D. C.

[Me66] **Meyer, R. A.** (1966). Induced radioactivity in food and electron sterilization. *Health Physics,* Vol. **12**, pp. 1027–1037.

[Mi87] **Miller, A. and Jensen, P. H.** (1987). Measurements of induced radioactivity in electron- and photon-irradiated beef. *Appl. Radiat. Isot.* **38**(7), 507–512.

[Na87a] **Nakamura, T., Uwamino, Y., Ohkubo, T., Hara. A.** (1987). Altitude variation of cosmic-ray neutrons. *Health Physics,* Vol. **53**(5), pp. 509–517.

[Na87b] **Nambi, K. S. V., and Soman, S. D.** (1987). Environmental radiation and cancer in India. *Health Physics,* Vol. **52**(5), pp. 653–657.

[Ok68] **Okulov, B. V.** (1968). Bremsstrahlung intensity near accelerators as a function of electron energy. Translated from: *Atomnaya Energiya* **25**(5), 426.

[Ra89a] **Ramachandran, T. V., and Mishra, U. C.** (1989). Measurement of natural radioactivity levels in Indian foodstuffs by gamma spectrometry. *Appl. Radiat. Isot.* **40**(8), 723–726.

[Ra89b] **Rassool, R. P., and Thompson, M. N.** (1989). Absolute photoneutron cross-section of ^{127}I. *Phys. Rev. C.* **39**(4), 1631–1632.

[Sa99] **Sandquist, G. M.; Kunze, J. F.; Muckerheide, J.** (1999). A Mathematical Explanation of the Health Effects of Low Level Ionizing Radiation. In: Proceedings of the International Conference on Future Nuclear Systems Aug. 29 to Sept. 3, 1999, Jackson Hole, Wyoming.

[Sm62] **Smith, H. D.** (1962). "Radioactivities produced in foods by high-energy electrons." Final report, report No. 17, dated March 15, 1962, under contract: DA 19-129-QM-1100. Stanford Research Institute Project No. PHU-2424. Quartermaster Food and Container Institute for the Armed Forces, Research and Engineering command, Quartermaster Corps, U. S. Army, Chicago, IL.

[Sm98] **Smith, B. J., Field, W., and Lynch, C. F.** (1998). Residential ^{222}Rn exposure and lung cancer: Testing the linear no-threshold theory with ecological data. *Health Phys.* **75**(1) 1998.

[Sa99] **Sandquist, G. M.; Kunze, J. F.; Muckerheide, J.** (1999). A mathematical explanation of the health effects of low level ionizing radiation. In: Proceedings of the International Conference on Future Nuclear Systems Aug. 29 to Sept. 3, 1999, Jackson Hole, Wyoming.

[Sw79a] **Swanson, W. P.** (1979a). Improved calculation of photoneutron yields released by incident electrons. *Health Phys.* **37**, 347–358.

[Sw79b] **Swanson, W. P.** (1979b). "Radiological safety aspects of the operation of electron linear accelerators." Technical Report Series No. 188. International Atomic Energy Agency, Vienna.

[WHO99] High-Dose Irradiation: Wholesomeness of Food Irradiated with Doses above 10 kGy. Report of a Joint FAO/IAEA/WHO Study Group, that met in Geneva 15–20 September 1997. World Health Organization Technical Report Series: 890, ISBN 92 4 120890 2, 1999.

[Wo79] **Woodworth, J. G., McNeill, K. G., Jury, J. W., Alvarez, R. A., Berman, B. L., Faul, D. D., and Meyer, P.** (1979). Photoneutron cross-sections for ^{18}O. *Phys. Rev. C.* **19**(5), 1667–1683.

TABLES

Table 1. Average of dose equivalent rates from various sources of natural background radiation in the United States of America [Anon80]

Radiation sources	Average dose equivalent rate in millisievert per year				
Radiation sources	Gonads	Lung	Bone Surface	Bone Marrow	G.I. tract
Cosmic radiation[A]	0.28	0.28	0.28	0.28	0.28
Cosmogenic radionuclides	0.007	0.007	0.008	0.007	0.007
External terrestrial[B]	0.26	0.26	0.26	0.26	0.026
Inhaled radionuclides[C]		1 – 4.5[D]			
Radionuclides in body[E]	0.27	0.24	0.6	0.24	0.24[F]
Totals (rounded)	0.8	1.8 – 5.3	1.15	0.8	0.8

[A] Assuming 10% reduction to account for structural shielding.
[B] Assuming 20% reduction for shielding by housing and 20% reduction for shielding by body.
[C] Dose rates to organs other than lung included in "Radionuclides in body".
[D] Local dose equivalent rate to segmental bronchi.
[E] Excluding cosmogenic contribution, which is shown separately.
[F] Excluding contribution from radionuclides in intestinal contents.

Table 2. Average annual effective dose equivalent[A] of ionizing background radiations to US population [BEIR V 90]

Source	**Effective dose equivalent in mSv**
Natural: Radon	2.0
Cosmic	0.27
Terrestrial	0.28
Internal	0.39
Total natural sources:	3.0
Other: X ray diagnosis	0.39
Nuclear medicine	0.14
Consumer products	0.10
Occupational	<0.01
Nuclear fuel	<0.01
Fallout	<0.01
Miscellaneous	<0.01
Total artificial:	0.63
Total natural and artificial:	3.6

[A] The "effective dose equivalent" means that the dose to a specific organ has been weighted by radiation quality factor and by the fraction of the organ relative to the whole body.

Table 3. Elemental composition of the reference food sample[A]

Atomic number	Chemical symbol	Elemental[b] concentration in mg/kg of reference food	Atomic number	Chemical symbol	Elemental[B] concentration in mg/kg of reference food
1	H	90 000	33	As	0.1
3	Li		34	Se	0.1
4	Be		35	Br	2
5	B		37	Rb	8
6	C	180 000	38	Sr	0.2
7	N	20 000	40	Zr	0.5
8	O	700 000	41	Nb	
11	Na	750	42	Mo	0.1
12	Mg	300	44	Ru	
13	Al	0.4	45	Rh	0.01
14	Si	10	47	Ag	0.02
15	P	2 000	48	Cd	0.1
16	S	2 200	49	In	0.01
17	Cl	560	50	Sn	0.1
19	K	4 000	51	Sb	0.01
20	Ca	140	52	Te	0.01
22	Ti	0.1	53	I	1
23	V	0.1	55	Cs	0.01
24	Cr	0.01	56	Ba	0.02
25	Mn	0.2	57	La	
26	Fe	50	79	Au	0.01
27	Co	0.01	80	Hg	0.05
28	Ni	0.1	81	Tl	
29	Cu	0.6	82	Pb	1
30	Zn	40	83	Bi	
31	Ga		88	Ra	
32	Ge	0.1	92	U	

A. This elemental composition is identical to that used by Becker [Be79], except that we have to his Table 1 added three elements: rubidium (Rb) 8 ppm, iodine (I) 1 ppm, and gold (Au) 0.01 ppm.

B. The listed concentrations are in parts per million (ppm); that is, in milligram of the element per kilogram of food.

Table 4. Typical concentration of some of the major trace elements in food[A]

Food	Na	Mg	P	S	Cl	K	Ca	Mn	Fe	Cu	Zn	Rb	I
Beef	840	240	1,670	2,300	760	3,380	110	0.24	28	0.80	5		0.092
Halibut	1,110	240	2,110	2,120	880	3,040	130	0.24	7	1.60	430		0.5
Oysters (raw)	4,710	390	1,430	1,800	6,280	2,040	940	0.39	56	36.00			1.000
Green beans	230	260	440	300	330	2,510	650	0.26	11	1.26			
Peaches	150	110	150	70	50	2,560	60	0.11	4	0.10			0.1
Chicken	910	270	2,000	2,520	790	3,720	140	0.27	15	3.00			
Mixed Veg.	400	380	1,010	460	140	1,130	80	0.38	4	0.80			0.05
Bacon	8,200	130	1,080	1,520	1,251	2,390	130	0.13	8				

A. All concentrations are in milligram of element per gram of food. The data are from Table 14 from [Kr60].

Table 5. Average elemental distribution in the body of a standard man (70 kg)[A] (From report of the Committee Two of ICRP: Permissible dose for internal radiation)

Atomic number	Chemical symbol	Concentration in mg/kg	Atomic number	Chemical symbol	Concentration in mg/kg
1	H	100 000	33	As	< 1.4
3	Li	< 0.013	34	Se	?
4	Be	< 0.028	35	Br	?
5	B	< 0.14	37	Rb	17
6	C	180 000	38	Sr	2
7	N	30 000	40	Zr	< 0.086
8	O	650 000	41	Nb	< 0.7
11	Na	1500	42	Mo	< 0.07
12	Mg	500	44	Ru	< 0.086
13	Al	1.4	45	Rh	?
14	Si	0.15	47	Ag	< 0.014
15	P	10 000	48	Cd	0.43
16	S	2 500	49	In	?
17	Cl	1 500	50	Sn	0.43
19	K	2 000	51	Sb	< 1.3
20	Ca	15 000	52	Te	?
22	Ti	< 0.21	53	I	0.43
23	V	< 0.0014	55	Cs	$< 1.4 \cdot 10^{-4}$
24	Cr	< 0.086	56	Ba	0.23
25	Mn	0.3	57	La	< 0.7
26	Fe	57	79	Au	< 0.014
27	Co	< 0.043	80	Hg	?
28	Ni	< 0.14	81	Tl	< 0.086
29	Cu	1.4	82	Pb	1.1
30	Zn	33	83	Bi	< 0.0043
31	Ga	$< 3 \cdot 10^{-5}$	88	Ra	$1.4 \cdot 10^{-9}$
32	Ge	?	92	U	$3 \cdot 10^{-5}$

A. All concentrations are in milligram of element per gram of human body that weighs about 70 kg.

Table 6. Isomers with lifetimes greater than 1 minute[A]

Isomer	Fractional abundance of the isotope in the element	Average abundance of element in mg/kg of humans	Abundance of the isotope in mg/kg	Half-life $T_{1/2}$ of isotope	Nuclear spin for the ground state and the isomeric state in units of h	Decay energy in MeV	E_{th} in MeV for (γ, n) and (γ, p) production
^{83m}Kr	0.115	<0.01	<0.001	1.86 h	9/2+, 1/2	0.0416	7.5 9.8
^{87m}Sr	0.07	0.2	0.014	2.81 h	9/2+, 1/2	0.388	8.4 9.4
^{93m}Nb	1	<0.01	<0.01	16.1 y	9/2+, 1/2	0.0304	8.8 6.0
^{103m}Rh	1	<0.01	<0.01	56.12 m	1/2, 7/2+	0.04	9.3 6.2
^{111m}Cd	0.128	0.1	0.013	48.5 m	1/2+, 11/2	0.396	7.0 9.1
^{113m}Cd	0.122	0.1	0.013	14.1 y	1/2+, 11/2	0.59	6.5 9.8
^{113m}In	0.043	<0.01	<0.0004	100 m	9/2+, 1/2	0.3917	9.4 6.1
^{115m}In	0.957	<0.01	<0.0096	4.486 h	9/2+, 1/2	0.385	9.0 6.8
^{117m}Sn	0.0768	0.1	0.008	13.6 d	1/2+, 11/2	0.3146	6.9 9.4
^{119m}Sn	0.0858	0.1	0.009	293 d	1/2+, 11/2	0.0896	6.5 9.9
^{123m}Te	0.0091	<0.01	0.0001	119.7 d	1/2+, 11/2	0.247	6.9 8.1
^{125m}Te	0.0712	<0.01	0.0007	58 d	1/2+, 11/2	0.145	6.6 8.7
^{129m}Xe	0.264	<0.01	0.0026	8.89 d	1/2+, 11/2	0.236	6.9 8.2
^{131m}Xe	0.212	<0.01	0.0021	11.9 d	3/2+, 11/2	0.164	6.6 8.8
^{135m}Ba	0.0659	0.02	0.0013	28.8 h	3/2+, 11/2	0.2682	7.0 8.3
^{137m}Ba	0.1123	0.02	0.0023	2.552 m	3/2+, 11/2	0.6617	6.9 8.7
^{176m}Lu	0.0259	<0.01	<0.0003	3.66 h	7, 1	1.315	6.3 6.0
^{180m}Hf	0.352	<0.01	<0.0035	5.52 h	0+, 8	1.1416	7.4 8.0
^{180m}Ta	0.0001	<0.01	<0.000001	8.15 h	1+, 9	0.835	6.6 5.8
^{189m}Os	0.161	<0.01	<0.0016	5.8 h	3/2+, 9/2	0.0308	5.9 7.3
^{190m}Os	0.264	<0.01	<0.0026	9.9 m	0+, 10	1.705	7.8 8.0
^{193m}Ir	0.627	<0.001	0.0006	10.53 d	3/2+, 11/2	0.0802	7.8 5.9
^{195m}Pt	0.338	<0.01	<0.0034	4.33 d	1/2-, 13/2+	0.2952	6.1 7.6
^{199m}Hg	0.169	0.05	0.0084	42.6 m	1/2, 13/2+	0.532	6.6 7.2
^{204m} Pb	0.014	1.0	0.015	67.2 m	0+, 9	2.185	8.4 6.6

A. Most of the nuclear data are from Table of the Isotopes (Revised 1991) by Norman E. Holden, at High Flux Beam Reactor, Reactor Division, Brookhaven National Laboratory, Upton. N.Y.11973. A similar version is also found in Handbook of Chemistry and Physics, 79th edition, 1998–1999, pp. 11–41 to 11–149. See reference [Ho99]. The data were supplemented by data from Table of the Isotopes compiled by Russel L. Heath, National Reactor Testing Station, Idaho Falls, Idaho, and published in Hand book of Chemistry and Physics, 49th edition (1968), and the different version ibid, 61st edition (1980). See reference [He80]. The last column is from Table 7.

Table 7. Threshold energies $E_{th}(\gamma, n)$ and $E_{th}(\gamma, p)$ in the natural isotopes, and the half-lives and decay modes of the produced isotopes[A]

Natural Isotope	% nat. abun-dance in	$E_{th}(\gamma, n)$	Isotope formed	Half-life of formed isotope	Decay Modes*	$E_{th}(\gamma, p)$	Isotope formed	Half-life of formed isotope	Decay Modes*
$^{1}_{1}H$	99.985								
$^{2}_{1}H$	0.015	2.225	$^{1}_{1}H$	Stable		2.225	$^{0}_{1}n$	(11 min)	
$^{3}_{2}He$	0.00013	7.72		Unstable		5.49	$^{2}_{1}H$	Stable	
$^{4}_{2}He$	99.9999	20.58	$^{3}_{2}He$	Stable		19.81	$^{3}_{1}H$	12.26 y	β^-
$^{6}_{3}Li$	7.42	5.66	$^{5}_{3}Li$	10^{-21}	p^+, α	4.59	$^{5}_{2}He$	$2\cdot10^{-21}$ s	n
$^{7}_{3}Li$	92.58	7.25	$^{6}_{3}Li$	Stable		9.97	$^{6}_{2}He$	0.82 s	β^-
$^{9}_{4}Be$	100	1.66	$^{8}_{4}Be$	10^{-14} s	$2\cdot\alpha$	16.87	$^{8}_{3}Li$	0.85 s	β^-, $2\cdot\alpha$
$^{10}_{5}B$	18.8	8.44	$^{9}_{5}B$	$3\cdot10^{-19}$ s	p^+, $2\cdot\alpha$	6.59	$^{9}_{4}Be$	Stable	
$^{11}_{5}B$	81.2	11.46	$^{10}_{5}B$	Stable		11.23	$^{10}_{4}Be$	$2.7\cdot10^{6}$ y	β^-
$^{12}_{6}C$	98.89	18.72	$^{11}_{6}C$	20.5 m	β^+, EC	15.96	$^{11}_{5}B$	Stable	
$^{13}_{6}C$	1.11	4.95	$^{12}_{6}C$	Stable		17.53	$^{12}_{5}B$	0.027 s	β^-, α
$^{14}_{7}N$	99.63	10.55	$^{13}_{7}N$	10.1 m	β^+	7.55	$^{13}_{6}C$	Stable	
$^{15}_{7}N$	0.37	10.83	$^{14}_{7}N$	Stable		10.21	$^{14}_{6}C$	5730 y	β^-
$^{16}_{8}O$	99.76	15.66	$^{15}_{8}O$	124 s	β^+	12.13	$^{15}_{7}N$	Stable	
$^{17}_{8}O$	0.04	4.14	$^{16}_{8}O$	Stable		13.78	$^{16}_{7}N$	7.2 s	β^-
$^{18}_{8}O$	0.20	8.04	$^{17}_{8}O$	Stable		15.94	$^{17}_{7}N$	4.16 s	β^-
$^{19}_{9}F$	100	10.43	$^{18}_{9}F$	109.7 m	β^+, EC	7.99	$^{18}_{8}O$	Stable	
$^{20}_{10}Ne$	90.51	16.87	$^{19}_{10}Ne$	17.5 s	β^+	12.85	$^{19}_{9}F$	Stable	
$^{21}_{10}Ne$	0.27	6.76	$^{20}_{10}Ne$	Stable		13.01	$^{20}_{9}F$	11.4 s	β^-
$^{22}_{10}Ne$	9.22	10.36	$^{21}_{10}Ne$	Stable		15.27	$^{21}_{9}F$	4.4 s	β^-
$^{23}_{11}Na$	100	12.42	$^{22}_{11}Na$	2.602 y	β^+, EC	8.79	$^{22}_{10}Ne$	Stable	
$^{24}_{12}Mg$	78.99	16.53	$^{23}_{12}Mg$	12.1 s	β^+	11.69	$^{23}_{11}Na$	Stable	
$^{25}_{12}Mg$	10.0	7.33	$^{24}_{12}Mg$	Stable		12.06	$^{24}_{11}Na$	15.0 h	β^-
$^{26}_{12}Mg$	11.01	11.09	$^{25}_{12}Mg$	Stable		14.14	$^{25}_{11}Na$	60 s	β^-
$^{27}_{13}Al$	100	13.06	$^{26}_{13}Al$	$7\cdot10^{5}$ y		8.27	$^{26}_{12}Mg$	Stable	

* β^+ stands for positron emission, β^- for electron emission, p for proton (H^+) emission, α for alpha-particle (He^{++}) emission, EC stands for orbital electron capture, and IT for isomeric transition.

Table 7. (cont.)

Natural Isotope	% nat. abun-dance	$E_{th}(\gamma, n)$	Isotope formed	Half-life of formed isotope	Decay modes	$E_{th}(\gamma, p)$	Isotope formed	Half-life of formed isotope	Decay modes
$^{28}_{14}Si$	92.23	17.18	$^{27}_{14}Si$	4.2 s	β^+	11.58	$^{27}_{13}Al$	Stable	
$^{29}_{14}Si$	4.67	8.47	$^{28}_{14}Si$	Stable		12.33	$^{28}_{13}Al$	2.31 m	β^-
$^{30}_{14}Si$	3.1	10.61	$^{29}_{14}Si$	Stable		13.51	$^{29}_{13}Al$	6.6 m	β^-
$^{31}_{15}P$	100	12.31	$^{30}_{15}P$	2.5 m	β^+	7.30	$^{30}_{14}Si$	Stable	
$^{32}_{16}S$	95.00	15.04	$^{31}_{16}S$	2.7 s	β^+	8.87	$^{31}_{15}P$	Stable	
$^{33}_{16}S$	0.76	8.64	$^{32}_{16}S$	Stable		9.57	$^{32}_{15}P$	14.3 d	β^-
$^{34}_{16}S$	4.22	11.42	$^{33}_{16}S$	Stable		10.88	$^{33}_{15}P$	25 d	β^-
$^{36}_{16}S$	0.02	9.89	$^{35}_{16}S$	88 d	β^-	13.02	$^{35}_{15}P$	?	(β^-, β^-)
$^{35}_{17}Cl$	75.77	12.65	$^{34}_{17}Cl$	1.56 s	β^+	6.37	$^{34}_{16}S$	Stable	
$^{37}_{17}Cl$	24.23	10.31	$^{36}_{17}Cl$	$3 \cdot 10^5$ y	β^+, EC, β^-	8.39	$^{36}_{16}S$	Stable	
$^{36}_{18}Ar$	0.34	15.25	$^{35}_{18}Ar$	1.83 s	β^+	8.51	$^{35}_{17}Cl$	Stable	
$^{38}_{18}Ar$	0.07	11.84	$^{37}_{18}Ar$	35 d	EC	10.24	$^{37}_{17}Cl$	Stable	
$^{40}_{18}Ar$	99.59	9.87	$^{39}_{18}Ar$	265 y	β^-	12.53	$^{39}_{17}Cl$	55.5 m	β^-
$^{39}_{19}K$	93.26	13.08	$^{38}_{19}K$	7.71 m	β^+, EC	6.38	$^{38}_{18}Ar$	Stable	
$^{40}_{19}K$	0.01	7.80	$^{39}_{19}K$	Stable		7.58	$^{39}_{18}Ar$	265 y	β^-
$^{41}_{19}K$	6.73	10.10	$^{40}_{19}K$	$1.3 \cdot 10^9$ y	β^-, β^+, EC	7.81	$^{40}_{18}Ar$	Stable	
$^{40}_{20}Ca$	96.941	15.64	$^{39}_{20}Ca$	0.87 s	β^+	8.33	$^{39}_{19}K$	Stable	
$^{42}_{20}Ca$	0.647	11.48	$^{41}_{20}Ca$	$8 \cdot 10^4$ y	EC	10.28	$^{41}_{19}K$	Stable	
$^{43}_{20}Ca$	0.135	7.93	$^{42}_{20}Ca$	Stable		10.68	$^{42}_{19}K$	12.4 h	β^-
$^{44}_{20}Ca$	2.086	11.13	$^{43}_{20}Ca$	Stable		12.17	$^{43}_{19}K$	22.4 h	β^-
$^{46}_{20}Ca$	0.004	10.40	$^{45}_{20}Ca$	165 d	β^-	13.82	$^{45}_{19}K$	16 m	β^-
$^{48}_{20}Ca$	0.187	9.94	$^{47}_{20}Ca$	4.53 d	β^-, β^-	15.81	$^{47}_{19}K$	?	$(\beta^-, \beta^-, \beta^-)$
$^{45}_{21}Sc$	100	11.33	$^{44}_{21}Sc$	3.92 h	β^+	6.89	$^{44}_{20}Ca$	Stable	
$^{46}_{22}Ti$	8.0	13.19	$^{45}_{22}Ti$	3.09 h	β^+, EC	10.34	$^{45}_{21}Sc$	Stable	
$^{47}_{22}Ti$	7.5	8.88	$^{46}_{22}Ti$	Stable		10.46	$^{46}_{21}Sc$	83.8 d	β^-
$^{48}_{22}Ti$	73.7	11.63	$^{47}_{22}Ti$	Stable		11.45	$^{47}_{21}Sc$	3.43 d	β^-
$^{49}_{22}Ti$	5.5	8.14	$^{48}_{22}Ti$	Stable		11.35	$^{48}_{21}Sc$	1.83 d	β^-
$^{50}_{22}Ti$	5.3	10.94	$^{49}_{22}Ti$	Stable		12.16	$^{49}_{21}Sc$	57.5 m	β^-

Table 7. (cont.)

Natural Isotope	% nat. abun-dance	$E_{th}(\gamma, n)$	Isotope formed	Half-life of formed isotope	Decay modes	$E_{th}(\gamma, p)$	Isotope formed	Half-life of formed isotope	Decay modes
$^{50}_{23}V$	0.25	9.33	$^{49}_{23}V$	330 d	EC	7.95	$^{49}_{22}Ti$	Stable	
$^{51}_{23}V$	99.75	11.05	$^{50}_{23}V$	Stable		8.06	$^{50}_{22}Ti$	Stable	
$^{50}_{24}Cr$	4.35	13.00	$^{49}_{24}Cr$	41.9 m	β^-	9.59	$^{49}_{23}V$	330 d	EC
$^{52}_{24}Cr$	83.79	12.04	$^{51}_{24}Cr$	27.8 d	EC	10.50	$^{51}_{23}V$	Stable	
$^{53}_{24}Cr$	9.50	7.94	$^{52}_{24}Cr$	Stable		11.13	$^{52}_{23}V$	3.76 m	β^-
$^{54}_{24}Cr$	2.36	9.72	$^{53}_{24}Cr$	Stable		12.37	$^{53}_{23}V$	2.0 m	β^-
$^{55}_{25}Mn$	100	10.23	$^{54}_{25}Mn$	303 d	EC	8.07	$^{54}_{24}Cr$	Stable	
$^{54}_{26}Fe$	5.8	13.38	$_{26}Fe^{53}$	8.5 m	β^+, EC	8.85	$^{53}_{25}Mn$	$2{\cdot}10^6$ y	EC
$^{56}_{26}Fe$	91.8	11.20	$^{55}_{26}Fe$	2.6 y	EC	10.18	$^{55}_{25}Mn$	Stable	
$^{57}_{26}Fe$	2.1	7.65	$^{56}_{26}Fe$	Stable		10.56	$^{56}_{25}Mn$	2.58 h	β^-
$^{58}_{26}Fe$	0.3	10.05	$^{57}_{26}Fe$	Stable		11.95	$^{57}_{25}Mn$	1.7 m	β^-
$^{59}_{27}Co$	100	10.49	$^{58}_{27}Co$	71.3 d	β^+, EC	8.27	$^{58}_{26}Fe$	Stable	
$^{58}_{28}Ni$	68.7	12.22	$^{57}_{28}Ni$	36.0 h	β^+, EC	8.17	$^{57}_{27}Co$	270 d	EC
$^{60}_{28}Ni$	26.10	11.39	$^{59}_{28}Ni$	$8{\cdot}10^4$ y	EC	9.53	$^{59}_{27}Co$	Stable	
$^{61}_{28}Ni$	1.13	7.82	$^{60}_{28}Ni$	Stable		9.86	$^{60}_{27}Co$	10.5 m 5.26 y	IT β^-
$^{62}_{28}Ni$	3.59	10.6	$^{61}_{28}Ni$	Stable		11.14	$^{61}_{27}Co$	1.65 h	β^-
$^{64}_{28}Ni$	0.91	9.66	$^{63}_{28}Ni$	92 y	β^-	12.55	$^{63}_{27}Co$	52 s	β^-
$^{63}_{29}Cu$	69.1	10.85	$^{62}_{29}Cu$	9.8 m	β^+, EC	6.12	$^{62}_{28}Ni$	Stable	
$^{65}_{29}Cu$	30.9	9.91	$^{64}_{29}Cu$	12.9 h	β^-, β^+, EC	7.45	$^{64}_{28}Ni$	Stable	
$^{64}_{30}Zn$	48.6	11.86	$^{63}_{30}Zn$	38.4 m	β^+, EC	7.71	$^{63}_{29}Cu$	Stable	
$^{66}_{30}Zn$	27.9	11.06	$^{65}_{30}Zn$	243.6 d	β^+, EC	8.93	$^{65}_{29}Cu$	Stable	
$^{67}_{30}Zn$	4.1	7.05	$^{66}_{30}Zn$	Stable		8.91	$^{66}_{29}Cu$	5.10 m	β^-
$^{68}_{30}Zn$	18.8	10.20	$^{67}_{30}Zn$	Stable		9.99	$^{67}_{29}Cu$	61.88 h	β^-
$^{70}_{30}Zn$	0.6	9.21	$^{69}_{30}Zn$	13.9 h, 58 m	IT β^-	11.11	$^{69}_{29}Cu$	2.8 m	β^-
$^{69}_{31}Ga$	60	10.31	$^{68}_{31}Ga$	68.3 m	β^+, EC	6.61	$^{68}_{30}Zn$	Stable	
$^{71}_{31}Ga$	40	9.31	$^{70}_{31}Ga$	21.1 m	β^-	7.87	$^{70}_{30}Zn$	Stable	

Table 7. (cont.)

Natural Isotope	% nat. abun-dance	$E_{th}(\gamma, n)$	Isotope formed	Half-life of formed isotope	Decay modes	$E_{th}(\gamma, p)$	Isotope formed	Half-life of formed isotope	Decay modes
$^{70}_{32}Ge$	20.5	11.5	$^{69}_{32}Ge$	39 h	β^+, EC	8.5	$^{69}_{31}Ga$	Stable	
$^{72}_{32}Ge$	27.4	10.7	$^{71}_{32}Ge$	0.02 s, 11.4 d	IT EC	9.7	$^{71}_{31}Ga$	Stable	
$^{73}_{32}Ge$	7.8	6.78	$^{72}_{32}Ge$	Stable		10.0	$^{72}_{31}Ga$	14.1 h	β^-
$^{74}_{32}Ge$	36.5	10.2	$^{73}_{32}Ge$	Stable		11.0	$^{73}_{31}Ga$	4.9 h	β^-
$^{76}_{32}Ge$	7.8	9.43	$^{75}_{32}Ge$	48.9 s 82.8 m	IT β^-	12.0	$^{75}_{31}Ga$	2 m	β^-
$^{75}_{33}As$	100	10.2	$^{74}_{33}As$	17.9 d	β^-, β^+, EC	6.9	$^{74}_{32}Ge$	Stable	
$^{74}_{34}Se$	0.9	12.1	$^{73}_{34}Se$	42 m	β^+, EC	8.6	$^{73}_{33}As$	80.3 d	EC
$^{76}_{34}Se$	9.0	11.2	$^{75}_{34}Se$	120.4 d	β^-	9.5	$^{75}_{33}As$	Stable	
$^{77}_{34}Se$	7.6	7.4	$^{76}_{34}Se$	Stable		9.6	$^{76}_{33}As$	26.5 h	β^-
$^{78}_{34}Se$	23.5	10.5	$^{77}_{34}Se$	17.5 s Stable	IT	10 4	$^{77}_{33}As$	38.8 h	β^-
$^{80}_{34}Se$	49.8	9.91	$^{79}_{34}Se$	$6.5 \cdot 10^4$ y	β^-	11.4	$^{79}_{33}As$	9.0 m	β^-
$^{82}_{34}Se$	9.2	9.28	$^{81}_{34}Se$	57 m 18.6 m	IT β^-	12.3	$^{81}_{33}As$	33 s	β^-
$^{79}_{35}Br$	50.69	10.7	$^{78}_{35}Br$	6.4 m	β^+, EC	6.3	$^{78}_{34}Se$	Stable	
$^{81}_{35}Br$	49.31	10.2	$^{80}_{35}Br$	4.4 h 17.6 m	IT β^+, EC	7.5	$^{80}_{34}Se$	Stable	
$^{78}_{36}Kr$	0.35	12.0	$^{77}_{36}Kr$	1.19 h	β^-, β^+, EC	8.2	$^{77}_{35}Br$	57 h	β^+, EC
$^{80}_{36}Kr$	2.25	11.5	$^{79}_{36}Kr$	34.9 h	β^+, EC	9.1	$^{79}_{35}Br$	Stable	
$^{82}_{36}Kr$	11.6	11.0	$^{81}_{36}Kr$	$2.1 \cdot 10^5$y	EC	9.9	$^{81}_{35}Br$	Stable	
$^{83}_{36}Kr$	11.5	7.5	$^{82}_{36}Kr$	Stable		9.8	$^{82}_{35}Br$	6.1 m 35.5 h	IT, β^- β^-
$^{84}_{36}Kr$	57.0	10.5	$^{83}_{36}Kr$	1.86 h Stable	IT	10.7	$^{83}_{35}Br$	2.41 h	β^+, EC
$^{86}_{36}Kr$	17.3	9.86	$^{85}_{36}Kr$	4.39 h 10.76 y	IT, β^- β^-	11.9	$^{85}_{35}Br$	31.8 m	β^+, EC

Table 7. (cont.)

Natural Isotope	% nat. abun-dance	$E_{th}(\gamma, n)$	Isotope formed	Half-life of formed isotope	Decay modes	$E_{th}(\gamma, p)$	Isotope formed	Half-life of formed isotope	Decay modes
$^{85}_{37}Rb$	72.17	10.5	$^{84}_{37}Rb$	20 m 33 d	EC, IT β^+, EC	7.0	$^{84}_{36}Kr$	Stable	
$^{87}_{37}Rb$	27.83	9.92	$^{86}_{37}Rb$	1.04 m 18.66 d	IT β^-	8.6	$^{86}_{36}Kr$	Stable	
$^{84}_{38}Sr$	0.5	12.0	$^{83}_{38}Sr$	33 h	β^+, EC	9.0	$^{83}_{37}Rb$	83 d	EC
$^{86}_{38}Sr$	9.9	11.5	$^{85}_{38}Sr$	70 m 64 d	IT, EC EC	9.6	$^{85}_{37}Rb$	Stable	
$^{87}_{38}Sr$	7.0	8.4	$^{86}_{38}Sr$	2.83 h Stable	IT, EC	9.4	$^{86}_{37}Rb$	64 s 18.66 d	IT β^-
$^{88}_{38}Sr$	82.6	11.1	$^{87}_{38}Sr$	Stable		10.6	$^{87}_{37}Rb$	Stable	
$^{89}_{39}Y$	100	11.5	$^{88}_{39}Y$	106.6 d	β^+, EC	7.1	$^{88}_{38}Sr$	Stable	
$^{90}_{40}Zr$	51.4	12.0	$^{89}_{40}Zr$	4.4 m 79 h	IT, β^+, EC EC, β^+	8.4	$^{89}_{39}Y$	Stable	
$^{91}_{40}Zr$	11.2	7.2	$^{90}_{40}Zr$	Stable		8.7	$^{90}_{39}Y$	3.2 h 64.2 h	IT β^-
$^{92}_{40}Zr$	17.1	8.6	$^{91}_{40}Zr$	Stable		9.4	$^{91}_{39}Y$	50 m 57.5 d	IT β^-
$^{94}_{40}Zr$	17.5	8.22	$^{93}_{40}Zr$	$9.5 \cdot 10^5$ y	β^-	10.3	$^{93}_{39}Y$	10.4 h	β^-
$^{96}_{40}Zr$	2.8	7.85	$^{95}_{40}Zr$	65 d	β^-	11.5	$^{95}_{39}Y$	11 m	β^-
$^{93}_{41}Nb$	100	8.83	$^{92}_{41}Nb$	10.1 d >350 y	IT, β^+, EC	6.0	$^{92}_{40}Zr$	Stable	
$^{92}_{42}Mo$	15.84	12.7	$^{91}_{42}Mo$	65 s 15.6 m	IT, β^+ β^+	7.5	$^{91}_{41}Nb$	62 d Long	IT EC
$^{94}_{42}Mo$	9.04	9.68	$^{93}_{42}Mo$	6.9 h 10^4 y	IT EC	8.5	$^{93}_{41}Nb$	3.7 y Stable	IT
$^{95}_{42}Mo$	15.72	7.4	$^{94}_{42}Mo$	Stable		8.6	$^{94}_{41}Nb$	6.3 m $2 \cdot 10^4$ y	IT, β^- β^-
$^{96}_{42}Mo$	16.53	9.2	$^{95}_{42}Mo$	Stable		9.3	$^{95}_{41}Nb$	90 h 35 d	IT β^-

Table 7. (cont.)

Natural Isotope	% nat. abun-dance	$E_{th}(\gamma, n)$	Isotope formed	Half-life of formed isotope	Decay modes	$E_{th}(\gamma, p)$	Isotope formed	Half-life of formed isotope	Decay modes
$^{97}_{42}Mo$	9.46	6.8	$^{96}_{42}Mo$	Stable		9.2	$^{96}_{41}Nb$	23.35 h	β^-
$^{98}_{42}Mo$	23.78	8.6	$^{97}_{42}Mo$	Stable		9.8	$^{97}_{41}Nb$	1.0 m 72 m	IT β^-
$^{100}_{42}Mo$	9.13	8.29	$^{99}_{42}Mo$	66 h	β^-	10.0	$^{99}_{41}Nb$	10 s 2.4 m	β^- β^-
$^{99}_{43}Tc$	~								
$^{96}_{44}Ru$	5.51	10.7	$_{44}Ru^{95}$	99 m	β^+, EC	7.4	$^{95}_{43}Tc$	61 d 20 h	EC, IT, EC
$^{98}_{44}Ru$	1.87	10.3	$_{44}Ru^{97}$	2.9 d	EC	8.3	$^{97}_{43}Tc$	90 d $2.6\cdot10^6$ y	IT EC
$^{99}_{44}Ru$	12.72	7.5	$^{98}_{44}Ru$	Stable		8.4	$^{98}_{43}Tc$	$1.5\cdot10^5$ y	β^-
$^{100}_{44}Ru$	12.62	9.7	$^{99}_{44}Ru$	Stable		9.2	$^{99}_{43}Tc$	6.0 h $2.1\cdot10^5$ y	IT β^-
$^{101}_{44}Ru$	17.07	6.8	$^{100}_{44}Ru$	Stable		9.4	$^{100}_{43}Tc$	17 s	β^-
$^{102}_{44}Ru$	31.61	9.2	$^{101}_{44}Ru$	Stable		10.1	$^{101}_{43}Tc$	14 m	β^-
$^{104}_{44}Ru$	18.58	8.91	$^{103}_{44}Ru$	40 d	β^-	10.5	$^{103}_{43}Tc$	50 s	β^-
$^{103}_{45}Rh$	100	9.3	$^{102}_{45}Rh$	206 d	β^+, EC, β^-	6.2	$^{102}_{44}Ru$	Stable	
$^{102}_{46}Pd$	0.96	10.6	$^{101}_{46}Pd$	8.4 h	EC, β^+	7.8	$^{101}_{45}Rh$	4.5 d 3.1 y	IT EC
$^{104}_{46}Pd$	10.97	10.0	$^{103}_{46}Pd$	17 d	EC	8.7	$^{103}_{45}Rh$	Stable	
$^{105}_{46}Pd$	22.23	7.1	$^{104}_{46}Pd$	Stable		8.8	$^{104}_{45}Rh$	4.4 m 43 s	IT, β^- β^-
$^{106}_{46}Pd$	27.33	9.6	$^{105}_{46}Pd$	Stable		9.3	$^{105}_{45}Rh$	45 s 35.9 h	IT β^-
$^{108}_{46}Pd$	26.71	9.22	$^{107}_{46}Pd$	21.3 s $7\cdot10^6$ y	IT β^-	10.0	$^{106}_{45}Rh$	130 m 30 s	β^- β^-
$^{110}_{46}Pd$	11.81	8.80	$^{109}_{46}Pd$	4.7 m 13.5 h	IT β^-	9.5	$^{108}_{45}Rh$	17 s	β^-

Table 7. (cont.)

Natural Isotope	% nat. abun-dance	$E_{th}(\gamma, n)$	Isotope formed	Half-life of formed isotope	Decay modes	$E_{th}(\gamma, p)$	Isotope formed	Half-life of formed isotope	Decay modes
$^{107}_{47}Ag$	51.82	9.53	$^{106}_{47}Ag$	8.4 d 24 m	EC β^+, EC	5.8	$^{106}_{46}Pd$	Stable	
$^{109}_{47}Ag$	48.18	9.19	$^{108}_{47}Ag$	>5 y 2.42 m	IT, EC β^-, β^+, EC	6.5	$^{108}_{46}Pd$	Stable	
$^{106}_{48}Cd$	1.22	10.9	$^{105}_{48}Cd$	55 m	EC, β^+	7.3	$^{105}_{47}Ag$	40 d	EC
$^{108}_{48}Cd$	0.88	10.3	$^{107}_{48}Cd$	6.5 h	EC, β^+	8.1	$^{107}_{47}Ag$	44 s Stable	IT
$^{110}_{48}Cd$	12.39	9.89	$^{109}_{48}Cd$	450 d	EC	8.9	$^{109}_{47}Ag$	40 s Stable	IT
$^{111}_{48}Cd$	12.75	7.0	$^{110}_{48}Cd$	Stable		9.1	$^{110}_{47}Ag$	253 d 24 s	IT, β^- β^-
$^{112}_{48}Cd$	24.07	9.4	$^{111}_{48}Cd$	49 m Stable	IT	9.6	$^{111}_{47}Ag$	74 s 7.5 d	IT β^-
$^{113}_{48}Cd$	12.26	6.5	$^{112}_{48}Cd$	Stable		9.8	$^{112}_{47}Ag$	3.2 h	β^-
$^{114}_{48}Cd$	28.86	9.0	$^{113}_{48}Cd$	14 y Stable	IT, β^-	10.3	$^{113}_{47}Ag$	1.2 m 5.3 h	IT, β^- β^-
$^{116}_{48}Cd$	7.58	8.70	$^{115}_{48}Cd$	43 d 2.3 d	β^- β^-	11.1	$^{115}_{47}Ag$	20 s 21.1 m	β^- β^-
$^{113}_{49}In$	4.28	9.44	$^{112}_{49}In$	0.042 s 21 m 14 m	IT IT β^-, EC, β^+	6.1	$^{112}_{48}Cd$	Stable	
$^{115}_{49}In$	95.72	9.03	$^{114}_{49}In$	2.5 s 50 d 72 s	IT IT EC, β^-, β^+	6.8	$^{114}_{48}Cd$	Stable	
$^{112}_{50}Sn$	1.0	10.8	$^{111}_{50}Sn$	35 m	EC, β^+	7.5	$_{49}In^{111}$	10 m 2.81 d	IT EC
$^{114}_{50}Sn$	0.7	10.3	$^{113}_{50}Sn$	20 m 118 d	IT EC	8.5	$_{49}In^{113}$	1.73 h Stable	IT
$^{115}_{50}Sn$	0.4	7.5	$_{50}Sn^{114}$	Stable		8.7	$_{49}In^{114}$	2.5 s 50 d 72 s	IT IT EC, β^-, β^+
$^{116}_{50}Sn$	14.7	9.6	$^{115}_{50}Sn$	Stable		9.3	$_{49}In^{115}$	4.5 h Stable	IT, β^-
$^{117}_{50}Sn$	7.7	6.9	$^{116}_{50}Sn$	Stable		9.4	$_{49}In^{116}$	2.16 s 54 m 14 s	IT β^- β^-
$^{118}_{50}Sn$	24.3	9.3	$^{117}_{50}Sn$	14 d Stable	IT	10.0	$_{49}In^{117}$	1.93 h 44 m	IT, β^- β^-
$^{119}_{50}Sn$	8.6	6.5	$^{118}_{50}Sn$	Stable		9.9	$_{49}In^{118}$	4.4 m 5 s	β^- β^-

Table 7. (cont.)

Natural Isotope	% nat. abun-dance	$E_{th}(\gamma, n)$	Isotope formed	Half-life of formed isotope	Decay modes	$E_{th}(\gamma, p)$	Isotope formed	Half-life of formed isotope	Decay modes
$^{120}_{50}Sn$	32.4	9.1	$^{119}_{50}Sn$	250 d Stable	IT	10.7	$_{49}In^{119}$	18 m 2.1 m	IT, β^- β^-
$^{122}_{50}Sn$	4.6	8.81	$^{121}_{50}Sn$	76 y 27 h	β^- β^-	11.4	$_{49}In^{121}$	3.1 m 30 s	β^- β^-
$^{124}_{50}Sn$	5.6	8.49	$^{123}_{50}Sn$	125 d 42 m	β^- β^-	12.1	$_{49}In^{123}$	36 s 10 s	β^- β^-
$^{121}_{51}Sb$	57.25	9.24	$^{120}_{51}Sb$	15.9 m	β^+, EC	5.8	$^{120}_{50}Sn$	Stable	
$^{123}_{51}Sb$	42.75	8.97	$^{122}_{51}Sb$	4.2 m 2.8 d	IT β^-, β^+, EC	6.6	$^{122}_{50}Sn$	Stable	
$^{120}_{52}Te$	0.1	10.3	$^{119}_{52}Te$	4.7 d 15.9 h	EC β^+, EC	7.2	$^{119}_{51}Sb$	38 h	EC
$^{122}_{52}Te$	2.5	9.84	$^{121}_{52}Te$	154 d 17 d	IT, EC, β^+ EC	8.0	$^{121}_{51}Sb$	Stable	
$^{123}_{52}Te$	0.9	6.9	$^{122}_{52}Te$	Stable		8.1	$^{122}_{51}Sb$	4.2 m 2.8 d	IT β^-, β^+, EC
$^{124}_{52}Te$ $^{125}_{52}Te$	4.6 7.0	9.4 6.6	$^{123}_{52}Te$ $^{124}_{52}Te$	117 d Stable Stable	IT	8.6 8.7	$^{123}_{51}Sb$ $^{124}_{51}Sb$	Stable 21 m 93 s 60 3 d	 IT IT, β^- β^-
$^{126}_{52}Te$	18.7	9.1	$^{125}_{52}Te$	58 d Stable	IT	9.1	$^{125}_{51}Sb$	2.7 y	β^-
$_{52}Te^{128}$	31.7	8.78	$^{127}_{52}Te$	109 d 9.4 h	IT, β^- β^-	9.6	$^{127}_{51}Sb$	93 h	β^-
$^{130}_{52}Te$	34.5	8.41	$^{129}_{52}Te$	34 d 69 m	EC, β^- β^-	10.0	$^{129}_{51}Sb$	4.3 h	β^-
$^{127}_{53}J$	100	9.14	$^{126}_{53}J$	13 d	β^+, EC, β^-	6.2	$^{126}_{52}Te$	Stable	
$^{124}_{54}Xe$	0.1	10.3	$^{123}_{54}Xe$	2.1 h	β^+, EC	6.8	$_{53}J^{123}$	13.3 h	EC

Table 7. (cont.)

Natural Isotope	% nat. abun-dance	$E_{th}(\gamma, n)$	Isotope formed	Half-life of formed isotope	Decay modes	$E_{th}(\gamma, p)$	Isotope formed	Half-life of formed isotope	Decay modes
$^{126}_{54}Xe$	0.1	10.1	$^{125}_{54}Xe$	55 s 17 h	IT EC	7.6	$_{53}J^{125}$	60 d	EC
$^{128}_{54}Xe$	1.9	9.61	$^{127}_{54}Xe$	75 s 36.4 d	IT EC	8.2	$_{53}J^{127}$	Stable	
$^{129}_{54}Xe$	26.4	6.9	$^{128}_{54}Xe$	Stable		8.2	$_{53}J^{128}$	25.08 m	β^+, EC, β^-
$^{130}_{54}Xe$	4.1	9.3	$^{129}_{54}Xe$	8.d Stable	IT	8.7	$_{53}J^{129}$	$1.7 \cdot 10^7$ y	β^-
$^{131}_{54}Xe$	21.2	6.6	$^{130}_{54}Xe$	Stable		8.8	$_{53}J^{130}$	8.82 m 12.3 h	IT β^-
$^{132}_{54}Xe$	26.9	8.9	$^{131}_{54}Xe$	11.8 d Stable	IT	9.1	$_{53}J^{131}$	8.07 d	β^-
$^{134}_{54}Xe$	10.4	8.53	$^{133}_{54}Xe$	2.26 d 5.27 d	IT β^-	9.6	$_{53}J^{133}$	20.9 h	β^-,
$^{136}_{54}Xe$	8.9	7.99	$^{135}_{54}Xe$	15.6 m 9.2 h	IT β^-	9.9	$_{53}J^{135}$	6.7 h	β^-
$^{133}_{55}Cs$	100	9.00	$^{132}_{55}Cs$	6.5 d	β^+, EC	6.1	$^{132}_{54}Xe$	Stable	

Table 7. (cont.)

Natural Isotope	% nat. abun-dance	$E_{th}(\gamma, n)$	Isotope formed	Half-life of formed isotope	Decay modes	$E_{th}(\gamma, p)$	Isotope formed	Half-life of formed isotope	Decay modes
$^{130}_{56}Ba$	0.1	10.4	$^{129}_{56}Ba$	2.5 h	β^+, EC	7.2	$^{129}_{55}Cs$	32 h	EC
$^{132}_{56}Ba$	0.1	9.80	$^{131}_{56}Ba$	15 m 12 d	IT EC	7.7	$^{131}_{55}Cs$	9.70 d	EC
$^{134}_{56}Ba$	2.4	9.47	$^{133}_{56}Ba$	38.9 h	IT, EC	8.2	$^{133}_{55}Cs$	Stable	
$^{135}_{56}Ba$	6.6	7.0	$^{134}_{56}Ba$	Stable		8.3	$^{134}_{55}Cs$	2.90 h 2.05 y	IT β^-
$^{136}_{56}Ba$	7.9	9.1	$^{135}_{56}Ba$	28.7 h Stable	IT	8.5	$^{135}_{55}Cs$	$3\cdot10^6$ y	β^-
$^{137}_{56}Ba$	11.2	6.9	$^{136}_{56}Ba$	0.32 s Stable	IT	8.7	$^{136}_{55}Cs$	13 d	β^-
$^{138}_{56}Ba$	71.7	8.6	$^{137}_{56}Ba$	2.55 m Stable	IT	9.0	$^{137}_{55}Cs$	30.23 y	β^-
$^{138}_{57}La$	0.09	7.47	$^{137}_{57}La$	$6\cdot10^7$ y	EC	6.0	$^{137}_{56}Ba$	2.55 m Stable	IT
$^{139}_{57}La$	99.91	8.8	$^{138}_{57}La$	Stable		6.2	$^{138}_{56}Ba$	Stable	
$^{136}_{58}Ce$	0.2	9.91	$^{135}_{58}Ce$	17.2 h	β^+, EC	6.9	$^{135}_{57}La$	19.5 h	EC
$^{138}_{58}Ce$	0.3	9.74	$^{137}_{58}Ce$	34.4 h 9.0 h	IT, EC β^+, EC	7.1	$^{137}_{57}La$	$6\cdot10^7$ y	EC
$^{140}_{58}Ce$	88.4	9.19	$^{139}_{58}Ce$	55 s 140 d	IT EC	8.1	$^{139}_{57}La$	Stable	
$^{142}_{58}Ce$	11.1	7.17	$^{141}_{58}Ce$	33 d	β^-	8.8	$^{141}_{57}La$	3.9 h	β^-
$^{141}_{59}Pr$	100	9.40	$^{140}_{59}Pr$	3.39 m	β^+, EC	5.2	$^{140}_{58}Ce$	Stable	
$^{142}_{60}Nd$	27.2	9.82	$^{141}_{60}Nd$	64 s 2.4 h	IT EC, β^+	7.2	$^{141}_{59}Pr$	Stable	
$^{143}_{60}Nd$	12.2	6.1	$^{142}_{60}Nd$	Stable		7.5	$^{142}_{59}Pr$	19.2 h	β^-
$^{144}_{60}Nd$	23.8	7.8	$^{143}_{60}Nd$	Stable		8.0	$^{143}_{59}Pr$	13.7 d	β^-
$^{145}_{60}Nd$	8.3	5.8	$^{144}_{60}Nd$	Stable		8.0	$^{144}_{59}Pr$	17.3 m	β^-
$^{146}_{60}Nd$	17.2	7.6	$^{145}_{60}Nd$	Stable		8.6	$^{145}_{59}Pr$	5.98 h	β^-
$^{148}_{60}Nd$	5.7	7.33	$^{147}_{60}Nd$	10.98 d 2.623 y	β^- β^-	9.3	$^{147}_{59}Pr$	12 m	β^-
$^{150}_{60}Nd$	5.6	7.38	$^{149}_{60}Nd$	1.73 h 2.212 d	β^- β^-	9.5	$^{149}_{59}Pr$	2.3 m 1.73 h	β^-, β^-, β^-

Table 7. (cont.)

Natural Isotope	% nat. abun-dance	$E_{th}(\gamma, n)$	Isotope formed	Half-life of formed isotope	Decay modes	$E_{th}(\gamma, p)$	Isotope formed	Half-life of formed isotope	Decay modes
$^{147}_{61}Pm$	0								
$^{144}_{62}Sm$	3.1	10.6	$^{143}_{62}Sm$	8.9 m	β^+, EC	6.3	$^{143}_{61}Pm$	265 d	EC
$^{147}_{62}Sm$	15.1	6.36	$^{146}_{62}Sm$	7.107 y	α	7.1	$^{146}_{61}Pm$	710 d	EC, β^-
$^{148}_{62}Sm$	11.3	8.14	$^{147}_{62}Sm$	Stable		7.6	$^{147}_{61}Pm$	2.5 y	β^-
$^{149}_{62}Sm$	13.9	5.9	$^{148}_{62}Sm$	Stable		7.6	$^{148}_{61}Pm$	42 d 5.39 d	IT, β^- β^-
$^{150}_{62}Sm$	7.4	8.0	$^{149}_{62}Sm$	Stable		8.3	$^{149}_{61}Pm$	53.1 h	β^-
$^{152}_{62}Sm$	26.7	8.26	$^{151}_{62}Sm$	90 y	β^-	8.7	$^{151}_{61}Pm$	28 h	β^-
$^{154}_{62}Sm$	22.6	7.97	$^{153}_{62}Sm$	46.8 y	β^-	9.0	$^{153}_{61}Pm$	?	?
$^{151}_{63}Eu$	47.8	7.94	$^{150m}_{63}Eu$	12.8 h 36 y	β^+,EC, β^- Ec	4.9	$^{150}_{62}Sm$	Stable	
$^{153}_{63}Eu$	52.2	8.55	$^{152}_{63}Eu$	13 y	β^+,EC, β^-	5.9	$^{152}_{62}Sm$	Stable	
$^{152}_{64}Gd$	0.2	8.59	$^{151}_{64}Gd$	120 d	EC, α	7.3	$^{151}_{63}Eu$	Stable	
$^{154}_{64}Gd$	2.2	8.89	$^{153}_{64}Gd$	242 d	EC	7.6	$^{153}_{63}Eu$	Stable	
$^{155}_{64}Gd$	14.8	6.5	$^{154}_{64}Gd$	Stable		7.6	$^{154}_{63}Eu$	16 y	β^-
$^{156}_{64}Gd$	20.5	8.5	$^{155}_{64}Gd$	Stable		8.0	$^{155}_{63}Eu$	1.81 y	β^-
$^{157}_{64}Gd$	15.7	6.4	$^{156}_{64}Gd$	Stable		8.0	$^{156}_{63}Eu$	15 d	β^-
$^{158}_{64}Gd$	24.8	7.9	$^{157}_{64}Gd$	Stable		8.5	$^{157}_{63}Eu$	15.2 h	β^-
$^{160}_{64}Gd$	21.8	7.45	$^{159}_{64}Gd$	18 h	β^-	9.3	$^{159}_{63}Eu$	18 m	β^-
$^{159}_{65}Tb$	100	8.13	$^{158}_{65}Tb$	11 s $1.2 \cdot 10^3$ y	IT EC, β^-	6.1	$^{158}_{64}Gd$	Stable	
$^{156}_{66}Dy$	0.06	9.44	$^{155}_{66}Dy$	10.2 h	β^+, EC	6.6	$^{155}_{65}Tb$	5.6 d	EC
$^{158}_{66}Dy$	0.1	9.06	$^{157}_{66}Dy$	8.1 h	EC	6.9	$^{157}_{65}Tb$	150 y	EC
$^{160}_{66}Dy$	2.34	8.58	$^{159}_{66}Dy$	144 d	EC	7.4	$^{159}_{65}Tb$	Stable	
$^{161}_{66}Dy$	18.9	6.5	$^{160}_{66}Dy$	Stable		7.5	$^{160}_{65}Tb$	73 d	β^-
$^{162}_{66}Dy$	25.5	8.2	$^{161}_{66}Dy$	Stable		8.0	$^{161}_{65}Tb$	6.9 d	β^-
$^{163}_{66}Dy$	24.9	6.3	$^{162}_{66}Dy$	Stable		7.9	$^{162}_{65}Tb$	7.5 m	β^-
$^{164}_{66}Dy$	28.2	7.7	$^{163}_{66}Dy$	Stable		8.5	$^{163}_{65}Tb$	7 m 6.5 h	β^- β^-

Table 7. (cont.)

Natural Isotope	% nat. abun-dance	$E_{th}(\gamma, n)$	Isotope formed	Half-life of formed isotope	Decay modes	$E_{th}(\gamma, p)$	Isotope formed	Half-life of formed isotope	Decay modes
$^{165}_{67}$Ho	100	8.04	$^{164}_{67}$Ho	37 m	β^-, EC	6.2	$^{164}_{66}$Dy	Stable	
$^{162}_{68}$Er	0.1	9.2	$^{161}_{68}$Er	3.1 h	β^+, EC	6.4	$^{161}_{67}$Ho	2.5 h	IT, EC
$^{164}_{68}$Er	1.6	8.85	$^{163}_{68}$Er	75 m	β^+, EC	6.9	$^{163}_{67}$Ho	$>10^3$ y	IT, EC
$^{166}_{68}$Er	33.4	8.48	$^{165}_{68}$Er	10.3 h	EC	7.3	$^{165}_{67}$Ho	Stable	
$^{167}_{68}$Er	22.9	6.4	$^{166}_{68}$Er	Stable		7.5	$^{166}_{67}$Ho	26.9 h $1.2\cdot10^3$ y	β^- β^-
$^{168}_{68}$Er	27.0	7.8	$^{167}_{68}$Er	Stable		8.0	$^{167}_{67}$Ho	3.1 h	β^-
$^{170}_{68}$Er	15.0	7.26	$^{169}_{68}$Er	9.4 d	β^-	8.6	$^{169}_{67}$Ho	4.8 m	β^-
$^{169}_{69}$Tm	100	8.03	$^{168}_{69}$Tm	87 d	EC	5.6	$^{168}_{68}$Er	Stable	
$^{168}_{70}$Yb	0.1	9.05	$^{167}_{70}$Yb	18 m	β^+, EC	6.3	$^{167}_{69}$Tm	9.6 d	EC
$^{170}_{70}$Yb	3.1	8.47	$^{169}_{70}$Yb	32 d	EC	6.8	$^{169}_{69}$Tm	Stable	
$^{171}_{70}$Yb	14.3	6.6	$^{170}_{70}$Yb	Stable		6.8	$^{170}_{69}$Tm	128.6 d	β^-
$^{172}_{70}$Yb	21.9	8.0	$^{171}_{70}$Yb	Stable		7.3	$^{171}_{69}$Tm	1.92 y	β^-
$^{173}_{70}$Yb	16.2	5.4	$^{172}_{70}$Yb	Stable		7.5	$^{172}_{69}$Tm	63.6 h	β^-
$^{174}_{70}$Yb	31.7	7.5	$^{173}_{70}$Yb	Stable		8.0	$^{173}_{69}$Tm	8.2 h	β^-
$^{176}_{70}$Yb	12.7	6.87	$^{175}_{70}$Yb	101 h	IT, β^-	8.5	$^{175}_{69}$Tm	20 m	β^-
$^{175}_{71}$Lu	97.4	7.67	$^{174}_{71}$Lu	140 d 3.6 y	IT, EC EC	5.5	$^{174}_{70}$Yb	Stable	
$^{176}_{71}$Lu	2.6	6.3	$^{175}_{71}$Lu	Stable		6.0	$^{175}_{70}$Yb	101 h	IT, β^-
$^{174}_{72}$Hf	0.2	8.63	$^{173}_{72}$Hf	23.6 h	EC	6.2	$^{173}_{71}$Lu	1.37 y	EC
$^{176}_{72}$Hf	5.2	8.17	$^{175}_{72}$Hf	70 d	EC	6.7	$^{175}_{71}$Lu	Stable	
$^{177}_{72}$Hf	18.5	6.4	$^{176}_{72}$Hf	Stable		6.8	$^{176m}_{71}$Lu $^{176}_{71}$Lu	3.66 h $3.8\cdot10^{10}$y	β^- β^-
$^{178}_{72}$Hf	27.1	7.6	$^{177}_{72}$Hf	Stable		7.3	$^{177m}_{71}$Lu $^{177}_{71}$Lu	160.7 d 6.75 d	IT, β^- β^-
$^{179}_{72}$Hf	13.8	6.1	$^{178m2}_{72}$Hf $^{178m1}_{72}$Hf	>10 y 5 s	IT IT	7.6	$^{178m}_{71}$Lu $^{178}_{71}$Lu	23.1 m 28.5 m	β^- β^-
$^{180}_{72}$Hf	35.2	7.4	$^{179m}_{72}$Hf	18.6 s	IT	8.0	$^{179}_{71}$Lu	4.6 h	β^-

Table 7. (cont.)

Natural Isotope	% nat. abun-dance	$E_{th}(\gamma, n)$	Isotope formed	Half-life of formed isotope	Decay modes	$E_{th}(\gamma, p)$	Isotope formed	Half-life of formed isotope	Decay modes
$^{180}_{73}Ta$	0.01	6.645	$^{179}_{73}Ta$	600 y	EC	5.75	$^{179m}_{72}Hf$	18.6 s	IT
$^{181}_{73}Ta$	99.99	7.577	$^{180m}_{73}Ta$	8.1 h	EC, β^-	5.94	$^{180m}_{72}Hf$	5.5 h	IT
$^{180}_{74}W$	0.1	8.412	$^{179}_{74}W$	5.2 m 38 m	IT EC	6.57	$^{179}_{73}Ta$	600 y	EC
$^{182}_{74}W$	26.3	8.063	$^{181}_{74}W$	140 d	IT, EC	7.09	$^{181}_{73}Ta$	Stable	
$^{183}_{74}W$	14.3	6.191	$^{182}_{74}W$	Stable		7.22	$^{182}_{73}Ta$	16.5 m 115 d	IT β^-
$^{184}_{74}W$	30.7	7.412	$^{183}_{74}W$	5.3 s	IT	7.70	$^{183}_{73}Ta$	5.1 d	β^-
$^{186}_{74}W$	28.6	7.195	$^{185}_{74}W$	1.62 m 75.8 d	IT β^-	8.40	$^{185}_{73}Ta$	50 m	β^-
$^{185}_{75}Re$	37.4	7.68	$^{184}_{75}Re$	169 d 3.8 d	IT EC	5.4	$^{184}_{74}W$	Stable	
$^{187}_{75}Re$	62.6	7.36	$^{186}_{75}Re$	90 h	β^-	6.0	$^{186}_{74}W$	Stable	
$^{184}_{76}Os$	0.02	9.3	$^{183}_{76}Os$	9.9 h 12 h	IT, EC EC	5.7	$^{183}_{75}Re$	71 d	EC
$^{186}_{76}Os$	1.58	8.3	$^{185}_{76}Os$	94 d	EC	6.5	$^{185}_{75}Re$	Stable	
$^{187}_{76}Os$	1.6	6.3	$^{186}_{76}Os$	Stable		6.6	$^{186}_{75}Re$	90 h	β^-
$^{188}_{76}Os$	13.3	8.0	$^{187}_{76}Os$	Stable		7.2	$^{187}_{75}Re$	Stable	
$^{189}_{76}Os$	16.1	5.9	$^{188}_{76}Os$	Stable		7.3	$^{188}_{75}Re$	18.7 m 16.7 h	IT β^-
$^{190}_{76}Os$	26.4	7.8	$^{189}_{76}Os$	5.7 h	IT	8.0	$^{189}_{75}Re$	24 h	β^-
$^{192}_{76}Os$	41	7.56	$^{191}_{76}Os$	13 h 15 d	IT β^-	9.8	$^{191}_{75}Re$	9.8 m	β^-
$^{191}_{77}Ir$	37.3	8.07	$^{190}_{77}Ir$	3.2 h 1.2 h 11 d	IT, β^+, EC IT EC	5.3	$^{190m}_{76}Os$	9.9 m	IT
$^{193}_{77}Ir$	62.7	7.76	$^{192}_{77}Ir$	>5 y 1.4 m 74 d	IT IT, β^- β^-, β^+, EC	5.9	$^{192}_{76}Os$	Stable	

Table 7. (cont.)

Natural Isotope	% nat. abun-dance	$E_{th}(\gamma, n)$	Isotope formed	Half-life of formed isotope	Decay modes	$E_{th}(\gamma, p)$	Isotope formed	Half-life of formed isotope	Decay modes
$^{190}_{78}Pt$	0.01	8.91	$^{189}_{78}Pt$	10.9 h	EC	6.17	$^{189}_{77}Ir$	13.3 d	EC
$^{192}_{78}Pt$	0.79	8.67	$^{191}_{78}Pt$	3.0 d	EC	6.88	$^{191m}_{77}Ir$	4.9 s	IT
$^{194}_{78}Pt$	32.9	8.37	$^{193}_{78}Pt$	4.3 d <500 y	IT EC	7.53	$^{193m}_{77}Ir$	12 d	IT
$^{195}_{78}Pt$	33.8	6.10	$^{194}_{78}Pt$	Stable		7.57	$^{194}_{77}Ir$	17.4 h	β^-
$^{196}_{78}Pt$	25.3	7.92	$_{78}Pt^{195}$	4.1 d	IT	8.26	$^{195}_{77}Ir$	4.2 h	β^-
$^{198}_{78}Pt$	7.2	7.56	$^{197m}_{78}Pt$ $^{197}_{78}Pt$	80 m 18 h	IT, β^- β^-	8.93	$^{197}_{77}Ir$	7 m	β^-
$^{197}_{79}Au$	100	8.07	$^{196}_{79}Au$	6.18 d	β^+, EC, β^-	5.78	$^{196}_{78}Pt$	Stable	
$^{196}_{80}Hg$	0.2	8.85	$^{195}_{80}Hg$	9.5 h	EC	6.6	$^{195}_{79}Au$	31 s 183 d	IT EC
$^{198}_{80}Hg$	10.1	8.49	$^{197}_{80}Hg$	24 h 65 h	IT, EC EC	7.1	$^{197m}_{79}Au$	7.2 s	IT
$^{199}_{80}Hg$	16.9	6.6	$^{198}_{80}Hg$	Stable		7.2	$^{198}_{79}Au$	2.693 d	β^-
$^{200}_{80}Hg$	23.1	8.0	$^{199m}_{80}Hg$	43 m	IT	7.7	$^{199}_{79}Au$	3.15 d	β^-
$^{201}_{80}Hg$	13.2	6.2	$^{200}_{80}Hg$	Stable		7.7	$^{200}_{79}Au$	48.4 m	β^-
$^{202}_{80}Hg$	29.7	7.8	$^{201}_{80}Hg$	Stable		8.4	$^{201}_{79}Au$	26 m	β^-
$^{204}_{80}Hg$	6.8	7.45	$^{203}_{80}Hg$	46.57 d	β^-	9.6	$^{203}_{79}Au$	5.5 s	β^-
$^{203}_{81}Tl$	29.5	7.7	$^{202}_{81}Tl$	12.0 d	EC	5.7	$^{202}_{80}Hg$	Stable	
$^{205}_{81}Tl$	70.5	7.5	$^{204}_{81}Tl$	3.8 y	β^-, EC	6.4	$^{204}_{80}Hg$	Stable	
$^{204}_{82}Pb$	1.4	8.4	$^{203}_{82}Pb$	6.1 s 52.1 h	IT EC	6.6	$^{203}_{81}Tl$	Stable	
$^{206}_{82}Pb$	24.1	8.1	$^{205}_{82}Pb$	4 ms $3 \cdot 10^7$ y	IT EC	7.3	$^{205}_{81}Tl$	Stable	
$^{207}_{82}Pb$	22.1	6.7	$^{206}_{82}Pb$	Stable		7.5	$^{206}_{81}Tl$	4.19 m	β^-
$^{208}_{82}Pb$	52.4	7.4	$^{207}_{82}Pb$	0.8 s	IT	8.0	$^{207}_{81}Tl$	1.3 s 4.78 m	IT β^-

Table 7. (cont.)

Natural Isotope	% nat. abun-dance	$E_{th}(\gamma, n)$	Isotope formed	Half-life of formed isotope	Decay modes	$E_{th}(\gamma, p)$	Isotope formed	Half-life of formed isotope	Decay modes
$^{209}_{83}$Bi	100	7.46	$^{208}_{83}$Bi	$3.7 \cdot 10^5$ y	EC	3.8	$^{208}_{82}$Pb	Stable	
$_{84}$Po	Trace								
$_{85}$ At	Trace								
$_{86}$Rn	Trace								
$_{87}$Fr	Trace								
$^{226}_{88}$Ra	Trace								
$_{89}$Ac	Trace								
$^{232}_{90}$Th		6.44	$^{231}_{90}$Th	25.5 h	β^-	7.7	$^{231}_{89}$Ac	15 m	β^-
$_{91}$Pa	Trace								
$^{234}_{92}$U	0.005	6.84	$^{233}_{92}$U	$1.6 \cdot 10^5$ y	α	6.6	$^{233}_{91}$Pa	27.0 d	β^-
$^{235}_{92}$U	0.720	5.30	$^{234}_{92}$U	$2.5 \cdot 10^5$ y	α	6.7	$^{234}_{91}$Pa	1,17 m 6.75 h	IT, β^- β^-
$^{238}_{92}$U	99.275	6.15	$^{237}_{92}$U	6.75 d	β^-	7.7	$^{237}_{91}$Pa	39 m	β^-

A.: The thresholds for (γ, n) and (γ, p) reactions are from the Tables of Keller, K. A., Lange, J., Münzel, H. (1973) Q-values and Excitation Functions of Nuclear Reactions, Editor: H. Schopper. *Landolt-Börnstein, Numerical Data and Functional Relationships in Science and Technology*, New Series, editor in chief: K.-H. Hellwege; Group I: Nuclear and Particle Physics, Vol. **5**, Part a. Springer-Verlag Berlin, Heidelberg, New York, 1973. The remaining values are from the Holden, N. E. (1991) *Table of the Isotopes.* Report (revised 1991) from the High Flux Beam Reactor, Reactor Division, Brookhaven National Laboratory, Upton, New York, 11973. A similar version is also found in *CRC Handbook of Chemistry and Physics*, 79th edition, 1998-1999; editor: D. R. Lide; CRC Press, Bocca Raton, Boston, London, New York, Washington DC; pp.

Table 8. Photoneutron activity produced in reference food irradiated with X rays[A]

Isotope	Weight of the elements in mg/kg of food	Number of isotope atoms per gram of food	Photo-neutron thres-hold in MeV	Isotope formed	Decay mode	Decay energy in MeV	Half-life	Bq/kg per kGy for 10 MeV X rays	Bq/kg per kGy for 7.5 MeV X rays
^{1}H	90 000	$5.38 \cdot 10^{22}$	-	-	-				
^{2}H		$8.07 \cdot 10^{18}$	2.2246	^{1}H	Stable		Stable	0	0
^{12}C	180 000	$8.92 \cdot 10^{21}$	18.72	^{11}C	β^+, EC→ ^{11}B	1.982	20.3 m	0	0
^{13}C		$1.00 \cdot 10^{20}$	4.95	^{12}C			Stable	0	0
^{14}N	20 000	$8.57 \cdot 10^{20}$	10.55	^{13}N	β^+→ ^{13}C	2.2205	9.97 m	0	0
^{15}N		$3.18 \cdot 10^{18}$	10.83	^{14}N			Stable	0	0
^{16}O	700 000	$2.63 \cdot 10^{22}$	15.67	^{15}O	β^+→ ^{15}N	2.754	2.022 m	0	0
^{17}O		$9.75 \cdot 10^{18}$	4.14	^{16}O			Stable	0	0
^{18}O		$5.37 \cdot 10^{19}$	8.04	^{17}O			Stable	0	0
^{23}Na	750	$1.96 \cdot 10^{19}$	12.42	^{22}Na	β^+, EC→ ^{22}Ne	2.842	2.605 y	0	0
^{24}Mg	300	$5.85 \cdot 10^{18}$	16.53	^{23}Mg	β^+→ ^{23}Na	4.058	11.32 s	0	0
^{25}Mg		$7.53 \cdot 10^{17}$	7.33	^{24}Mg			Stable	0	0
^{26}Mg		$8.30 \cdot 10^{17}$	11.09	^{25}Mg			Stable	0	0
^{27}Al	0.4	$8.93 \cdot 10^{15}$	13.06	^{26}Al	β^+, EC→ ^{26}Mg	4.005	$7.1.10^{5}$ y	0	0
^{28}Si	10	$1.98 \cdot 10^{17}$	17.18	^{27}Si	β^+→ ^{27}Al	4.812	4.14 s	0	0
^{29}Si		$1.01 \cdot 10^{16}$	8.47	^{28}Si			Stable	0	0
^{30}Si		$6.63 \cdot 10^{15}$	10.61	$^{Si}29$			Stable	0	0
^{31}P	2 000	$3.89 \cdot 10^{19}$	12.31	^{30}P	β^+→ ^{30}Si	4.226	2.50 m	0	0
^{32}S	2 200	$3.93 \cdot 10^{19}$	15.04	^{31}S	β^+→ ^{31}P	5.396	2.56 s	0	0
^{33}S		$3.14 \cdot 10^{17}$	8.64	^{32}S			Stable	0	0
^{34}S		$1.74 \cdot 10^{18}$	11.42	^{33}S			Stable	0	0
^{36}S		$8.26 \cdot 10^{15}$	9.89	^{35}S	β^-→ ^{35}Cl	0.1674	87.2 d	$3.6.10^{-6}$	0
^{35}Cl	560	$7.19 \cdot 10^{18}$	12.64	^{34m}Cl ^{34}Cl	β^+→ ^{34}S IT→ ^{34}Cl β^+→ ^{34}S	5.65, 0.146 5.492	32.2 m 1.528 s	0 0	0 0
^{37}Cl		$2.33 \cdot 10^{18}$	10.31	^{36}Cl ^{36}Cl	β^-→ ^{36}Ar, 98% β^+, EC→ ^{36}S, 2%	0.7093 1.142	$3.01 \cdot 10^{5}$ y $3.01 \cdot 10^{5}$ y	0	0
^{39}K	4 000	$5.75 \cdot 10^{19}$	13.08	^{38m}K ^{38}K	β^+→ ^{38}Ar, 100% β^+→ ^{38}Ar, 99.8%	6.742 5.913	0.942 s 7.63 m	0 0	0
^{40}K		$7.21 \cdot 10^{15}$	7.80	^{39}K			Stable	0	0
^{41}K		$4.15 \cdot 10^{18}$	10.10	^{40}K ^{40}K	β^+, EC→ ^{40}Ar, 11% β^-→ ^{40}Ca, 89%	1.50 1.31	$1.26.10^{9}$ y $1.26.10^{9}$ y	0 0	0 0
^{40}Ca	140	$2.04 \cdot 10^{18}$	15.64	^{39}Ca	β^+→ ^{39}K	6.531	0.86 s	0	0
^{42}Ca		$1.35 \cdot 10^{16}$	11.48	^{41}Ca	EC→ ^{41}K	0.421	$1.03 \cdot 10^{5}$ y	0	0
^{43}Ca		$3.05 \cdot 10^{15}$	7.93	^{42}Ca			Stable	0	0
^{44}Ca		$4.33 \cdot 10^{16}$	11.13	^{43}Ca			Stable	0	0
^{46}Ca		$6.94 \cdot 10^{13}$	10.40	^{45}Ca	β^-→ ^{45}Sc	0.257	162.7 d	0	0
^{48}Ca		$3.93 \cdot 10^{15}$	9.94	^{47}Ca ^{47}Sc	β^-→ ^{47}Sc β^-→ ^{47}Ti	1.988 0.601	4.536 d, 3.349 d	$7.2 \cdot 10^{-6}$ $9.8 \cdot 10^{-6}$	0 0

Table 8. (cont.)[A]

Isotope	Weight of the elements in mg/kg of food	Number of isotope atoms per gram of food	Photo-neutron thres-hold in MeV	Isotope formed	Decay mode	Decay energy in MeV	Half-life	Bq/kg per kGy for 10 MeV X rays	Bq/kg per kGy for 7.5 MeV X rays
^{46}Ti	0.1	$1.01\cdot10^{14}$	13.19	^{45}Ti	β^+, EC→ ^{45}Sc	2.063	3.078 h	0	0
^{47}Ti		$9.78\cdot10^{13}$	8.88	^{46}Ti			Stable	0	0
^{48}Ti		$9.88\cdot10^{14}$	11.63	^{47}Ti			Stable	0	0
^{49}Ti		$7.37\cdot10^{13}$	8.14	^{48}Ti			Stable	0	0
^{50}Ti		$6.79\cdot10^{13}$	10.94	^{49}Ti			Stable	0	0
^{50}V	0.1	$2.96\cdot10^{12}$	9.34	^{49}V	EC→^{49}Ti	0.601	337 d	$1.0\cdot10^{-7}$	0
^{51}V		$1.18\cdot10^{15}$	11.05	^{50}V			Stable	0	0
^{50}Cr	0.01	$5.03\cdot10^{12}$	13.00	^{49}Cr ^{49}V	β^+, EC→ ^{49}V EC→^{49}Ti	2.627 0.601	42.3 m 337 d	0 0	0 0
^{52}Cr		$9.70\cdot10^{13}$	12.04	^{51}Cr	EC→^{51}V	0.751	27.7 d	0	0
^{53}Cr		$1.10\cdot10^{13}$	7.94	^{52}Cr			Stable	0	0
^{54}Cr		$2.74\cdot10^{12}$	9.72	^{53}Cr			Stable	0	0
^{55}Mn	0.2	$2.19\cdot10^{15}$	10.23	^{54}Mn	EC→^{54}Cr	1.377	312.2 d	0	0
^{54}Fe	50	$3.18\cdot10^{16}$	13.38	^{53m}Fe ^{53}Fe ^{53}Mn	IT→ ^{53}Fe β^+→ ^{53}Mn EC→ ^{53}Cr	3.041 3.774 0.596	2.6 m 8.51 m $3.7.10^6$ y	0 0 0	0 0 0
^{56}Fe		$4.95\cdot10^{17}$	11.20	^{55}Fe	EC→^{55}Mn	0.2314	2.73 y	0	0
^{57}Fe		$1.13\cdot10^{16}$	7.65	^{56}Fe			Stable	0	0
^{58}Fe		$1.51\cdot10^{15}$	10.05	^{57}Fe			Stable	0	0
^{59}Co	0.01	$1.02\cdot10^{14}$	10.49	^{58m}Co ^{58}Co	IT→^{58}Co β^+, EC→ ^{58}Fe	0.03 2.30	9.1 h 70.88 d	0 0	0 0
^{58}Ni	0.1	$6.98\cdot10^{14}$	12.22	^{57}Ni ^{57}Co	β^+, EC→ ^{57}Co EC→ ^{57}Fe	3.265 0.836	1.4833 d 271.8 d	0 0	0 0
^{60}Ni		$2.69\cdot10^{14}$	11.39	^{59}Ni	EC→ ^{59}Co	1.072	$7.6\cdot10^4$ y	0	0
^{61}Ni		$1.17\cdot10^{13}$	7.82	^{60}Ni			Stable	0	0
^{62}Ni		$3.73\cdot10^{13}$	10.60	^{61}Ni			Stable	0	0
^{64}Ni		$9.50\cdot10^{12}$	9.66	^{63}Ni	β^- → ^{63}Cu	0.065	100 y	$5.3\cdot10^{-10}$	0
^{63}Cu	0.6	$3.93\cdot10^{15}$	10.85	^{62}Cu	β^+, EC→^{62}Ni	3.95	9.74 m	0	0
^{65}Cu		$1.75\cdot10^{15}$	9.91	^{64}Cu ^{64}Cu	β^- → ^{64}Zn, 39% β^+, EC→ ^{64}Ni	0.578 1.675	12.7 h	$*1.0\cdot10^{-4}$	0
^{64}Zn	40	$1.79\cdot10^{17}$	11.86	^{63}Zn	β^+, EC→ ^{63}Cu	3.367	38.5 m	0	0
^{66}Zn		$1.03\cdot10^{17}$	11.06	^{65}Zn	β^+, EC→ ^{65}Cu	1.352	243.8 d	0	0
^{67}Zn		$1.51\cdot10^{16}$	7.05	^{66}Zn			Stable	0	0
^{68}Zn		$6.93\cdot10^{16}$	10.20	^{67}Zn			Stable	0	0
^{70}Zn		$2.21\cdot10^{15}$	9.21	^{69m}Zn ^{69}Zn	IT→ ^{69}Zn, 99% β^- → ^{69}Ga	0.439 0.905	13.76 h 56 m	$<1.1\cdot10^{-1}$	0 0
^{70}Ge	0.1	$1.76\cdot10^{14}$	11.5	^{69}Ge	β^+, EC→ ^{69}Ga	2.225	1.63 d	0	0
^{72}Ge		$2.27\cdot10^{14}$	10.7	^{71m}Ge ^{71}Ge	IT→ ^{71}Ge EC→ ^{71}Ga	0.0234 0.236	20.4 ms 11.2 d	0	0
^{73}Ge		$6.47\cdot10^{13}$	6.78	^{72}Ge			Stable	0	0
^{74}Ge		$2.98\cdot10^{14}$	10.2	^{73}Ge			Stable	0	0
^{76}Ge		$6.17\cdot10^{13}$	9.43	^{75m}Ge ^{75}Ge	IT→ ^{75}Ge β^- → ^{75}As	0.1397 1.178	48 s 1.38 h	$1.2\cdot10^{-2}$	0

Table 8. (cont.)[A]

Isotope	Weight of the elements in mg/kg of food	Number of isotope atoms per gram of food	Photo-neutron thres-hold in MeV	Isotope formed	Decay mode	Decay energy in MeV	Half-life	Bq/kg per kGy for 10 MeV X rays	Bq/kg per kGy for 7.5 MeV X rays
^{75}As	0.1	$8.04 \cdot 10^{14}$	10.2	^{74}As, ^{74}As	$\beta^- \rightarrow {}^{74}$Se, 32% β^+, EC$\rightarrow {}^{74}$Ge	1.354 2.562	17.78 d	0 0	0 0
^{74}Se	0.1	$6.79 \cdot 10^{12}$	12.1	^{73m}Se ^{73}Se ^{73}As	IT$\rightarrow {}^{73}$Se, 73% β^+, EC$\rightarrow {}^{73}$As EC$\rightarrow {}^{73}$Ge	0.0257 2.74 0.346	42 m 7.1 h 80.3 d	0 0 0	0 0 0
^{76}Se		$7.14 \cdot 10^{13}$	11.2	^{75}Se	EC$\rightarrow {}^{75}$As	0.865	119.78 d	0	0
^{77}Se		$5.78 \cdot 10^{13}$	7.4	^{76}Se			Stable	0	0
^{78}Se		$1.81 \cdot 10^{14}$	10.5	^{77}Se			Stable	0	0
^{80}Se		$3.78 \cdot 10^{14}$	9.9	^{79m}Se ^{79}Se	IT$\rightarrow {}^{79}$Se $\beta^- \rightarrow {}^{79}$Br	0.096 0.149	3.92 m $6.5 \cdot 10^4$ y	$<8.9 \cdot 10^{-3}$ $<1.0 \cdot 10^{-12}$	0 0
^{82}Se		$6.67 \cdot 10^{13}$	9.3	^{81}Se	$\beta^- \rightarrow {}^{81}$Br	1.59	18.5 m	$1.2 \cdot 10^{-1}$	0
^{79}Br	2.0	$7.64 \cdot 10^{15}$	10.7	^{78}Br	β^+, EC$\rightarrow {}^{78}$Se	3.574	6.45 m	0	0
^{81}Br		$7.43 \cdot 10^{15}$	10.2	^{80m}Br ^{80}Br ^{80}Br	IT$\rightarrow {}^{80}$Br $\beta^- \rightarrow {}^{80}$Kr, 92% β^+, EC$\rightarrow {}^{80}$Se, 8%	0.0489 2.00 1.87	4.42 h 17.66 m 17.66 m	0 0 0	0 0 0
^{85}Rb	8	$4.07 \cdot 10^{16}$	10.5	^{84m}Rb ^{84}Rb ^{84}Rb	IT$\rightarrow {}^{84}$Rb β^+, EC$\rightarrow {}^{84}$Kr, 97% $\beta^- \rightarrow {}^{84}$Sr, 3%	0.216 2.682 0.893	20.3 m 32.9 d 32.9 d	0 0 0	0 0 0
^{87}Rb		$1.57 \cdot 10^{16}$	9.9	^{86m}Rb ^{86}Rb	IT$\rightarrow {}^{86}$Rb $\beta^- \rightarrow {}^{86}$Sr	0.556 1.775	1.018 m 18.65 d	<1.6 $<5.9 \cdot 10^{-5}$	0 0
^{84}Sr	0.2	$7.70 \cdot 10^{12}$	12.0	^{83m}Sr ^{83}Sr ^{83}Rb	IT$\rightarrow {}^{83}$Sr EC$\rightarrow {}^{83}$Rb β^+, EC$\rightarrow {}^{83}$Rb EC$\rightarrow {}^{83}$Kr	0.2591 2.53 2.27 0.93	5 s 32.4 h 86.2 d	0 0 0	0 0 0
^{86}Sr		$1.36 \cdot 10^{14}$	11.5	^{85m}Sr ^{85}Sr	IT$\rightarrow {}^{85}$Sr, 87% EC$\rightarrow {}^{85}$Rb, 13% EC$\rightarrow {}^{85}$Rb	0.2387 1.3037 1.065	1.127 h 64.84 d	0 0	0 0
^{87}Sr		$9.62 \cdot 10^{13}$	8.43	^{87m}Sr ^{86}Sr	IT$\rightarrow {}^{87}$Sr	0.3884	2.80 h Stable	<0.22 0	 0
^{88}Sr		$1.13 \cdot 10^{15}$	11.1	^{87m}Sr	IT$\rightarrow {}^{87}$Sr	0.3884	2.80 h	0	0
^{90}Zr	0.5	$1.70 \cdot 10^{15}$	12.0	^{89m}Zr ^{89}Zr	IT$\rightarrow {}^{89}$Zr, 94% β^+, EC$\rightarrow {}^{89}$Y, 6% β^+, EC$\rightarrow {}^{89}$Y	0.5877 3.42 2.832	4.18 m 3.267 d	0 0	0 0
^{91}Zr		$3.7 \cdot 10^{14}$	7.2	^{90}Zr		-	Stable	0	0
^{92}Zr		$5.64 \cdot 10^{14}$	8.6	^{91}Zr		-	Stable	0	0
^{94}Zr		$5.78 \cdot 10^{14}$	8.2	^{93}Zr	$\beta^- \rightarrow {}^{93}$Nb	0.09	$1.5 \cdot 10^6$ y	$4.6 \cdot 10^{-10}$	0
^{96}Zr		$9.24 \cdot 10^{13}$	7.8	^{95}Zr ^{95}Nb	$\beta^- \rightarrow {}^{95}$Nb $\beta^- \rightarrow {}^{95}$Mo	1.125 0.926	64.02 d 34.97 d	$< 1.2 \cdot 10^{-3}$ $< 2.2 \cdot 10^{-3}$	0 0

Table 8. (cont.)

Isotope	Weight of elements in mg/kg of food	Number of isotope atoms per gram of food	Photo-neutron thres-hold in MeV	Isotope formed	Decay mode	Decay energy in MeV	Half-life	Bq/kg per kGy for 10 MeV X rays	Bq/kg per kGy for 7.5 MeV X rays
^{92}Mo	0.1	$9.31\cdot10^{13}$	12.7	^{91m}Mo ^{91m}Mo ^{91}Mo ^{91m}Nb ^{91}Nb	IT→ ^{91}Mo, 50% β^+, EC→ ^{91m}Nb β^+, EC→ ^{91}Nb IT→ ^{91}Nb EC→ ^{91}Zr	0.653 5.093 4.44 0.1045 1.254	1.08 m 15.5 m 62 d 700 y	0 0 	0 0
^{94}Mo		$5.81\cdot10^{13}$	9.7	^{93m}Mo ^{93}Mo	IT→ ^{93}Mo EC→ ^{93}Nb	2.425 0.406	6.9 h $3.5\cdot10^3$ y	$<4.1\cdot10^{-4}$ $<9.3\cdot10^{-11}$	0 0
^{95}Mo		$9.99\cdot10^{13}$	7.4	^{94}Mo		-	Stable	0	0
^{96}Mo		$1.05\cdot10^{14}$	9.2	^{95}Mo		-	Stable	0	0
^{97}Mo		$5.99\cdot10^{13}$	6.8	^{96}Mo		-	Stable	0	0
^{98}Mo		$1.51\cdot10^{14}$	8.6	^{97}Mo		-	Stable	0	0
^{100}Mo		$6.04\cdot10^{13}$	8.3	^{99}Mo ^{99m}Tc ^{99}Tc	β^-→ ^{99m}Tc IT→ ^{99}Tc β^-→ ^{99}Ru	1.357 0.142 0.293	2.75 d 6.01 h $2.13\cdot10^5$ y	$*\ 6.0\cdot10^{-3}$	0
^{103}Rh	0.01	$5.85\cdot10^{13}$	9.3	^{103m}Rh ^{102m}Rh ^{102}Rh	IT→ ^{102}Rh IT→ ^{102}Rh, 5% β^+, EC→ ^{102}Ru, 76% β^-→ ^{102}Pd, 19% β^-→ ^{102}Pd	0.04 2.28	56.12 m 207 d 2.9 y	$<3.3\cdot10^{-2}$ $<8.2\cdot10^{-6}$ $<1.6\cdot10^{-6}$	0
^{107}Ag	0.02	$5.79\cdot10^{13}$	9.5	^{106m}Ag ^{106}Ag	EC→ ^{106}Pd β^+, EC→ ^{106}Pd	>2.97 2.97	8.4 d 24 m	$<*8.3.10^{-5}$ $<*4.2\cdot10^{-2}$	0 0
^{109}Ag		$5.49\cdot10^{13}$	9.2	^{108m}Ag ^{108m}Ag ^{108}Ag	IT→ ^{108}Ag, 8% EC→ ^{108}Pd, 92% β^+, EC→ ^{108}Pd, 3% β^-→ ^{108}Cd, 97%	0.079 2.00 1.92 1.65	130 y 130 y 2.39 m 2.39 m	$<*7.9\cdot10^{-8}$ $<*2.27$ 	0 0
^{106}Cd	0.1	$4.77\cdot10^{12}$	10.9	^{105}Cd ^{105}Ag	β^+, EC→ ^{105}Ag EC→ ^{105}Pd	2.74 1.34	55.5 m 41.3 d	0 0	0 0
^{108}Cd		$4.77\cdot10^{12}$	10.3	^{107}Cd	β^+, EC→ ^{107}Ag	1.417	6.52 h	0	0
^{110}Cd		$6.69\cdot10^{13}$	9.9	^{109}Cd	EC→ ^{109}Ag	0.214	462 d	$1.3\cdot10^{-8}$	0
^{111}Cd		$6.86\cdot10^{13}$	7.0	^{111m}Cd ^{110}Cd	IT→ ^{111}Cd	0.396	48.5 m Stable	< 4.9 0	<0.023 0
^{112}Cd		$1.29\cdot10^{14}$	9.4	^{111m}Cd ^{111}Cd	IT→ ^{111}Cd	0.396	48.5 m Stable	$< 7.4\cdot10^{-2}$	0
^{113}Cd		$6.55\cdot10^{13}$	6.5	^{113m}Cd ^{112}Cd	IT→ ^{113}Cd	0.59	14.1 y Stable	$< 4.9\cdot10^{-5}$ 0	$<1.15\cdot10^{-6}$ 0
^{114}Cd		$1.54\cdot10^{14}$	9.0	^{113m}Cd ^{113}Cd	β^-→ ^{113}In	0.59	14.1 y Stable	$< 2.7\cdot10^{-6}$	0
^{116}Cd		$4.01\cdot10^{13}$	8.7	^{115m}Cd ^{115}Cd	β^-→ ^{115}In β^-→ ^{115m}In ^{115m}In → ^{115}In	1.629 1.448 0.336	44.6 d 2.23 d 4.486 h	$< 1.8\cdot10^{-4}$ $<3.7\cdot10^{-3}$	0 0

Table 8. (cont.)

Isotope	Weight of the elements in mg/kg of food	Number of isotope atoms per gram of food	Photo-neutron thres-hold in MeV	Isotope formed	Decay mode	Decay energy in MeV	Half-life	Bq/kg per kGy for 10 MeV X rays	Bq/kg per kGy for 7.5 MeV X rays
^{113}In	0.01	$2.26 \cdot 10^{12}$	9.4	^{113m}In ^{112m}In ^{112}In	IT→ ^{113}In IT→ ^{112}In β^+, EC→^{112}Cd β^-→^{112}Sn, 44%	0.3917 0.155 2.588 0.66	1.658 h 20.8 m 14.4 m 14.4 m	$< 6.5 \cdot 10^{-4}$ $< 3.1 \cdot 10^{-3}$ $< 4.4 \cdot 10^{-3}$	 0 0
^{115}In		$5.02 \cdot 10^{13}$	9.0	^{115m}In ^{115m}In ^{114m}In ^{114m}In ^{114}In ^{114}In	IT→^{115}In, 95% β^-→^{115}Sn, 5% IT→^{114}In, 97% EC→^{114}Cd, 3% β^-→^{114}Sn, 97% EC→^{114}Cd, 3%	0.336 0.83 0.190 2.18 1.989 1.451	4.486 h 4.486 h 49.51 d 49.51 d 1.198 m 1.198 m	$<3.1 \cdot 10^{-7}$ $<*8.3 \cdot 10^{-5}$ $<*4.9$	 0 0
^{112}Sn	0.1	$4.92 \cdot 10^{12}$	10.8	^{111}Sn ^{111}In	β^+, EC→ ^{111}In EC→ ^{111}Cd	2.45 0.86	35 m 2.804 d	0	0
^{114}Sn		$3.30 \cdot 10^{12}$	10.3	^{113m}Sn ^{113m}Sn ^{113}Sn	IT→ ^{113}Sn, 92% EC→ ^{113}In, 8% EC→ ^{113}In	0.077 1.115 1.038	21.4 m 115.1 d	0 0	0 0
^{115}Sn		$1.83 \cdot 10^{12}$	7.5	^{114}Sn		-	Stable	0	0
^{116}Sn		$7.37 \cdot 10^{13}$	9.6	^{115}Sn		-	Stable	0	0
^{117}Sn		$3.90 \cdot 10^{13}$	6.9	^{117m}Sn ^{116}Sn	IT→ ^{117}Sn	0.3146	13.6 d Stable	$<1.1 \cdot 10^{-2}$ 0	$<8 \cdot 10^{-5}$ 0
^{118}Sn		$1.23 \cdot 10^{14}$	9.3	^{117m}Sn ^{117}Sn	IT→ ^{117}Sn	0.3146	13.6 d Stable	$<*4.2 \cdot 10^{-4}$ 0	0 0
^{119}Sn		$4.35 \cdot 10^{13}$	6.5	^{119m}Sn ^{118}Sn	IT→ ^{119}Sn	0.0896	293 d Stable	$<5.4 \cdot 10^{-4}$ 0	$<1.3 \cdot 10^{-5}$ 0
^{120}Sn		$1.65 \cdot 10^{14}$	9.1	^{119m}Sn ^{119}Sn	IT→ ^{119}Sn	0.0896	293 d Stable	$<*3.5 \cdot 10^{-5}$	0 0
^{122}Sn		$2.35 \cdot 10^{13}$	8.8	^{121m}Sn ^{121m}Sn ^{121}Sn	IT→^{121}Sn, 78% β^-→^{121}Sb, 22% β^-→^{121}Sb,	0.006 0.394 0.388	55 y 1.128 d	$<2.0 \cdot 10^{-7}$ $<3.5 \cdot 10^{-3}$	0 0
^{124}Sn		$2.94 \cdot 10^{13}$	8.5	^{123m}Sn ^{123}Sn	β^-→ ^{123}Sb β^-→ ^{123}Sb	1.428 1.403	40.1 m 129 d	$<*8.2 \cdot 10^{-2}$ $<*1.8 \cdot 10^{-5}$	0 0
^{121}Sb	0.01	$2.84 \cdot 10^{13}$	9.2	^{120m}Sb ^{120}Sb	EC→ ^{120}Sb EC, β^+→ ^{120}Sb	~2.7 2.68	5.76 d 15.89 m	$<*4.2 \cdot 10^{-4}$ $<*2.2 \cdot 10^{-1}$	0 0
^{123}Sb		$2.11 \cdot 10^{13}$	9.0	^{122m}Sb ^{122}Sb ^{122}Sb	IT→ ^{122}Sb β^-→^{122}Te, 98% β^+→^{122}Sn, 2%	0.162 1.980 1.619	4.19 m 2.72 d 2.72 d	$<*6.2 \cdot 10^{-1}$ $<*6.6 \cdot 10^{-4}$	0 0

Table 8. (cont.)

Isotope	Weight of the elements in mg/kg of food	Number of isotope atoms per gram of food	Photo-neutron thres-hold in MeV	Isotope formed	Decay mode	Decay energy in MeV	Half-life	Bq/kg per kGy for 10 MeV X rays	Bq/kg per kGy for 7.5 MeV X rays
^{120}Te	0.01	$4.48\cdot10^{10}$	10.3	^{119m}Te ^{119}Te ^{119}Sb	EC→ ^{119}Sb β^+, EC→ ^{119}Sb EC→ ^{119}Sn	2.6 2.29 0.59	4.69 d 16.0 h 1.588 d	0 0 0	0 0 0
^{122}Te		$1.22\cdot10^{12}$	9.3	^{121m}Te ^{121}Te	IT→ ^{121}Te, 89% EC→ ^{121}Sb, 11% EC→ ^{121}Sb	0.212 1.25 1.04	154 d 16.8 d	$<2.7\cdot10^{-7}$ $<2.4\cdot10^{-6}$	0 0
^{123}Te		$4.27\cdot10^{11}$	6.9	^{123m}Te ^{122}Te	IT→ ^{123}Te	0.247	119.7 d Stable	$<1.1\cdot10^{-5}$ 0	 0
^{124}Te		$2.26\cdot10^{12}$	9.4	^{123m}Te ^{123}Te	IT→ ^{123}Te	0.247	119.7 d Stable	$<4.1\cdot10^{-7}$ 0	0 0
^{125}Te		$3.36\cdot10^{12}$	6.6	^{125m}Te ^{124}Te	IT→ ^{125}Te	0.145	58 d Stable	$<2.2\cdot10^{-4}$ 0	 0
^{126}Te		$8.93\cdot10^{12}$	9.1	^{125m}Te ^{125}Te	IT→ ^{125}Te	0.145	58 d Stable	$<1.1\cdot10^{-5}$	0
^{128}Te		$1.50\cdot10^{13}$	8.8	^{127m}Te ^{127m}Te ^{127}Te	IT→ ^{127}Te, 98% β^-→ ^{127}I, 2% β^-→ ^{127}I	0.088 0.77 0.697	109 d 9.4 h	$<*1.9\cdot10^{-5}$ $<*5.3\cdot10^{-3}$	0 0
^{130}Te		$1.60\cdot10^{13}$	8.4	^{129m}Te ^{129}Te ^{129}I	IT→ ^{129}Te, 63% β^-→ ^{129}I, 37% β^-→ ^{129}I β^-→ ^{129}Xe	0.105 1.606 1.501 0.191	33.6 d 1.16 h $1.7\cdot10^7$ y	$<*1.9\cdot10^{-4}$ $<*1.3\cdot10^{-1}$ $<*1.1\cdot10^{-12}$	0 0 0
^{127}I	0.5	$2.373\cdot10^{15}$	9.14	^{126}I	EC→ ^{126}Te, 55% β^+→ ^{126}Te, 1% β^-→ ^{126}Xe, 44%	2.15 1.26	13.0 d	$*\ 1.35\cdot10^{-2}$	0
^{133}Cs	0.01	$4.53\cdot10^{13}$	9.0	^{132}Cs	EC→ ^{132}Xe, 98% β^+→ ^{132}Xe, 0.3% β^-→ ^{132}Ba, 1.7%	2.12 1.28	6.48 d	$<7.5\cdot10^{-4}$	0
^{130}Ba	0.02	$9.30\cdot10^{10}$	10.4	^{129m}Ba ^{129}Ba ^{129}Cs	EC, β^+→ ^{129}Cs, 98% EC→ ^{129}Xe EC, β^+→ ^{129}Cs EC→ ^{129}Xe	≈ 2.55 2.43 1.192	2.17 h 2.2 h 1.336 d	0	0
^{132}Ba		$8.86\cdot10^{10}$	9.8	^{131m}Ba ^{131}Ba ^{131}Cs	IT→ ^{131}Ba EC→ ^{131}Cs EC → ^{131}Xe	0.187 1.36 0.35	14.6 m 11.7 d 9.69 d	$<7.4\cdot10^{-6}$ $<6.4\cdot10^{-9}$ $<7.7\cdot10^{-9}$	0 0 0
^{134}Ba		$2.12\cdot10^{12}$	9.5	^{133m}Ba ^{133}Ba	IT→ ^{133}Ba EC→ ^{133}Cs	0.288 0.516	1.621 d 10.53 y	$<1.8\cdot10^{-5}$ $<7.4\cdot10^{-9}$	0 0
^{135}Ba		$5.78\cdot10^{12}$	7.0	^{135m}Ba ^{134}Ba	IT→ ^{135}Ba	0.2682	1.2 d Stable	$<1.4\cdot10^{-2}$ 0	0
^{136}Ba		$6.88\cdot10^{12}$	9.1	^{135m}Ba ^{135}Ba	IT→ ^{135}Ba	0.2682	1.2 d	$<4.6\cdot10^{-4}$	0
^{137}Ba		$9.85\cdot10^{12}$	6.9	^{137m}Ba ^{136}Ba	IT→ ^{137}Ba	0.6617	2.552 m Stable	$<*18.2$ 0	 0
^{138}Ba		$6.29\cdot10^{13}$	8.6	^{137m}Ba ^{137}Ba	IT→ ^{137}Ba	0.6617	2.552 m Stable	$<*10.7$ 0	0

Table 8. (cont.)

Isotope	Weight of the elements in mg/kg of food	Number of isotope atoms per gram of food	Photo-neutron thres-hold in MeV	Isotope formed	Decay mode	Decay energy in MeV	Half-life	Bq/kg per kGy for 10 MeV X rays	Bq/kg per kGy for 7.5 MeV X rays
^{197}Au	0.01	$3.06 \cdot 10^{13}$	8.07	^{196m2}Au ^{196m1}Au ^{196}Au	IT→ ^{196}Au IT→ ^{196}Au EC→ ^{196}Pt	0.5954 0.0846 1.505	9.7 h 8.1 s 6.18 d	$<*4.3 \cdot 10^{-2}$ $<*2.8 \cdot 10^{-3}$	0 0
^{196}Hg	0.05	$2.25 \cdot 10^{11}$	9.8	^{195m}Hg ^{195m}Hg ^{195}Hg ^{195}Au	IT→ ^{195}Hg, 54% EC→ ^{195}Au, 46% EC→ ^{195}Au EC→ ^{195}Pt	0.3186 1.52 0.227	1.67 d 9.5 h 186.12 d	$<1.7 \cdot 10^{-7}$ $<7.2 \cdot 10^{-7}$	0 0
^{198}Hg		$1.50 \cdot 10^{13}$	8.3	^{197m}Hg ^{197}Hg	IT→ ^{197}Hg EC→ ^{197}Au	0.2989 0.599	23.8 h 2.672 d	$<1.2 \cdot 10^{-2}$ $<4.4 \cdot 10^{-3}$	0 0
^{199}Hg		$2.53 \cdot 10^{13}$	6.6	^{199m}Hg ^{198}Hg	IT→ ^{199}Hg	0.532	42.6 m Stable	<5.4 0	<0.1 0
^{200}Hg		$3.47 \cdot 10^{13}$	8.0	^{199m}Hg ^{199}Hg	IT→ ^{199}Hg	0.532	42.6 m Stable	<1.5	0
^{201}Hg		$1.98 \cdot 10^{13}$	6.2	^{200}Hg			Stable	0	0
^{202}Hg		$4.48 \cdot 10^{13}$	7.8	^{201}Hg			Stable	0	0
^{204}Hg		$1.03 \cdot 10^{13}$	7.5	^{203}Hg	$\beta^- \rightarrow ^{203}$Tl	0.492	46.61 d	$5.7 \cdot 10^{-4}$	0
^{204}Pb	1	$4.07 \cdot 10^{13}$	8.4	^{204m}Pb ^{203}Pb	IT→ ^{204}Pb EC→ ^{203}Tl	2.185 0.98	1.12 h 2.1615 d	$<5.8 \cdot 10^{-1}$ $<1.3 \cdot 10^{-2}$	0
^{206}Pb		$7.00 \cdot 10^{14}$	8.1	^{205}Pb	EC→ ^{205}Tl	0.0512	$1.5 \cdot 10^{7}$ y	$1.4 \cdot 10^{-10}$	0
^{207}Pb		$6.42 \cdot 10^{14}$	6.7	^{206}Pb			Stable	0	0
^{208}Pb		$1.52 \cdot 10^{15}$	7.4	^{207}Pb			Stable	0	0

A.: Most of the nuclear data are from Table of the Isotopes by Norman E. Holden, at High Flux Beam Reactor, Reactor Division, Brookhaven National Laboratory, Upton. N.Y.11973. [Ho99] The data were supplemented by data from Table of the Isotopes compiled by Russel L. Heath, National Reactor Testing Station, Idaho Falls, Idaho, and published in Handbook of Chemistry and Physics, 49th edition (1968), and the different version ibid. 61st edition (1980). [He80] The two last columns are derived as discussed in Section 5.1 to 5.4.

Table 9. Photoneutron activity produced in reference food irradiated with electrons[A]

Isotope	Weight of the element in mg/kg of food	Number of isotope atoms per gram of food	Photo-neutron threshold in MeV	Isotopes formed	Decay mode	Decay energy in MeV	Half-life	Activity in Bq/kg per kGy for 10 MeV electron irradiation	Decay Energy times activity in MeV·Bq/kg per kGy for 10 MeV electron irradiation
^{36}S		$8.26\cdot10^{15}$	9.89	$^{35}S\rightarrow\ ^{35}Cl$	β^-	0.1674	87.2 d	7.510^{-9}	$1.25\cdot10^{-9}$
^{48}Ca		$3.93\cdot10^{15}$	9.94	$^{47}Ca\rightarrow\ ^{47}Sc$ $^{47}Sc\rightarrow\ ^{47}Ti$	β^- β^-	1.988 0.601	4.536 d, 3.349 d	$1.5\cdot10^{-8}$ $2.0\cdot10^{-8}$	$3.0\cdot10^{-8}$ $1.2\cdot10^{-8}$
^{50}V	0.1	$2.96\cdot10^{12}$	9.34	$^{49}V\rightarrow\ ^{49}Ti$	EC	0.601	337 d	$2.1\cdot10^{-10}$	$1.3\cdot10^{-10}$
^{64}Ni		$9.50\cdot10^{12}$	9.66	$^{63}Ni\rightarrow\ ^{63}Cu$	β^-	0.065	100 y	$1.1\cdot10^{-12}$	$7.2\cdot10^{-14}$
^{65}Cu		$1.75\cdot10^{15}$	9.91	$^{64}Cu\rightarrow\ ^{64}Zn$ $^{64}Cu\rightarrow\ ^{64}Ni$	β^-, 39% β^+, EC	0.578, 1.675	12.7 h	$*2.1\cdot10^{-7}$	$*2.5\cdot10^{-7}$
^{70}Zn		$2.21\cdot10^{15}$	9.21	$^{69m}Zn\rightarrow\ ^{69}Zn$ $^{69}Zn\rightarrow\ ^{69}Ga$	IT, 99% β^-	0.439 0.905	13.76 h then 56m	$<2.31\cdot10^{-4}$ $<2.6\cdot10^{-4}$	$<3.1\cdot10^{-4}$
^{76}Ge		$6.17\cdot10^{13}$	9.43	$^{75}Ge\rightarrow\ ^{75}As$	β^-	1.178	1.38 h	$2.6\cdot10^{-5}$	$3.1\cdot10^{-5}$
^{80}Se		$3.78\cdot10^{14}$	9.9	$^{79m}Se\rightarrow\ ^{79}Se$ $^{79}Se\rightarrow\ ^{79}Br$	β^-	0.096 0.149	3.92 m $6.5.10^4$ y	$<1.8\cdot10^{-5}$ $<2.1\cdot10^{-15}$	$<1.7\cdot10^{-6}$ $<3.1\cdot10^{-16}$
^{82}Se		$6.67\cdot10^{13}$	9.3	$^{81}Se\rightarrow\ ^{81}Br$	β^-	1.59	18.5 m	$2.6\cdot10^{-4}$	$4.1\cdot10^{-4}$
^{87}Rb		$1.57\cdot10^{16}$	9.9	$^{86m}Rb\rightarrow\ ^{86}Rb$ $^{86}Rb\rightarrow\ ^{86}Sr$	IT β^-	0.556 1.775	1.018 m 18.65 d	$<3.4\cdot10^{-3}$ $<1.3\cdot10^{-5}$	$<1.9\cdot10^{-3}$ $<2.3\cdot10^{-7}$
^{94}Zr		$5.78\cdot10^{14}$	8.2	$^{93}Zr\rightarrow\ ^{93}Nb$	β^-	0.09	$1.5\cdot10^6$ y	$1.0\cdot10^{-12}$	$8.7\cdot10^{-14}$
^{96}Zr		$9.24\cdot10^{13}$	7.8	$^{95}Zr\rightarrow\ ^{95}Nb$ $^{95}Nb\rightarrow\ ^{95}Mo$	IT, β^- β^-	1.125 0.926	64.02 d 34.97 d	$<2.6\cdot10^{-6}$	$<5.2\cdot10^{-6}$
^{94}Mo		$5.81\cdot10^{13}$	9.7	$^{93m}Mo\rightarrow\ ^{93}Mo$ $^{93}Mo\rightarrow\ ^{93}Nb$	IT EC	2.425 0.406	6.9 h $3.5\cdot10^3$ y	$<8.6\cdot10^{-7}$ $<1.9\cdot10^{-13}$	$<2.1\cdot10^{-6}$ $<7.9\cdot10^{-14}$
^{100}Mo		$6.04\cdot10^{13}$	8.3	$^{99}Mo\rightarrow\ ^{99}Tc$	β^-	1.357	2.75 d	$*1.3\cdot10^{-5}$	$*1.8\cdot10^{-5}$
^{103}Rh	0.01	$5.85\cdot10^{13}$	9.3	$^{102}Rh\rightarrow\ ^{93}Ru$	EC	2.28	2.9 y	$3.4\cdot10^{-9}$	$7.7\cdot10^{-9}$
^{107}Ag	0.02	$5.79\cdot10^{13}$	9.5	$^{106m}Ag\rightarrow\ ^{106}Pd$ $^{106}Ag\rightarrow\ ^{106}Pd$	EC β^+, EC	>2.97 2.97	8.4 d 24 m	$<*1.7\cdot10^{-7}$ $<*8.8\cdot10^{-5}$	$<*5.1\cdot10^{-7}$ $<*2.6\cdot10^{-4}$
^{109}Ag		$5.49\cdot10^{13}$	9.2	$^{108m}Ag\rightarrow\ ^{108}Ag$ ^{108}Pd $^{108}Ag\rightarrow\ ^{108}Cd$ $^{108}Ag\rightarrow\ ^{108}Pd$	IT, 8% EC, 92% β^-, 97% β^+, EC	0.079 1.65 1.92	130 y 2.39 m	$<*1.7\cdot10^{-10}$ $<*4.8\cdot10^{-8}$	$<*1.4\cdot10^{-11}$ $<*8.0\cdot10^{-3}$
^{110}Cd		$6.69\cdot10^{13}$	9.9	$^{109}Cd\rightarrow\ ^{109}Ag$	EC	0.214	462 d	$2.7\cdot10^{-11}$	$5.8\cdot10^{-12}$
^{111}Cd		$6.86\cdot10^{13}$	7.0	^{111m}Cd ^{110}Cd	IT→ ^{111}Cd	0.396	48.5 m Stable	$< 9.1\cdot10^{-3}$ 0	$<3.6\cdot10^{-3}$ 0
^{112}Cd		$1.29\cdot10^{14}$	9.4	$^{111m}Cd\rightarrow\ ^{111}Cd$ ^{111}Cd	IT	0.396 -	48.5 m	$<1.6\cdot10^{-4}$	$<6.3\cdot10^{-5}$
^{113}Cd		$6.55\cdot10^{13}$	6.5	$^{113m}Cd\ ^{112}Cd$	IT→ ^{113}Cd	0.59	14.1 y Stable	$< 9.1\cdot10^{-8}$ 0	$<5.3\cdot10^{-8}$ 0
^{114}Cd		$1.54\cdot10^{14}$	9.0	$^{113m}Cd\rightarrow\ ^{113}In$ ^{113}Cd	β^-	0.59 -	14.1 y	$<5.7\cdot10^{-9}$	$<3.4\cdot10^{-9}$
^{116}Cd		$4.01\cdot10^{13}$	8.7	$^{115m}Cd\rightarrow\ ^{115}In$ $^{115}Cd\rightarrow\ ^{115}In$	β^- β^-	1.629 1.448	44.6 d 2.23 d	$<3.7\cdot10^{-7}$ $<7.5\cdot10^{-6}$	$<6.1\cdot10^{-7}$ $<1.1\cdot10^{-5}$

Table 9. (cont.)

Isotope	Weight of the element in mg/kg of food	Number of isotope atoms per gram of food	Photo-neutron thres-hold in MeV	Isotopes formed	Decay mode	Decay energy in MeV	Half-life	Activity in Bq/kg per kGy for 10 MeV electron irradiation	Decay Energy times activity in MeV·Bq/kg per kGy for 10 MeV electron irradiation
^{113}In	0.01	$2.26\cdot10^{12}$	9.4	^{112m}In→ ^{112}In ^{112}In→ ^{112}Cd ^{112}Sn	IT β^+, EC β^-, 44%	0.155 2.588 0.66	20.8 m 14.4 m	$<6.4\cdot10^{-6}$ $<9.3\cdot10^{-6}$	$<1.0\cdot10^{-6}$ $<1.6\cdot10^{-5}$
^{115}In		$5.02\cdot10^{13}$	9.0	^{114m}In→ ^{114}In ^{114m}In→ ^{114}Cd ^{114}In→ ^{114}Sn ^{114}In→ ^{114}Cd	IT, 97% EC, 3% β^-, 97% EC, 3%	0.190 1.989 	49.51 d 1.198 m 	$<*1.7\cdot10^{-7}$ $<*1.0\cdot10^{-2}$ 	$<*8.3\cdot10^{-5}$ $<*1.2\cdot10^{-2}$
^{117}Sn		$3.90\cdot10^{13}$	6.9	^{117m}Sn ^{116}Sn	IT→ ^{117}Sn	0.3146	13.6 d Stable	$<2.0\cdot10^{-5}$ 0	$<6.4\cdot10^{-6}$ 0
^{118}Sn		$1.23\cdot10^{14}$	9.3	^{117m}Sn→ ^{117}Sn	IT	0.3146	13.6 d	$*8.8\cdot10^{-7}$	$*2.8\cdot10^{-7}$
^{119}Sn		$4.35\cdot10^{13}$	6.5	^{119m}Sn ^{118}Sn	IT→ ^{119}Sn	0.0896	293 d Stable	$<1.0\cdot10^{-6}$ 0	$<8.9\cdot10^{-8}$ 0
^{120}Sn		$1.65\cdot10^{14}$	9.1	^{119m}Sn→ ^{119}Sn	IT	0.0896	293 d	$*7.4\cdot10^{-6}$	$*6.6\cdot10^{-9}$
^{122}Sn		$2.35\cdot10^{13}$	8.8	^{121m}Sn→ ^{121}Sn ^{121m}Sn→ ^{121}Sb ^{121}Sn→ ^{121}Sb	IT β^- β^-	0.006 0.394 0.388	55 y 1.125 d	$<4.2\cdot10^{-10}$ $<7.4\cdot10^{-6}$	$<1.7\cdot10^{-10}$ $<2.9\cdot10^{-6}$
^{124}Sn		$2.94\cdot10^{13}$	8.5	^{123m}Sn→ ^{123}Sb ^{123}Sn→ ^{123}Sb	β^- β^-	1.428 1.403	40.1 m 129 d	$<*1.7\cdot10^{-4}$ $<*3.7\cdot10^{-8}$	$<*2.4\cdot10^{-4}$ $<*5.3\cdot10^{-8}$
^{121}Sb	0.01	$2.84\cdot10^{13}$	9.2	^{120m}Sb→ ^{120}Sb ^{120}Sb→ ^{120}Sb	EC EC, β^+	~2.7 2.68	5.76 d 15.89 m	$<*8.8\cdot10^{-7}$ $<*4.6\cdot10^{-4}$	$<*2.4\cdot10^{-6}$ $<*1.2\cdot10^{-3}$
^{123}Sb		$2.11\cdot10^{13}$	9.0	^{122m}Sb→ ^{122}Sb ^{122}Sb→ ^{122}Te ^{122}Sb→ ^{122}Sb	IT β^-, 98% β^+, 2%	0.162 1.980 1.619	4.19 m 2.72 d 	$<*1.3\cdot10^{-3}$ $<*1.4\cdot10^{-6}$ 	$<*2.1\cdot10^{-4}$ $<*2.8\cdot10^{-6}$
^{122}Te		$1.22\cdot10^{12}$	9.3	^{121m}Te→ ^{121}Te ^{121m}Te→ ^{121}Sb ^{121}Te→ ^{121}Sb	IT, 89% EC, 11% EC	0.212 1.25 1.04	154 d 16.8 d	$<5.6\cdot10^{-10}$ $<5.1\cdot10^{-9}$	$<1.9\cdot10^{-10}$ $<5.3\cdot10^{-9}$
^{124}Te		$2.26\cdot10^{12}$	9.4	^{123m}Te→ ^{123}Te ^{123}Te	IT	0.247	119.7 d	$<8.6\cdot10^{-10}$	$<2.1\cdot10^{-10}$
^{126}Te		$8.93\cdot10^{12}$	9.1	^{125m}Te→ ^{125}Te ^{125}Te	IT	0.145	58 d	$<2.3\cdot10^{-8}$	$<3.3\cdot10^{-9}$
^{128}Te		$1.50\cdot10^{13}$	8.8	^{127m}Te→ ^{127}Te ^{127m}Te→ ^{127}I ^{127}Te→ ^{127}I	IT, 98% β^-, 2% β^-	0.088 0.77 0.697	109 d 9.4 h	$<*4.0\cdot10^{-8}$ $<*1.1\cdot10^{-5}$	$<*4.1\cdot10^{-9}$ $<*7.7\cdot10^{-6}$
^{130}Te		$1.60\cdot10^{13}$	8.4	^{129m}Te→ ^{129}Te ^{129m}Te→ ^{129}I ^{129}Te→ ^{129}I ^{129}I→ ^{129}Xe	IT, 63% β^-, 37% β^- β^-	0.105 1.606 1.501 0.191	33.6 d 1.16 h $1.7\cdot10^7$ y	$<*4.0\cdot10^{-7}$ $<*2.7\cdot10^{-4}$ $<*2.3\cdot10^{-15}$	$<*2.6\cdot10^{-7}$ $<*4.1\cdot10^{-4}$ $<*4.4\cdot10^{-16}$
^{127}I	0.5	$2.373\cdot10^{15}$	9.14	^{126}I→ ^{126}Te ^{126}I→ ^{126}Xe	EC, β^+ β^-, 44%	2.151 1.26	13.0 d	$*2.8\cdot10^{-5}$	$*4.9\cdot10^{-5}$

Table 9. (cont.)

Isotope	Weight of the elements in mg/kg of food	Number of isotope atoms per gram of food	Photo-neutron thres-hold in MeV	Isotopes formed	Decay mode	Decay energy in MeV	Half-life	Activity in Bq/kg per kGy for 10 MeV electron irradiation	Decay Energy times activity in MeV·Bq/kg per kGy for 10 MeV electron irradiation
^{133}Cs	0.01	$4.53\cdot10^{13}$	9.0	^{132}Cs→ ^{132}Xe ^{132}Cs→ ^{132}Ba	EC, 98% β^+, 0.3% β^-, 1.7%	2.121 1.28	6.48 d	$<1.6\cdot10^{-6}$	$<3.3\cdot10^{-6}$
^{132}Ba		$8.86\cdot10^{10}$	9.8	^{131m}Ba→ ^{131}Ba ^{131}Ba→ ^{131}Cs ^{131}Cs→ ^{131}Xe	IT EC EC	0.187 1.36 0.35	14.6 m 11.7 d 9.69 d	$<1.6\cdot10^{-8}$ $<1.4\cdot10^{-11}$ $<1.6\cdot10^{-11}$	$<2.9\cdot10^{-9}$ $<1.9\cdot10^{-11}$ $<5.6\cdot10^{-12}$
^{134}Ba		$2.12\cdot10^{12}$	9.5	^{133m}Ba→ ^{133}Ba ^{133}Ba→ ^{133}Cs	IT EC	0.288 0.516	1.621 d 10.53 y	$<3.7\cdot10^{-8}$ $<1.6\cdot10^{-11}$	$<1.1\cdot10^{-8}$ $<8.0\cdot10^{-12}$
^{136}Ba		$6.88\cdot10^{12}$	9.1	^{135m}Ba→ ^{135}Ba ^{135}Ba	IT	0.2682	1.2 d	$<1.0\cdot10^{-6}$	$<2.6\cdot10^{-7}$
^{138}Ba		$6.29\cdot10^{13}$	8.6	^{137m}Ba→ ^{137}Ba ^{137}Ba	IT	0.6617	2.552 m	$<*2.3\cdot10^{-2}$	$<*1.5\cdot10^{-2}$
^{197}Au	0.01	$3.06\cdot10^{13}$	8.07	^{196m2}Au→ ^{196}Au ^{196m1}Au→ ^{196}Au ^{196}Au→ ^{196}Pt	IT IT EC	0.5954 0.0846 1.505	9.7 h 8.1 s 6.18 d	$<*8.0.10^{-5}$ $<*5.2.10^{-6}$	$<*5.4.10^{-5}$ $<*8.9.10^{-6}$
^{196}Hg	0.05	$2.25\cdot10^{11}$	9.8	^{195m}Hg→ ^{195}Hg ^{195m}Hg→ ^{195}Au ^{195}Hg→ ^{195}Au	IT, 54% EC, 46% EC	0.3186 1.52	1.67 d 9.5 h	$<3.1.10^{-10}$ $<1.3.10^{-9}$	$<1.1.10^{-10}$ $<2.4.10^{-9}$
^{198}Hg		$1.50\cdot10^{13}$	8.3	^{197m}Hg→ ^{197}Hg ^{197}Hg→ ^{197}Au	IT EC	0.2989 0.599	23.8 h 2.672 d	$<2.2\cdot10^{-5}$ $<8.1\cdot10^{-6}$	$<7.4\cdot10^{-6}$ $<5.5\cdot10^{-6}$
^{199}Hg		$2.53\cdot10^{13}$	6.6	^{199m}Hg ^{198}Hg	IT→ ^{199}Hg	0.532	42.6 m Stable	<0.01 0	$<5.3\cdot10^{-3}$ 0
^{200}Hg		$3.47\cdot10^{13}$	8.0	^{199m}Hg→ ^{199}Hg ^{199}Hg	IT	0.532	42.6 m	$<2.8\cdot10^{-3}$	$<1.7\cdot10^{-3}$
^{204}Hg		$1.03\cdot10^{13}$	7.5	^{203}Hg→ ^{203}Tl	β^-	0.492	46.61 d	$1.2\cdot10^{-6}$	$5.9\cdot10^{-7}$
^{204}Pb	1	$4.07\cdot10^{13}$	8.4	^{203}Pb→ ^{203}Tl	EC	0.97	2.1615 d	$2.7\cdot10^{-5}$	$2.6\cdot10^{-5}$
^{204}Pb	1	$4.07\cdot10^{13}$	8.4	^{204m}Pb→ ^{204}Pb ^{203}Pb→ ^{203}Tl	IT EC	2.185 0.98	1.12 h 2.1615 d	$<1.1\cdot10^{-3}$ $<2.4\cdot10^{-5}$	$<2.3\cdot10^{-3}$ $<2.4\cdot10^{-5}$
^{206}Pb		$7.00\cdot10^{14}$	8.1	^{205}Pb→ ^{205}Tl	EC	0.053	$1.5\cdot10^{7}$ y	$3.0\cdot10^{-13}$	$1.6\cdot10^{-14}$

A.: The data in the first eight columns are obtained from the relevant columns in Table 8. The data in the penultimate column (the 9th column) are obtained from the penultimate column in Table 8 by multiplying them with the relevant factor derived in Section 5 and 6. The last column, which gives the activity in column 9 multiplied by the disintegration energy released in the decay (see column 7) is a rough indicator of the damaging effects of the radiation.

Table 10. The dose in mSv/year from photoneutron activity when consuming 50 kg/year of reference food sterilized by 60 kGy with 10 MeV electrons[A]

Isotope produced	Activity in Bq/(kg·kGy) of food irradiated by 10 MeV electrons	Half-life of the isotope	Decay energy in MeV	Conversion factor from becquerel to sievert	Dose in mSv/year for consumption of 50 kg/year of reference food exposed to dose of 60 kGy
^{120m}Sb	$< 4.6 \cdot 10^{-4}$	15.89 m	2.68	$1.4 \cdot 10^{-11}$	$< 1.93 \cdot 10^{-8}$
^{81}Se	$2.6 \cdot 10^{-4}$	18.5 m	1.59	$2.7 \cdot 10^{-11}$	$2.11 \cdot 10^{-8}$
^{106}Ag	$< 8.82 \cdot 10^{-5}$	24.0 m	2.97	$3.2 \cdot 10^{-11}$	$< 8.46 \cdot 10^{-9}$
^{123m}Sn	$< 1.72 \cdot 10^{-4}$	40.1 m	1.428	$3.8 \cdot 10^{-11}$	$< 1.96 \cdot 10^{-8}$
^{199m}Hg	$< 3.15 \cdot 10^{-3}$	42.6 m	0.532	$3.1 \cdot 10^{-11}$	$< 2.93 \cdot 10^{-7}$
^{111m}Cd	$< 1.55 \cdot 10^{-4}$	48.5 m	0.396	$(9.0 \cdot 10^{-12})$	$< 4.19 \cdot 10^{-9}$
^{129}Te	$< 2.7 \cdot 10^{-4}$	1.16 h	1.501	$6.3 \cdot 10^{-11}$	$< 5.10 \cdot 10^{-8}$
^{75}Ge	$< 2.6 \cdot 10^{-5}$	1.38 h	1.178	$4.6 \cdot 10^{-11}$	$< 3.59 \cdot 10^{-9}$
^{93m}Mo	$< 8.6 \cdot 10^{-7}$	6.9 h	2.43	$2.8 \cdot 10^{-10}$	$<7.22 \cdot 10^{-10}$
^{127}Te	$< 1.1 \cdot 10^{-5}$	9.4 h	0.697	$1.7 \cdot 10^{-10}$	$< 5.61 \cdot 10^{-9}$
^{196m2}Au	$< 9.0 \cdot 10^{-5}$	9.7 h	0.5954	$(2.4 \cdot 10^{-10})$	$< 6.48 \cdot 10^{-8}$
^{69m}Zn + ^{69}Zn	$< 2.31 \cdot 10^{-4}$	13.76 h	1.34	$3.3 \cdot 10^{-10}$	$< 2.29 \cdot 10^{-7}$
^{197m}Hg	$< 2.5 \cdot 10^{-5}$	23.8 h	0.2989	$3.4 \cdot 10^{-10}$	$< 2.55 \cdot 10^{-8}$
^{121}Sn	$<7.4 \cdot 10^{-6}$	1.125 d	0.388	$2.3 \cdot 10^{-10}$	$< 5.11 \cdot 10^{-9}$
^{203}Pb	$2.7 \cdot 10^{-5}$	2.16 d	0.97	$2.4 \cdot 10^{-10}$	$1.94 \cdot 10^{-8}$
^{135m}Ba	$< 1.0 \cdot 10^{-6}$	1.2 d	0.2682	$4.5 \cdot 10^{-10}$	$< 1.35 \cdot 10^{-9}$
^{203}Pb	$2.7 \cdot 10^{-5}$	2.16 d	0.97	$2.4 \cdot 10^{-10}$	$1.94 \cdot 10^{-8}$
^{115}Cd	$< 7.8 \cdot 10^{-6}$	2.23 d	1.448	$1.4 \cdot 10^{-9}$	$< 3.28 \cdot 10^{-8}$
^{197}Hg	$< 9.2 \cdot 10^{-6}$	2.672 d	0.599	$2.3 \cdot 10^{-10}$	$< 6.35 \cdot 10^{-9}$
^{122}Sb	$< 1.4 \cdot 10^{-6}$	2.72 d	1.973	$1.7 \cdot 10^{-9}$	$< 7.14 \cdot 10^{-9}$
^{99}Mo	$< 1.3 \cdot 10^{-5}$	2.75 d	1.357	$1.2 \cdot 10^{-9}$	$< 4.68 \cdot 10^{-8}$
^{120m}Sb	$< 8.8 \cdot 10^{-7}$	5.76 d	2.7	$1.2 \cdot 10^{-9}$	$< 3.17 \cdot 10^{-9}$
^{196}Au	$< 5.9 \cdot 10^{-6}$	6.18 d	1.505	$(2.5 \cdot 10^{-9})$	$<4.43 \cdot 10^{-8}$
^{132}Cs	$< 1.6 \cdot 10^{-6}$	6.48 d	2.107	$5.0 \cdot 10^{-10}$	$< 2.40 \cdot 10^{-9}$
^{106m}Ag	$< 1.7 \cdot 10^{-7}$	8.4 d	2.97	$(1.5 \cdot 10^{-9})$	$< 7.65 \cdot 10^{-10}$
^{126}I	$< 2.9 \cdot 10^{-5}$	13.0 d	1.759	$2.9 \cdot 10^{-8}$	$< 2.41 \cdot 10^{-6}$
^{129m}Te	$< 4.0 \cdot 10^{-7}$	33.6 d	0.66	$3.0 \cdot 10^{-9}$	$< 3.0 \cdot 10^{-9}$
^{95}Nb	$< 4.6 \cdot 10^{-6}$	34.97 d	0.926	$5.8 \cdot 10^{-10}$	$< 8.00 \cdot 10^{-9}$
^{115m}Cd	$<3.7 \cdot 10^{-7}$	44.6 d	1.629	$3.3 \cdot 10^{-9}$	$<3.66 \cdot 10^{-9}$
^{203}Hg	$1.2 \cdot 10^{-6}$	46.61 d	0.492	$5.4 \cdot 10^{-10}$	$1.94 \cdot 10^{-9}$
^{114m}In	$< 1.7 \cdot 10^{-7}$	49.51 d	2.15	$4.1 \cdot 10^{-9}$	$< 2.09 \cdot 10^{-9}$
^{95}Zr	$< 2.6 \cdot 10^{-6}$	64.02 d	2.051	$8.8 \cdot 10^{-10}$	$< 6.86 \cdot 10^{-9}$
^{35}S	$7.5 \cdot 10^{-9}$	87.2 d	0.1674	$1.9 \cdot 10^{-10}$	$4.25 \cdot 10^{-12}$

A. For explanation of this table, see Section 6.4.

Table 11. The number of neutrons produced per gram of reference food per kGy of X ray dose as function of the electron energy [A]

Incident electron energy in MeV	^{2}H	^{13}C	^{14}N	^{17}O	^{18}O	^{23}Na	^{25}Mg+ ^{26}Mg	^{31}P	^{33}S+ ^{36}S+ ^{34}S	^{37}Cl+ ^{35}Cl	Sum
3	$8.0\cdot10^{4}$										$8.0\cdot10^{4}$
4	$2.7\cdot10^{5}$										$2.7\cdot10^{5}$
5	$4.3\cdot10^{5}$	1.3		$1.2\cdot10^{3}$							$4.3\cdot10^{5}$
6	$5.3\cdot10^{5}$	$2.5\cdot10^{4}$		$6.4\cdot10^{3}$							$5.3\cdot10^{5}$
7	$6.0\cdot10^{5}$	$1.1\cdot10^{5}$		$1.5\cdot10^{4}$							$7.3\cdot10^{5}$
8	$6.3\cdot10^{5}$	$2.7\cdot10^{5}$		$2.5\cdot10^{4}$			3.7·10 1				$9.3\cdot10^{5}$
9	$6.5\cdot10^{5}$	$4.7\cdot10^{5}$		$3.6\cdot10^{4}$	$2.2\cdot10^{4}$		$3.1\cdot10^{2}$		$1.3\cdot10^{1}$		$1.2\cdot10^{6}$
10	$6.6\cdot10^{5}$	$6.6\cdot10^{5}$		$6.5\cdot10^{4}$	$1.5\cdot10^{5}$		$9.6\cdot10^{2}$		$3.5\cdot10^{2}$		$1.5\cdot10^{6}$
11	$6.6\cdot10^{5}$	$8.7\cdot10^{5}$	$1.7\cdot10^{4}$	$8.3\cdot10^{4}$	$4.3\cdot10^{5}$		$3.2\cdot10^{3}$		$1.2\cdot10^{3}$	$1.9\cdot10^{3}$	$2.1\cdot10^{6}$
12	$6.5\cdot10^{5}$	$1.2\cdot10^{6}$	$3.0\cdot10^{5}$	$1.0\cdot10^{5}$	$7.8\cdot10^{5}$		$6.2\cdot10^{3}$		$2.6\cdot10^{3}$	$9.4\cdot10^{3}$	$3.1\cdot10^{6}$
13	$6.4\cdot10^{5}$	$1.5\cdot10^{6}$	$9.9\cdot10^{5}$	$1.3\cdot10^{5}$	$1.1\cdot10^{6}$	$1.6\cdot10^{3}$	$8.8\cdot10^{3}$	$5.0\cdot10^{3}$	$6.7\cdot10^{3}$	$2.0\cdot10^{4}$	$4.4\cdot10^{6}$
14	$6.3\cdot10^{5}$	$1.9\cdot10^{6}$	$2.0\cdot10^{6}$	$1.5\cdot10^{5}$	$1.4\cdot10^{6}$	$1.7\cdot10^{4}$	$1.2\cdot10^{4}$	$4.2\cdot10^{4}$	$2.0\cdot10^{4}$	$3.6\cdot10^{4}$	$6.2\cdot10^{6}$

[A] The number of neutrons is obtained by numerical integration of Eq. (20) in Section 8.

Table 12. The number of neutrons produced per kJ of incident electron beam impinging on thick targets of tungsten, tantalum, gold, and iron[A]

Incident electron energy in MeV	Tungsten	Tantalum	Gold	Iron
6.5	$6.2\cdot10^{5}$	0	0	
7.0	$1.1\cdot10^{8}$	$3.4\cdot10^{3}$	0	
7.5	$4.8\cdot10^{8}$	$4.8\cdot10^{4}$	0	
8.0	$1.5\cdot10^{9}$	$5.7\cdot10^{7}$	0	1.1·105
8.5	$4.1\cdot10^{9}$	$5.9\cdot10^{8}$	$1.0\cdot10^{8}$	$1.8\cdot10^{6}$
9.0	$9.2\cdot10^{9}$	$2.1\cdot10^{9}$	$1.1\cdot10^{9}$	$7.9\cdot10^{6}$
9.5	$1.8\cdot10^{10}$	$5.3\cdot10^{9}$	$3.9\cdot10^{9}$	$2.2\cdot10^{7}$
10.0	$3.1\cdot10^{10}$	$1.1\cdot10^{10}$	$9.5\cdot10^{9}$	$4.7\cdot10^{7}$
10.5	$4.6\cdot10^{10}$	$1.9\cdot10^{10}$	$1.8\cdot10^{10}$	$8.7\cdot10^{7}$
11.0	$6.5\cdot10^{10}$	$3.0\cdot10^{10}$	$3.0\cdot10^{10}$	$1.5\cdot10^{8}$
11.5	$9.0\cdot10^{10}$	$4.5\cdot10^{10}$	$4.7\cdot10^{10}$	$2.3\cdot10^{8}$
12.0	$1.1\cdot10^{11}$	$6.4\cdot10^{10}$	$6.9\cdot10^{10}$	$4.0\cdot10^{8}$
12.5	$1.4\cdot10^{11}$	$8.9\cdot10^{10}$	$9.7\cdot10^{10}$	$7.8\cdot10^{8}$
13.0	$1.8\cdot10^{11}$	$1.2\cdot10^{11}$	$1.3\cdot10^{11}$	$1.5\cdot10^{9}$
13.5	$2.1\cdot10^{11}$	$1.5\cdot10^{11}$	$1.7\cdot10^{11}$	$2.8\cdot10^{9}$
14.0	$2.6\cdot10^{11}$	$2.0\cdot10^{11}$	$2.2\cdot10^{11}$	$4.7\cdot10^{9}$
14.5	$3.1\cdot10^{11}$	$2.5\cdot10^{11}$	$2.8\cdot10^{11}$	$7.5\cdot10^{9}$
15.0	$3.7\cdot10^{11}$	$3.0\cdot10^{11}$	$3.5\cdot10^{11}$	$1.1\cdot10^{10}$

[A] The number of neutrons is obtained by using the analysis by Swanson [Sw79a] as indicated in Section 8.2.

Table 13. Forward emitted X ray energy as % of the incident beam energy [A]

Half-angle of the X ray cone in degrees	5 MeV incident electrons	7.5 MeV incident electrons	10 MeV incident electrons
0^0	0	0	0
15^0	1.1	1.8	2.8
30^0	2.4	4.3	7.0
45^0	4.0	7.4	10.9
60^0	5.6	10.0	14.5
75^0	7.0	12.3	17.4
90^0	8.2	14.1	19.7

[A] The number of neutrons is obtained as indicated in Section 8.4.

Table 14. Neutron-capture activity in food and relevant characteristics of isotopes. The isotope abundance in food; the thermal neutron cross-sections; the number of neutrons absorbed if the fluence of neutrons per cm^2 is equal to one; the half-lives of the isotopes produced; the correspon-ding number of disintegrations per sec per gram of food; and the isotope produced and particle emitted. (See Section 10.1 for explanation of the different columns)[A]

Isotope	Natural isotope abun-dance in %	Atomic mass	Weight of the element in ppm of food	Number of atoms per gram of food	Thermal neutron capture cross-section in barns	Number of neutrons absorbed per gram of food	Half-lives	Number of decays per sec per gram of food	Isotope produced and particles emitted	Decay energy in MeV
H		1.008	90000	$5.38 \cdot 10^{22}$	0.332	$1.79 \cdot 10^{-2}$				
^{1}H	99.985			$5.38 \cdot 10^{22}$	0.332	$1.79 \cdot 10^{-2}$	Stable		^{2}H	
^{2}H	0.015			$8.06 \cdot 10^{18}$	0.00051	$4.11 \cdot 10^{-9}$	12.32 y	$7.3 \cdot 10^{-18}$	^{3}H, β^-, ^{3}He	0.0186
^{3}H				$7.30 \cdot 10^{7}$	$<6 \cdot 10^{-6}$			(0.133)	^{3}H, β^-, ^{3}He	0.0186
C		12.01	180000	$9.02 \cdot 10^{21}$	0.0035	$3.16 \cdot 10^{-5}$				
^{12}C	98.9			$8.92 \cdot 10^{21}$	0.0035	$3.12 \cdot 10^{-5}$	Stable		^{13}C	
^{13}C	1.1			$1.00 \cdot 10^{20}$	0.0014	$1.40 \cdot 10^{-7}$	5715 y	$5.38 \cdot 10^{-19}$	^{14}C, β^-, ^{14}N	0.1565
^{14}C				$1.20 \cdot 10^{10}$	$<1 \cdot 10^{-6}$		5,715	(0.046)	^{14}C, β^-, ^{14}N	0.1565
N		14.01	20000	$8.60 \cdot 10^{20}$	1.88	$1.62 \cdot 10^{-3}$				
^{14}N	99.63			$8.57 \cdot 10^{20}$	0.08	$6.86 \cdot 10^{-5}$	Stable		^{15}N	
					1.83 p	$1.57 \cdot 10^{-3}$	5715 y	$6.03 \cdot 10^{-15}$	p, ^{14}C, β^-, ^{14}N	0.1565
^{15}N	0.37			$3.15 \cdot 10^{18}$	0.00004	$1.26 \cdot 10^{-10}$	7.13 s	$1.22 \cdot 10^{-11}$	^{16}N, β^-, ^{16}O	10.419
O		16	700000	$2.635 \cdot 10^{22}$	0.00029	$7.64 \cdot 10^{-6}$				
^{16}O	99.759			$2.63 \cdot 10^{22}$	0.00019	$5.00 \cdot 10^{-6}$	Stable		^{17}O	

Table 14. (cont.)

Isotope	Natural isotope abun-dance in %	Atomic mass	Weight of the element in ppm of food	Number of atoms per gram of food	Thermal neutron capture cross-section in barns	Number of neutrons absorbed per gram of food	Half-lives	Number of decays per sec per gram of food	Isotope produced and particles emitted	Decay energy in MeV
^{17}O	0.037			$9.75\cdot10^{18}$	0.24He	$2.34\cdot10^{-6}$	5715 y	$9.01\cdot10^{-18}$	^{14}C, β^-, ^{14}N	0.1565
^{18}O	0.204			$5.37\cdot10^{19}$	0.00016	$8.60\cdot10^{-9}$	26.9 s	$2.22\cdot10^{-10}$	^{19}O, β^-, ^{19}F	4.819
Na		22.99	750	$1.965\cdot10^{19}$	0.525	$1.03\cdot10^{-5}$				
^{23}Na	100			$1.96\cdot10^{19}$	0.525	$1.03\cdot10^{-5}$	14.96 h	$1.33\cdot10^{-10}$	^{24}Na, β^-, ^{24}Mg	5.514
Mg		24.305	300	$7.433\cdot10^{18}$	0.066	$4.90\cdot10^{-7}$				
^{24}Mg	78.99			$5.87\cdot10^{18}$	0.053		Stable		^{25}Mg	
^{25}Mg	10.00			$7.43\cdot10^{17}$	0.20		Stable		^{26}Mg	
^{26}Mg	11.01			$8.18\cdot10^{17}$	0.038	$3.11\cdot10^{-8}$	9.45 m	$3.80\cdot10^{-11}$	^{27}Mg, β^-, ^{27}Al	2.610
Al		26.982	0.4	$8.928\cdot10^{15}$	0.230	$2.15\cdot10^{-9}$				
^{27}Al	100			$8.93\cdot10^{15}$	0.23	$2.05\cdot10^{-9}$	2.25 m	$1.05\cdot10^{-11}$	^{28}Al, β^-, ^{28}Si	4.642
Si		28.086	10.0	$2.144\cdot10^{17}$	0.166	$3.64\cdot10^{-8}$				
^{28}Si	92.23			$1.98\cdot10^{17}$	0.17		Stable		^{29}Si	
^{29}Si	4.67			$1.01\cdot10^{16}$	0.12		Stable		^{30}Si	
^{30}Si	3.10			$6.65\cdot10^{15}$	0.107	$7.12\cdot10^{-10}$	2.62 h	$5.23\cdot10^{-14}$	^{31}Si, β^-, ^{31}P	1.49
P		30.974	2000	$3.889\cdot10^{19}$	0.17	$7.39\cdot10^{-6}$		$4.15\cdot10^{-12}$		
^{31}P	100			$3.89\cdot10^{19}$	0.17	$6.61\cdot10^{-6}$	14.28 d	$3.715\cdot10^{-12}$	^{32}P, β^-, ^{32}S	1.71
S		32.066	2200	$4.132\cdot10^{19}$	0.54	$2.15\cdot10^{-5}$				
^{32}S	95.02			$3.93\cdot10^{19}$	0.55 $5\cdot10^{-4}$ α	$1.93\cdot10^{-5}$ $<2\cdot10^{-8}$	Stable Stable		^{33}S α, ^{29}Si	
^{33}S	0.75			$3.10\cdot10^{17}$	0.46 $2\cdot10^{-3}$ p	$1.42\cdot10^{-7}$ $6.2\cdot10^{-10}$	Stable 25.3 d	$2.0\cdot10^{-16}$	^{34}S p, $^{33}P\rightarrow\beta^-$, ^{33}S	0.249
^{34}S	4.21			$1.74\cdot10^{18}$	0.30	$5.22\cdot10^{-7}$	87.2 d	$4.8\cdot10^{-14}$	^{35}S, β^-, ^{35}Cl	0.167
^{36}S	0.02			$8.26\cdot10^{15}$	0.23	$1.90\cdot10^{-9}$	5.05 m	$4.35\cdot10^{-12}$	^{37}S, β^-, ^{37}Cl	4.865
Cl		35.453	560	$9.512\cdot10^{18}$	33.6	$3.20\cdot10^{-4}$				
^{35}Cl	75.77			$7.21\cdot10^{18}$	43.7 0.44 p $8\cdot10^{-5}$ α	$3.15\cdot10^{-4}$ $3.17\cdot10^{-6}$ $5.8\cdot10^{-10}$	$3\cdot10^5$ y 87.2 d 14.28 d	$2.3\cdot10^{-17}$ $2.92\cdot10^{-13}$ $3.24\cdot10^{-16}$	^{36}Cl, β^-, ^{36}A, 98% ^{36}Cl, β^+, ^{36}S, 2% p, $^{35}S\rightarrow\beta^-$, ^{35}Cl α, $^{32}P\rightarrow\beta^-$, ^{32}S	0.7093 1.142 0.167
^{37}Cl	24.23			$2.30\cdot10^{18}$	0.43	$9.91\cdot10^{-7}$	37.2 m	$3.08\cdot10^{-10}$	^{38}Cl, β^-, ^{38}A	4.917
K		39.098	4000	$6.161\cdot10^{19}$	2.1	$1.21\cdot10^{-4}$				
^{39}K	93.258			$5.75\cdot10^{19}$	2.1 0.00005 0.0043	$1.21\cdot10^{-4}$ $2.88\cdot10^{-9}$ $2.47\cdot10^{-7}$	$1.26\cdot10^9$ y 268 y $3.01\cdot10^5$ y	$2.1\cdot10^{-21}$ $2.36\cdot10^{-19}$ $1.8\cdot10^{-20}$	^{40}K, β^-, ^{40}Ca, 89% ^{40}K, β^+, ^{40}A, 10.7% p, $^{39}Ar\rightarrow\beta^-$, ^{39}K α, $^{36}Cl\rightarrow\beta^-$, ^{36}Ar	1.312 1.50

Table 14. (cont.)

Isotope	Natural isotope abun-dance in %	Atomic mass	Weight of the element in ppm of food	Number of atoms per gram of food	Thermal neutron capture cross-section in barns	Number of neutrons absorbed per gram of food	Half-lives	Number of decays per sec per gram of food	Isotope produced and particles emitted	Decay energy in MeV
^{40}K	0.0117			$7.21\cdot10^{15}$		$7.21\cdot10^{15}$	$1.26\cdot10^{9}$ y	(0.1259) nat. activ.	^{40}K, β^-, ^{40}Ca, 89% ^{40}K, β^+, ^{40}A, 10.7%	1.312 1.50
^{40}K	0.0117			$7.21\cdot10^{15}$	30 4.4 p 0.42 α		Stable Stable Stable Stable		^{41}K ^{40}Ar p, ^{40}Ar α, ^{37}Cl	
^{41}K	6.7302			$4.15.10^{18}$	1.46	$6.05\cdot10^{-6}$	12.36 h	$9.43\cdot10^{-11}$	^{42}K, β^-, ^{42}Ca	3.523
Ca		40.078	140	$2.104\cdot10^{18}$	0.43	$9.04\cdot10^{-7}$				
^{40}Ca	96.941			$2.04\cdot10^{18}$	0.41 0.13 α	$8.36\cdot10^{-7}$ $2.65\cdot10^{-7}$	$1.02\cdot10^{5}$ y 35.0 d	$1.8\cdot10^{-19}$ $6.08\cdot10^{-14}$	^{41}Ca, EC, ^{41}K α, ^{37}Ar$\rightarrow$EC, ^{37}Cl	0.421
^{42}Ca	0.647			$1.35\cdot10^{16}$	0.65		Stable		^{43}Ca	
^{43}Ca	0.135			$3.05\cdot10^{15}$	6		Stable		^{44}Ca	
^{44}Ca	2.086			$4.39\cdot10^{16}$	0.8	$3.51\cdot10^{-8}$	162.7 d	$1.73\cdot10^{-15}$	^{45}Ca, β^-, ^{45}Sc	0.257
^{46}Ca	0.004			$6.94\cdot10^{13}$	0.70	$5.86\cdot10^{-11}$	4.536 d 3.349 d	$8.6\cdot10^{-17}$	^{47}Ca, β^-, ^{47}Sc, ^{47}Sc, β^-, ^{47}Ti	1.988 0.60
^{48}Ca	0.187			$3.93\cdot10^{15}$	1.1	$4.33\cdot10^{-9}$	8.72 m 57.3 m	$5.73\cdot10^{-12}$ $<8.7\cdot10^{-13}$	^{49}Ca, β^-, ^{49}Sc, ^{49}Sc, β^-, ^{49}Ti	5.263 2.005
Ti		47.88	0.1	$1.258\cdot10^{15}$	6.1	$7.67\cdot10^{-9}$				
^{46}Ti	8.0			$1.01\cdot10^{14}$	0.6		Stable		^{47}Ti	
^{47}Ti	7.3			$9.78\cdot10^{13}$	1.6		Stable		^{48}Ti	
^{48}Ti	73.8			$9.88\cdot10^{14}$	7.9		Stable		^{49}Ti	
^{49}Ti	5.5			$7.37\cdot10^{13}$	1.9		Stable		^{50}Ti	
^{50}Ti	5.4			$6.79\cdot10^{13}$	0.179	$1.22\cdot10^{-11}$	5.76 m	$2.4\cdot10^{-14}$	^{51}Ti, β^-, ^{51}V	2.472
V		50.941	0.1	$1.182\cdot10^{15}$	5.0	$5.91\cdot10^{-9}$				
^{50}V	0.25			$2.96\cdot10^{12}$	21		Stable		^{51}V	
^{51}V	99.75			$1.18\cdot10^{15}$	4.9	$5.78\cdot10^{-9}$	3.76 m	$1.78\cdot10^{-11}$	^{52}V, β^-, ^{52}Cr	3.976
Cr		51.996	0.01	$1.158\cdot10^{14}$	3.0	$3.47\cdot10^{-10}$				
^{50}Cr	4.345			$5.03\cdot10^{12}$	15	$7.55\cdot10^{-11}$	27.7 d	$2.2\cdot10^{-17}$	^{51}Cr, EC, ^{51}V	0.751
^{52}Cr	83.79			$9.70\cdot10^{13}$	0.8		Stable		^{53}Cr	
^{53}Cr	9.5			$1.10\cdot10^{13}$	18		Stable		^{54}Cr	
^{54}Cr	2.365			$2.74\cdot10^{12}$	0.36	$9.86\cdot10^{-13}$	3.50 m	$3.3\cdot10^{-15}$	^{55}Cr, β^-, ^{55}Mn	2.603

Table 14. (cont.)

Isotope	Natural isotope abun-dance in %	Atomic mass	Weight of the element in ppm of food	Number of atoms per gram of food	Thermal neutron capture cross-section in barns	Number of neutrons absorbed per gram of food	Half-lives	Number of decays per sec per gram of food	Isotope produced and particles emitted	Decay energy in MeV
Mn		54.938	0.2	$2.192 \cdot 10^{15}$	13.3	$2.91 \cdot 10^{-8}$				
^{55}Mn	100			$2.19 \cdot 10^{15}$	13.3	$2.92 \cdot 10^{-8}$	2.58 h	$2.2 \cdot 10^{-12}$	^{56}Mn, β^-, ^{56}Fe	3.696
Fe		55.847	50.0	$5.391 \cdot 10^{17}$	2.56	$1.38 \cdot 10^{-6}$				
^{54}Fe	5.9			$3.18 \cdot 10^{16}$	2.7	$8.59 \cdot 10^{-8}$	2.73 y	$6.9 \cdot 10^{-16}$	^{55}Fe, EC, ^{55}Mn	0.2314
^{56}Fe	91.72			$4.95 \cdot 10^{17}$	2.6		Stable		^{57}Fe	
^{57}Fe	2.1			$1.13 \cdot 10^{16}$	2.5		Stable		^{58}Fe	
^{58}Fe	0.28			$1.51 \cdot 10^{15}$	1.3	$1.96 \cdot 10^{-9}$	44.5 d	$3 \cdot 5.10^{-16}$	^{59}Fe, β^-, ^{59}Co	1.565
Co		58.933	0.01	$1.02 \cdot 10^{14}$	37.19	$3.79 \cdot 10^{-9}$				
^{59}Co	100			$1.02 \cdot 10^{14}$	20.7 16.5+21	$2.12 \cdot 10^{-9}$ $3.80 \cdot 10^{-9}$	10.5 m 5.27y	$2.3 \cdot 10^{-12}$- $1.59 \cdot 10^{-17}$	^{60m}Co, IT, ^{60}Co, 99.8% ^{60m}Co, β^-, ^{60}Ni, 0.02% ^{60}Co, β^-, ^{60}Ni	0.059 2.883 2.824
Ni		58.693	0.1	$1.026 \cdot 10^{15}$	4.5	$4.62 \cdot 10^{-9}$				
^{58}Ni	68.077			$6.98 \cdot 10^{14}$	4.6 $3 \cdot 10^{-5}$ α	$3.21 \cdot 10^{-9}$ $2.1 \cdot 10^{-14}$	$7.6 \cdot 10^{4}$ y 2.73 y	$9.30 \cdot 10^{-22}$ $1.69 \cdot 10^{-22}$	^{59}Ni, EC, ^{59}Co α, ^{55}Fe$\rightarrow$ EC, ^{55}Mn	1.072 0.2314
^{60}Ni	26.223			$2.69 \cdot 10^{14}$	2.9		Stable		^{61}Ni	
^{61}Ni	1.140			$1.17 \cdot 10^{13}$	2.5 $3 \cdot 10^{-5}$ α		Stable Stable		^{62}Ni α, ^{58}Fe	
^{62}Ni	3.634			$3.73 \cdot 10^{13}$	15	$5.59 \cdot 10^{-10}$	100 y	$1.23 \cdot 10^{-19}$	^{63}Ni, β^-, ^{63}Cu	0.065
^{64}Ni	0.926			$9.50 \cdot 10^{12}$	1.5,1.6	$1.52 \cdot 10^{-11}$	2.517 h	$1.16 \cdot 10^{-15}$	^{65}Ni, β^-, ^{65}Cu	2.134
Cu		63.546	0.6	$5.686 \cdot 10^{15}$	3.8	$2.16 \cdot 10^{-8}$				
^{63}Cu	69.17			$3.93 \cdot 10^{15}$	4.5	$1.77 \cdot 10^{-8}$	12.7 h	$2.68 \cdot 10^{-13}$	^{64}Cu, β^-, ^{64}Zn, 39% ^{64}Cu, β^+, ^{64}Ni, 19% ^{64}Cu, EC, ^{64}Ni, 41%	0.578 1.675 1.675
^{65}Cu	30.83			$1.75 \cdot 10^{15}$	2.17	$3.80 \cdot 10^{-9}$	5.1 m	$8.6 \cdot 10^{-12}$	^{66}Cu, β^-, ^{66}Zn,	2.642
Zn		65.39	40.0	$3.684 \cdot 10^{17}$	1.1	$4.05 \cdot 10^{-7}$				
^{64}Zn	48.6			$1.79 \cdot 10^{17}$	0.74 $1.2 \cdot 10^{-5}$, p $1.1 \cdot 10^{-5}$, α	$1.32 \cdot 10^{-7}$	243.8 d Stable Stable	$4.36 \cdot 10^{-15}$	^{65}Zn, EC, β^+, ^{65}Cu p, ^{64}Cu α, ^{61}Ni	1.352
^{66}Zn	27.9			$1.03 \cdot 10^{17}$	0.9 $2 \cdot 10^{-5}$, α	$2.06 \cdot 10^{-12}$	Stable 100 y	$4.5 \cdot 10^{-22}$	^{67}Zn α, ^{63}Ni$\rightarrow\beta^-$, ^{63}Cu	0.065
^{67}Zn	4.1			$1.51 \cdot 10^{16}$	6.9 $4 \cdot 10^{-4}$, α		Stable Stable		^{68}Zn α, ^{64}Ni	
^{68}Zn	18.8			$6.93 \cdot 10^{16}$	0.072 0.8 $2 \cdot 10^{-5}$, α	$5.00 \cdot 10^{-9}$ $5.54.10^{-8}$ $1.39 \cdot 10^{-12}$	13.76 h 56 m 2.517 h	$7.00 \cdot 10^{-14}$ $1.43.10^{-11}$ $1.06 \cdot 10^{-16}$	^{69m}Zn, IT, ^{69}Zn ^{69}Zn, β^-, ^{69}Ga α, ^{65}Ni$\rightarrow$ β^-, ^{65}Cu	0.439 0.905 2.134

Table 14. (cont.)

Isotope	Natural isotope abun-dance in %	Atomic mass	Weight of the element in ppm of food	Number of atoms per gram of food	Thermal neutron capture cross-section in barns	Number of neutrons absorbed per gram of food	Half-lives	Number of decays per sec per gram of food	Isotope produced and particles emitted	Decay energy in MeV
^{70}Zn	0.06			$2.21\cdot10^{15}$	0.0081 0.083	$1.79.10^{-11}$ $1.83\cdot10^{-10}$	3.97 h 2.4 m	$8.7.10^{-16}$ $8.8.10^{-13}$	^{71m}Zn, β^-, ^{71}Ga ^{71}Zn, β^-, ^{71}Ga	2.61
Ge		72.61	0.1	$8.294\cdot10^{14}$	2.2	$1.82\cdot10^{-9}$				
^{70}Ge	21.24			$1.76\cdot10^{14}$	0.3 2.7+0.3	$5.28\cdot10^{-11}$ $5.28\cdot10^{-10}$	0.0204 s 11.2 d	$3.8\cdot10^{-16}$	^{71m}Ge, IT, ^{71}Ge ^{71}Ge, EC, ^{71}Ga	0.259
^{72}Ge	27.66			$2.27\cdot10^{14}$	0.9		Stable		^{73}Ge	
^{73}Ge	7.72			$6.47\cdot10^{13}$	15		Stable		^{74}Ge	
^{74}Ge	35.94			$2.98\cdot10^{14}$	0.14 +0.28	$4.17\cdot10^{-10}$ $1.25\cdot10^{-10}$	48 s 82.8 m	$6.0\cdot10^{-13}$ $1.7\cdot10^{-14}$	^{75m}Ge, IT, ^{75}Ge ^{75}Ge, β^-, ^{75}As	1.178
^{76}Ge	7.44			$6.17\cdot10^{13}$	0.09 0.06+ 0.09·0.2	$5.55\cdot10^{-12}$ $4.81\cdot10^{-12}$	53 s 11.30 h 38.8 h	$7.3\cdot10^{-14}$ $8.2\cdot10^{-17}$ $2.39\cdot10^{-17}$	^{77m}Ge, IT, ^{77}Ge, 20% ^{77m}Ge, β^-, ^{77}As, 80% ^{77}Ge, β^-, ^{77}As ^{77}As, β^-, ^{77}Se	0.16 2.861 2.70 0.683
As		74.922	0.1	$8.038\cdot10^{14}$	4.0	$3.21\cdot10^{-9}$				
^{75}As	100			$8.04\cdot10^{14}$	4.0	$3.21\cdot10^{-9}$	26.3 h	$2.35\cdot10^{-14}$	^{76}As, β^-, ^{76}Se	2.97
Se		78.96	0.1	$7.627\cdot10^{14}$	12	$9.15\cdot10^{-9}$				
^{74}Se	0.89			$6.79\cdot10^{12}$	50	$3.39\cdot10^{-10}$	119.8 d	$2.3\cdot10^{-17}$	^{75}Se, EC, ^{75}As	0.864
^{76}Se	9.36			$7.14\cdot10^{13}$	22 +63		17.4 s Stable		(^{77m}Se, IT, ^{77}Se) ^{77}Se	
^{77}Se	7.63			$5.78\cdot10^{13}$	42		Stable		^{78}Se	
^{78}Se	23.77			$1.81\cdot10^{14}$	0.38 +0.2	$6.89\cdot10^{-11}$ $1.05\cdot10^{-10}$	3.92 m $6.5\cdot10^{4}$ y	$2.0.10^{-13}$ $3.6\cdot10^{-23}$	^{79m}Se, IT, ^{79}Se, then ^{79}Se, β^-, ^{79}Br	0.0957 0.149
^{80}Se	49.61			$3.78.10^{14}$	0.06 +0. 35	$2.27\cdot10^{-11}$ $1.32\cdot10^{-10}$	57.3 m 18.5 m 18.5 m	$4.57\cdot10^{-15}$ $4.53\cdot10^{-15}$ $8.3\cdot10^{-14}$	^{81m}Se, IT, ^{81}Se, 99% then ^{81}Se, β^-, ^{81}Br ^{81}Se, β^-, ^{81}Br	0.1031 1.59 1.59
^{82}Se	8.74			$6.67\cdot10^{13}$	0.039 +0.0052	$2.60\cdot10^{-12}$ $3.47\cdot10^{-13}$ $2.95\cdot10^{-12}$	70 s 22.3 m 2.40 h	$2.6\cdot10^{-14}$ $1.8\cdot10^{-16}$ <$2.4.10^{-16}$	^{83m}Se, β^-, ^{83}Br, and ^{83}Se, β^-, ^{83}Br, then ^{83}Br, β^-, ^{83}Kr	3.96 3.67 0.98
Br		79.904	2	$1.507\cdot10^{16}$	6.8	$1.02\cdot10^{-7}$				
^{79}Br	50.69			$7.64\cdot10^{15}$	2.5 +8.3	$1.91\cdot10^{-8}$ $6.34\cdot10^{-8}$	4.42 h 17.66 m	$8.3\cdot10^{-13}$ $4.1\cdot10^{-11}$	^{80m}Br,IT, ^{80}Br, then ^{80}Br, β^-, ^{80}Kr, 92% ^{80}Br,EC,β^+, ^{80}Se, 8% ^{80}Br, β^-, ^{80}Kr, 92% ^{80}Br,EC,β^+, ^{80}Se, 8%	0.0488 2.00 1.87 2.00 1.87

Table 14. (cont.)

Isotope	Natural isotope abun-dance in %	Atomic mass	Weight of the element in ppm of food	Number of atoms per gram of food	Thermal neutron capture cross-section in barns	Number of neutrons absorbed per gram of food	Half-lives	Number of decays per sec per gram of food	Isotope produced and particles emitted	Decay energy in MeV
^{81}Br	49.31			$7.43\cdot10^{15}$	2.4 +0.24	$1.78\cdot10^{-8}$ $1.93\cdot10^{-8}$	6.1 m 35.3 h	$3.4\cdot10^{-11}$ $1.1\cdot10^{-13}$	^{82m}Br, IT, ^{82}Br, 98%, and ^{82m}Br, β$^-$, ^{82}Kr, 2% ^{82}Br, β$^-$, ^{82}Kr	0.046 3.139 3.094
Rb		85.468	8	$5.637\cdot10^{16}$	0.4	$2.25\cdot10^{-8}$				
^{85}Rb	72.17			$4.07\cdot10^{16}$	0.06 +0.38	$2.44\cdot10^{-9}$ $1.8\cdot10^{-8}$	1.018 m 18.65 d	$2.8\cdot10^{-11}$ $7.7\cdot10^{-15}$	^{86m}Rb,IT, ^{86}Rb, ^{86}Rb, β$^-$, ^{86}Sr	0.556 1.775
^{87}Rb	27.83			$1.57\cdot10^{16}$	0.1	$1.57\cdot10^{-9}$	17.7 m	$1.0\cdot10^{-12}$	^{88}Rb, β$^-$, ^{88}Sr	5.316
Sr		87.62	0.2	$1.37\cdot10^{15}$	1.2	$1.64\cdot10^{-9}$				
^{84}Sr	0.56			$7.70\cdot10^{12}$	0.6 +0.2	$4.62\cdot10^{-12}$ $6.16\cdot10^{-12}$	67.6 m 64.84 d	$7.9\cdot10^{-16}$ $7.6\cdot10^{-19}$	^{85m}Sr, IT, ^{85}Sr, 87% ^{85m}Sr, EC, ^{85}Rb, 13% ^{85}Sr, EC, ^{85}Rb	0.237 1.302 1.065
^{86}Sr	9.9			$1.36\cdot10^{14}$	0.81	$1.10\cdot10^{-10}$	2.80 h	$7.5\cdot10^{-15}$	^{87m}Sr, IT, ^{87}Sr	0.3884
^{87}Sr	7.0			$9.62\cdot10^{13}$	16		Stable		^{88}Sr	
^{88}Sr	82.6			$1.13\cdot10^{15}$	0.0058	$6.55\cdot10^{-12}$	50.52 d	$1.04\cdot10^{-18}$	^{89}Sr, β$^-$, ^{89}Y	1.492
Zr		91.22	0.5	$3.30\cdot10^{15}$	0.19	$6.27\cdot10^{-10}$				
^{90}Zr	51.45			$1.70\cdot10^{15}$	0.014	$2.38\cdot10^{-11}$	Stable			
^{91}Zr	11.22			$3.70\cdot10^{14}$	1.2	$4.44\cdot10^{-10}$	Stable			
^{92}Zr	17.15			$5.64\cdot10^{14}$	0.2	$1.13\cdot10^{-10}$	$1.5\cdot10^{6}$ y	$1.7\cdot10^{-24}$	^{93}Zr, β$^-$, 93Nb	0.09
^{94}Zr	17.38			$5.74\cdot10^{14}$	0.049	$2.81\cdot10^{-11}$	64.02 d 3.61 d 34.97 d	$3.5\cdot10^{-18}$ ≈$3.5\cdot10^{-18}$	^{95}Zr, β$^-$, ^{95m}Nb, and ^{95}Nb ^{95m}Nb, IT, ^{95}Nb 97.5% ^{95}Nb, β$^-$, ^{95}Mo	1.162 0.2357 0.926
^{96}Zr	2.8			$9.24\cdot10^{13}$	0.020	$1.85\cdot10^{-12}$	16.8 h 58.1 s 1.23 h	$2.1\cdot10^{-17}$ ≈$2.1\cdot10^{-17}$	^{97}Zr, β$^-$, ^{97m}Nb and ^{97}Nb ^{97m}Nb, IT, ^{97}Nb ^{97}Nb, β$^-$, ^{97}Mo	2.658 1.934
Mo		95.94	0.1	$6.277\cdot10^{14}$	2.5	$1.57\cdot10^{-9}$				
^{92}Mo	14.84			$9.31\cdot10^{13}$	0.0002 + 0.06	$1.9\cdot10^{-14}$ $5.6\cdot10^{-12}$	6.9 h $3.5\cdot10^{3}$ y	$5.2\cdot10^{-19}$ $3.5\cdot10^{-23}$	^{93m}Mo, IT, ^{93}Mo ^{93}Mo, EC, ^{93}Nb	2.425 0.406
^{94}Mo	9.25			$5.81\cdot10^{13}$	0.02		Stable		^{95}Mo	
^{95}Mo	15.92			$9.99\cdot10^{13}$	13.4		Stable		^{96}Mo	
^{96}Mo	16.68			$1.05\cdot10^{14}$	0.5		Stable		^{97}Mo	
^{97}Mo	9.55			$5.99\cdot10^{13}$	2.5	$1.50\cdot10^{-10}$	Stable		^{98}Mo	
^{98}Mo	24.13			$1.51\cdot10^{14}$	0.14	$2.12\cdot10^{-11}$	65.94 h 6.01h $2.13\cdot10^{5}$ y	$6.2\cdot10^{-17}$ $6.8\cdot10^{-16}$ $2.2.10^{-24}$	^{99}Mo, β$^-$, ^{99m}Tc ^{99m}Tc, IT, ^{99}Tc, 100% ^{99}Tc, β$^-$, ^{99}Ru	1.357 0.142 0.294
^{100}Mo	9.63			$6.04\cdot10^{13}$	0.19	$1.15\cdot10^{-11}$	14.6 m 14.2 m	$9.1\cdot10^{-15}$ $9.3\cdot10^{-15}$	^{101}Mo, β$^-$, ^{101}Tc ^{101}Tc, β$^-$, ^{101}Ru	2.82 1.61

Table 14. (cont.)

Isotope	Natural isotope abun-dance in %	Atomic mass	Weight of the element in ppm of food	Number of atoms per gram of food	Thermal neutron capture cross-section in barns	Number of neutrons absorbed per gram of food	Half-lives	Number of decays per sec per gram of food	Isotope produced and particles emitted	Decay energy in MeV
Rh		102.91	0.01	$5.85 \cdot 10^{13}$	145	$8.48 \cdot 10^{-9}$				
^{103}Rh	100			$5.85 \cdot 10^{13}$	11 +134	$6.44 \cdot 10^{-10}$ $7.84 \cdot 10^{-9}$	4.36 m 42.3 s	$1.7 \cdot 10^{-12}$ $1.3.10^{-10}$	^{104m}Rh, IT, ^{104}Rh, 99+% ^{104}Rh, β^-, ^{104}Pd ^{104}Rh, β^-, ^{104}Pd, 99+% ^{104}Rh, EC, ^{104}Ru, 0.4%	0.129 2.44 2.44 1.14
Ag		107.9	0.02	$1.12 \cdot 10^{14}$	63.2	$7.08 \cdot 10^{-9}$				
^{107}Ag	51.839			$5.79 \cdot 10^{13}$	0.37 + 35	$2.14 \cdot 10^{-11}$ $2.03 \cdot 10^{-9}$	$1.3 \cdot 10^{2}$ y 2.39 m	$3.6 \cdot 10^{-21}$ $9.8 \cdot 10^{-12}$	^{108m}Ag, EC, ^{108}Cd, or ^{108m}Ag, IT, ^{108}Ag, 8% ^{108}Ag, β^-, ^{108}Cd, 97% or EC, β^+, ^{108}Pd, 3%	1.73 0.079 1.65 1.92
^{109}Ag	49.161			$5.49 \cdot 10^{13}$	4.2 + 87	$2.31 \cdot 10^{-10}$ $4.78 \cdot 10^{-9}$	249.8 d 24.6 s	$7.4 \cdot 10^{-18}$ $1.3 \cdot 10^{-10}$	^{110m}Ag, β^-, ^{110}Cd, 99% or IT, ^{110}Ag, β^-, ^{110}Cd ^{110}Ag, β^-, ^{110}Cd	3.008 3.123 2.892
Cd		112.41	0.1	$5.358 \cdot 10^{14}$	2,520	$1.35 \cdot 10^{-6}$				
^{106}Cd	1.25			$6.70 \cdot 10^{12}$	0.20	$1.34 \cdot 10^{-12}$	6.52 h	$4.0 \cdot 10^{-17}$	^{107}Cd, EC, β^+, ^{107}Ag	1.42
^{108}Cd	0.89			$4.77 \cdot 10^{12}$	1	$4.77 \cdot 10^{-12}$	462.0 d	$8.3 \cdot 10^{-20}$	^{109}Cd, EC, ^{109}Ag	0.214
^{110}Cd	12.49			$6.69 \cdot 10^{13}$	0.06 + 11	$4.02 \cdot 10^{-12}$	48.5 m Stable	$9.6 \cdot 10^{-16}$	^{111m}Cd, IT, ^{111}Cd ^{111}Cd	0.151
^{111}Cd	12.8			$6.86 \cdot 10^{13}$	3.5		Stable		^{112}Cd	
^{112}Cd	24.13			$1.29 \cdot 10^{14}$	0.012 + 2.2	$1.55 \cdot 10^{-12}$	14.1 y Stable	$2.4 \cdot 10^{-21}$	^{113m}Cd, β^-, ^{113}In ^{113}Cd	0.59
^{113}Cd	12.22			$6.55 \cdot 10^{13}$	20,600	$1.35 \cdot 10^{-6}$	Stable		^{114}Cd	
^{114}Cd	28.73			$1.54 \cdot 10^{14}$	0.04 0 + 0.29	$6.16 \cdot 10^{-12}$ $4.47 \cdot 10^{-11}$	44.6 d 2.228 d	$1.1.10^{-18}$ $1.6 \cdot 10^{-16}$	^{115m}Cd, β^-, ^{115}In ^{115}Cd, β^-, ^{115}In	1.629 1.448
^{116}Cd	7.49			$4.01 \cdot 10^{13}$	0.026 + 0.052	$1.04 \cdot 10^{-12}$ $3.13 \cdot 10^{-12}$	3.4 h (1.94 h) 2.49 h (44 m)	$5.9 \cdot 10^{-17}$ <$5.9 \cdot 10^{-17}$ <$2.4 \cdot 10^{-16}$ <$2.4 \cdot 10^{-16}$	^{117m}Cd, β^-, ^{117m}In ^{117m}In, β^-, ^{117}Sn ^{117m}In, IT, ^{117}In ^{117}Cd, β^-, ^{117}In, then ^{117}In, β^-, ^{117}Sn	2.66 1.769 2.53 1.45
In		114.8	0.01	$5.246 \cdot 10^{13}$	197	$1.02 \cdot 10^{-8}$				

Table 14. (cont.)

Isotope	Natural isotope abun-dance in %	Atomic mass	Weight of the element in ppm of food	Number of atoms per gram of food	Thermal neutron capture cross-section in barns	Number of neutrons absorbed per gram of food	Half-lives	Number of decays per sec per gram of food	Isotope produced and particles emitted	Decay energy in MeV
^{113}In	4.3			$2.26\cdot10^{12}$	3.1 +5.4 +3.9	$7.00\cdot10^{-12}$ $1.22\cdot10^{-11}$ ($1.6\cdot10^{-11}$)	2.5 s 49.51 d (71.9 s)	$1.9\cdot10^{-12}$ $2.0\cdot10^{-18}$ $1.5\cdot10^{-13}$	^{114m2}In, IT, ^{114}In, 100% ^{114m1}In, IT, ^{114}In, 97% ^{114m}In, EC, ^{114}Cd, 3% ^{114}In, β^-, ^{114}Sn, 97% ^{114}In, EC, ^{114}Cd, 3%	0.150 0.190 1.641 1.989 1.453
^{115}In	95.7			$5.02\cdot10^{13}$	88 +73 +44	$4.42\cdot10^{-9}$ $3.66\cdot10^{-9}$ ($6.63\cdot10^{-9}$)	2.16 s 54.1 m 14.1 s	$1.42\cdot10^{-9}$ $7.8\cdot10^{-13}$ $3.3\cdot10^{-10}$	^{116m2}In, IT, ^{116}In ^{116m1}In, β^-, ^{116}Sn ^{116}In, β^-, ^{116}Sn	0.162 3.39 3.27
Sn		118.71	0.1	$5.073\cdot10^{14}$	0.61	$3.09\cdot10^{-10}$				
^{112}Sn	0.97			$4.92\cdot10^{12}$	0.15 +0.40	$7.38\cdot10^{-13}$ $1.97\cdot10^{-12}$	21.4 m 115.1 d	$4.0\cdot10^{-16}$ $1.4\cdot10^{-19}$	^{113m}Sn,IT, ^{113}Sn, 92% ^{113m}Sn, EC, ^{113}In, 8% ^{113}Sn, EC, ^{113}In	0.077 1.115 1.038
^{114}Sn	0.66			$3.35\cdot10^{12}$	0.12		Stable		^{115}Sn	
^{115}Sn	0.34			$1.72\cdot10^{12}$	0.00006		Stable		α, ^{112}Cd	
^{116}Sn	14.54			$7.38\cdot10^{13}$	0.006 +0.14	$4.43\cdot10^{-13}$	13.60 d Stable	$2.6\cdot10^{-19}$	^{117m}Sn, IT, ^{117}Sn ^{117}Sn	0.3146
^{117}Sn	7.68			$3.90\cdot10^{13}$	1.1		Stable		^{118}Sn	
^{118}Sn	24.22			$1.23\cdot10^{14}$	0.004	$4.91\cdot10^{-13}$	293 d	$1.3\cdot10^{-20}$	^{119m}Sn, IT, ^{119}Sn	0.0896
^{119}Sn	8.58			$4.35\cdot10^{13}$	2		Stable		^{120}Sn	
^{120}Sn	32.59			$1.65\cdot10^{14}$	0.001 +0.13	$1.65\cdot10^{-13}$ $2.15\cdot10^{-11}$	55 y 1.128 d	$6.6\cdot10^{-23}$ $1.5\cdot10^{-16}$	^{121m}Sn, IT, ^{121}Sn, 78% ^{121m}Sn, β^-, ^{121}Sb, 22% ^{121}Sn, β^-, ^{121}Sb	0.006 0.394 0.388
^{122}Sn	4.63			$2.35\cdot10^{13}$	0.15 +0.001	$3.52\cdot10^{-12}$ $2.35\cdot10^{-14}$	40.1 m 129.2 d	$1.0\cdot10^{-15}$ $8.8\cdot10^{-20}$	^{123m}Sn, β^-, ^{123}Sb ^{123}Sn, β^-, ^{123}Sb	1.428 1.403
^{124}Sn	5.79			2.94·1013	0.13 +0.005	$3.82\cdot10^{-12}$ $1.47\cdot10^{-13}$ $3.97\cdot10^{-12}$	9.51 m 9.63 d 2.758 y	$4.6\cdot10^{-15}$ $1.2\cdot10^{-19}$ $3.2\cdot10^{-20}$	^{125m}Sn, β^-, ^{125}Sb ^{125}Sn, β^-, ^{125}Sb, then ^{125}Sb, β^-, ^{125}Te	2.387 2.360 0.767
Sb		121.76	0.01	$4.946\cdot10^{13}$	5.2	$2.57\cdot10^{-10}$				
^{121}Sb	57.21			$2.830\cdot10^{13}$	0.4 +5.6	$1.13\cdot10^{-11}$ $1.70\cdot10^{-10}$	4.19 m 2.72 d	$3.12\cdot10^{-14}$ $5.01\cdot10^{-16}$	^{122m}Sb, IT, ^{122}Sb ^{122}Sb, β^-, ^{122}Te, 98% ^{122}Sb, β^+, ^{122}Sn, 2%	0.162 1.980 1.619
^{123}Sb	42.79			$2.116\cdot10^{13}$	0.02 +0.04 +4.0	$4.23\cdot10^{-13}$ $8.47\cdot10^{-13}$ $8.47\cdot10^{-11}$	20.3 m 1.6 m 60.2 d	$2.4\cdot10^{-16}$ $6.1\cdot10^{-15}$ $1.1\cdot10^{-17}$	^{124m2}Sb, IT, ^{124}Sb ^{124m1}Sb, IT, ^{124}Sb, 80% ^{124m1}Sb, β^-, ^{124}Te, 20% ^{124}Sb, β^-, ^{124}Te	0.035 0.010 2.915 2.905
Te		127.6	0.01	$4.719\cdot10^{13}$	4.7	$2.22\cdot10^{-10}$				

Table 14. (cont.)

Isotope	Natural isotope abun-dance in %	Atomic mass	Weight of the ele-ment in ppm of food	Number of atoms per gram of food	Thermal neutron capture cross-section in barns	Number of neutrons absorbed per gram of food	Half-lives	Number of decays per sec per gram of food	Isotope produced and particles emitted	Decay energy
^{120}Te	0.09			$4.25 \cdot 10^{10}$	0.25 2.0	$1.06 \cdot 10^{-14}$ $8.49 \cdot 10^{-14}$	154 d 16.8 d	$5.5 \cdot 10^{-22}$ $4.1 \cdot 10^{-20}$	^{121m}Te,IT, ^{121}Te, 89% ^{121m}Te,EC, ^{121}Sb, 11% ^{121}Te, EC, ^{121}Sb	0.2122 1.25 1.04
^{122}Te	2.55			$1.20 \cdot 10^{12}$	2.4	$2.89 \cdot 10^{-12}$	119.7 d	$1.94 \cdot 10^{-19}$	^{123m}Te, IT, ^{123}Te	0.247
^{123}Te	0.89			$4.20 \cdot 10^{11}$	370	$1.55 \cdot 10^{-10}$	Stable		^{124}Te	
^{124}Te	4.74			$2.24 \cdot 10^{12}$	0.05 +7	$1.12 \cdot 10^{-13}$ $1.57 \cdot 10^{-11}$	58 d Stable	$1.55 \cdot 10^{-20}$	^{125m}Te, IT, ^{125}Te ^{125}Te	0.15
^{125}Te	7.07			$3.34 \cdot 10^{12}$	1.6	$5.34 \cdot 10^{-12}$	Stable		^{126}Te	
^{126}Te	18.84			$8.89 \cdot 10^{12}$	0.12 0.8	$1.07 \cdot 10^{-12}$ $7.11 \cdot 10^{-12}$	109 d 9.4 h	$7.9 \cdot 10^{20}$ $1.5 \cdot 10^{-16}$	^{127m}Te, IT, ^{127}Te ^{127m}Te, β^-, ^{127}I, 2% ^{127m}Te, β^-, ^{127}I	0.088 0.77 0.697
^{128}Te	31.74			$1.50 \cdot 10^{13}$	0.016 0.20	$2.40 \cdot 10^{-13}$ $2.99 \cdot 10^{-12}$	33.6 d 1.16 h $1.7 \cdot 10^{7}$ y 1.16 h $1.7 \cdot 10^{7}$ y	$5.7 \cdot 10^{-20}$ $4.0 \cdot 10^{-17}$ $3.1 \cdot 10^{-28}$ $5.0 \cdot 10^{-16}$ $3.9 \cdot 10^{-27}$	^{129m}Te,IT, ^{129}Te, 63% ^{129m}Te, β^-, ^{129}I, 37% ^{129}Te, β^-, ^{129}I, then ^{129}I, β^-, ^{129}Xe ^{129}Te, β^-, ^{129}I, then ^{129}I, β^-, ^{129}Xe	0.105 1.60 1.501 0.191 1.501 0.191
^{130}Te	34.08 33.87			$1.61 \cdot 10^{13}$	0.03 0.20	$4.82 \cdot 10^{-13}$ $3.22 \cdot 10^{-12}$	1.35 d 8.04 d 25.0 m 8.04 d	$2.9 \cdot 10^{-18}$ $1.49 \cdot 10^{-15}$	^{131m}Te, β^-, ^{131}I, 78% ^{131m}Te, IT , ^{131}Te, 22% ^{131}Te, β^-, ^{131}I, then ^{131}I, β^-, ^{131}Xe ^{131}Te, β^-, ^{131}I, then ^{131}I, β^-, ^{131}Xe	2.4 0.18 2.251 0.971 2.251 0.971
I		126.9	1	$4.745 \cdot 10^{15}$	6.15	$2.94 \cdot 10^{-8}$				
^{127}I	100			$4.745 \cdot 10^{15}$	6.15	$2.94 \cdot 10^{-8}$	25.0 m	$1.4 \cdot 10^{-11}$	^{128}I, β^-, ^{128}Xe ^{128}I, EC, ^{128}Te	2.125 1.256

Table 14. (cont.)

Isotope	Natural isotope abun-dance in %	Atomic mass	Weight of the ele-ment in ppm of food	Number of atoms per gram of food	Thermal neutron capture cross-section in barns	Number of neutrons absorbed per gram of food	Half-lives	Number of decays per sec per gram of food	Isotope produced and particles emitted	Decay energy
Cs		130.9	0.01	$4.531 \cdot 10^{13}$	30	$1.36 \cdot 10^{-9}$				
^{133}Cs	100			$4.531 \cdot 10^{13}$	2.7 +27.7	$1.22 \cdot 10^{-10}$ $1.38 \cdot 10^{-9}$	2.91 h 2.065 y	$8.1 \cdot 10^{-15}$ $1.5 \cdot 10^{-17}$	^{134m}Cs, IT, ^{134}Cs ^{134}Cs, β^-, ^{134}Ba	0.139 2.059
Ba		137.33	0.02	$8.770 \cdot 10^{13}$	1.3	$1.14 \cdot 10^{-10}$				
^{130}Ba	0.106			$9.30 \cdot 10^{10}$	1 + 8	$9.30 \cdot 10^{-14}$ $8.37 \cdot 10^{-13}$	14.6 m 11.7 d 9.69 d	$7.36 \cdot 10^{-17}$ $5.74 \cdot 10^{-19}$ $6.93 \cdot 10^{-19}$	^{131m}Ba, IT, ^{131}Ba ^{131}Ba, EC, ^{131}Cs ^{131}Cs, EC, ^{131}Xe	0.187 1.36 0.35
^{132}Ba	0.101			$8.86 \cdot 10^{10}$	0.84 + 9.7	$7.44 \cdot 10^{-14}$ $9.34 \cdot 10^{-13}$	1.621d 10.53 y	$3.68 \cdot 10^{-19}$ $1.9 \cdot 10^{-21}$	^{133m}Ba, IT, ^{133}Ba ^{133}Ba, EC, ^{133}Cs	0.288 0.516
^{134}Ba	2.42			$2.12 \cdot 10^{12}$	0.1 + 1.3	$2.12 \cdot 10^{-13}$	1.20 d Stable	$1.42 \cdot 10^{-18}$	^{135m}Ba, IT, ^{135}Ba ^{135}Ba	0.2682
^{135}Ba	6.593			$5.78 \cdot 10^{12}$	0.014 +5.8	$8.09 \cdot 10^{-14}$	0.308 s Stable	$1.8 \cdot 10^{-13}$	^{136m}Ba, IT, ^{136}Ba ^{136}Ba	2.0305

Table 14. (cont.)

Isotope	Natural isotope abun-dance in %	Atomic mass	Weight of the ele-ment in ppm of food	Number of atoms per gram of food	Thermal neutron capture cross-section in barns	Number of neutrons absorbed per gram of food	Half-lives	Number of decays per sec per gram of food	Isotope produced and particles emitted	Decay energy
^{136}Ba	7.85			$6.88 \cdot 10^{12}$	0.010 + 0.44	$6.88 \cdot 10^{-14}$	2.552 m Stable	$3.1 \cdot 10^{-16}$	^{137m}Ba, IT, ^{137}Ba ^{137}Ba	0.6617
^{137}Ba	11.23			$9.85 \cdot 10^{12}$	5		Stable		^{138}Ba	
^{138}Ba	71.7			$6.29 \cdot 10^{13}$	0.41	$2.58 \cdot 10^{-11}$	1.396 h	$8.6 \cdot 10^{-15}$	^{139}Ba, β^-, ^{139}La	2.314
Au		196.97	0.01	$3.057 \cdot 10^{13}$	98.7	$3.02 \cdot 10^{-9}$				
^{197}Au	100			$3.057 \cdot 10^{13}$	98.7	$3.02 \cdot 10^{-9}$	2.30 d 2.694 d	$1.1 \cdot 10^{-14}$ $9.0 \cdot 10^{-15}$	^{198m}Au, IT, ^{198}Au ^{198}Au, β^-, ^{198}Hg	0.812 1.373
Hg		200.59	0.05	$1.501 \cdot 10^{14}$	370	$5.55 \cdot 10^{-8}$				
^{196}Hg	0.15			$2.25 \cdot 10^{11}$	105 + 3000	$2.36 \cdot 10^{-11}$ $6.99 \cdot 10^{-10}$	23.8 h 2.672 d	$1.9 \cdot 10^{-16}$ $2.1 \cdot 10^{-15}$	^{197m}Hg, IT, ^{197}Hg ^{197}Hg, EC, ^{197}Au	0.2989 0.599
^{198}Hg	9.97			$1.50 \cdot 10^{13}$	0.017 + 2.0	$2.54 \cdot 10^{-12}$	42.6 m Stable	$6.9 \cdot 10^{-17}$	^{199m}Hg, IT, ^{199}Hg ^{199}Hg	0.532
^{199}Hg	16.87			$2.53 \cdot 10^{13}$	2,100		Stable		^{200}Hg	
^{200}Hg	23.10			$3.47 \cdot 10^{13}$	<60		Stable		^{201}Hg	
^{201}Hg	13.18			$1.98 \cdot 10^{13}$	<60		Stable		^{202}Hg	
^{202}Hg	29.86			$4.48 \cdot 10^{13}$	4.9	$2.20 \cdot 10^{-10}$	46.61d	$3.8 \cdot 10^{-17}$	^{203}Hg, β^-, ^{203}Tl	0.492
^{204}Hg	6.87			$1.03 \cdot 10^{13}$	0.4	$4.12 \cdot 10^{-12}$	5.2 m	$9.2 \cdot 10^{-15}$	^{205}Hg, β^-, ^{205}Tl	1.53
Pb		207.2	1	$2.906 \cdot 10^{15}$	0.172	$5.00 \cdot 10^{-10}$				
^{204}Pb	1.4			$4.07 \cdot 10^{13}$	0.68	$2.77 \cdot 10^{-11}$	$1.5 \cdot 10^{7}$ y	$4.0 \cdot 10^{-26}$	^{205}Pb, EC, ^{205}Tl	0.053
^{206}Pb	24.1			$7.00 \cdot 10^{14}$	0.03	$2.10 \cdot 10^{-11}$	0.80 s	$1.8 \cdot 10^{-11}$	^{207m}Pb, IT, ^{207}Pb	1.632
^{207}Pb	22.1			$6.42 \cdot 10^{14}$	0.7	$4.50 \cdot 10^{-10}$	Stable		^{208}Pb	
^{208}Pb	52.4			$1.52 \cdot 10^{15}$	0.49	$7.46 \cdot 10^{-10}$	3.25 h	$4.4 \cdot 10^{-14}$	^{209}Pb, β^-, ^{209}Bi	0.644

A.: Most of the nuclear data are from Table of the Isotopes by Norman E. Holden, at High Flux Beam Reactor, Reactor Division, Brookhaven National Laboratory, Upton. N.Y.11973. See reference [Ho99]. The data were supplemented by data from Table of the Isotopes compiled by Russel L. Heath, National Reactor Testing Station, Idaho Falls, Idaho, and published in Hand book of Chemistry and Physics, 49th edition (1968), and the different version ibid, 61st edition (1980). See reference [He80].

Table 15. The number of atoms in 100 kg of food that absorb a neutron if the neutron fluence is one per cm^{2}[A]

Isotope in the food	Number of atoms that absorb a neutron per 100 kg of food	% of the neutrons that are absorbed in each element of food
H	1790	89.303
C	3.16	0.158
N	162	8.082
O	0.76	0.038
Na	1.03	0.051
Mg	0.05	0.002
P	0.74	0.037
S	2.15	0.107
Cl	32.0	1.596
K	12.1	0.604
Ca	0.09	0.004
Fe	0.14	0.007
Zn	0.04	0.002
Br	0.01	0.001
Cd	0.14	0.007
Sum	2004.41	100.00

[A] The numbers in column 2 are derived from column 7 of Table 14. Column 3 gives the values in column 2 as a percentage of the sum. See explanations in Section 10.1.

Table 16. Neutron capture activity dose in mSv/year from consumption of reference food exposed to fluences of 10^5 and $3 \cdot 10^8$ neutrons per cm^2.[A]

Isotope produced	Activity in Bq/g of food for one neutron/cm^2	Half-life of the isotope	Decay energy in MeV	Conversion factor for becquerel to sievert	Dose in mSv/year from consumption of 40 kg/year of reference food exposed to fluence of 10^5 neutron/cm^2	Dose in mSv/year from consumption of 40 kg/year of reference food exposed to fluence of $3 \cdot 10^8$ neutron/cm^2
^{80}Br	$4.1 \cdot 10^{-11}$	17.7 m	2.00	$3.1 \cdot 10^{-11}$	$5.08 \cdot 10^{-9}$	$1.5 \cdot 10^{-5}$
^{88}Rb	$1.0 \cdot 10^{-12}$	17.7 m	5.32	$9.0 \cdot 10^{-11}$	$3.60 \cdot 10^{-10}$	$1.1 \cdot 10^{-6}$
^{81}Se	$9.2 \cdot 10^{-14}$	18.5 m	1.59	$2.7 \cdot 10^{-11}$	$9.94 \cdot 10^{-12}$	$3.0 \cdot 10^{-8}$
^{128}I	$1.4 \cdot 10^{-11}$	25.0 m	1.78	$4.6 \cdot 10^{-11}$	$2.58 \cdot 10^{-9}$	$7.7 \cdot 10^{-6}$
^{38}Cl	$3.0 \cdot 10^{-10}$	37.2 m	4.92	$1.2 \cdot 10^{-10}$	$1.44 \cdot 10^{-7}$	$4.3 \cdot 10^{-4}$
^{116m1}In	$1.9 \cdot 10^{-12}$	54.1 m	3.35	$6.4 \cdot 10^{-11}$	$4.86 \cdot 10^{-10}$	$1.5 \cdot 10^{-6}$
^{69}Zn	$1.4 \cdot 10^{-11}$	56.0 m	0.91	$3.1 \cdot 10^{-11}$	$1.77 \cdot 10^{-9}$	$5.3 \cdot 10^{-6}$
^{49}Sc	$8.7 \cdot 10^{-13}$	57.5 m	2.01	$8.2 \cdot 10^{-11}$	$2.85 \cdot 10^{-10}$	$8.6 \cdot 10^{-7}$
^{75}Ge	$1.7 \cdot 10^{-14}$	1.4 h	1.18	$4.6 \cdot 10^{-11}$	$3.13 \cdot 10^{-12}$	$9.4 \cdot 10^{-9}$
^{56}Mn	$2.2 \cdot 10^{-12}$	2.6 h	3.70	$2.5 \cdot 10^{-10}$	$2.20 \cdot 10^{-9}$	$6.6 \cdot 10^{-6}$
^{31}Si	$5.3 \cdot 10^{-14}$	2.6 h	1.49	$1.6 \cdot 10^{-10}$	$3.39 \cdot 10^{-11}$	$1.0 \cdot 10^{-7}$
^{134m}Cs	$7.5 \cdot 10^{-15}$	2.9 h	0.14	$2.0 \cdot 10^{-11}$	$6.00 \cdot 10^{-13}$	$1.8 \cdot 10^{-9}$
^{80m}Br	$8.3 \cdot 10^{-13}$	4.4 h	2.04	$1.1 \cdot 10^{-10}$	$3.65 \cdot 10^{-10}$	$1.1 \cdot 10^{-6}$
^{42}K	$9.4 \cdot 10^{-11}$	12.4 h	3.52	$4.3 \cdot 10^{-10}$	$1.62 \cdot 10^{-7}$	$4.9 \cdot 10^{-4}$
^{64}Cu	$2.7 \cdot 10^{-13}$	12.7 h	1.23	$1.2 \cdot 10^{-10}$	$1.30 \cdot 10^{-10}$	$3.9 \cdot 10^{-7}$
^{69m}Zn	$7.0 \cdot 10^{-14}$	13.8 h	0.44	$3.3 \cdot 10^{-10}$	$9.24 \cdot 10^{-11}$	$2.8 \cdot 10^{-7}$
^{24}Na	$1.3 \cdot 10^{-10}$	15.0 h	5.52	$4.3 \cdot 10^{-10}$	$2.29 \cdot 10^{-7}$	$6.9 \cdot 10^{-4}$
^{76}As	$2.5 \cdot 10^{-14}$	1.1 d	2.97	$1.6 \cdot 10^{-9}$	$1.60 \cdot 10^{-10}$	$4.8 \cdot 10^{-7}$
^{82}Br	$1.1 \cdot 10^{-13}$	1.5 d	3.14	$5.4 \cdot 10^{-10}$	$2.38 \cdot 10^{-10}$	$7.1 \cdot 10^{-7}$
^{115}Cd	$1.7 \cdot 10^{-16}$	2.2 d	1.45	$1.4 \cdot 10^{-9}$	$9.52 \cdot 10^{-13}$	$2.9 \cdot 10^{-9}$
^{12}2Sb	$4.9 \cdot 10^{-16}$	2.7 d	3.60	$1.7 \cdot 10^{-9}$	$3.36 \cdot 10^{-12}$	$1.0 \cdot 10^{-8}$
^{47}Ca	$8.8 \cdot 10^{-17}$	4.5 d	1.99	$1.6 \cdot 10^{-9}$	$5.63 \cdot 10^{-13}$	$1.7 \cdot 10^{-9}$
^{32}P	$3.5 \cdot 10^{-12}$	14.3 d	1.71	$2.4 \cdot 10^{-9}$	$3.36 \cdot 10^{-8}$	$1.0 \cdot 10^{-4}$
^{86}Rb	$8.9 \cdot 10^{-15}$	18.6 d	1.78	$2.8 \cdot 10^{-9}$	$9.96 \cdot 10^{-11}$	$3.0 \cdot 10^{-7}$
^{33}P	$1.5 \cdot 10^{-15}$	25.3 d	0.25	$2.4 \cdot 10^{-10}$	$1.44 \cdot 10^{-12}$	$4.3 \cdot 10^{-9}$
^{59}Fe	$3.5 \cdot 10^{-16}$	44.5 d	1.56	$1.8 \cdot 10^{-9}$	$2.52 \cdot 10^{-12}$	$7.6 \cdot 10^{-9}$
^{35}S	$2.6 \cdot 10^{-13}$	87.2 d	0.17	$7.7 \cdot 10^{-10}$	$8.01 \cdot 10^{-10}$	$2.4 \cdot 10^{-6}$
^{45}Ca	$1.7 \cdot 10^{-15}$	162.7 d	0.26	$7.6 \cdot 10^{-10}$	$5.17 \cdot 10^{-12}$	$1.6 \cdot 10^{-8}$
^{65}Zn	$4.5 \cdot 10^{-15}$	243.6 d	1.35	$3.9 \cdot 10^{-9}$	$7.10 \cdot 10^{-11}$	$2.1 \cdot 10^{-7}$
^{134}Cs	$1.4 \cdot 10^{-17}$	2.065 y	2.06	$1.9 \cdot 10^{-8}$	$1.06 \cdot 10^{-12}$	$3.2 \cdot 10^{-9}$
^{55}Fe	$6.9 \cdot 10^{-16}$	2.73 y	0.23	$3.3 \cdot 10^{-10}$	$9.11 \cdot 10^{-13}$	$2.7 \cdot 10^{-9}$
^{60}Co	$1.6 \cdot 10^{-17}$	5.27 y	2.82	$3.4 \cdot 10^{-9}$	$2.16 \cdot 10^{-13}$	$6.5 \cdot 10^{-10}$
^{14}C	$5.8 \cdot 10^{-15}$	5715 y	0.16	$5.8 \cdot 10^{-10}$	$1.35 \cdot 10^{-11}$	$4.1 \cdot 10^{-8}$

[A] See Section 10.2 for explanations.

FIGURES

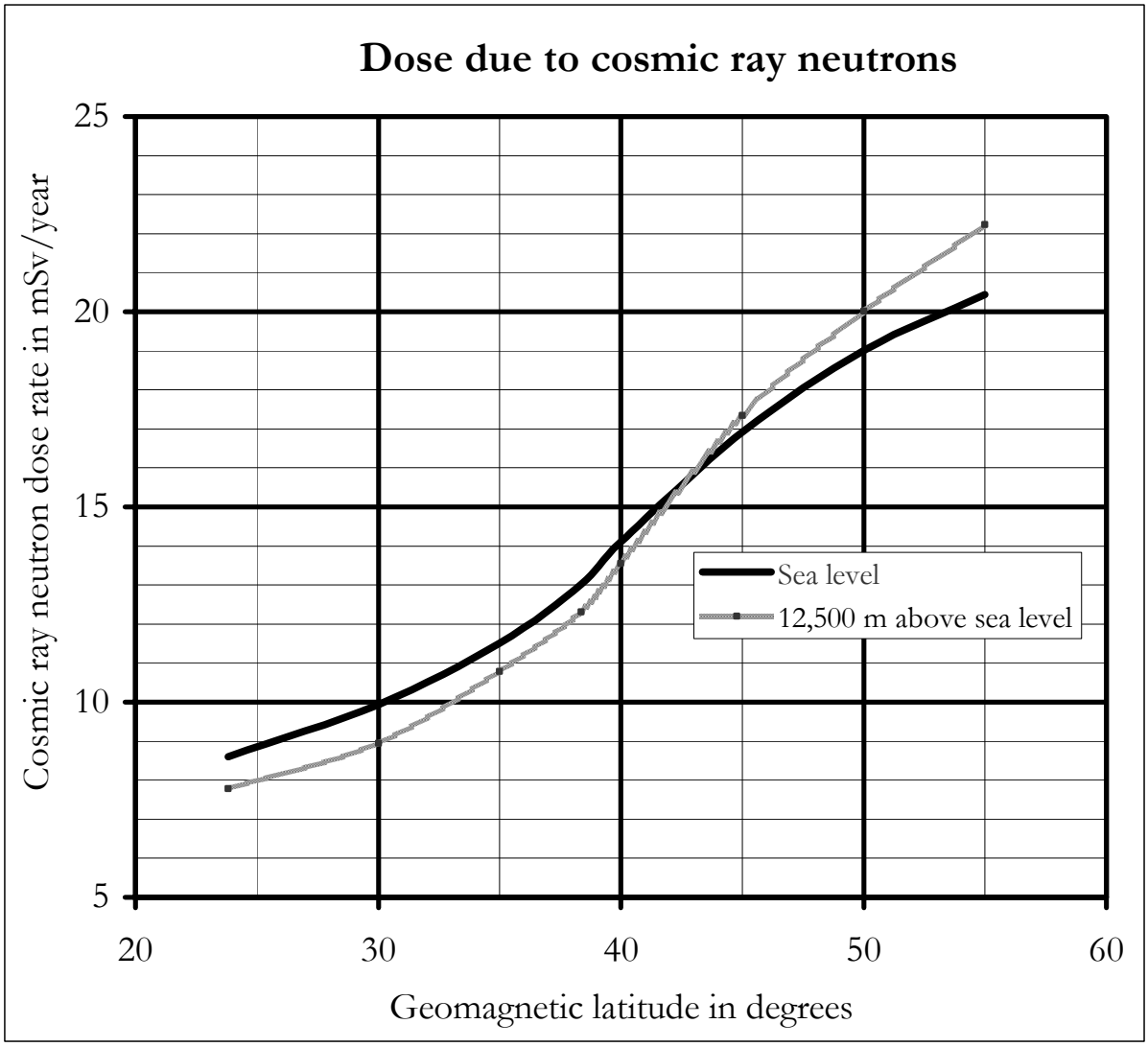

Fig.1. The ordinate shows the neutron dose-rate. The curve with lower slope shows the cosmic neutron dose rate at sea level multiplied by 300 as a function of the magnetic latitude on the abscissa. The steeper curve shows the cosmic neutron dose rate at 12,500 meters altitude as a function of the magnetic latitude. Thus, at magnetic latitude of 50^0 the cosmic neutron dose at a height of 12,500 m over sea level is about 20 mSv/year, while at ground level and at the same magnetic latitude the cosmic ray neutron dose is about 19/300=0.063 mSv/year. The neutron dose rate at sea level and magnetic latitude of 43^0 is seen to be roughly 300 times smaller than that at 12,500 m over sea level. (See [Na87a])

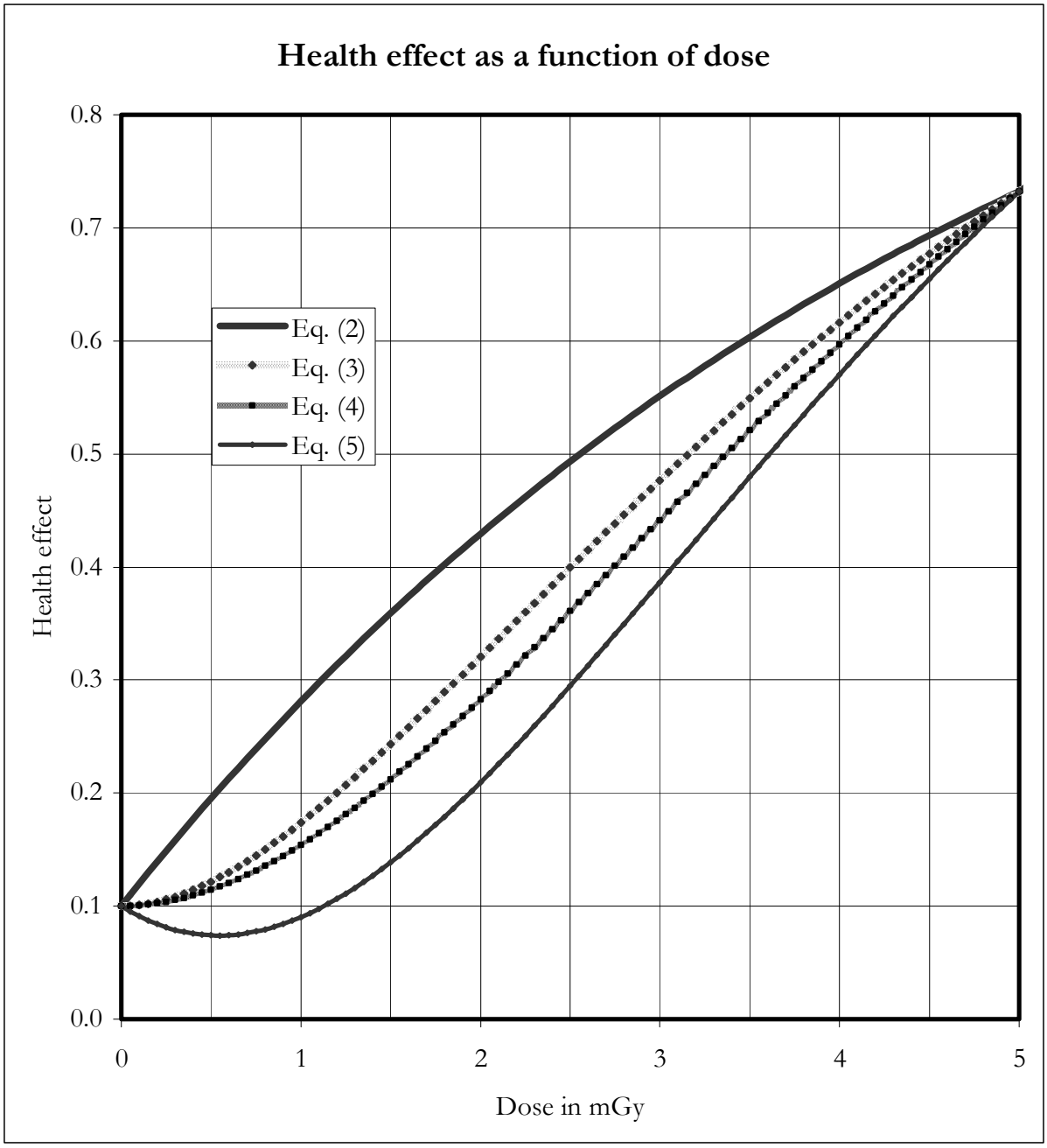

Fig. 2. The effects observed at high doses may be extrapolated to low doses in different ways as the four curves indicate. The top curve, shows the relation indicated by Eq. (2). It can be considered equivalent to the LNT model given by Eq. (1). The next two curves show the relations indicated by Eqs. (3) and (4). In case of these two curves a linear extrapolation from high doses would indicate a threshold dose. The lowest curve shows relation indicated by Eq. (5), which at very low doses shows a small beneficial effect. However, the beneficial effect is small and it would be extremely difficult to confirm it experimentally. For this illustration, the curves given by the equations have been adjusted to go through the same points at (0, 0.1) and at (5, 0.7321); and in case of equation (5), the value of A =1.5 and B = 0.5.

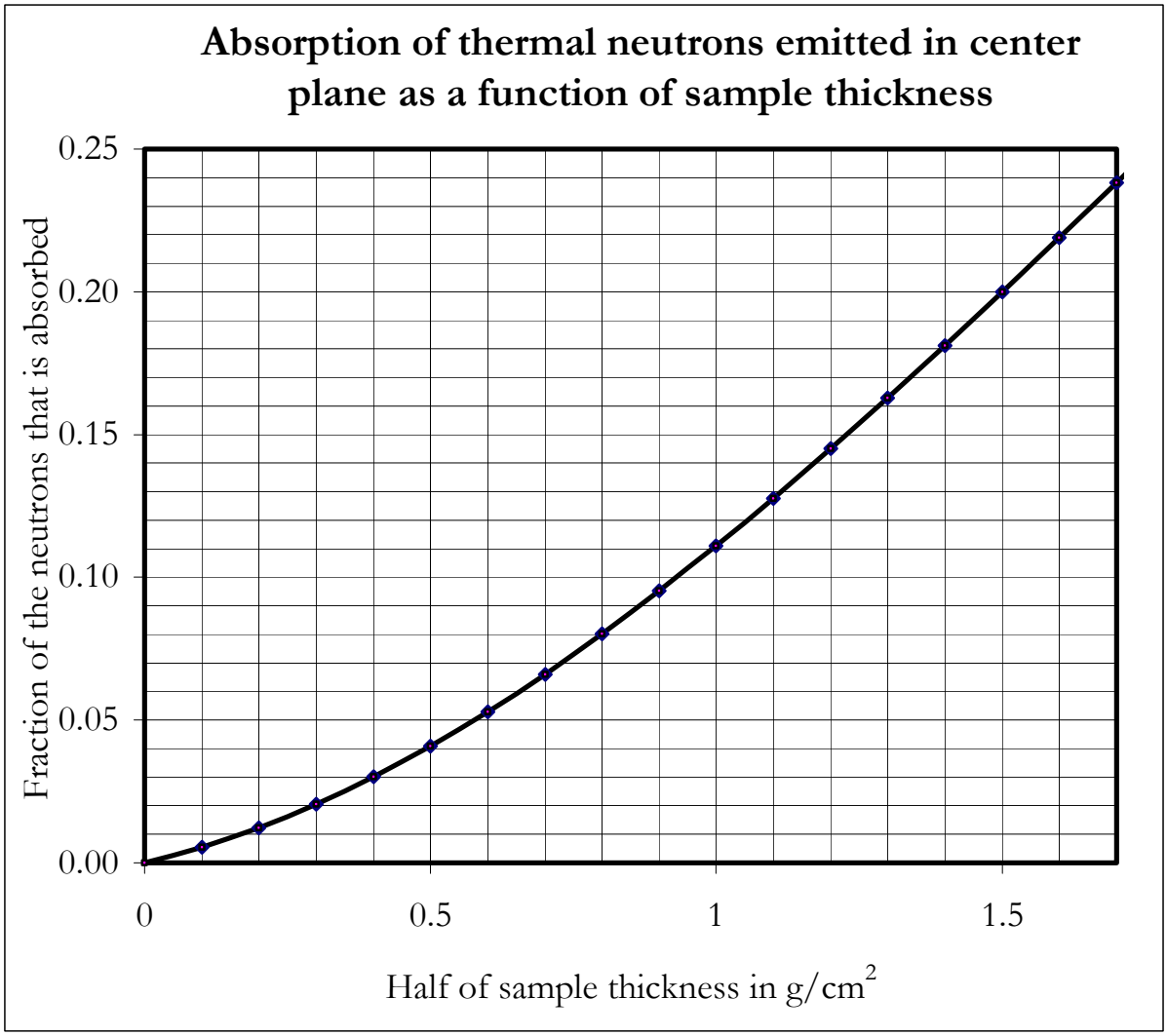

Fig. 3. Probability for absorption of a thermal neutron emitted in the center plane of a sample with half-thickness shown on the abscissa.

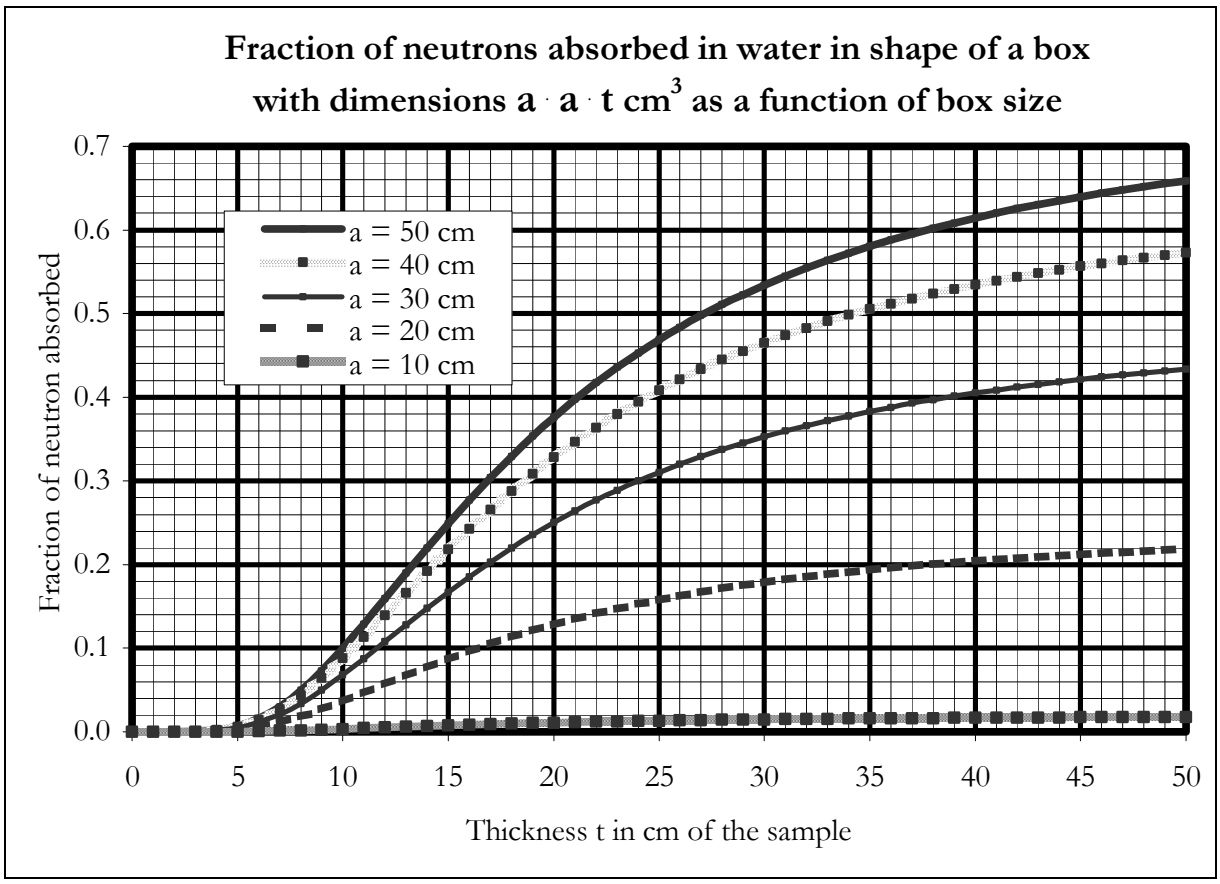

Fig. 4. The ordinate shows the fraction of the emitted fast neutrons that are slowed down thermalized and absorbed in a water sample. This water sample is in form of a rectangular box with dimensions a, a, and t, where the thickness t is shown on the abscissa. The 5 curves from the top are for the dimension a equal to: 50, 40, 30, 20, and 10 cm, respectively. For example, the middle curve shows that the fraction 0.3, or 30 %, of the produced neutrons are absorbed in a water sample with dimensions: 30 cm, 30 cm, and 24 cm, while 70 % of the produced neutrons are scattered out or diffused out of the sides of the sample. The same curve shows that about 10 % of the neutrons are absorbed if the dimensions are 30, 30, and 12 cm, respectively. It is also seen that less than 1 % of the neutrons are absorbed when the samples are less than 4 cm thick. It is assumed that none of the neutrons that are scattered out or diffused out of the sample are reflected back into the sample.

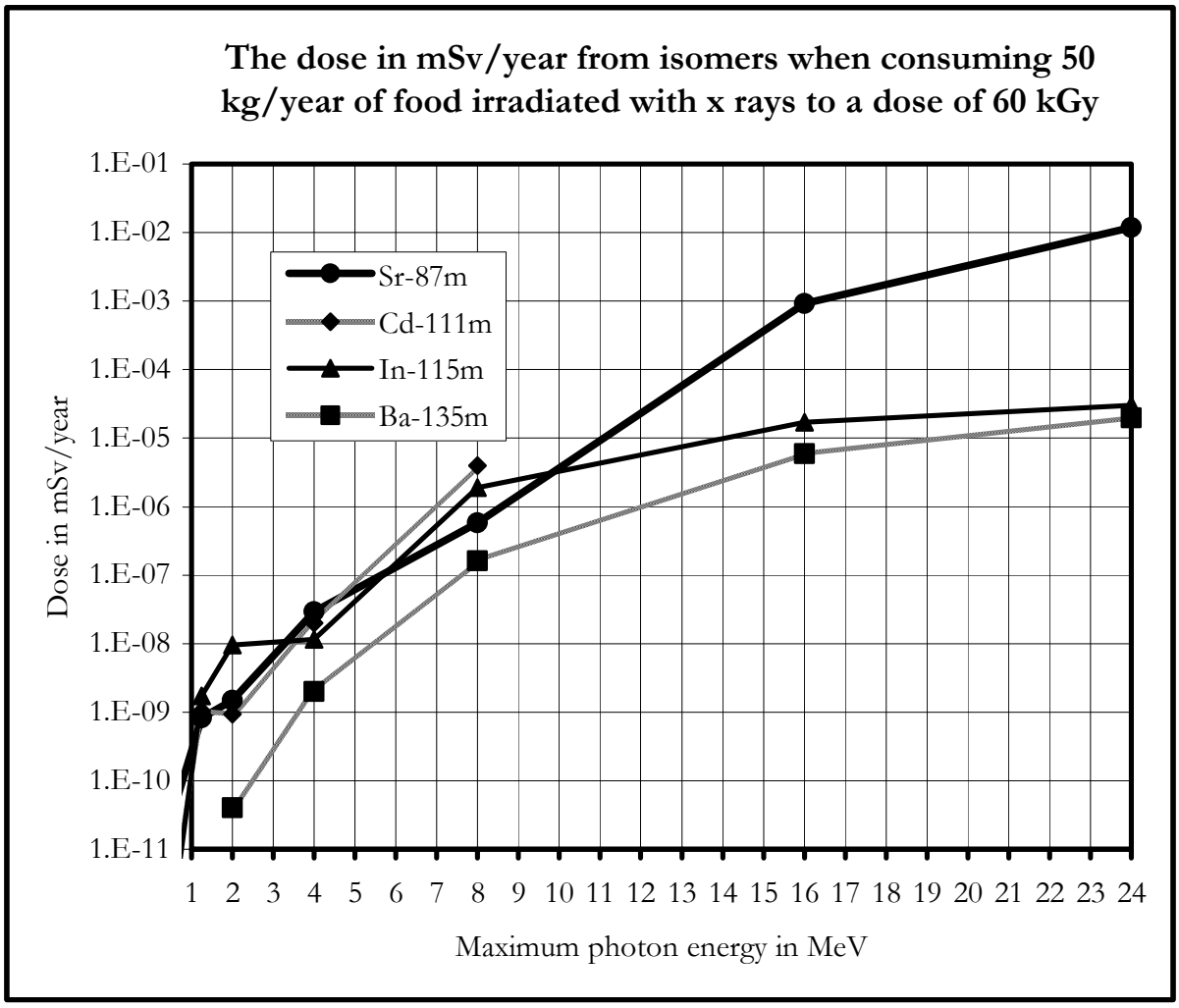

Fig. 5. Dose from isomeric activity as a function of the photon energy. The three curves, ^{87m}Sr, ^{115m}In, and ^{135m}Ba, go to 24 MeV. The curve for ^{111m}Cd goes to 8 MeV. It is assumed that 50 kg of food is consumed per year; and that all the food has been irradiated with 60 kGy of absorbed photon energy (γ-ray photons from Co-60 and Cs-137, or X ray photons produced by 4, 8, 16 and 24 MeV electrons). It is also assumed that the food is consumed immediately following irradiation.

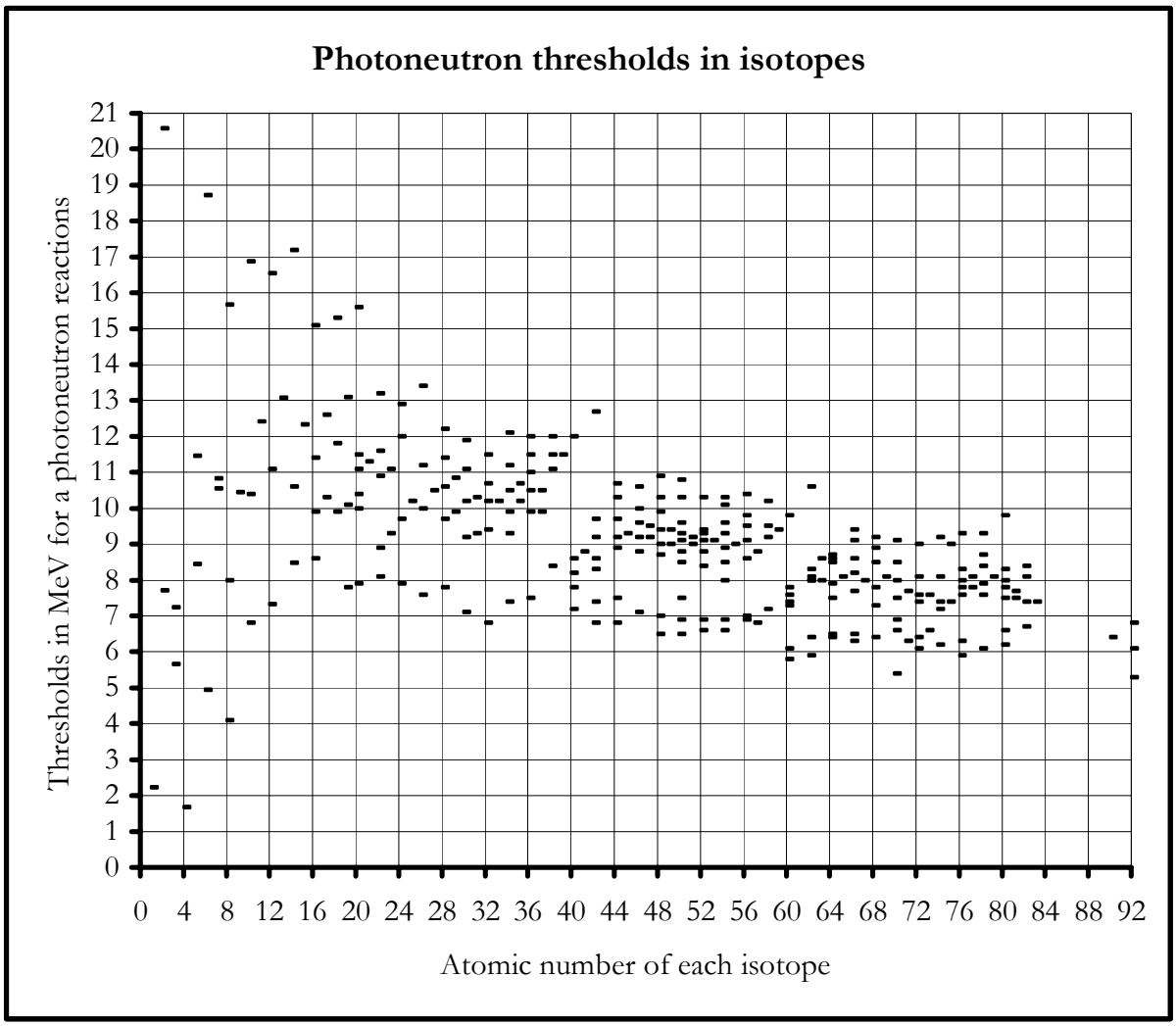

Fig. 6. Thresholds for (γ, n) reactions are shown on the ordinate as a function of the atomic number on the abscissa. It is seen that many isotopes have thresholds below 10 MeV. However, the cross-section is usually small just above the threshold and reaches a maximum usually about 8 MeV above the threshold. Many of the isotope formed are either stable or if excited will have decayed to a stable isotope before exciting the irradiation room. For example, the threshold for deuterium, ^{2}H, is 2.225 MeV is very low, but the hydrogen isotope ^{1}H is stable. The ^{3}He (7.72 MeV), ^{6}Li (5.66), ^{7}Li (7.25), ^{9}Be (1.66), and ^{10}B (8.44) are not found or only in trace amount in food. Even if one of these isotopes was found in the food, the formed isotope would have decayed to a stable isotope long before it left the irradiation room. ^{13}C (4.95 MeV), ^{17}O(4.14 MeV), and ^{18}O (8.14) are found in low concentrations, but they all result in stable isotopes ^{12}C, ^{16}O, and ^{17}O. If an isotope results in radioactivity, the magnitude and biological significance must be estimated. In this way each and every isotope has to be evaluated.

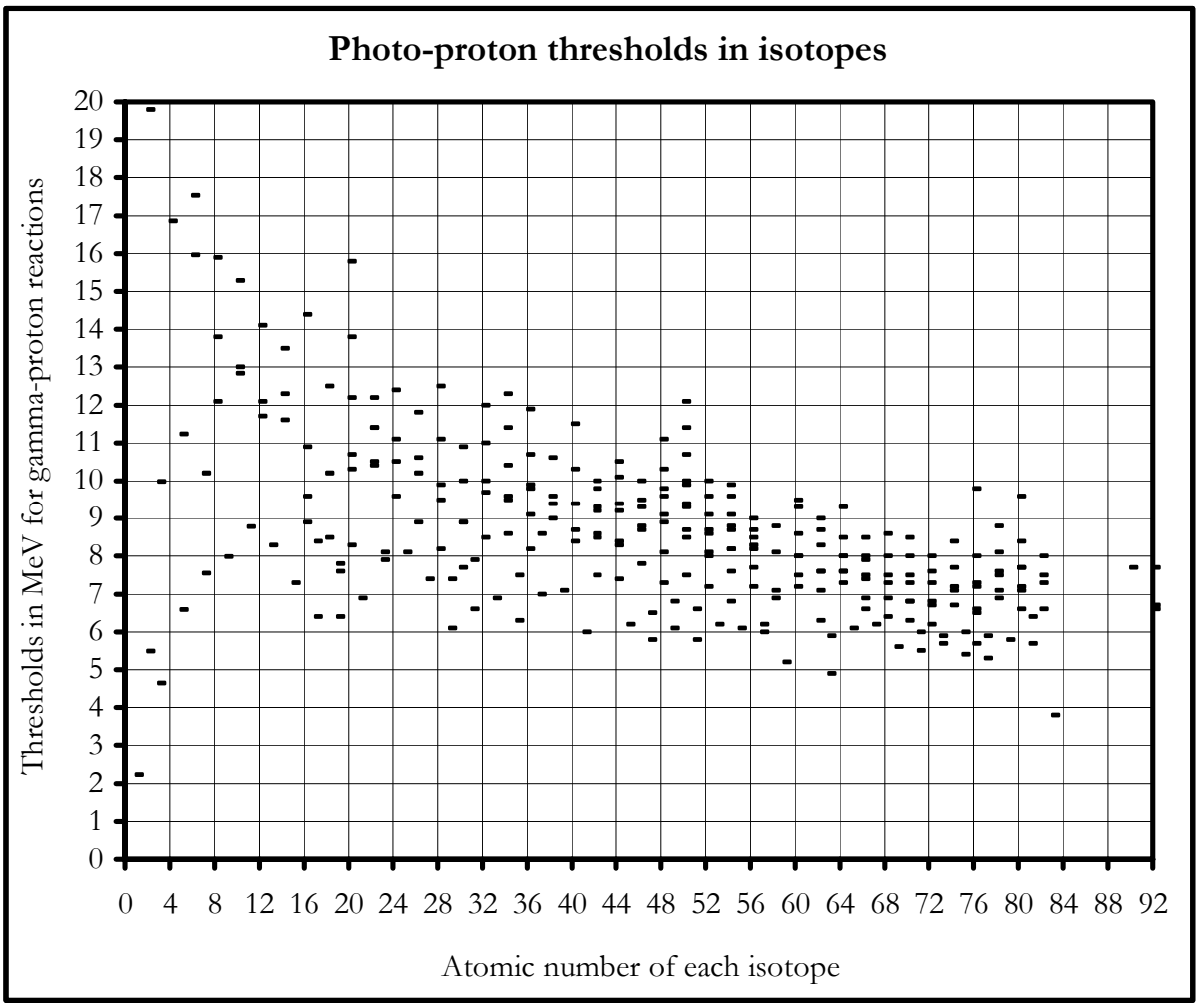

Fig. 7. Thresholds for (γ, p) reactions are shown on the ordinate as a function of the atomic number on the abscissa. It is seen that many isotopes have thresholds below 10 MeV. However, the cross-section are extremely small because the protons have to penetrate the coulomb barrier, which rises above the binding energy as explained in Section 7. The coulomb barrier, given by Eq. (18), is small for the lowest atomic numbers. In these cases the (γ, p) reactions result in stable isotopes as shown in Section 7 and Table 7. For example, the threshold for deuterium, ^{2}H, is 2.225 MeV is very low, but the hydrogen isotope ^{1}H is stable. The ^{3}He (5.49 MeV) results in stable ^{2}H. ^{6}Li (4.59) results in ^{5}He, which disintegrates immediately. ^{7}Li (9.97) results in ^{6}He, which decays in 0.82 seconds. ^{10}B (6.59) results in stable ^{9}Be. ^{14}N (7.55) results in relatively stable ^{14}C. If an isotope results in radioactivity, the magnitude and biological significance must be estimated. In this way each and every isotope has to be evaluated.

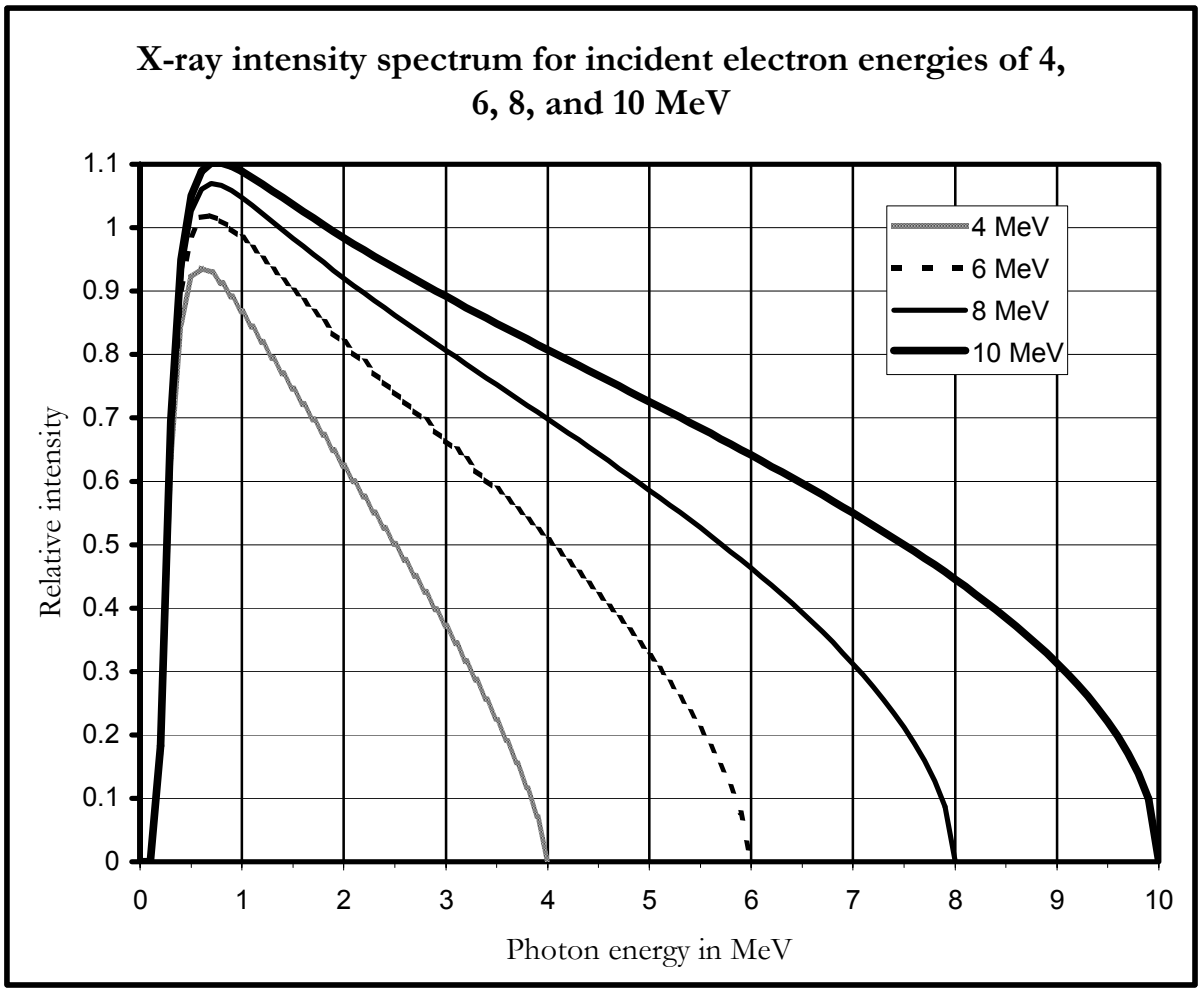

Fig. 8. The four curves give the X ray spectrum produced by 4, 6, 8, and 10 MeV electrons impinging on an X ray target. The spectral intensity is used to calculate the X ray dose as well as the cross-sections for photoneutron production. All neutron yields and activities are reported per unit (kGy) dose; therefore, the values of the absolute intensities do not affect the results. The decreasing intensity at very low photon energies is due to photoelectric absorption of low energy photons in the X ray target made of tungsten.

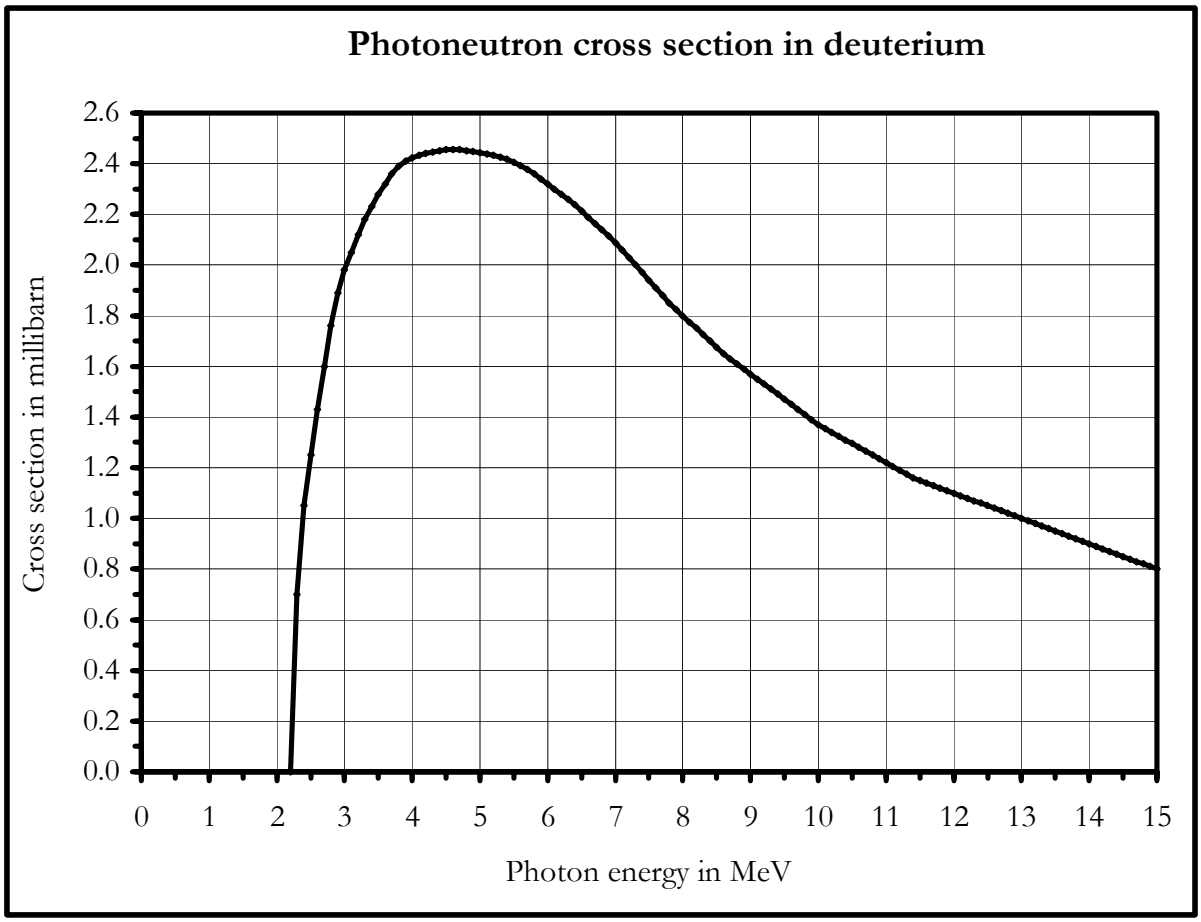

Fig. 9. The cross-section, $\sigma(\gamma, n)$, in millibarn (= 10^{-27} cm^2) in deuterium for production of photoneutrons by x ray photons is shown as a function of the incident photon energy.

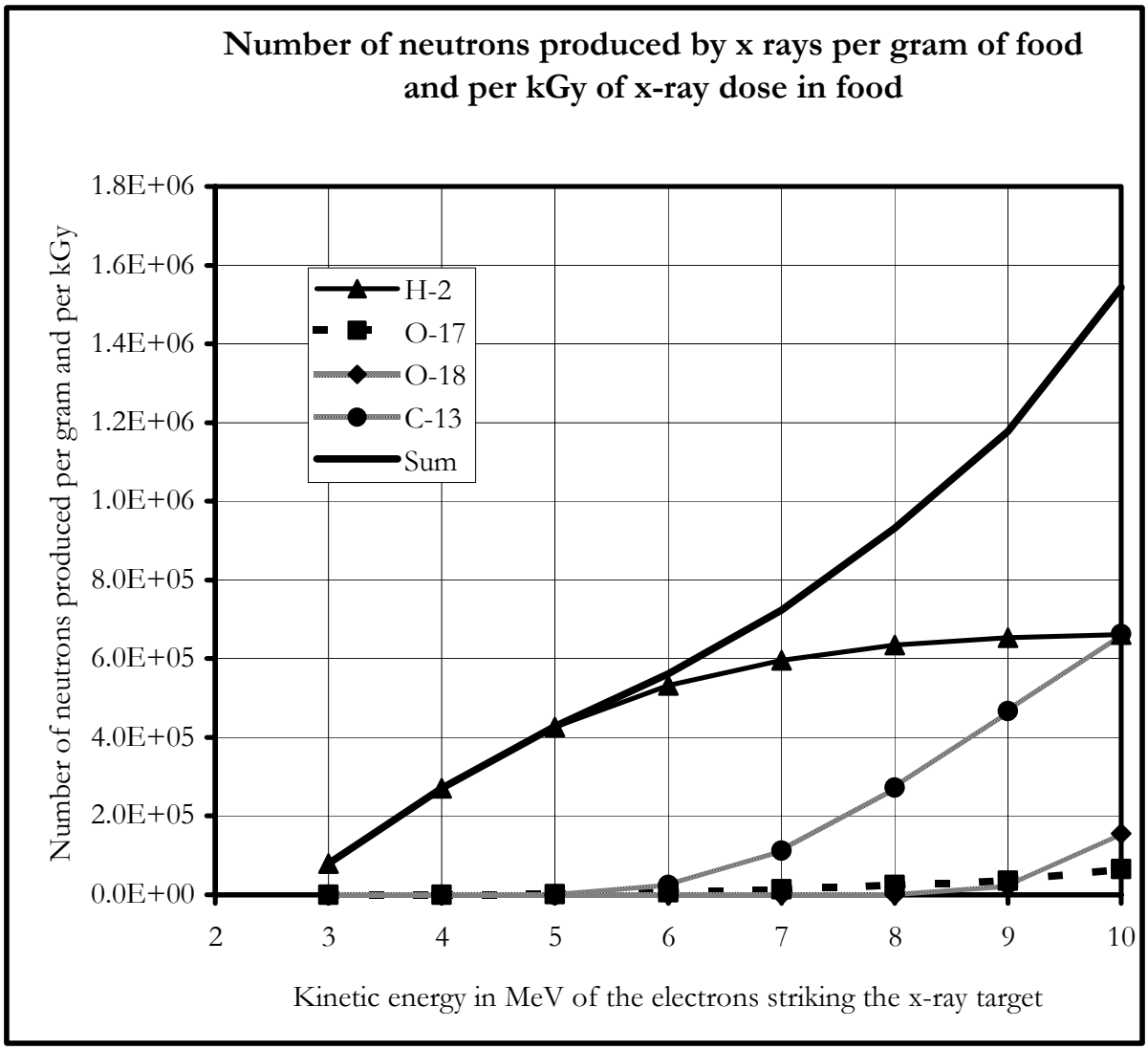

Fig. 10. The number of neutrons produced per gram and per kGy in the reference food irradiated with X rays is shown as a function of the kinetic energy in MeV of the incident electrons striking the X ray target. The energy range is 3 to 10 MeV. The summation (Sum) of neutron from all the isotopes in reference food is $1.54 \cdot 10^6$ at 10 MeV, $8.27 \cdot 10^5$ at 7.5 MeV, and $4.27 \cdot 10^5$ at 5 MeV.

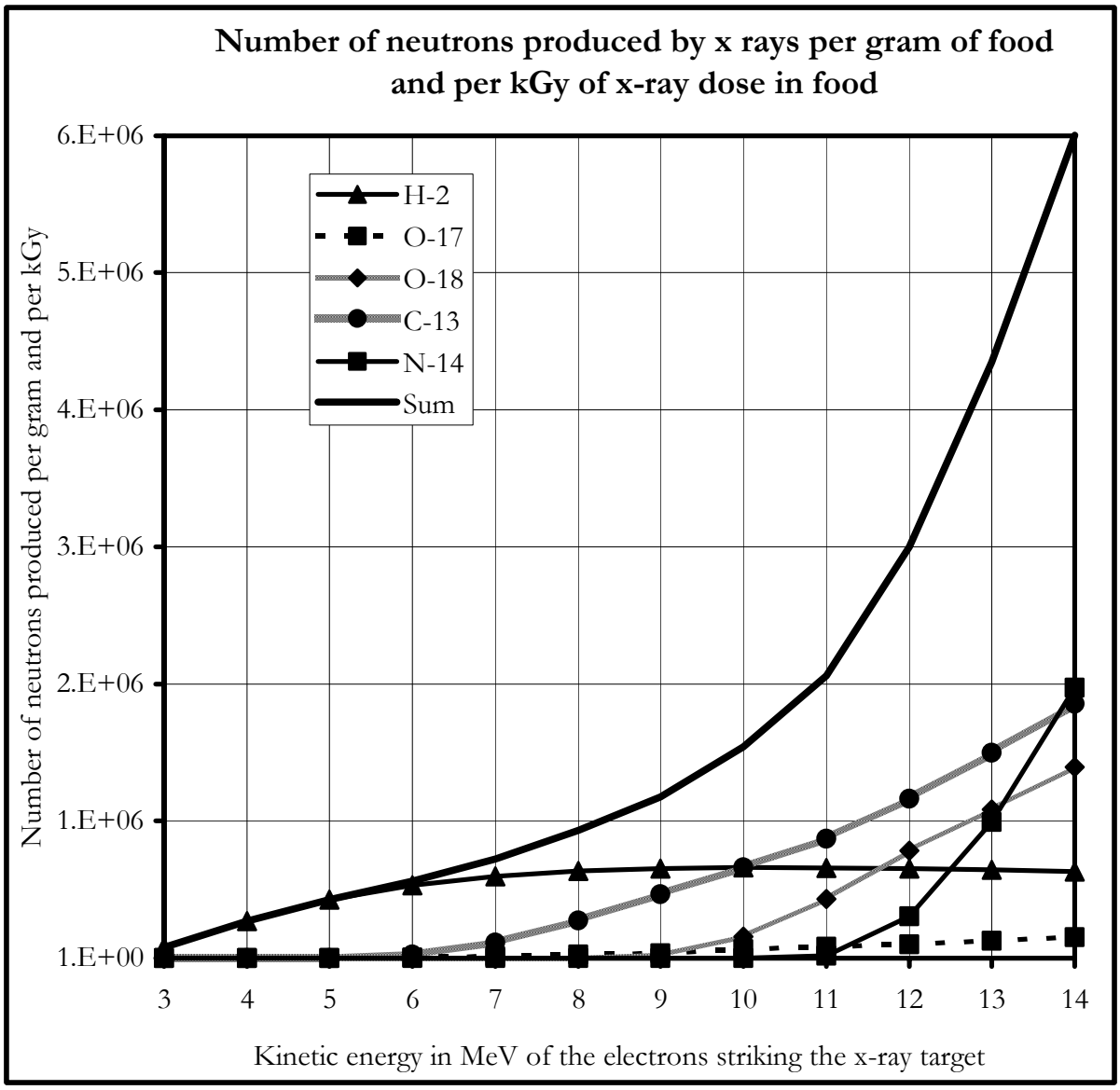

Fig. 11. The number of neutrons produced per gram and per kGy in the reference food irradiated with X rays is shown as a function of the kinetic energy in MeV of the incident electrons striking the X ray target. The energy range is 3 to 14 MeV.

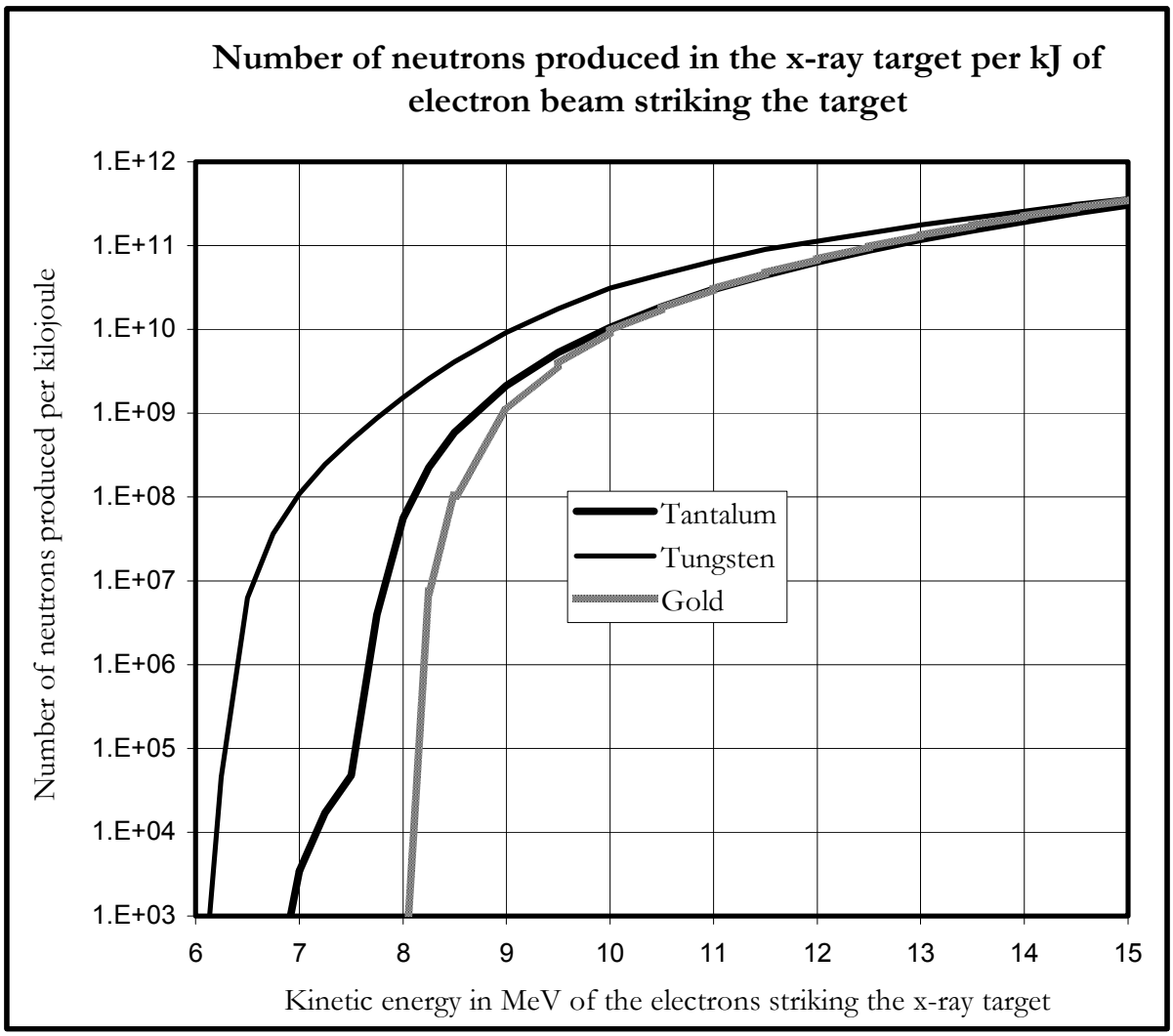

Fig. 12. The number of neutrons produced per kJ of electron beam striking a thick X ray target is shown as a function of the incident electron energy. The three curves from right to left are for X ray targets of gold, tantalum, and tungsten, respectively (see Table 12).

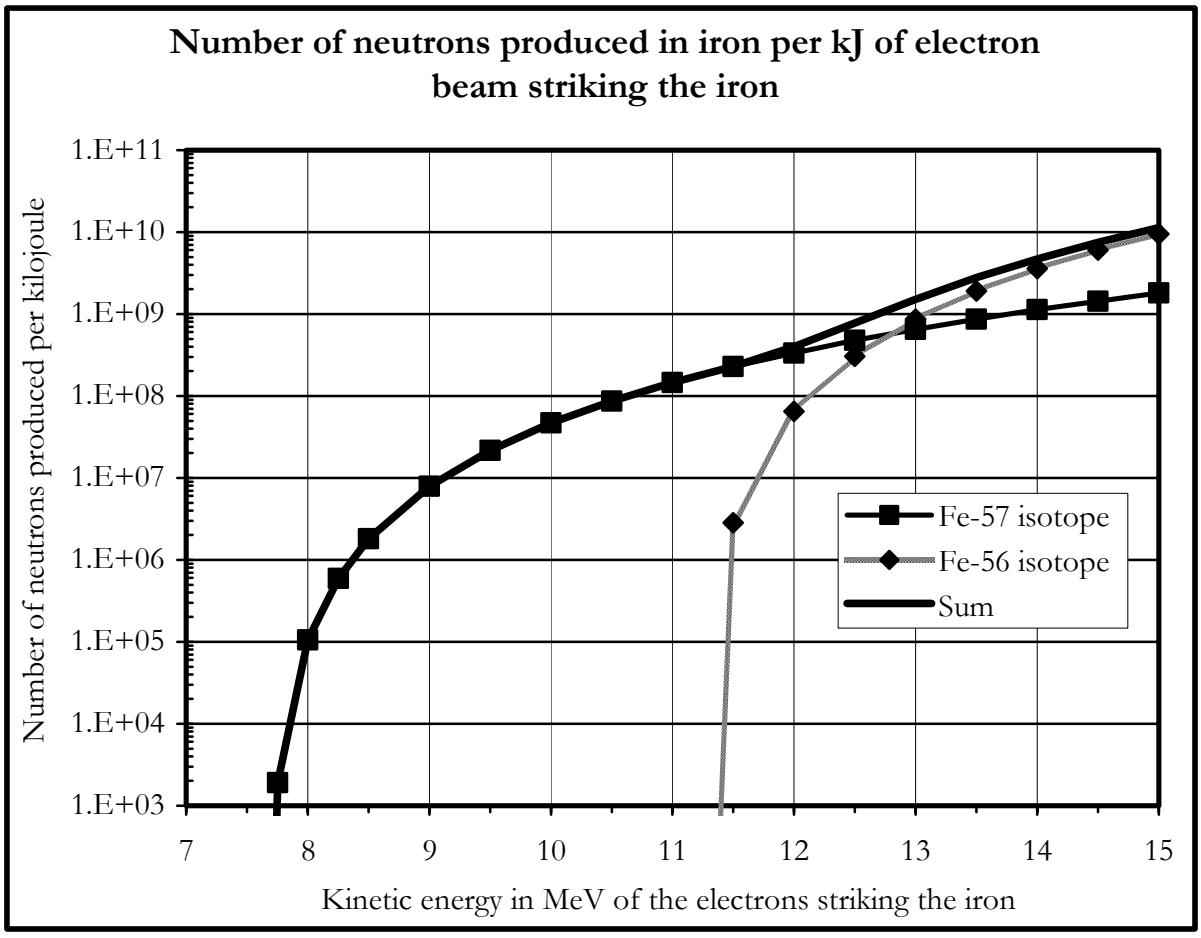

Fig. 13. The number of neutrons produced per kJ of electron beam striking a thick target of iron is shown as a function of the incident electron energy. The two lower curves show the contribution of the two iron isotopes Fe-57 and Fe-56. The top curve shows the summation of these two contributions (see Table 12).

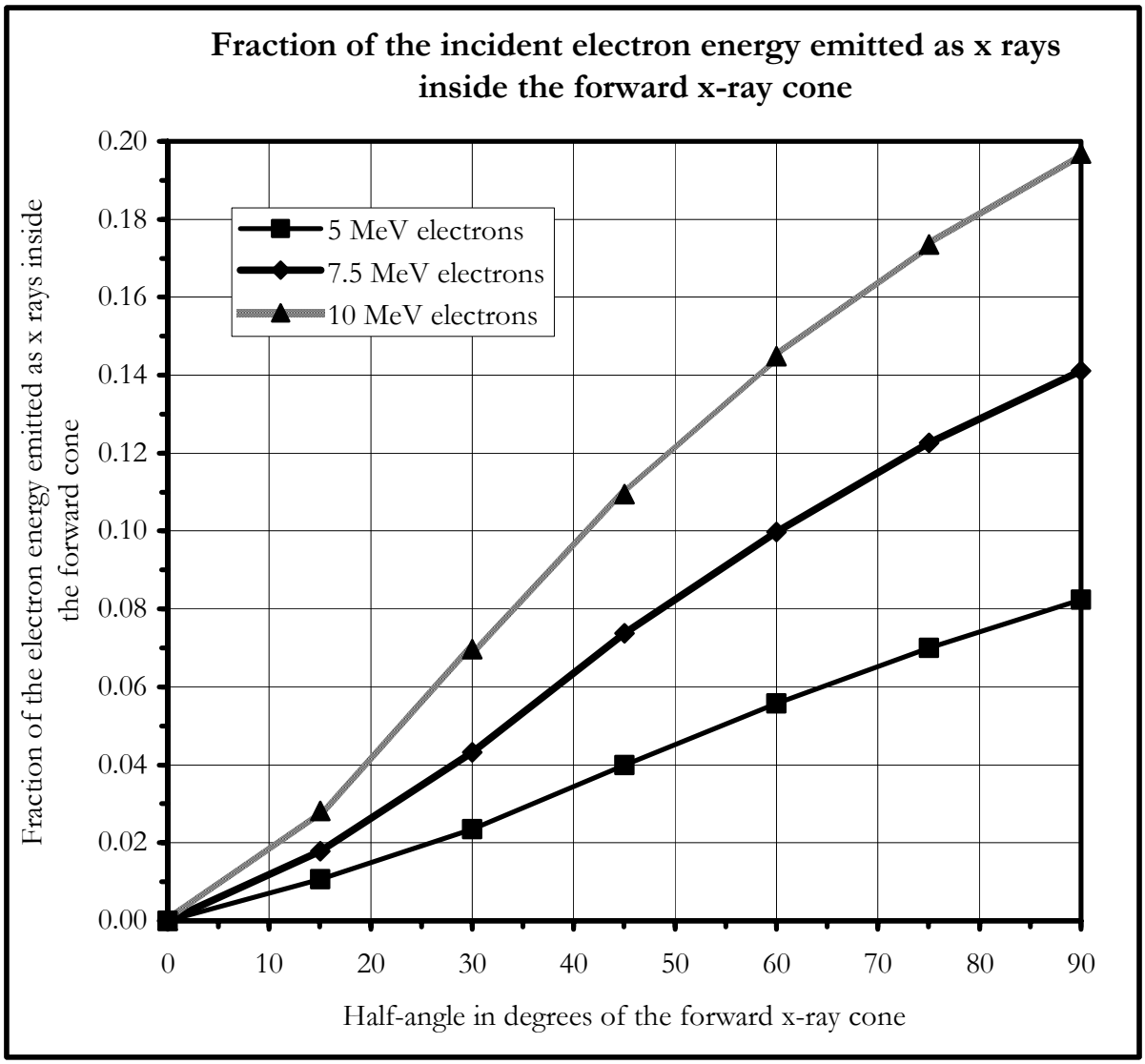

Fig. 14. The ordinate gives the fraction of the incident electron beam energy that is emitted within a forward X ray cone. The half-angle of the cone in degrees is shown on the abscissa for 10, 7.5, and 5 MeV incident electron beam.

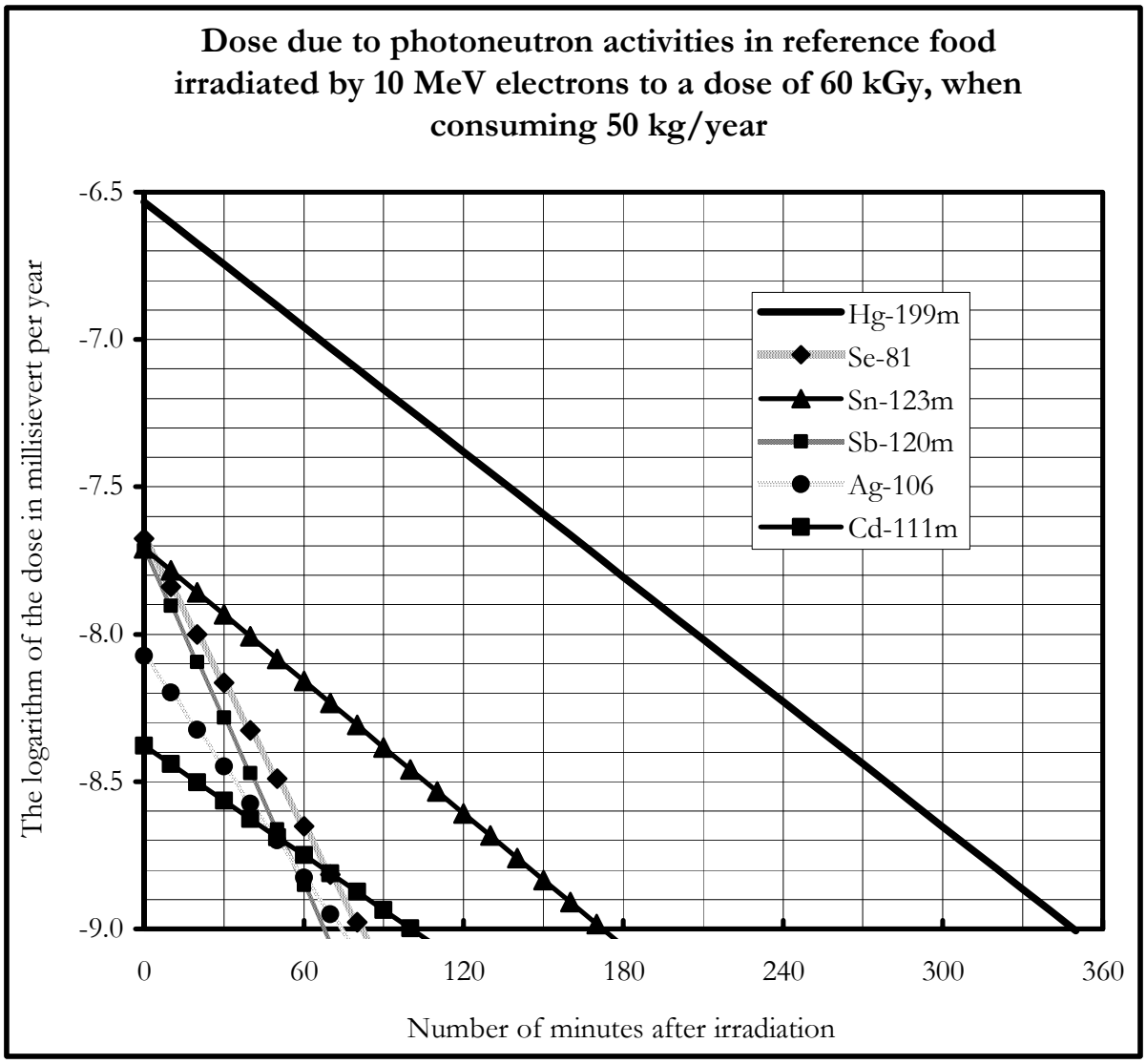

Fig. 15. The dose from short lived (half-life < 1 hour) photoneutron activities. The ordinate gives the dose in millisievert/year humans receive after consuming 50 kg/year of food minutes (shown on the abscissa) after irradiation to a dose of 60 kGy with 10 MeV electrons. It is seen that even if the food is consumed about an hour after irradiation, the isotope 199mHg with highest activity would cause less than 10^{-7} mSv/year. Usually, a sterilized food would be consumed many days after irradiation and the short lived isotopes would have disappeared before the food is consumed. The natural background radiation is about 3 mSv/year.

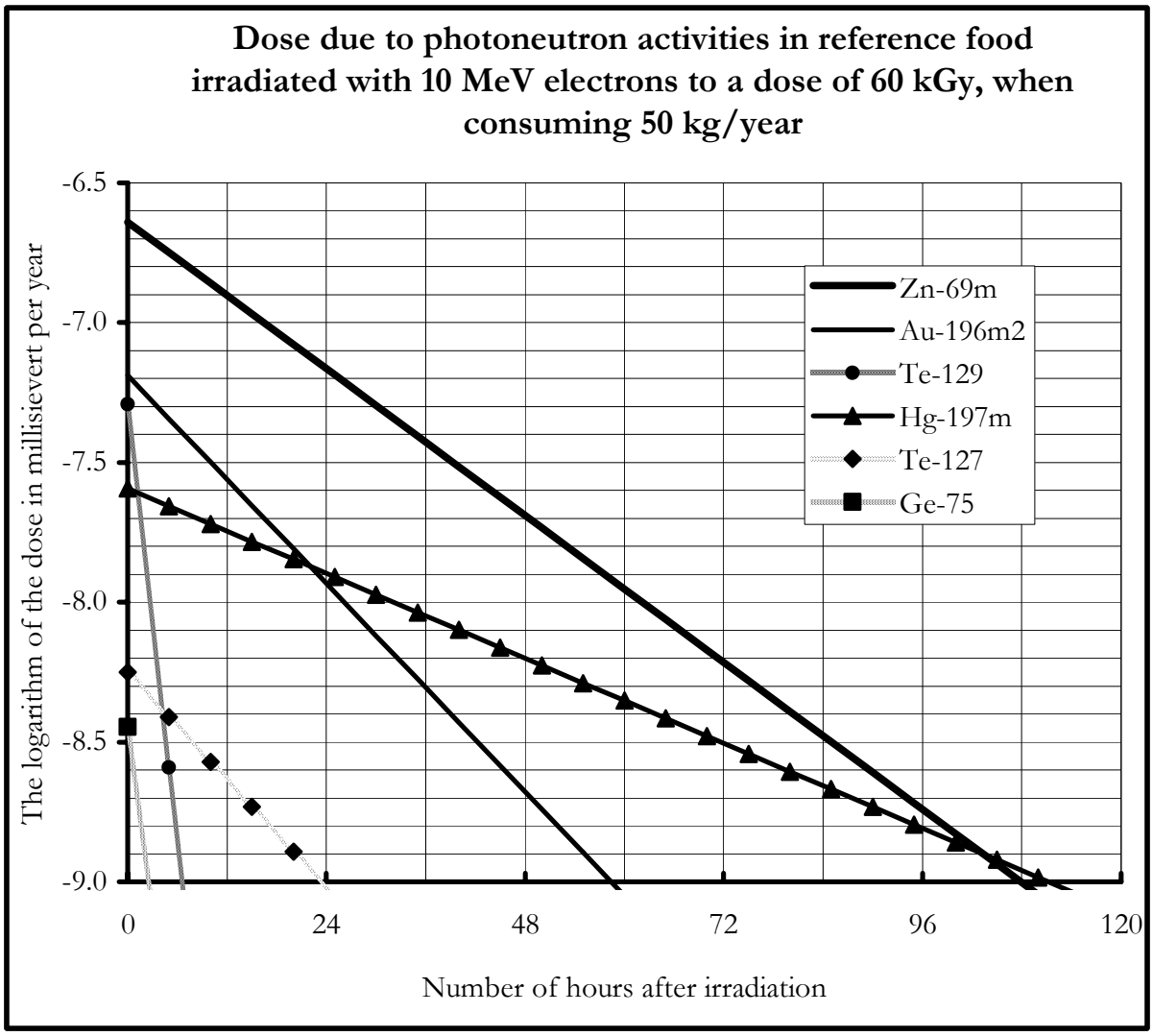

Fig. 16. The dose from relatively short lived (1 hour < half-life < 24 hour) photoneutron activities. The ordinate gives the logarithm of the dose in millisievert/year humans receive after consuming 50 kg/year of food hours (shown on the abscissa) after irradiation to a dose of 60 kGy with 10 MeV electrons. It is seen that even if the food was consumed about 17 hours after irradiation, the isotope ^{69m}Zn with highest activity would cause less than 10^{-7} mSv/year. Usually, a sterilized food would be consumed many days and usually months after irradiation. The relatively short lived isotopes would then have disappeared before the food is consumed. The natural background radiation is about 3 mSv/year.

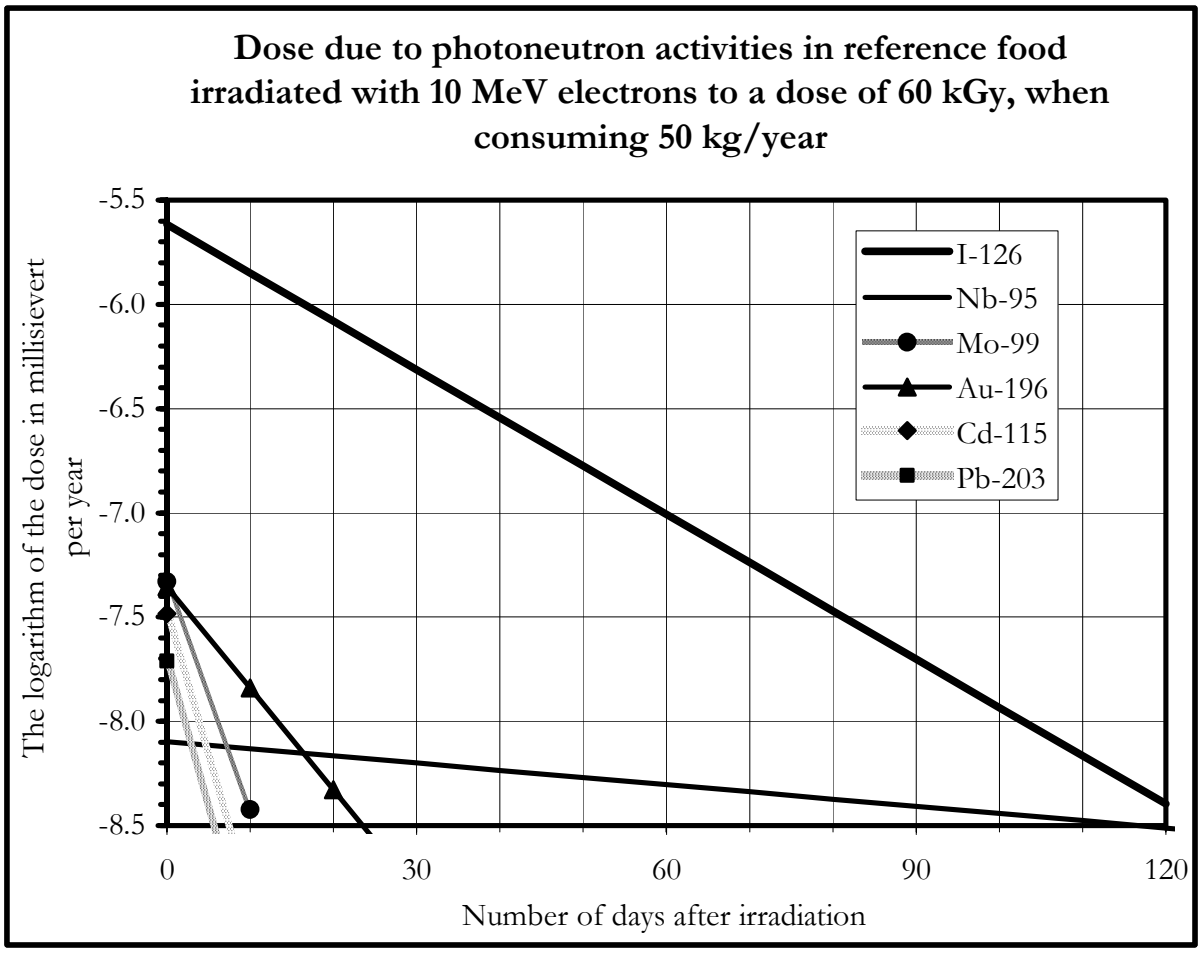

Fig. 17. The dose from relatively long lived (half-life >1 day) photoneutron activities. The ordinate gives the dose in millisievert/year humans receive after consuming 50 kg/year of food days (shown on the abscissa) after irradiation to a dose of 60 kGy with 10 MeV electrons. The principal activity is that of ^{126}I, which decays with a half-life of 13 hours. It is seen that even if the 50 kg of reference food is consumed immediately after irradiation, the dose would be $2.4 \cdot 10^{-6}$ mSv/year, which is about $8 \cdot 10^{-7}$ of the natural background of 3 mSv/year. This is a conservative estimate as the concentration of iodine in the reference food was assumed to be 0.5 ppm, while the measurements in food such as beef (see Table 3) indicate a value of 0.1 ppm. Further, the sterilized food is likely to be consumed many days and usually months after irradiation. At the time of consumption the activity in beef is likely to be, therefore, below 1/10,000,000 of the natural background.

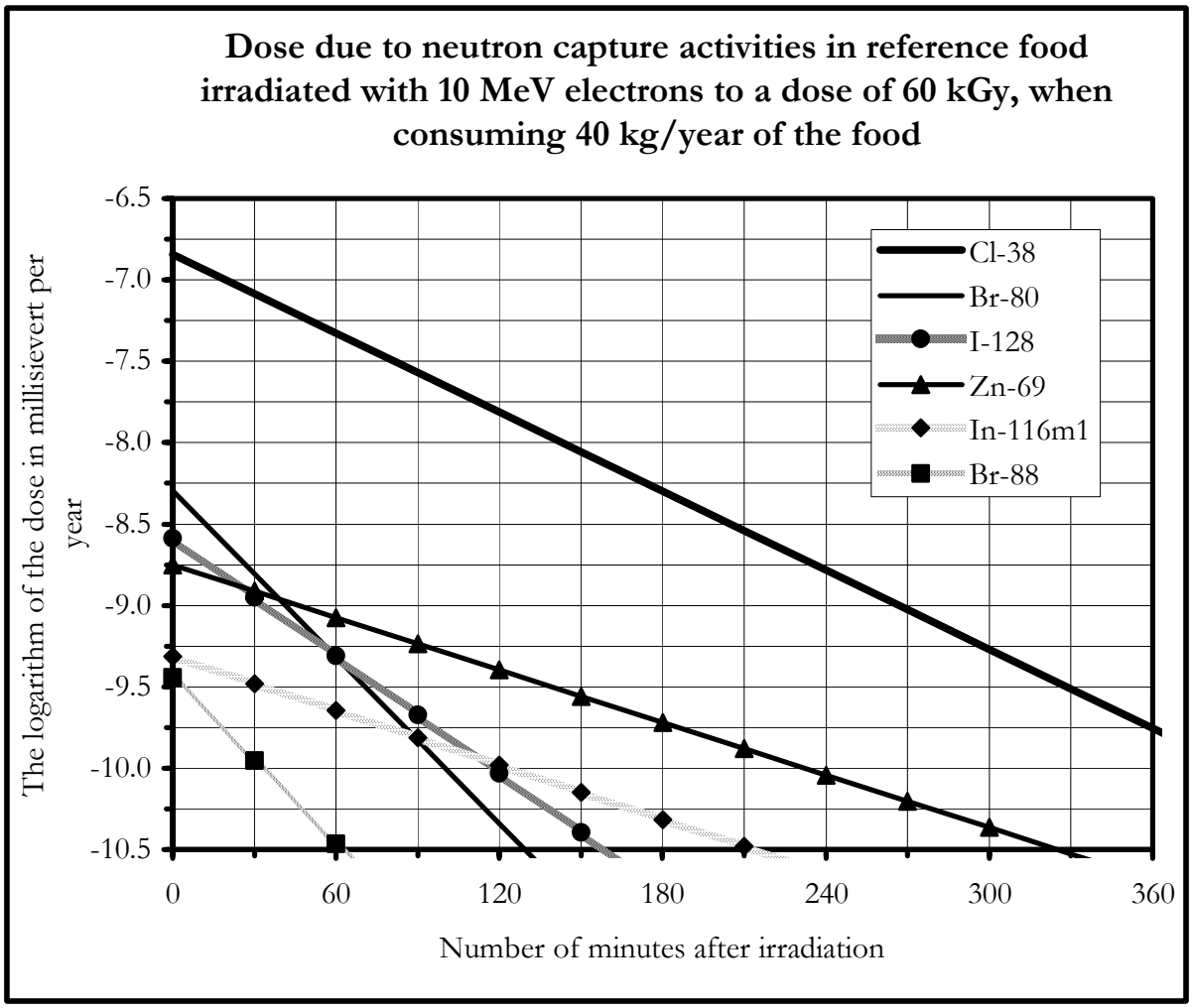

Fig. 18. The ordinate shows the logarithm of the dose from short lived (half-life < 1 hour) neutron capture activities. The units of dose are in millisievert/year humans receive after consuming 40 kg/year of food minutes (shown on the abscissa) after exposure to a neutron fluence of 10^5 neutrons per cm^2. This neutron fluence corresponds approximately to an irradiation by a dose of 60 kGy with 10 MeV electrons. The highest activity, $1.4 \cdot 10^{-7}$ mSv/year, is that of ^{38}Cl isotope with half-life of 37.2 minutes. All activity will have disappeared at the time of expected consumption. The natural background radiation is about 3 mSv/year.

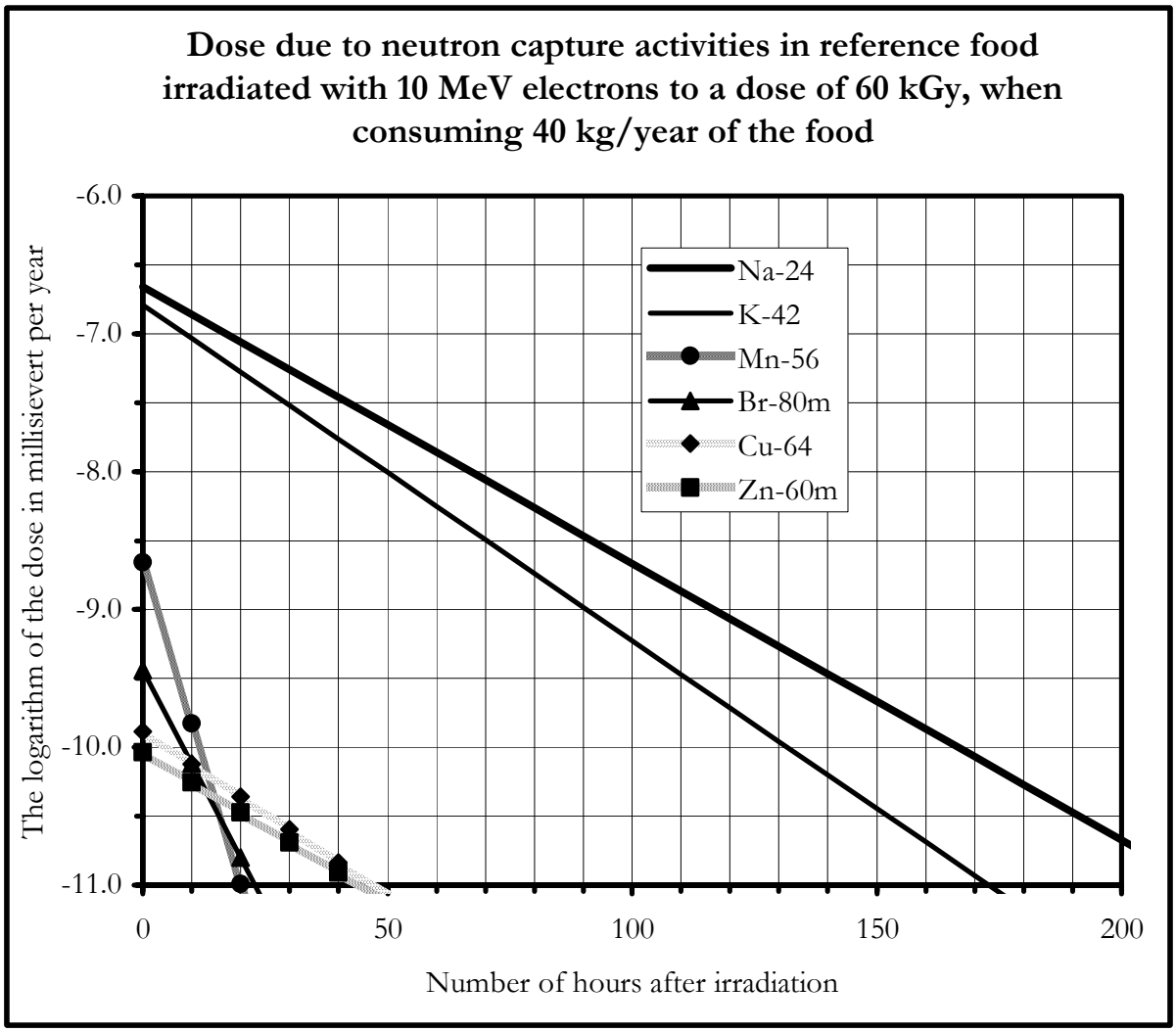

Fig. 19. The ordinate shows the logarithm of dose from relatively short lived (1 hour < half-life < 24 hour) neutron-capture activities. The unit of dose is in millisievert/year humans receive after consuming 40 kg/year of food hours (shown on the abscissa) after exposure to a neutron fluence of 10^5 neutrons per cm^2. This neutron fluence corresponds approximately to an irradiation by a dose of 60 kGy with 10 MeV electrons. The highest activities are $2.3 \cdot 10^{-7}$ mSv/year from ^{24}Na with half-life of 15.0 hours, and $1.6 \cdot 10^{-7}$ mSv/year from ^{42}K with half-life of 13.4 hours. These activities are insignificant immediately after irradiation and even less at the time of consumption. The natural background radiation is about 3 mSv/year.

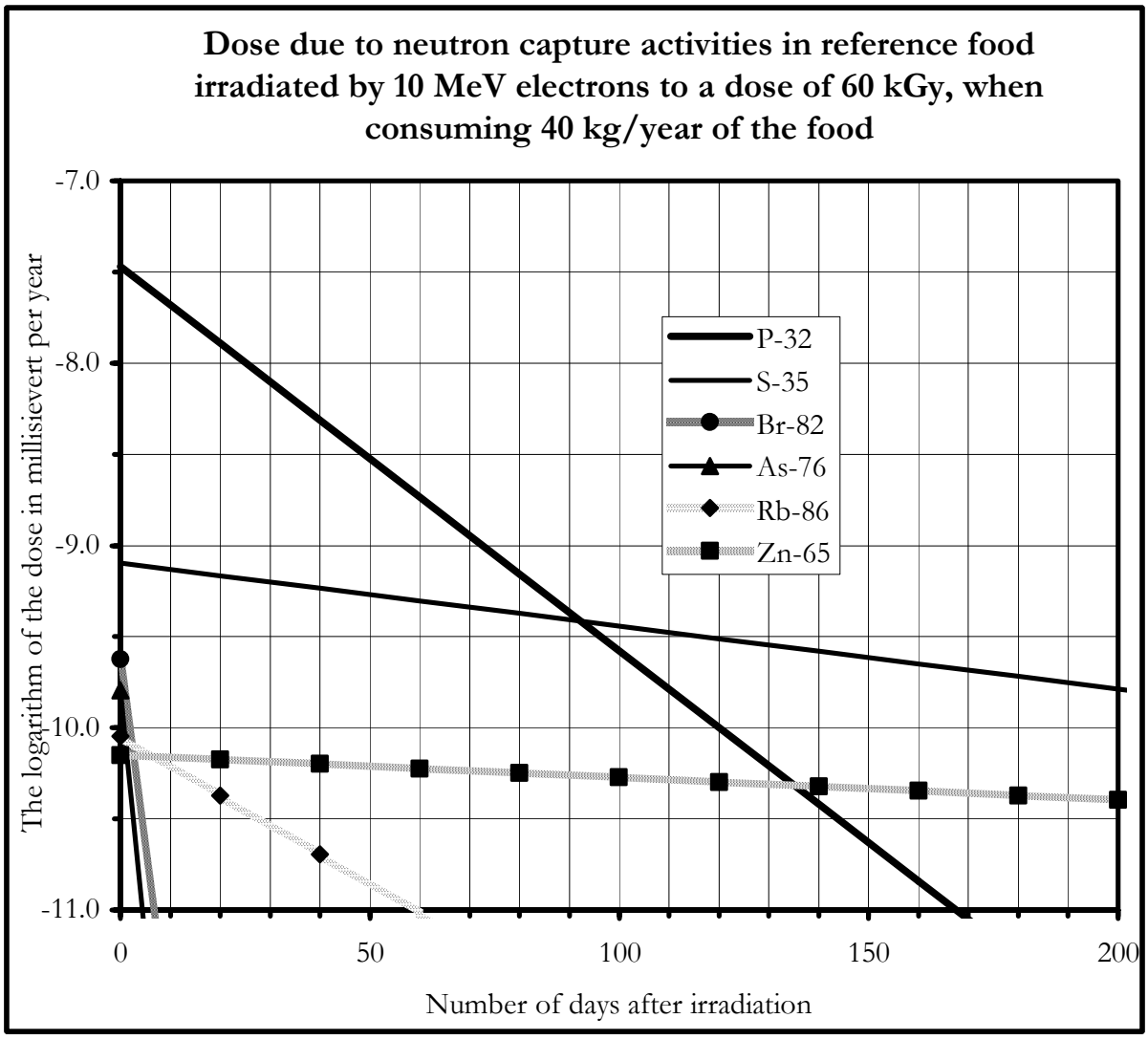

Fig. 20. The dose from relatively long-lived (half-life >1 day) neutron-capture activities. The ordinate gives the dose in millisievert/year humans receive after consuming 40 kg/year of food days (shown on the abscissa) after exposure to a neutron fluence of 10^5 neutrons per cm^2. This neutron fluence corresponds approximately to irradiation by a dose of 60 kGy with 10 MeV electrons. The principal activity is that of ^{32}P, which decays with a half-life of 14.28 days. The activities are insignificant immediately after irradiation and even less at the time of consumption. The natural background radiation is about 3 mSv/year.

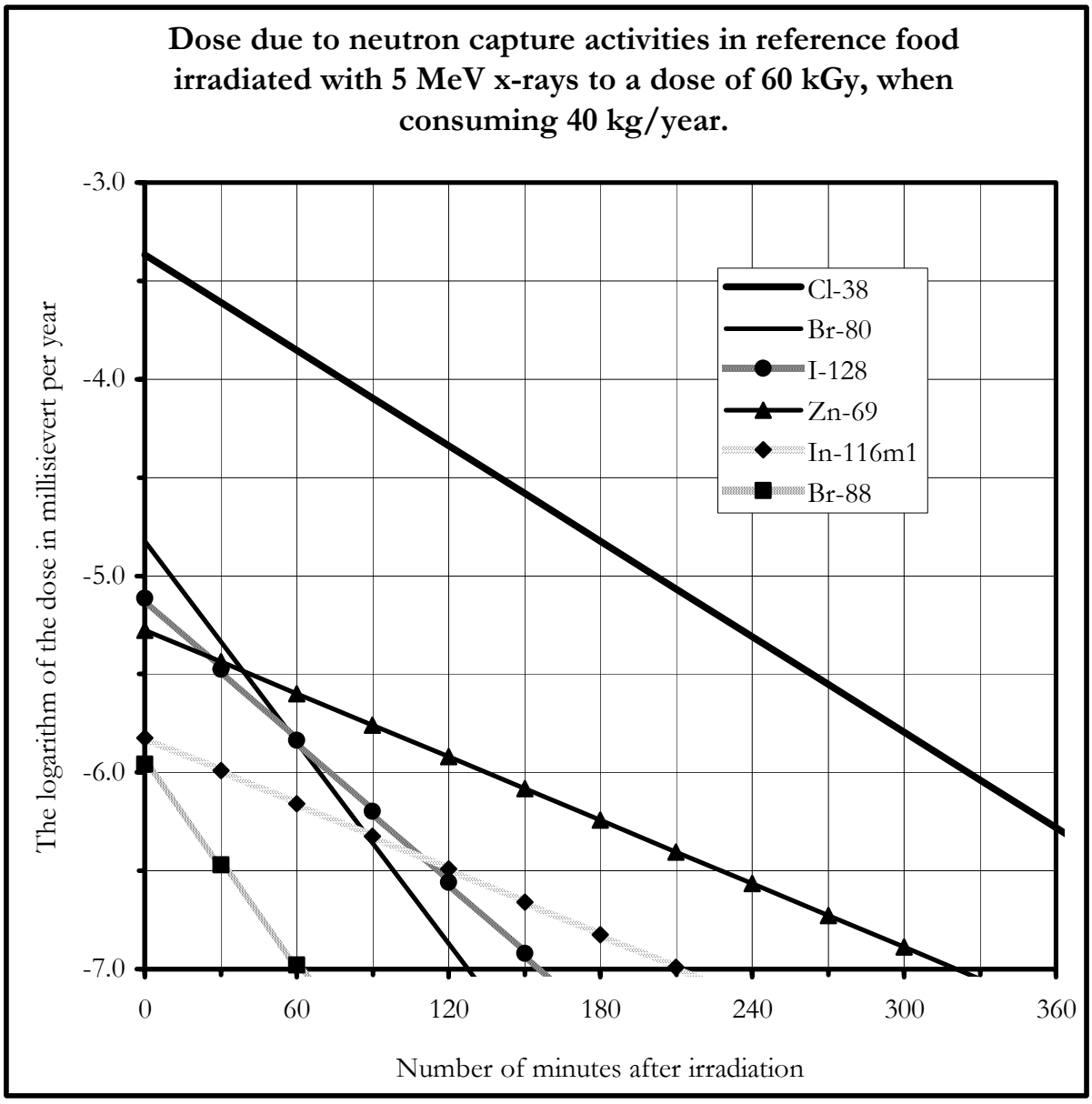

Fig. 21. The ordinate shows the logarithm of the dose from short lived (half-life < 1 hour) neutron-capture activities. The dose is in units of millisievert/year humans receive after consuming 40 kg/year of food minutes (shown on the abscissa) after irradiation with a fluence of $3 \cdot 10^{8}$ neutrons per cm^2. This neutron fluence corresponds approximately to irradiation to a dose of 60 kGy with 5 MeV x rays, or to a dose of 30 kGy with 7.5 MeV X rays. The highest activity, $4.3 \cdot 10^{-4}$ mSv/year, is that of ^{38}Cl with a half-life is 37.2 minutes. All the short lived activities will have practically disappeared at the time of consumption. The natural background radiation is about 3 mSv/year.

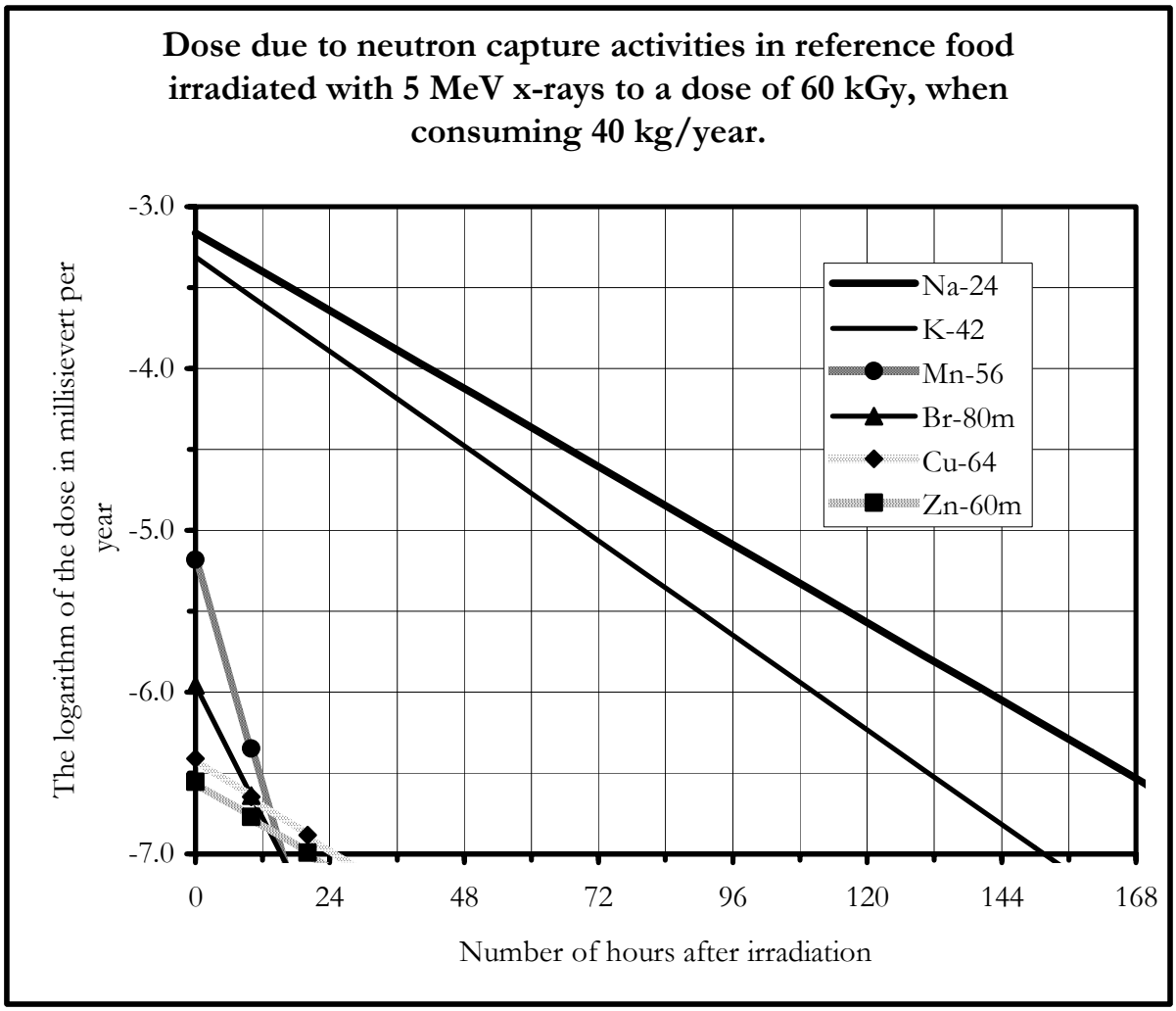

Fig. 22. The ordinate shows the logarithm of dose from short lived (1 hour < half-life < 24 hour) neutron-capture activities. The dose is in units of millisievert/year humans receive after consuming 40 kg/year of food hours (shown on the abscissa) after exposure to a neutron fluence of $3 \cdot 10^8$ neutrons per cm^2. This neutron fluence corresponds approximately to irradiation by a dose of 60 kGy with 5 MeV x rays, or to a dose of 30 kGy with 7.5 MeV X rays. The highest activities are: $6.9 \cdot 10^{-4}$ mSv/year from ^{24}Na, and $4.9 \cdot 10^{-4}$ mSv/year from ^{42}K with half-lives of 15.0 and 13.4 hours, respectively. The sum of the activities is $1.18 \cdot 10^{-3}$ mSv/year, if the food is consumed immediately after irradiation. If the sterilized food is consumed 28 hours after irradiation, the dose will be 1/10,000 of the natural background, which is about 3 mSv/year. If the sterilized food is consumed 126 hours after irradiation, the dose will be about 1/1,000,000 of the natural background.

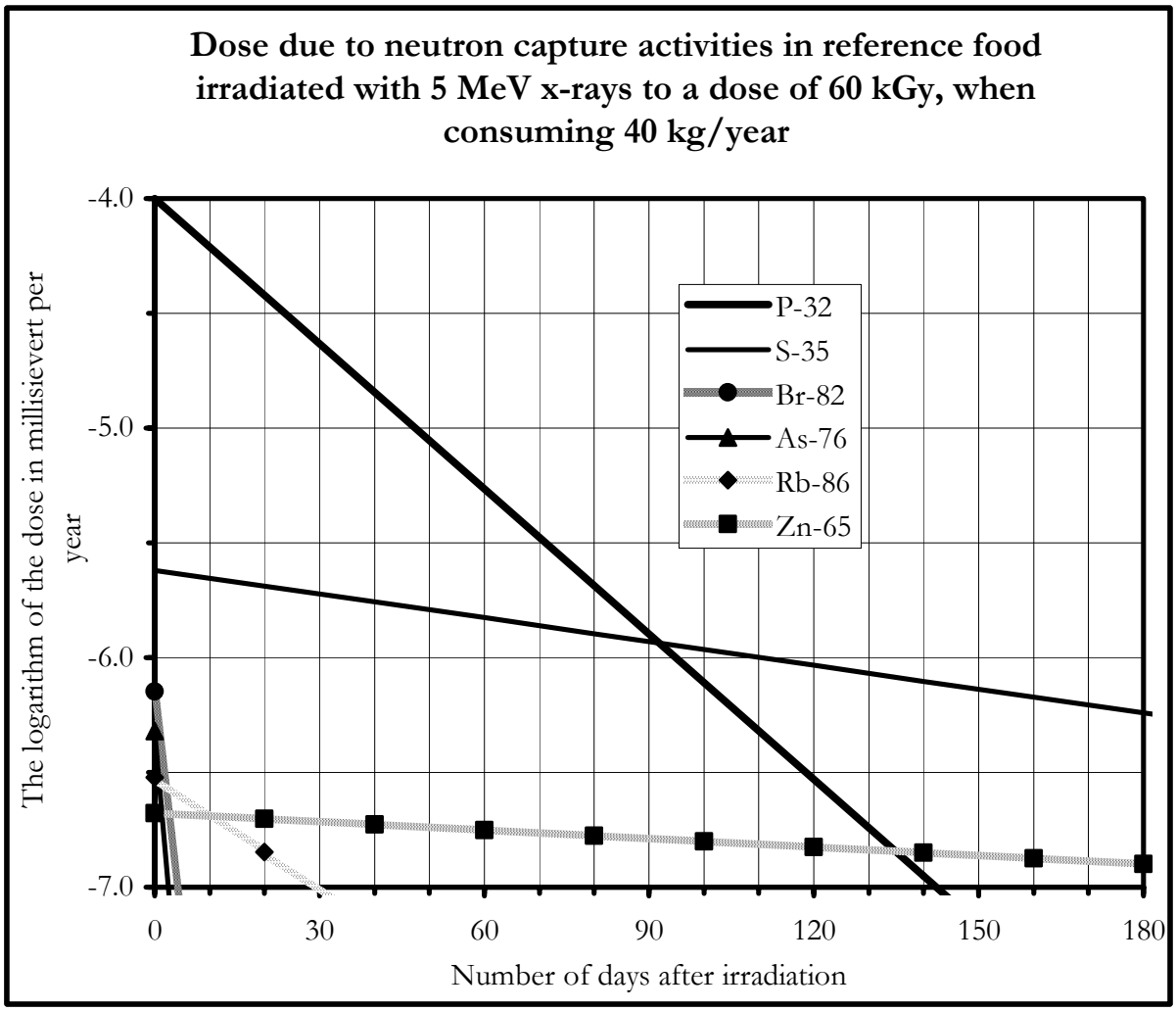

Fig. 23. The ordinate shows the logarithm of the dose from relatively long-lived (half-life >1 day) neutron capture activities. The unit of the dose is in millisievert/year humans receive after consuming 40 kg/year of food in days (shown on the abscissa) after exposure to a neutron fluence of $3 \cdot 10^8$ neutrons per cm^2. This neutron fluence corresponds approximately to irradiation by a dose of 60 kGy with 5 MeV x rays, or to a dose of 30 kGy with 7.5 MeV X rays. The principal activity is that of ^{32}P, which decays with a half-life of 14.28 days. The activity immediately after irradiation is 10^{-4} mSv/year or 1/30,000 of the natural background, which is about 3 mSv/year. This is a rather slowly decaying isotope.

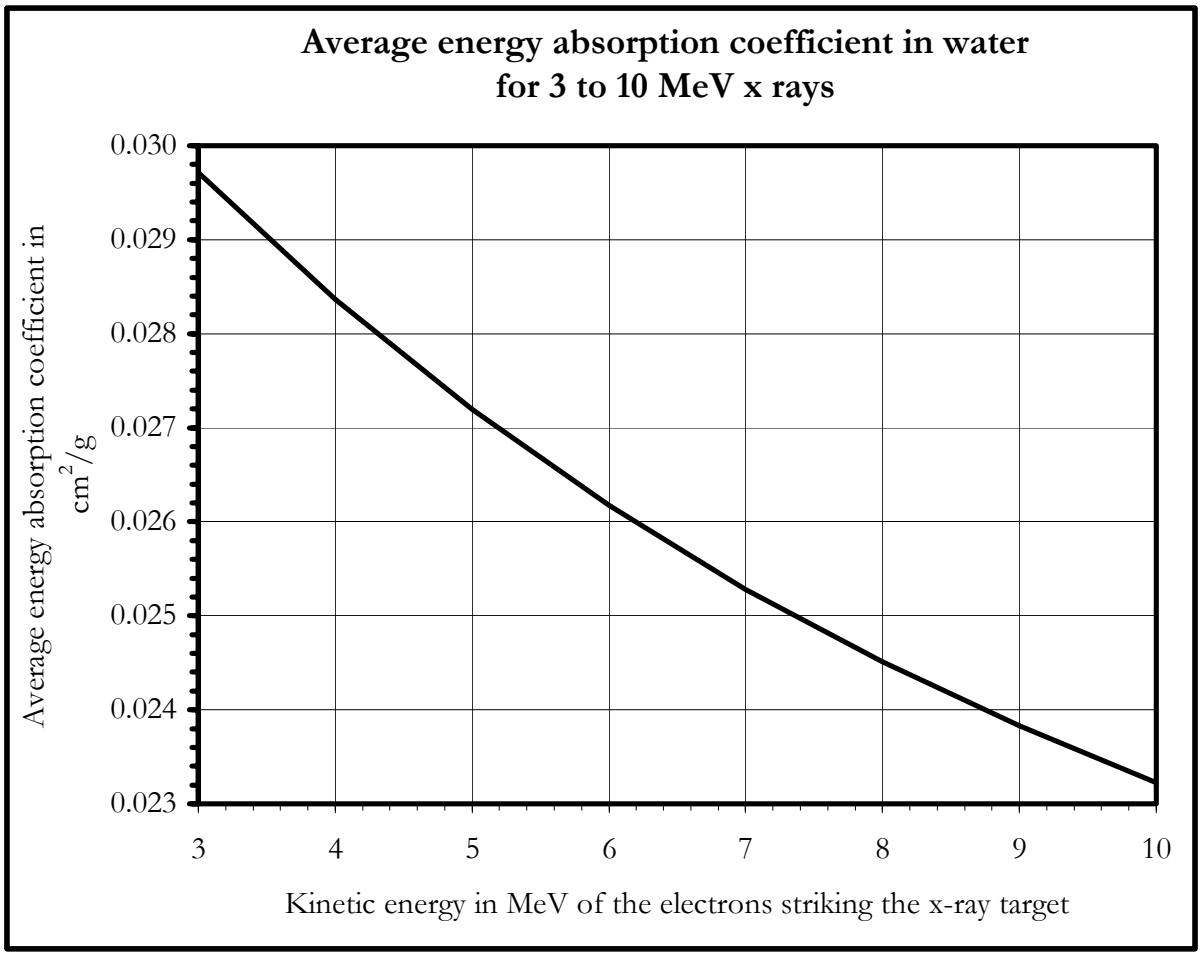

Fig. 24. The ordinate gives the average energy absorption coefficient in cm^2 /g in food irradiated with X rays from an X ray target, such as tantalum. It is seen that for 10 MeV X rays, the absorptions coefficient is about 0.0232 cm^2/g.

HISTORICAL BACKGROUND

The hope of many was that the awesome power of the atomic energy could be diverted to peaceful uses. Responding to this hope President Eisenhower announced on December 8, 1953 at the United Nations the "Atoms for Peace Program" and proposed international cooperation. This subsequently led to the first International Conference on the Peaceful Uses of Atomic Energy in Geneva, Switzerland, August 8–20, 1955, and establishment of the International Atomic Energy Agency (IAEA). In those days food borne diseases, malnutrition, and famines in the world were much more rampant than today, although the number of people was only half of that today. Increasing the harvest and preserving the food were some of the most promising peaceful uses suggested at the Conference.

Besides the United States, many countries, and international organizations became engaged in promoting research for the benefit of agriculture, food production, food preservation, and medical sterilization, and of course energy production. Many thought of using radioactive sources, such as cesium-137, used fuel elements from the nuclear reactors, as well as cobalt-60 for preserving the food. Others thought that accelerators, which are independent of the nuclear technology, would be better suited for many industrial applications.

W. Huber and A. Brasch of Electronized Chemicals Corporation using a Capacitron did early experiments using electrons directly from accelerators. (See: Electronics, 1945, **21**, 74; Science, 1947, **105**, 112; Science, 1948, **108**, 536; Proc. Rudolph Virchow med. Soc. N.Y., 1949, **8**, 3; Huber: Naturwissenschaften, 1951, **38**, 21; Food Technology, 1953, **7**, 109.) Huber and Brasch pointed out many of the advantages in using electron accelerators, and were the first to point out the advantage of irradiating the meats in frozen state. They correctly named "irradiated food" "electronized food"; and "to irradiate food" "to electronize food", because the electrons are the ones that produce all the effects, even in case of irradiation with gamma rays. Nickerson, Goldblith and Proctor at MIT named the process "electronic food sterilization". The MIT Food irradiation researchers used van de Graaff electron accelerator, X rays, and γ rays intermittently. John G. Trump helped MIT researchers with electron irradiation. He carried out the best electron scattering and depth dose distributions experiments for energies below 3 MeV. Bellamy at General Electric and others also did fine experiments. All these researchers used low energy accelerators. At the beginning of 1957 the low energy accelerators included: van de Graaff accelerators (High Voltage Engineering) up to 3 MeV and 3 kW; Resonant Transformers (General Electric) up to 4 MeV and 4 kW; Capacitron (Electronized Chemical Co.) up to 2 MeV and 3 kW. For these low energy accelerator the induced activity was not in question.

The first microwave driven linear accelerator built at Stanford University in Palo Alto in 1946–7 was used mainly for medical treatment and research. (W. W. Hansen wanted to design a medical accelerator when he invented the microwave generator in 1938, which led to the development of radar technology during the World War II. After the war Hansen's dream about building an accelerator for medical purpose was realized at Standford.) The Hammersmith linear accelerator in London was built and installed by Meropolitan Vickers Company in 1953. It was also used mainly for medical research.

Many practical applications in food irradiation required high-energy accelerators. The plans for an Irradiation Center at Stockton, California, included a 24 MeV (32 maximum) linear accelerator with 18 kW beam power. The contract to build the accelerator was awarded in March 29, 1957. Researchers responsible for the Army's Program, including the outstanding scientist and administrator Dr. Ralph G. H. Siu and his advisors recommended the accelerator. This high energy was based on the desire to irradiate food in No. 10 cans, which are 6 inches in diameter. Craig Nunan at Varian Associates, in Palo Alto was educated at Stanford and specialized in linear accelerators. He was in charge of the team building the 24 MeV accelerator.

The detrimental health effects of radiation on living organisms were well recognized. The possible problem of induced activity in irradiated food was not of concern as the energy of available gamma rays, X rays, and electrons was too low to induce activity, and use of neutron irradiation was not contemplated. However, it was not known if induced activity would be a problem at higher energies. The U. S. Department of Army which coordinated most of U. S. efforts in food irradiation initiated research into the induced activity problem already in early 1955.

At the Atomic Research Establishment Risø in Denmark, we drew in 1957 a broad plan for future radiation research and recommended a 10 MeV linear accelerator with about 5 kW beam power for food and medical research as well as pulsed radiation chemistry. The accelerator was to be horizontal with the electron beam bent 90^0 downwards and scanned in a plane perpendicular to the accelerator. This design permitted us to monitor **continuously** the electron energy, the scanner width, and the beam current. The plan, submitted to Danish AEC on December 1, 1957, was well received and forwarded immediately through channels to the Danish Rigsdag (Parliament), which approved and appropriated the funds already in April 1958. The contract for building the accelerator was awarded to Varian Associates in September 1958. Rough calculations had indicated to us that 10 MeV was a reasonable limit for no induced activity. At the time, we did not know the exact plans in USA, which included a 24 MeV linear accelerator.

The 10 MeV linear accelerator from Varian was installed at Risø and accepted in May 1960. The overall design was good, although there were a few minor problems. The Varian design of the electronics of the scanner system did not work well, and we replaced it with our own design at Risø, which included exact triangular waveform of the magnetic field in the scanner. The corresponding triangular current in the scanner magnet creates a rectangular voltage wave in an induction coil in the scanner magnet.

This rectangular wave can be compared with a good rectangular wave from an electronic generator, and the difference adjusted to zero by a good operation amplifier feedback system to assure triangular current in the scanner magnet. The height of the rectangular wave from the electronic generator is varied to give the right scanner width. This system was reliable and gave a uniform surface dose over the scanner width within measurement accuracy of 1%. This good dose uniformity was important for research and practical applications.

The current from the secondary monitor of the beam current was fed over a resistor, which was used as a potentiometer. This voltage was compared to the voltage from a tachometer generator measuring the speed of the conveyor. The difference voltage was then amplified to control the speed of the conveyor. This feedback system controlled the conveyor speed within about 0.25%. Thus, we made the beam current control the conveyor speed and thereby the dose within 1%. The dose is controlled simply by the potentiometer settings.

We could then keep the energy constant by varying slightly the beam current, which then automatically controls the conveyor speed. Thus the energy, scanner width and the dose is kept constant at the prescribed value. These changes in the scanner and the dose control were made in June to July 1960. All these parameters were monitored and recorded continuously.

Similar control over energy, scanner system, and dose was introduced at Natick, during my training of the staff there in September 1962 to August 1963. The system was described at an International Conference on Radiation Research at US Army Natick Laboratories Natick, MA January 14–16, 1963, which was sponsored by National Academy of Sciences- National Research Council and published by U. S. Department of Commerce, Office of Technical Services, 1963. A description of the system has also been published in a Risø Report No. 53 issued in April 1963. My coworkers have also described it several variants of it in subsequent publications.

Both at Risø and Natick, the energy could be monitored continuously, because of the 90 degrees bending of the beam. Two plates collecting the secondary electrons from the scanner

window inside the scanner registered the position of the beam. This then was used to monitor the energy. The energy was calibrated by the activation of copper, which emits positrons. The thresholds for the two isotopes are at 10.85 and 9.91 MeV. The activities are measured by anticoincidence detector, which reduces the background to nearly zero. The activities increase with third power of the energy difference. It is therefore easy to find the exact energy, as the activity increases proportional to $(E - E_{th})^3$.

The significance of the system of bending and the two collectors of secondary electrons is that the energy can be monitored and recorded continuously. It can be controlled by slightly changing the beam current, which controls the conveyor speed. In this way both the energy and the dose can be controlled to be constant and monitored automatically, even when the different parameters change slightly during heating of the accelerator or due to ripples on the high voltage lines. We draw attention to these details, because it is important to know that all the important parameters can be controlled and monitored during processing.

The accelerator arrived at Natick without the bending magnet, but a copy of the design introduced at Risø accelerator was quickly installed. The Natick accelerator did not have a conveyor. The building did not allow for the beam to be bent downward with a conveyor underneath as at Risø. Therefore, the beam was bent 90 degrees sidewise. We stipulated the design of the overhang conveyor at Natick, which was to include lightweight, overhang see-through carriers made of 2S-aluminum. This design minimizes induced activity. The pure aluminum has a threshold of 13.06 MeV, which assures no neutrons or induced activity when the energy is below 13 MeV; and the long life ($7 \cdot 10^5$ years) of ^{26}Al, means that even at higher energy, radioactivity in the carriers is not of concern for workers protection. The "see-through" carriers meant that most of the neutrons created in the food would not be slowed down and absorbed in the food, but escape into the walls which could be covered with neutron absorbers if necessary. (For example, the inside walls were covered with small blocks of boron concrete.) The beam catchers were also made of 2S-aluminum. They were made of three pieces insulated from each other by glass. This design permits continuous monitoring of the beam current, scanner width, and scanner position. The short life of ^{28}Al meant that also the small neutron absorption would not create a problem.

Several measurements were made to assure that the calculations of the shielding and radioactivity estimates were adequate. In 1960 at Risø, we also measured the induced radioactivity in food. We did this by exposing the food to a very high dose, about 5,000 kGy, by electrons; that is, to a dose 100 times higher than that used for sterilization. It was clear from the measurements that the neutron-capture reaction rather than (γ, n) reaction set the limit for 10 MeV X rays. Using 10 MeV X rays on salty ham at sterilizing doses was unacceptable. On the other hand, the 10 MeV electron irradiation was safe. However, the detection equipment was not as sophisticated or as well calibrated as those of US Army contractors. We considered these experiments, therefore, only as preliminary, and did not publish the results. The objective was only to assure safety, and to assure that our rough calculations were correct. We were not in doubt when we recommended use of 10 MeV electrons as safe. But we recommended against 10 MeV X rays; and we did not want to increase the energy beyond 10 MeV electrons, because we then increase the (γ, n) reactions, which increase with third power of the energy difference.

Natick submitted the petition for Co-60 γ-irradiation of bacon on August 17, 1962, (accepted for filing August 27). It was approved February 15, 1963, a month after the International Conference at Natick, January 14–16.

The wheat petition for irradiation with Co-60 γ rays was submitted October 4, 1962 by professor Brownell et al. and approved on August 21, 1963.

On June 5, 1963 General Electric submitted a petition for use of 5 MeV electrons on bacon. It was quickly approved on August 30, 1963.

On Dec 18, 1963 High Voltage Engineering submitted a petition for use of 5 MeV electrons on wheat. It was not approved before February 26, 1966.

On August 23, 1963, U. S. Army submitted a petition for extending it to 10 MeV electrons. It took FDA a long time to approve. The petition was not approved before April 21, 1965.

However, there was not a consensus. Many of my co-workers at Natick thought it should be higher. Dr. Richard Meyer was well trained in activation analyzes. He made a good analysis of the findings in the different reports of U.S. Army's contractors. Dr. H. William Koch, of National Bureau of Standards (now NIST), an outstanding physicist (the author with J. W. Motz of the best analyses of X ray production and X ray spectrum, Rev. of Mod. Phys. **31**, 920, 1959) was involved. At the time, he was the Chairman of the National Research Councils Advisory Committee to Natick on Radiation Sources. He was well capable of good assessment of induced radioactivity. Like Dr. Richard Meyer, he thought the limit should be higher. This is clear from Koch's paper with E. H. Eisenhower at the International Conference on Radiation Preservation of Food in September 27–30, 1964, Boston MA. This is also clear from his paper at the Symposium on Radiation Preservation of Foods at the meeting of the American Chemical Society September 16–17, 1965.

In a Memorandum for the Record dated May 24, 1999, Dr. Edward S. Josephson, who was in charge of the food irradiation program, reports that he and Dr. Koch had a meeting with FDA early in1964 to try to persuade FDA to approve 14 MeV. They were unsuccessful, but FDA agreed instead to increase the limit to 10 MeV. As mentioned above, the 10 MeV was not formally approved before in April 21, 1965.

The 5 MeV X ray petition for irradiation of bacon was submitted by Radiation Dynamics Inc. on July 23, 1964, and was approved relatively quickly on December 19, 1964. My former coworker, Mr. Robert Jarrett told me in 1995 (while at a meeting in Vienna) that Radiation Dynamics had consulted Natick. Dr. Richard Meyer was by then familiar with the many contract reports, and it is understandable that the researchers at Natick Laboratories were supportive and supplied Radiation Dynamics with all the available information.

In Denmark the main focus was on medical sterilization of disposable medical equipment such as syringes, catheters, bandages, catgut, and artificial lung heart machines used during open heart-surgery, etc. This program was initiated in the summer 1960. The irradiation facilities were being used for research during daytime but for industry during evenings, nights, and weekends as required. At this time it was the largest medical sterilization facility in Europe. As a consequence, the Danish industry increased very significantly its export of these items. The radiation sterilization of medical products was greatly appreciated by the Danish and other Scandinavian hospitals and by the medical health authorities in the Scandinavian countries. Due to heavy load, the Danish industry was advised to erect a 10 MeV electron facility for medical sterilization. This led to A/S Radest (now Raychem A/S) building a 10 MeV electron accelerator facility. The British had a low power 4.3 MeV linear accelerator for research. Their focus was on building cobalt-60 facilities; and most industrial sterilization of medical products throughout the world made use of cobalt-60 facilities.

At a Joint FAO/IAEA/WHO Expert Committee meeting in Rome, April 21–28, 1964 on the technical Basis for Legislation on Irradiated Food, the question of maximum electron energy came up. Dr. Josephson attended the meeting as an advisor to FAO. On his way to Rome he stopped at Risø and told me that the British were proposing 5 MeV as a maximum. I assured him that 10 MeV was safe. He was able to convince the other participants except the British at the meeting, and the Committee voted in favor of 10 MeV for electrons with the British delegation abstaining. The British participants were distinguished scientists, but their experts at home had concern about 10 MeV. (Dr. Josephson memorandum of May 24, 1999 discusses the meeting. See also the WHO Tech Report series No. 316; or the FAO Atomic Energy Series Report No. 6). FDA approved 10 MeV electrons one year later, or on April 21, 1965.

The first International Symposium on Ionizing Radiation and the Sterilization of Medical Products was held at Risø December 6–9, 1964. All the delegates could see the 10 MeV accelerator in operation. It became well known, therefore, that the 10 MeV worked well. In Germany a similar 10 MeV accelerator from Varian was installed in 1966 in Karlsruhe. Dr. Z. P. Zagórski, a leading radiation chemist from Warsaw, Poland work as a visiting scientist in my laboratory at Risø. He subsequently returned to Poland and had a similar 10 MeV accelerator installed in Warsaw. This accelerator was built by the Russians' accelerator center in Leningrad. Previously, Prof. Niels Bohr had invited his old friend Dr. Peter Kapitza who was in England from 1924 to 1935, working on low-temperature and magnetism, but when returning to Russia became a leading man there in radar technology. He brought with him his son Sergei, who was the leader of the accelerator development in Leningrad. While Bohr talked to Peter Kapitza, I was asked to entertain his son and show him the linear accelerator. He was quick at understanding everything. When Zagórski from Polen asked him to build one like that, he had no problems. Several others came to imitate what we did at Risø. It therefore was clearly recognized everywhere that 10 MeV linear accelerator was practical and did not produce any induced activity problems.

Dr. Richard A. Meyer who had analyzed thoroughly the reports of the different contractors on induced activity found that the induced activity produced by 24 MeV electrons was safe to use. In his report he states:

"In general it was found that sterilization of food with 24 MeV electrons will produce a slight increase in the activity level of the food. Such an increase is insignificant when compared to the natural activity in food or the two to ten fold increase in activity by use of certain food additives. It can be stated that no radioactivity is induced in foods up to around 14 MeV. Current research is aimed at determining this threshold value."

It is thus understandable why Dr. Josephson and Dr. Koch asked FDA in early 1964 to raise the limit for electron energy to 14. There were also a few objections to Dr. Meyer's conclusion.

(1) The fact, as pointed out by Dr. Meyer, that several permitted food additives contain much more radioactivity than the irradiated food, is usually irrelevant. The radioactivity in these food additives is due mainly to natural potassium. When we change the concentration of potassium in the food the body will regulate the concentration to be nearly constant. Even if the body concentration changes slightly, the chemical and physiological effects on the body are more important than any added radioactivity.

(2) Meyer like Koch and the contractors pointed out that the induced radioactivity was much less than the maximum permissible concentration (MPC) of the radioisotopes in the body as set by the National Committee on Radiation Protection. For example, the concentration of the long lived (half-life 2.6 y) Na-22 isotope was only 0.5% of MPC value (in ham it may be 14 times higher). This comparison may be rejected on the grounds that these MPC levels have to do with a limit for rejection (and necessary destruction) of food that has become artificially contaminated by nuclear war or something similar. These levels are not set to justify intentional introduction of radioactivity in to the food.

(3) Meyer pointed out that the long lived radioactivity introduced in 24 MeV irradiation was only about 5% of the natural radioactivity in beef. However, in ham (and bacon) it could be 70%. He said: "In general, it is reasonable to estimate that the long lived activity induced in foods will not exceed the amount present without irradiation and in most cases will be insignificant in comparison to the natural activity."

His arguments reflected the mainstream view at the time, which held that the fallout, which at that time increased the background by about 13% was acceptable. Others thought that these levels most likely were too high. At the Natick Radiation Laboratory, we continued to carry out many experiments at about 24 MeV, for example, dose distribution experiments and shielding

experiments. However, as soon as these experiments were finished, we changed the 24 MeV 18 kW accelerator at Natick to a 10 MeV 9 kW accelerator by removing half of the accelerator sections. All food irradiation experiments and radiation chemistry experiments at Natick Laboratories were subsequently done using 10 MeV. Some were unhappy about the change, but others felt strongly that we were in the business of developing food irradiation and should not open any discussion or fear about induced radioactivity. The 10 MeV electron irradiation limit was well accepted everywhere.

In 1975, we were approaching petitions for several foods, and we wanted to strengthen the justification for the energy levels used. A contract was awarded for thorough analyzes of the induced activity. Mr. Thomas G. Martin III, a certified health physicist and competent in theoretical calculations was the project officer. Professor Robert R. Becker, a good nuclear physicist, got the contract. He and Tom worked closely and did some experiments at Natick to confirm the calculations.

In 1980, at the Meeting of the Joint FAO/IAEA/WHO Expert Committee on the Wholesomeness of Irradiated Food recommended 10 MeV electrons and 5 MeV X rays. US FDA, as mentioned above, had already accepted both of these limits. They were also in accordance with the recommendation of FAO/IAEA Advisory Group on International Acceptance of Irradiated Food that met November 28 to December 1, 1977 in Wageningen, Netherlands, following the International Conference in Wageningen 21 to 25 November. In 1980 the Joint FAO/IAEA/WHO Expert Committee on the Wholesomeness of Irradiated Food, therefore accepted these limits, which then also were incorporated in the Codex Alimentarius Standards, which were accepted in 1983.

A meeting on “Food Safety Aspects Relating to the Application of X ray Surveillance Equipment” was sponsored by IAEA and FAO at Neuherberg, Munich, Germany November 13–17, 1989. Chairman was John W. Hubble of NIST, Gaithersburg. This meeting recommended approval of use of 10 MeV X rays for X raying whole shipping containers (truckloads) containing food. [Anon90] The maximum dose is only 0.5 Gy, or a dose that is a very small fraction, $5 \cdot 10^{-5}$, of the 10 kGy dose approved for 5 MeV X rays. The number of neutrons from the X ray target can be reduced by use of iron instead of heavy metals such as tungsten, tantalum or gold in the X ray target. The high energy X rays are needed to facilitate detection of contraband in truckloads of food in international trade. The request for consideration came from the State of Qatar. In light of the extremely low maximum dose of 0.5 Gy, the Committee considered the 10 MeV X rays acceptable.

The FAO/IAEA Consultants’ Meeting on the Development of X ray Machines for Food Irradiation, that met October 16–18, 1995 in Vienna, Austria concluded that irradiation of food with 7.5 MeV X rays was safe.

The FAO/IAEA/WHO Study Group on High Dose Irradiation that met at WHO Headquarters September 15 to 20, 1997 found (see reference [WHO99]) that it was generally accepted that only the following sources are suitable for radiation processing of food:

Radioisotope sources: cobalt-60 or caesium-137;

Machine sources: electrons up to 10 MeV and X rays from electrons up to 5 MeV.

The present publication gives some of the details of the information supplied to the Committee, and the reasons for the limitation.